

USING THE D1D5 CFT TO UNDERSTAND BLACK HOLES

DISSERTATION

Presented in Partial Fulfillment of the Requirements for the Degree Doctor of
Philosophy in the Graduate School of The Ohio State University

By

Steven G. Avery, B.S.

Graduate Program in Physics

The Ohio State University

2018

Dissertation Committee:

Samir D. Mathur, Advisor

Richard Kass

Yuri Kovchegov

Stuart Raby

© Copyright by
Steven G. Avery
2018

ABSTRACT

The bound state of D1-branes and D5-branes in IIB string theory is an exceptionally fertile system for the study of black holes. The D1D5 system has two dual descriptions: a gravitational and a conformal field theory (CFT) description. Here, we focus on using the two-dimensional CFT to understand black hole physics.

After reviewing the D1D5 system, we first show how to perturbatively relax the decoupling limit to calculate the emission *out* of the AdS/CFT into the asymptotic flat space. We take the effect of the neck into account and fix the coupling between the CFT and the asymptotic flat space. This calculation is distinguished from other AdS–CFT calculations which only work in the strict decoupling limit and use the gravitational description to learn about strongly coupled field theory.

We apply the formalism to particular smooth, horizonless three-charge nonextremal geometries. In the fuzzball proposal, these geometries are interpreted as black hole microstates, but they suffer from a classical instability. At first, the instability seems problematic in the fuzzball proposal; however, it was argued that if one used the D1D5 CFT then the instability could be interpreted as precisely the Hawking radiation process for the particular microstates. That the instability is classical, and not quantum mechanical results from a large Bose enhancement. In this document, we perform calculations that confirm this interpretation and demonstrate the above emission formalism.

All of the calculations discussed thus far, and most of the calculations in the literature on the D1D5 CFT, are at the “orbifold point” in moduli space. This point is far from the black hole physics of interest, but some calculations agree anyway. To understand black holes better it seems likely that moving off of the orbifold point will become necessary. We present several calculations demonstrating the effect of a single application of the marginal deformation operator that moves the D1D5 CFT off its orbifold point. The deformation operator twists two copies of the orbifold CFT, which we show produces a “squeezed state” with an arbitrary number of excitations. Thus, initial high-energy excitations can fragment into many low-energy excitations. This deformation, should give rise to thermalization and other important black hole dynamics.

Finally, we close with a brief summary and mention some opportunities for future work.

To my grandmother, for telling me that integrals are “fun.”

ACKNOWLEDGMENTS

I am indebted to numerous people who have provided encouragement, discussion, and enlightenment throughout my academic career. Perhaps most importantly, I am grateful to my advisor, Professor Samir Mathur. My understanding has benefited from many conversations about physics and mathematics with him. I am grateful to have had the opportunity to work with someone with such strong physical intuition and insight. On a more personal note, he has helped me navigate through the bureaucracies of graduate school and beyond. I would also like to thank Professors Richard Kass, Yuri Kovchegov, and Stuart Raby for serving on my candidacy and doctoral committees. They and my advisor surely deserve recognition for, if nothing else, reading my lengthy candidacy exam paper and this lengthy dissertation. Professors Kovchegov and Raby have also had important, positive influences on my graduate school experience through their classes and informal discussions.

I am grateful for all of the individuals who have taught me science and mathematics over the course of my life. Especially noteworthy are my high school math teacher, Mr. Wells, from whom I learned trigonometry, calculus, combinatorics, and some linear algebra; my first physics teacher, Mr. Olivieri, who taught me to think deeply about simple things and that I cannot depend on someone else to always tell me the answer; my undergraduate advisor, Professor Vatche Sahakian, who gave me my first taste of general relativity, string theory, and field theory; and my advisor, Professor Samir Mathur, whose lectures on particle physics, group theory, general relativity, and string theory, I will always cherish. From my time as an undergraduate, I am also grateful to Professor John Townsend for his encouragement, occasional criticism, and for making me pass out of “Frosh Physics.” There are numerous others who I have not mentioned here whose lectures and teaching have allowed me to progress. I would like to thank all of the professors I had at Harvey Mudd College; their dedication to undergraduate teaching was mostly unappreciated by me at the time—I hope they can forgive my occasional nap in class.

An important part of graduate school is learning to discuss physics. I have been privileged with great physics conversations with Archana Anandakrishnan, Greg Baker, Iosif Bena, Nikolay Bobev, Konstantin Bobkov, Borun Chowdhury, Ben Dundee, Stefano Giusto,

Sarang Gopalakrishnan, Josh Lapan, Samir Mathur, Jeremy Michelson, Joseph Polchinski, Stuart Raby, Yogesh Srivastava, and Anastasios Taliotis. Of marked importance in this regard are my collaborators: Borun Chowdhury, Samir Mathur, and Jeremy Michelson. While working through projects, they have helped my understanding of diverse topics immeasurably.

I should also thank those who read through and offered advice on drafts of this dissertation: Borun Chowdhury, Ben Dundee, Sarang Gopalakrishnan, Bart Horn, and my wife Elizabeth Avery. Their suffering deserves commendation. Others I have consulted about various technical points, and I am grateful for their responses: Jan de Boer, Borun Chowdhury, Josh Lapan, Emil Martinec, Joseph Polchinski, Carlos Tamarit, and Amitabh Virmani. On past projects, the results of which are presented here, I or my collaborators have also benefited from discussion with Sumit Das, Justin David, Antal Jevicki, Yuri Kovchegov, Per Kraus, Oleg Lunin, Emil Martinec, Mohit Randeria, Masaki Shigemori, and Yogesh Srivastava. I also extend my gratitude to the Kavli Institute for Theoretical Physics (KITP) at the University of California, Santa Barbara for supporting me while much of this document was written. Relatedly, I am grateful to Archana Anandakrishnan and Mike Hinton for being my “agents” in Columbus, while I was in Santa Barbara. Without their help, I could not have fulfilled the graduate school requirements.

There is more to life than physics, and there are many people that have provided support and companionship through my academic journey that I have not yet thanked. First and foremost, I am grateful to my family. My parents not only foot the bill of my early education, but have also provided inestimable encouragement and support throughout my life. I am especially grateful to my wife, Elizabeth, whose emotional support, encouragement, and patience have sustained me, even as she has overcome her own graduate school hurdles.

I am grateful for the friendship of Jeremy Bridge from high school onward. From my time as an undergraduate, I would like to thank the rest of “the triangle” for their various antics: Eric Malm and Jason Murcko. I am also grateful for friendship with Brad Greer, and *many* others during my time at Harvey Mudd College. At The Ohio State University, I thank all of my officemates; as well as Chris Porter, Bill Schneider, Ben Dundee, and Mike Hinton; and the rest of the graduate students, for their general camaraderie. I want to also thank my KITP officemates and fellow KITP graduate fellows for friendship and often asinine conversations: Claudia De Grandi, John Biddle, and Sarang Gopalakrishnan. The postdocs at the KITP have also been most welcoming.

The work presented here was supported in part by DOE grant DE-FG02-91ER-40690. My stay at the KITP and the writing of this document was supported in part by the National Science Foundation under Grant No. PHY05-51164.

VITA

January 27, 1983 Born—Tarzana, CA

May, 2005 B.S., Harvey Mudd College, Claremont,
CA

Autumn 2005–Spring 2008 Graduate Teaching Associate, OSU,
Columbus, OH

Summer 2008–Summer 2010 Graduate Research Associate, OSU,
Columbus, OH

Autumn 2010 KITP Graduate Fellow, UCSB, Santa Bar-
bara, CA

Publications

- S. G. Avery and B. D. Chowdhury, “Intertwining Relations for the Deformed D1D5 CFT,” arXiv:1007.2202 [hep-th].
- S. G. Avery, B. D. Chowdhury and S. D. Mathur, “Excitations in the deformed D1D5 CFT,” JHEP **1006**, 032 (2010) [arXiv:1003.2746 [hep-th]].
- S. G. Avery, B. D. Chowdhury and S. D. Mathur, “Deforming the D1D5 CFT away from the orbifold point,” JHEP **1006**, 031 (2010) [arXiv:1002.3132 [hep-th]].
- S. G. Avery and B. D. Chowdhury, “Emission from the D1D5 CFT: Higher Twists,” JHEP **1001**, 087 (2010) [arXiv:0907.1663 [hep-th]].
- S. G. Avery, B. D. Chowdhury and S. D. Mathur, “Emission from the D1D5 CFT,” JHEP **0910**, 065 (2009) [arXiv:0906.2015 [hep-th]].
- S. G. Avery and J. Michelson, “Mechanics and Quantum Supermechanics of a Monopole Probe Including a Coulomb Potential,” Phys. Rev. D **77**, 085001 (2008) [arXiv:0712.0341 [hep-th]].

S. G. Avery, E. Malm, and E. Harley, "The Myth of 'The Myth of Fingerprints'," *The UMAP Journal*, Fall 2004, 25(3) 215–230.

Fields of Study

Major Field: Physics

Table of Contents

| | Page |
|----------------------------------|------|
| Abstract | ii |
| Dedication | iv |
| Acknowledgments | v |
| Vita | vii |
| List of Figures | xiii |
| List of Tables | xiv |

Chapters

| | |
|--|-----------|
| 1 Introduction | 1 |
| 1.1 Why Quantum Gravity? | 1 |
| 1.1.1 Singularities | 2 |
| 1.1.2 Quantum Fields on Classical Geometry | 4 |
| 1.2 Obstacles to a Theory of Quantum Gravity | 11 |
| 1.2.1 Recent Attempts | 13 |
| 1.3 String Theory | 14 |
| 1.3.1 The Worldsheet | 15 |
| 1.3.2 D-branes | 20 |
| 1.3.3 The AdS–CFT Correspondence | 24 |
| 1.4 The Fuzzball Proposal | 28 |
| 1.5 Outline | 31 |
| 2 The D1D5 System | 33 |
| 2.1 IIB on a Torus | 34 |
| 2.1.1 IIB on T^5 | 34 |
| 2.1.2 Relationship with IIB on T^4 | 35 |
| 2.2 Supergravity Description | 36 |
| 2.2.1 The Two-charge Extremal Black Hole | 36 |
| 2.2.2 Generalizations | 38 |
| 2.2.3 The Near-Horizon Limit | 39 |
| 2.3 The Brane Description | 41 |
| 2.3.1 Gauge Theory Description | 42 |
| 2.3.2 Instanton Description | 49 |
| 2.4 The Correspondence | 51 |
| 2.5 The Orbifold Model of the D1D5 CFT | 52 |

| | | |
|----------|---|------------|
| 2.5.1 | The Symmetries and Action | 52 |
| 2.5.2 | Twist Operators | 55 |
| 2.5.3 | Chiral Primaries and Short Multiplets | 56 |
| 2.5.4 | Marginal Deformations | 62 |
| 2.5.5 | Spectral Flow | 64 |
| 2.5.6 | The Ramond Sector | 65 |
| 2.6 | Overview | 65 |
| 3 | Coupling the CFT to Flat Space | 66 |
| 3.1 | The Geometry | 67 |
| 3.2 | The Coupling between Gravity Fields and CFT Operators | 69 |
| 3.3 | The Outer Region | 72 |
| 3.4 | The Intermediate Region | 73 |
| 3.5 | The Interaction | 74 |
| 3.6 | Emission | 75 |
| 4 | Emission from JMaRT Geometries | 78 |
| 4.1 | JMaRT Geometries | 79 |
| 4.1.1 | Features of the Geometries | 79 |
| 4.1.2 | Ergoregion Emission | 86 |
| 4.2 | Reproducing $\kappa = 1$ Emission using the Orbifold CFT | 87 |
| 4.2.1 | The Initial State, the Final State, and the Vertex Operator | 88 |
| 4.2.2 | Using Spectral Flow | 93 |
| 4.2.3 | Evaluating the CFT Amplitude | 95 |
| 4.2.4 | Combinatorics | 96 |
| 4.2.5 | The Rate of Emission | 99 |
| 4.2.6 | Emission from Nonextremal Microstates | 101 |
| 4.3 | Reproducing $\kappa > 1$ Emission | 106 |
| 4.3.1 | Emission from κ -orbifolded Geometries | 107 |
| 4.3.2 | The “Unphysical” Amplitude | 110 |
| 4.3.3 | Relating the Computed CFT Amplitude to the Physical Problem | 114 |
| 4.3.4 | Method of Computation | 116 |
| 4.3.5 | Computing the Twist Jacobian Factor T | 117 |
| 4.3.6 | Computing the Mode Jacobian Factor M | 121 |
| 4.3.7 | The CFT Amplitude | 124 |
| 4.3.8 | Combinatorics | 125 |
| 4.3.9 | The Rate of Emission | 128 |
| 4.4 | Discussion | 129 |
| 5 | Moving off the Orbifold Point | 131 |
| 5.1 | The Deformation Operator | 132 |
| 5.1.1 | Normalization of σ_2^+ | 132 |
| 5.2 | Applying the Deformation Operator to the Vacuum | 134 |
| 5.2.1 | Outline of the Computation | 135 |
| 5.2.2 | Mode Expansions on the Cylinder | 138 |
| 5.2.3 | The $G_{A,-\frac{1}{2}}^-$ Operator | 139 |

| | | |
|----------|---|------------|
| 5.2.4 | Ansatz for $ \chi\rangle$ | 140 |
| 5.2.5 | The First Spectral Flow | 141 |
| 5.2.6 | Mode Expansions on the z Plane | 142 |
| 5.2.7 | Mapping to the Covering Space | 142 |
| 5.2.8 | The Second Spectral Flow | 144 |
| 5.2.9 | Computing γ_{mn}^B and γ_{mn}^F | 145 |
| 5.2.10 | The State $ \psi\rangle$ | 149 |
| 5.3 | Applying the Deformation Operator to Excited States | 150 |
| 5.3.1 | The Action of $\sigma_2^+(w_0)$ on a Single Bosonic Mode | 152 |
| 5.3.2 | The Action of $\sigma_2^+(w_0)$ on a Single Fermionic Mode | 157 |
| 5.3.3 | Two Bosonic Modes | 159 |
| 5.3.4 | Two Fermionic Modes | 161 |
| 5.3.5 | Complete Action of the Deformation Operator on a Bosonic Mode | 162 |
| 5.4 | Intertwining Relations | 163 |
| 5.4.1 | Basic Derivation | 163 |
| 5.4.2 | Problems | 167 |
| 5.4.3 | A More Rigorous Derivation | 169 |
| 5.5 | An Example: Intertwining Relations for J_n^a | 175 |
| 5.5.1 | The Contour Method | 175 |
| 5.5.2 | The Composite Method | 178 |
| 5.6 | Discussion | 180 |
| 6 | Conclusions and Outlook | 183 |

Appendices

| | | |
|----------|--|------------|
| A | Notation and Conventions for the Orbifold CFT | 185 |
| A.1 | Symmetries and Indices | 185 |
| A.2 | Field Content | 186 |
| A.3 | Currents | 186 |
| A.4 | Hermitian Conjugation | 187 |
| A.5 | OPE | 187 |
| A.6 | Mode Algebra | 189 |
| A.7 | Useful Identities | 190 |
| A.8 | n -twisted Sector Mode Algebra | 190 |
| A.9 | Spectral Flow | 191 |
| A.10 | Ramond Sector | 194 |
| B | Cartesian to Spherical Clebsch–Gordan Coefficients | 196 |
| C | Normalizing the CFT state and the Vertex Operator | 202 |
| C.1 | Normalizing the Initial State | 202 |
| C.2 | Normalizing the Vertex Operator | 203 |
| D | Computing Correlation Functions of $S_{N_1 N_5}$-twist Operators | 206 |
| D.1 | Basic Method | 206 |

| | | |
|----------|--|------------|
| D.2 | Spherical Correlation Functions of Twist Operators | 208 |
| D.3 | Properties of the Map | 209 |
| D.4 | Computing the Liouville Action | 210 |
| D.4.1 | Kinetic Contributions to the Liouville Action | 213 |
| D.4.2 | The Curvature Contribution | 218 |
| D.5 | The Unnormalized Correlator | 219 |
| D.6 | Normalizing the Twist Operators | 220 |
| D.7 | The General Correlator | 221 |
| D.7.1 | Checking the Correlator | 223 |
| E | The Exponential Ansatz | 224 |
| F | Some Useful Series | 227 |
| | Bibliography | 228 |

List of Figures

| Figure | Page |
|--|------|
| 1.1 Penrose diagram for black hole formation | 5 |
| 1.2 The pants diagram | 14 |
| 1.3 Closed string worldsheet | 15 |
| 1.4 The topology expansion of a string correlator | 18 |
| 1.5 Open strings on a D-brane | 22 |
| 1.6 Open string interactions | 23 |
| 1.7 Two different ways of picturing a closed string scattering off of a D-brane | 26 |
| 1.8 An illustration of open–closed string duality | 26 |
| 2.1 The NS vacuum and global AdS | 54 |
| 2.2 The twist operator σ_3 | 55 |
| 2.3 The short multiplets | 60 |
| 3.1 An illustration of the geometry created by stacks of branes | 67 |
| 4.1 The gravity description of the emission process | 87 |
| 4.2 The effect of spectral flow on the NS vacuum | 102 |
| 4.3 The initial and final states for emission | 103 |
| 4.4 The initial and final states for nonextremal emission | 104 |
| 4.5 Initial and final states for $\kappa = 2$ | 109 |
| 4.6 Initial and final states of the “unphysical” amplitude | 112 |
| 4.7 The branch cuts created by the twist operators | 116 |
| 4.8 The initial and final states of the “unphysical” amplitude for $\nu = 2$ excitations | 127 |
| 5.1 The effect of the twisting part of the deformation | 133 |
| 5.2 The deformation operator on the cylinder | 135 |
| 5.3 Manipulating the supercharge contour | 139 |
| 5.4 The t -plane for a $\sigma_2(z_0)$ | 143 |
| 5.5 Deforming the contour in the z -plane | 170 |
| 5.6 A close-up of contours C_2 and C_3 | 170 |
| 5.7 The contours in the t -plane | 171 |
| D.1 The map to the covering space | 211 |

List of Tables

| Table | | Page |
|-------|---|------|
| 1.1 | Low-energy excitations of IIA and IIB string theory | 20 |
| 2.1 | The D1D5 brane configuration | 33 |
| 2.2 | The charges and gauge fields of IIB strings compactified on T^4 | 35 |
| 2.3 | The near-horizon supergravity moduli | 40 |
| 2.4 | The chiral primaries in the n -twisted sector | 58 |
| 2.5 | The structure of a short multiplet | 61 |
| 2.6 | Moduli of the orbifold CFT | 64 |

Chapter 1

INTRODUCTION

In this chapter we give an overview of the background material, upon which the rest of the dissertation rests. We begin by reviewing the basic motivations for and difficulties of quantum gravity, which leads us to study of black holes in string theory. We give a very basic introduction to string theory. We then discuss the fuzzball proposal for the interior structure of black holes. We conclude the introduction with an outline of the rest of the remaining chapters.

The material presented here is probably insufficient for a complete understanding of the topics covered, but cites the relevant literature and serves as review that focuses on the issues pertinent here. It also serves as an apologia for string theory, which has received some negative attention in recent years.

1.1 Why Quantum Gravity?

The body of this dissertation is framed within the general context of string theory, which we review in Section 1.3. Before jumping into technical details, however, we must first ask: Do we *really* need a theory of quantum gravity? One may ask this question in two ways. First, the pragmatic question of what value such a theory would have; it almost certainly will not affect the daily life of a lay person, or even of most physicists—most likely there will be no experiments in the near future that are able to rigorously test the details of such a theory. Second, seeing as even gravitational waves have not yet been observed [1], one might wonder whether gravity actually *is* quantized in Nature. Indeed, Feynman entreats us to “keep an open mind” [2]:

It is still possible that quantum theory does not absolutely guarantee that gravity *has* to be quantized. I don’t want to be misunderstood here—by an open mind I do not mean an empty mind—I mean that perhaps if we consider alternative theories which do not seem *a priori* justified, and we calculate what things would be like if such a theory were true, we might all of a sudden discover that’s the way it really is!...In this spirit, I would like to suggest that it is

possible that quantum mechanics fails at large distances and for large objects.

Feynman, 1962

Despite this admonition, there are sundry reasons to believe that gravity *is* actually quantized, and furthermore that understanding quantum gravity is of central importance in our ongoing quest to understand Nature. Classical general relativity leaves us with many important questions that one would hope quantum gravity could answer: most prominently, the nature of the initial Big Bang singularity and the cosmological constant problem. A successful treatment of these problems with quantum gravity would be of fundamental importance to the cosmological understanding of the universe, and might have important astrophysically observable signals. Moreover, classical general relativity and quantum field theory are inconsistent without important quantum gravitational corrections.

1.1.1 Singularities

We address both the pragmatic form and the more fundamental form of the “why quantum gravity” question simultaneously. It is well-established that general relativity is a good description of classical gravity. In fact, general relativity is the most reasonable theory of gravitation one could consider that is consistent with special relativity and the simplest observations. That we get static gravitational fields implies that gravity is mediated by an integer-spin bosonic field; that gravity acts over long ranges suggests that gravity is mediated by a massless field. Odd-integer spin fields lead to forces that are both attractive and repulsive. Since gravity is universally attractive we should consider even-spin fields. A spin zero field could only couple to the trace of the stress–energy tensor $T^\mu{}_\mu$ and thus could not couple to the photon, which has traceless stress–energy tensor. The fact that light is deflected by gravity is now well-established.

General relativity is a very successful theory of gravity; however, there are some issues within the theory that may make one uncomfortable. Most prominently there are solutions that have singularities—regions of infinite curvature. The most famous example is the Schwarzschild black hole with metric (with Newton’s constant $G = 1$)

$$ds^2 = - \left(1 - \frac{2M}{r} \right) dt^2 + \frac{dr^2}{1 - \frac{2M}{r}} + r^2 d\Omega_2^2, \quad (1.1)$$

where M is the mass of the black hole and $d\Omega_2^2$ is the differential angular area element. At the Schwarzschild radius $r = 2M$, the coordinates break down, but the underlying spacetime manifold is perfectly smooth as is clear in other coordinizations. At $r = 0$, however, the geometry is singular, as can be seen by considering a coordinate invariant measure of curvature,

$$R^{\mu\nu\lambda\rho} R_{\mu\nu\lambda\rho} = \frac{48M^2}{r^6}. \quad (1.2)$$

An in-falling observer can reach the geometric singularity at $r = 0$ in finite proper time. This means that an adventurous physicist could reach the singularity and perform experiments (if he or she could withstand the tidal forces). The results of such experiments are at best ill-defined. The singularity has one saving grace: it is censored by the event horizon at $r = 2M$. The adventurous physicist could never publish the results of the experiments in a journal distributed outside the black hole. See Figure 1.1 for a Penrose diagram of spherically symmetric matter collapsing into a black hole. Note that the singularity is hidden behind the horizon in dashed red.

One might not be very troubled that singular solutions to Einstein's equations exist. Perhaps they are never realized in Nature, or perhaps we should simply discard them as unphysical. Unfortunately, this is a difficult position to hold. Hawking and Penrose [3, 4] demonstrated that singularities arise in general relativity from perfectly reasonable smooth initial conditions. For instance, if one starts with a cloud of pressureless dust, then it will collapse into a singularity [5].¹ Again, the only consolation would be that some form of cosmic censorship holds, and all the singularities are hidden behind event horizons so that we don't have to worry about "seeing" the breakdown of physics.

Even appropriately censored, these singularities are philosophically troublesome. This is not an esoteric concern, since there is strong evidence for the existence of astrophysical black holes in Nature [6], and furthermore there is an uncensored singularity at the original Big Bang event in the Friedmann–Robertson–Walker–Lemaître metric that best describes our universe. The metric describing a homogeneous, isotropic and flat cosmology is [7]

$$ds^2 = -d\tau^2 + a^2(\tau)(dx^2 + dy^2 + dz^2), \quad (1.3)$$

with scale factor $a(\tau)$. The exact form of $a(\tau)$ depends on the matter content of the universe; however, one typically finds that $a(\tau)$ is proportional to some positive power of τ . From which it follows that the Ricci scalar diverges at the origin of the universe, $\tau = 0$:

$$R = 6 \left(\frac{\ddot{a}}{a} + \frac{\dot{a}^2}{a^2} \right) \sim \frac{1}{\tau^2}. \quad (1.4)$$

We find, then, that we cannot simply turn a blind eye to the singularities that arise in general relativity. Instead it seems that general relativity is predicting its own downfall, and forcing us to consider quantum gravity. The unique length scale one can form from the fundamental constants G , \hbar , and c

$$\ell_{\text{pl}} = \sqrt{\frac{G\hbar}{c^3}}, \quad (1.5)$$

¹In a realistic case, one expects matter pressure to play a role; however, there is no obstacle to making the cloud massive enough to overcome the pressure.

the Planck length, is the natural length scale for a theory of quantum gravity. Thus, when the curvature becomes on the order of $R \sim 1/\ell_{\text{pl}}^2$, we expect large quantum gravity corrections. Presumably, any theory of quantum gravity should resolve the singularities that arise in general relativity (at least those singularities that arise from smooth initial data [8]).

There is another cosmological question on which a theory of quantum gravity might provide insight. For the Big Bang, we may also desire a theory of initial conditions. If a theory of quantum gravity can make robust physical predictions about the very early universe, then it can have observable consequences for current experiments measuring the cosmic microwave background or, alternatively, help explain the smallness of the cosmological constant [9]. Finally, we should note that the most successful theory of cosmology that explains the homogeneity of the observed universe, namely inflation, is a quantum gravity effect.

1.1.2 Quantum Fields on Classical Geometry

Above, we argue that the singularities arising in general relativity encourage the study of quantum gravity. Not only are they philosophically problematic, but the singularities are also an avenue for quantum gravity to become an experimental (or at least observational) field of physics. The above problems manifest themselves entirely within classical general relativity, and should presumably be resolved by a theory of quantum gravity.

We now consider what happens when we put quantum fields on curved background geometries, which more dramatically illustrates the need for a theory of quantum gravity. Let us first comment, however, that it is probably not consistent to think of some aspect of Nature as fundamentally classical, while the rest is fundamentally quantum. If, for example, gravity were classical, it would be difficult to imagine what gravitational field arises due to an electron that is in a quantum superposition of different positions. Suppose, for instance, we claimed that Einstein's equations were

$$G_{\mu\nu} = 8\pi\langle T_{\mu\nu} \rangle, \tag{1.6}$$

then we would get curvature originating from the different superposed positions. What happens when we make a measurement? The metric must jump acausally and nonlocally to a new configuration with curvature originating from only one location [2, 7]. If we insist gravity is classical, then it seems we are forced to discard quantum mechanics as fundamental. This tension becomes greater in the sequel.

As we discuss above, black holes are a robust prediction of general relativity, and there is evidence that they are realized in Nature. Above, our main concern was the geometric singularity where the curvature diverges—we now consider the event horizon. In the presence of a horizon, Hawking [10, 11] demonstrated that black holes are unstable and

emit black-body radiation at infinity. The energy of the emitted particles is compensated by negative energy particles that travel into the black hole, decreasing its mass. Thus, black holes are quantum mechanically unstable and will eventually decay, albeit slowly. For instance, Page [12] estimates that a solar mass black hole takes 10^{66} years to completely evaporate, which is many many orders of magnitude longer than the age of the universe (on the order of 10^{10} years).

Computing Hawking Radiation

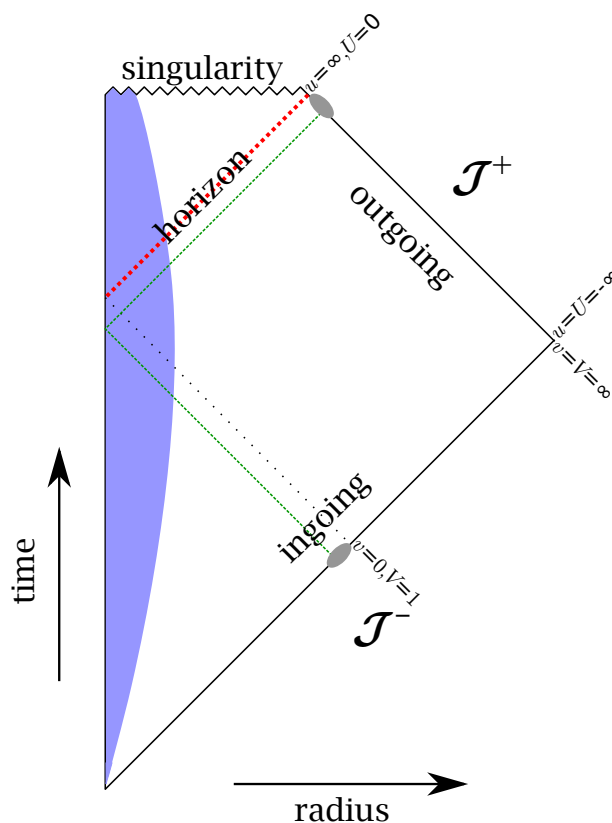


Figure 1.1: The Penrose diagram for some matter (light blue) collapsing into a Schwarzschild black hole. Outside of the matter, the metric is Schwarzschild. The Penrose diagram does *not* correctly indicate *distances* between spacetime events; only *angles* are correctly indicated. Null geodesics are lines at $\pm 45^\circ$, like the green dashed curve illustrating the connection between coordinates on future null infinity, \mathcal{J}^+ , and past null infinity, \mathcal{J}^- . The gray shading on \mathcal{J}^+ and \mathcal{J}^- indicates the region where geometric optics is a good approximation.

Let us sketch the essential details needed to understand Hawking radiation. Consider a noninteracting, massless, minimally-coupled scalar field, ϕ , in the background geometry corresponding to the formation of a Schwarzschild black hole. The action for ϕ is

$$S = \int d^4x \sqrt{-g} g^{\mu\nu} \partial_\mu \phi \partial_\nu \phi, \quad (1.7)$$

where $g_{\mu\nu}$ is the spacetime metric. The Penrose diagram for the collapse geometry is depicted in Figure 1.1. Outside of the collapsing matter, the metric is Schwarzschild, as in Equation (1.1). For this calculation, we do not need the details of the metric inside the collapsing matter, which depends on what the matter is.

The equations of motion for the field ϕ are given by

$$\square\phi = \frac{1}{\sqrt{-g}} \partial_\mu (\sqrt{-g} g^{\mu\nu} \partial_\nu \phi) = 0. \quad (1.8)$$

For simplicity, we consider only the s -wave emission by imposing the ansatz

$$\phi = \frac{f(r) e^{-i\omega t}}{r}. \quad (1.9)$$

The s -wave dominates the radiation spectrum, making this also a physically reasonable assumption [13]. Plugging into the equations of motion one finds that f must satisfy

$$\frac{r-2m}{r^2} \frac{d}{dr} \left[r(r-2m) \frac{d}{dr} \left(\frac{f(r)}{r} \right) \right] + \omega^2 f(r) = 0. \quad (1.10)$$

We are interested in finding how plane wave solutions near the horizon evolve into plane wave solutions near asymptotic infinity. Since the equations of motion are linear, there is a linear relationship between these two sets of modes. The connection defines a Bogolyubov transformation between the particle modes near the horizon and the asymptotic infinity particle modes.

To improve the asymptotic behavior of Equation (1.10), we introduce the “tortoise” radial coordinate

$$r_* = r + 2m \log \left| \frac{r-2m}{2m} \right|, \quad (1.11)$$

which gives equations that may be written in the form

$$f''(r_*) + \left[\omega^2 - \frac{2m}{r^3} \left(1 - \frac{2m}{r} \right) \right] f(r_*) = 0. \quad (1.12)$$

In the above, r is an implicit function of r_* given in Equation (1.11). For both asymptotic infinity $r \approx \infty$ and near-horizon $r \approx 2m$, Equation (1.12) simplifies and the field behaves as

$$\phi \propto \frac{e^{-i\omega(t \pm r_*)}}{r}. \quad (1.13)$$

Let us define null tortoise coordinates, u and v , as

$$u = t - r_*, \quad v = t + r_*. \quad (1.14)$$

The null surface \mathcal{J}^- has $u = -\infty$ and is parameterized by v . We define $v = 0$ as the point on \mathcal{J}^- connected to the point where the horizon forms by a null curve. See Figure 1.1. The null surface \mathcal{J}^+ has $v = \infty$ and is parameterized by u .

In a spacetime with no global timelike Killing vector, such as that of a black hole, there is no canonical notion of particle [7, 14]. There are two useful ways to describe the quantum mechanics of the scalar field. First, we can think about the “ingoing” Hilbert space which is defined along the null surface \mathcal{J}^- . This Hilbert space defines our in-states. We define the ingoing Hilbert space by expanding ϕ in terms of modes on \mathcal{J}^- . Near $v = 0$, the expansion takes the form

$$\phi_{\omega}^{(\text{in})} \sim a_{\omega} \frac{e^{-i\omega(t+r_*)}}{\sqrt{2\omega r}} + a_{\omega}^{\dagger} \frac{e^{i\omega(t+r_*)}}{\sqrt{2\omega r}}. \quad (1.15)$$

The second description of ϕ is in terms of the direct product of an “outgoing” Hilbert space and a horizon Hilbert space. The outgoing Hilbert space is defined in terms of modes along the null surface \mathcal{J}^+ , whereas the horizon Hilbert space is defined in terms of modes along the horizon. We do not need the details of the horizon here. Near the horizon, we can expand ϕ in terms of “outgoing modes” as

$$\phi_{\omega}^{(\text{out})} \sim b_{\omega} \frac{e^{-i\omega(t-r_*)}}{\sqrt{2\omega r}} + b_{\omega}^{\dagger} \frac{e^{i\omega(t-r_*)}}{\sqrt{2\omega r}}. \quad (1.16)$$

We wish to consider the situation when there are no incoming particles. This means we want the ingoing vacuum. What we find is that the ingoing vacuum has nonzero overlap with excited states of the outgoing Hilbert space. How do we see this? We need to understand how the ingoing modes at infinity are related to the outgoing modes near the horizon; we need to relate the a and a^{\dagger} ’s to the b and b^{\dagger} ’s. What we can do is consider an outgoing mode $\phi_{\omega}^{(\text{out})}$ and use the equation of motion (1.8) to evolve it from the near-horizon outgoing region into the ingoing region in Figure 1.1. We find that each outgoing mode evolves into a linear combination of the ingoing modes, with the coefficients telling us the exact relation between a ’s and b ’s.

The inner product on the ingoing Hilbert space can be stated in terms of the functions f :

$$\int_{-\infty}^{\infty} dv f_{\omega}(v) f_{\omega'}^*(v) = \int_{-\infty}^{\infty} dv \frac{e^{-i(\omega-\omega')v}}{2\sqrt{\omega\omega'}} = 2\pi \frac{\delta(\omega - \omega')}{2\omega}. \quad (1.17)$$

We wish to consider an outgoing mode near the horizon on \mathcal{J}^+ ,

$$g_{\omega}(u) = \frac{e^{-i\omega u}}{\sqrt{2\omega}}, \quad (1.18)$$

evolve it backwards in time to the null surface \mathcal{J}^- , and compute the overlap of that function with the in-modes. To evolve the outgoing mode backwards, we use the geometric optical approximation—that is, we assume that light rays travel on null geodesics. As we approach the horizon, the frequency of the outgoing mode increases making the approximation better and better. In null Kruskal coordinates,

$$U = -e^{-\frac{u}{4m}} \quad V = e^{\frac{v}{4m}}, \quad (1.19)$$

and the metric becomes

$$ds^2 = -16m^2 e^{-\frac{r}{2m}} dU dV + r^2 d\Omega_2^2. \quad (1.20)$$

From this form, it is clear that null geodesics in the r - t plane are curves of constant U or constant V . Let us trace an outgoing particle at coordinate u on \mathcal{J}^+ backward onto a point v on \mathcal{J}^- , following the path shown in Figure 1.1. From \mathcal{J}^- we follow a null geodesic with constant U until we reach $r = 0$, then we follow a null geodesic with constant V from $r = 0$ until we reach v . This gives the relation

$$(1 - U)V = 1 \quad \implies \quad v = -4m \log \left(1 + e^{-\frac{u}{4m}} \right) \approx -4m e^{-\frac{u}{4m}}, \quad (1.21)$$

near the horizon. Hence,

$$g_\omega(u) \longrightarrow g_\omega(v) \approx \begin{cases} 0 & v > 0 \\ \frac{1}{\sqrt{2\omega}} e^{i4m\omega \log(-\frac{v}{4m})} & v < 0, \end{cases} \quad (1.22)$$

where it should be clear from Figure 1.1 that propagating an outgoing mode onto \mathcal{J}^- can only give negative v . Let us define functions $\alpha_{\omega\omega'}$ and $\beta_{\omega\omega'}$ that describe the overlap of g_ω with the $f_\omega(v)$ on \mathcal{J}^- :

$$g_\omega(v) = \int_0^\infty \frac{d\omega'}{2\pi} (\alpha_{\omega\omega'} f_{\omega'}(v) + \beta_{\omega\omega'} f_{\omega'}^*(v)). \quad (1.23)$$

We can compute the coefficients α and β from the measure in Equation (1.17) to find [13]

$$\begin{aligned} \alpha_{\omega\omega'} &\approx \sqrt{\frac{\omega'}{\omega}} \int_0^\infty dv e^{-i\omega'v} \left(\frac{v}{4m} \right)^{i4m\omega} = -\frac{i}{\sqrt{\omega\omega'}} (i4m\omega')^{-i4m\omega} \Gamma(1 + i4m\omega) \\ \beta_{\omega\omega'} &\approx \sqrt{\frac{\omega'}{\omega}} \int_0^\infty dv e^{i\omega'v} \left(\frac{v}{4m} \right)^{i4m\omega} = \frac{i}{\sqrt{\omega\omega'}} (-i4m\omega')^{-i4m\omega} \Gamma(1 + i4m\omega). \end{aligned} \quad (1.24)$$

We see from the above that

$$\beta_{\omega\omega'} = -e^{-4\pi m\omega} \alpha_{\omega\omega'} \quad (1.25)$$

The coefficients tell us that a lowering operator a becomes a linear combination of raising and lowering operators b . The transformation we have outlined above that relates a and a^\dagger

operators on the incoming Hilbert space to b and b^\dagger operators on the outgoing Hilbert space is an example of a Bogolyubov transformation. It follows from the above [10, 13] that if we start with the incoming vacuum, the expectation value of the number of outgoing particles is given by

$$N_\omega = {}_a \langle 0 | b_\omega^\dagger b_\omega | 0 \rangle_a \sim \frac{1}{\frac{|\alpha|^2}{|\beta|^2} - 1} \sim \frac{1}{e^{8\pi m\omega} - 1}. \quad (1.26)$$

Thus, we conclude that if we start with the vacuum in the background of a Schwarzschild black hole, then we end with a Planckian distribution of outgoing particles corresponding to a black body with temperature $T = 1/(8\pi m)$. We have skipped over some important details in this discussion, especially with regard to what happens with the horizon Hilbert space. A more careful treatment allows one to see that energy is conserved by negative energy particles falling into the black hole. See [7, 10, 11, 13] for more complete discussions. Let us also comment, as emphasized in [15], that the Hawking process is quite general and only requires that there be a future horizon.²

Prior to Hawking's calculation, Bekenstein [17] argued that black holes have an entropy proportional to the horizon area. When combined with Hawking's calculation, one fixes the constant of proportionality and finds the Bekenstein–Hawking entropy,

$$S_{\text{BH}} = \frac{A}{4}. \quad (1.27)$$

So even without knowing the microscopic degrees of freedom, we can indirectly argue that black holes are thermodynamical objects with temperature and entropy.

The Information Paradox

Having derived that black holes emit radiation, let us consider the following process. We start with a bunch of matter in some quantum state $|\psi\rangle_{\text{in}}$ that undergoes gravitational collapse into a black hole. The black hole then emits radiation thermally until it entirely evaporates. All that remains of the state $|\psi\rangle_{\text{in}}$, then, is thermal radiation—a mixed state that can only be described by a density matrix! Thus, we see an apparent breakdown in quantum mechanics. Since any black hole formed by gravitational collapse would not have evaporated in the age of the universe, one might feel that this is not a problem; however, it may still be possible that small primordial black holes could have evaporated, or that one could tunnel into a small black hole state [12]. Regardless of whether it is actually realized, there is nothing to forbid this scenario within our best physical models of the universe and any inconsistencies still indicate a failure in our understanding of Nature.

²In fact, an experimental group has claimed to observe the Hawking process in an optical (non-gravitational) analogue [16].

This breakdown is frequently described as a loss of unitarity, but that may be misleading. If the time-evolution operator for a quantum system is non-unitary, then probability is not conserved. Typically this means that degrees of freedom are entering or leaving the system. For example, one can model alpha-decay with a non-Hermitian Hamiltonian, where the imaginary part of the energy is the decay rate corresponding to degrees of freedom leaving the system. With Hawking radiation, however, the generator of time evolution is not described by some non-Hermitian Hamiltonian. Instead time evolution could only be described in terms of a density matrix. This is a much more drastic situation, since all of our most fundamental laws are formulated in the language of quantum mechanics.

One may not find the information paradox as stated very compelling. After all, if one were to burn this dissertation, then the emitted radiation would presumably be described by a Planckian distribution; however, that would be a coarse-grained description. In fact, the radiation would result from some unitary evolution of the quantum mechanical state of all the atoms in the dissertation. In a similar spirit, one might think that back-reaction or some small quantum gravitational effect would restore unitary evolution. These and other effects certainly do alter the thermal distribution, but one can show that the information paradox is quite robust and has little to do with the actual distribution of the emitted particles.

The real problem is that the emitted radiation is entangled with negative energy particles that fall into the black hole, and once the black hole evaporates the emitted radiation is entangled with nothing [18–23]. In [22, 23], it was shown that quantum mechanics breaks down under the very general assumptions of locality and that quantum gravitational corrections are confined to the Planck scale.

Thus, if we assume that Nature is fundamentally quantum mechanical and local, then we are forced to conclude that quantum gravitational effects (at least in the presence of a black hole) are *not* confined to the Planck length. This breakdown of dimensional analysis indicates that some nontrivial physics is at work. The preceding discussion of singularities and Hawking radiation suggests understanding quantum gravity can have observable, and fundamentally important effects.

Some may question the virtues of pursuing a new theory that is motivated only by theoretical tensions between existing theories, and not by experimental data. After all, was it not a failure to consult with experiments that led Aristotelian physics astray? We suggest a more apt historical analogue would be to special relativity. Einstein’s main motivation for the introduction of special relativity was probably not the Michelson–Morley experiment, but rather a theoretical inconsistency between Galilean relativity and Maxwell’s equations [24].

1.2 Obstacles to a Theory of Quantum Gravity

Having shown why quantum gravity is important, let us now explain why it is difficult. While different people may have different requirements for a successful theory of quantum gravity, there are two main obstacles to a quantum description of gravity. First, there is a conceptual difficulty in formulating a field theory where the field also defines the underlying spacetime [7]. For instance, for a quantum bosonic field $\hat{\phi}$ on classical metric g , causality demands that spacelike separated measurements be independent, meaning

$$[\hat{\phi}(x), \hat{\phi}(y)] = 0 \quad (x - y)^2 > 0, \quad (1.28)$$

where $(x - y)^2$ is the spacetime interval, which depends on $g_{\mu\nu}(x)$. Clearly, we would like a similar statement to hold for $\hat{g}_{\mu\nu}$ when we quantize the metric; gravitons should not violate the causality of the underlying spacetime. We might try to write something like

$$[\hat{g}_{\mu\nu}(x), \hat{g}_{\rho\sigma}(y)] = 0 \quad (x - y)^2 > 0, \quad (1.29)$$

but this is not a sensible statement. Whether or not x and y are spacelike depends on the measured value of $g_{\mu\nu}$, but the commutation relation is supposed to be an operator statement, independent of the eigenstate measured. More broadly, we see that the notion of causality becomes problematic when spacetime is quantized [7]. Another problem that stems from the dual roles of $g_{\mu\nu}$ arises in describing topology-changing transitions. Topology changes should arguably be allowed within a theory of quantum gravity, but a canonical quantization description seems intractable since we depend on spacelike foliations of spacetime [7]. One may try a path integral description, but it is problematic to associate a transition amplitude with it, since it is not clear what the gauge-invariant observables are [7].

The second major difficulty is that naive quantizations of general relativity give non-renormalizable perturbative expansions. For instance, if we expand the metric about a flat background $\eta_{\mu\nu}$ ³

$$g_{\mu\nu} = \eta_{\mu\nu} + \sqrt{G_N} \tilde{h}_{\mu\nu}, \quad (1.30)$$

then the action for \tilde{h} in 4 dimensions is very schematically given by

$$\begin{aligned} S_{\text{Einstein-Hilbert}} &= \frac{1}{16\pi G_N} \int d^4x \sqrt{-g} R \\ &\sim \int d^4x (\partial \tilde{h}_{\mu\nu} \partial \tilde{h}^{\mu\nu} + \sqrt{G_N} (\partial \tilde{h})^2 \tilde{h} + G_N (\partial \tilde{h})^2 \tilde{h}^2 + \dots). \end{aligned} \quad (1.31)$$

³we put in the factor of G_N to canonically normalize the action for the field \tilde{h} .

We have only kept a few terms, but these are sufficient to argue that the action is nonrenormalizable. In 4 dimensions, the coupling G_N has dimensions

$$[G_N] = (\text{length})^2. \quad (1.32)$$

Perturbation theory can be thought of as a power series expansion in the coupling G_N . For instance, consider the cross-section for graviton–graviton scattering. Cross-sections have dimensions of area and the only other length scale is the center of mass energy, E , so the perturbative expansion must be of the form

$$\sigma \sim G_N (a_0 + a_1(G_N E^2) + a_2(G_N E^2)^2 + \dots), \quad (1.33)$$

where the a_i are dimensionless constants. At high energies, then, σ violates the Froissart bound, which states that unitarity requires the cross-section at high energies grow no faster than $\log^2 E$ [25]. One can bypass this simple dimensional analysis by introducing another mass scale into the problem: either an explicit cutoff Λ or new massive excitations. From the above, we see that the new excitations should enter at an energy scale less than roughly $1/\sqrt{G_N} \sim 1/\ell_{\text{pl}}$. This is precisely what string theory does. Alternatively, one might hope that the dimensionless constants a_i vanish due to some symmetry or happy coincidence—as it happens they do not, e.g. [26–28].

Historically, some viewed renormalizability as a fundamental requirement of a well-defined quantum field theory. A more modern perspective is that nonrenormalizable field theories (and indeed even renormalizable field theories) should be viewed as effective descriptions valid at low energies. As one tries to extrapolate to higher energies in a nonrenormalizable theory, one gets more and more new terms with undetermined parameters. The ever-increasing number of undetermined parameters signals a loss of predictivity from a low-energy point of view; however, if we imagine starting from a UV theory with a finite number of parameters, then we see that all of those coefficients are fixed by a finite number of UV parameters. Thus, the distinction between renormalizable and nonrenormalizable theories simply reflects how sensitive the low-energy effective theory is to the high-energy (short-distance) physics that we may not know. For renormalizable theories, all of the short-distance physics can be encoded in a finite number of variables that can be determined experimentally, whereas a nonrenormalizable theory, like gravity, gives an infinite number of low-energy parameters.

The canonical example of this point of view is Fermi weak theory, a nonrenormalizable but useful description of low-energy weak interactions. At right about the energy scale predicted by the Froissart bound argument, one finds new massive degrees of freedom: the W and Z bosons. Thus, we say that the Glashow–Salam–Weinberg electroweak theory flows in the infrared, or low-energy, to Fermi weak theory. Applying these lessons to

gravity suggests that rather than trying to naively quantize general relativity, we should try looking for a high-energy theory that flows in the infrared to general relativity. Of course, finding such a theory with the desired properties is notoriously difficult.

1.2.1 Recent Attempts

There are at least three active programs attempting to find a consistent quantization of gravity:⁴ loop quantum gravity with its many variations, asymptotically safe gravity, and string theory. Both loop quantum gravity and asymptotically safe gravity take the attitude that perhaps the nonrenormalizability suggested by (1.33) indicates not a failure of the theory but of the perturbative expansion. Loop quantum gravity attempts to quantize gravity directly, without splitting the metric into a background and a small perturbation [31]. Asymptotically safe gravity, on the other hand, suggests that Equation (1.33) is an expansion about the wrong ultraviolet fixed point. We considered the $\partial\tilde{h}\partial\tilde{h}$ term the free theory about which we perturbed—this is implicitly an expansion about the Gaussian RG fixed point. The asymptotic safety program suggests that there may be a nontrivial fixed point, for which the interactions are renormalizable [32–35]. While the two alternatives to string theory mentioned above are active areas of research, this dissertation follows the string theory approach. String theory seems to be the most promising approach, and has far more tools for answering the questions of interest.

There are a couple of reasons to believe that quantum gravity cannot be a theory of local quantum fields. For instance, one can think of general relativity as the gauge theory of diffeomorphisms. Typically, when quantizing a gauge field theory, the fundamental degrees of freedom are local, gauge-invariant fields $\phi(x)$; however, in the case of general relativity x itself transforms under gauge transformations making such an identification impossible [36]. This suggests that a complete theory of quantum gravity cannot be formulated as a theory of local fields [37].

There is a second argument that quantum gravity cannot be a field theory. Since general relativity predicts that a black hole forms whenever enough energy is packed into a given region of space, it follows that the high energy spectrum of gravity should be dominated by black holes. From the Schwarzschild solution and the Bekenstein–Hawking formula, Equations (1.1) and (1.27), the entropy grows with energy like

$$S_{\text{black hole}} \sim E^2. \quad (1.34)$$

On the other hand, the high-energy behavior of any field theory is expected to be a conformal field theory, whose entropy grows like

$$S_{\text{CFT}} \sim E^{\frac{3}{4}} \quad (1.35)$$

⁴See [29] for another attempt, and [30] for a discussion of its current status.

in four dimensions. Thus, we should not expect a field theory description of gravity. See [38–40] for more precise and more general arguments that quantum gravity cannot be a field theory. This leads us to consider string theory.

1.3 String Theory

We now introduce string theory, one of the most promising theories of quantum gravity. While the full theory remains to be fully defined, there are certain limits of string theory that are understood very well. Our best description comes from the worldsheet formalism of a single string propagating through a fixed background. This is analogous to the quantum mechanical description of a single particle. The full description of interacting particles requires quantum field theory. Similarly, people think about “string field theories” that have creation and annihilation operators of whole strings, a topic we discuss no further here. Although the worldsheet description is restrictive, it contains a lot more physics than the quantum mechanics of a single particle might suggest.

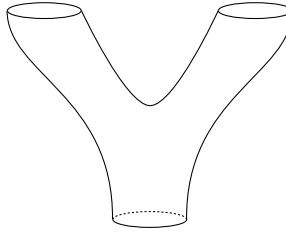


Figure 1.2: A closed string splits into two closed strings in the “pants diagram.” Note that a single worldsheet describes this three-point function. Thus the string worldsheet description is far richer than the analogous worldline theory of a particle.

Because the string worldsheet can have many different topologies and excitations, we can actually describe interactions between many different string states. See Figure 1.2 for an illustration. Computations of this type have been the most fundamental tool for exploring the consequences of the theory. What we learn from analysis of the worldsheet theory is that string theory is a theory of quantum gravity that is finite, reduces to general relativity in the low-energy limit, and has no free parameters [41–44]. One other interesting and unexpected consequence of the theory is a prediction of the spacetime dimension: (super)string theory is consistent only in 10 spacetime dimensions [41, 42, 44].

That string theory is formulated in 10 dimensions, while we clearly observe only 4 dimensions might seem like a deal-breaker for the theory; however, there are at least three

reasons why the theory is still worth pursuing. Firstly, quantum gravity is *hard* as emphasized above. String theory seems to resolve a lot of the difficulties in an elegant and consistent manner. This alone merits the study of string theory. Furthermore, there are enough powerful tools within string theory that we can use to perform explicit calculations addressing some of the puzzles about gravity mentioned above. Secondly, we can consider string theory on a very small six-dimensional compact manifold. Such a theory would appear to be four-dimensional in the length scales that have been explored so far. The process of compactifying to four-dimensions introduces new degrees of freedom from the four-dimensional perspective, à la Kaluza–Klein theory. By these means, the extra six dimensions give us enough freedom to potentially recover the Standard Model of particle physics, giving us the hope that string theory can unify all of known physics [42, 44]. Thirdly, string theory allows one to relate strongly coupled gauge theory correlators in flat space to weakly coupled gravity calculations in one higher dimension via “gravitational holography” [45–47]. These tools can give insight into problems in other areas of physics, for instance, nuclear theory [48] and condensed matter theory [49, 50].

1.3.1 The Worldsheet

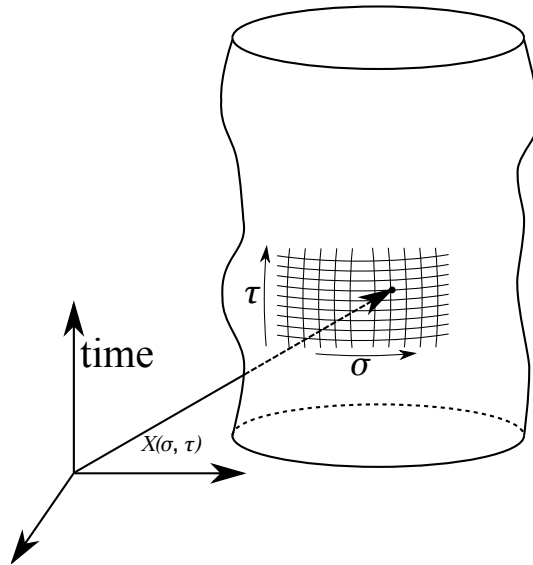


Figure 1.3: A closed string propagating through time sweeps out a worldsheet. We parameterize the worldsheet with functions $X(\sigma, \tau)$. We can think of X as fields living in a two-dimensional field theory with coordinates (σ, τ) .

Let us briefly introduce the worldsheet description of string theory. For details, see the standard references [41–44] or, alternatively, some more recent texts [51–53]. We can describe the classical motion of a string through spacetime by giving its path with a Lorentz vector $X^\mu = X^\mu(\sigma, \tau)$. The parameters σ and τ are not coordinates for physical spacetime, and so we are free to rescale them as we wish. Most treatments of string theory begin with the Nambu–Goto action,

$$S_{\text{NG}} = -T(\text{area of worldsheet}) = -T \int d\tau d\sigma \sqrt{-\det(\partial_a X^\mu \partial_b X_\mu)}, \quad (1.36)$$

the action for a relativistic string traveling through flat space. Here, a and b correspond to either σ or τ . This is the analogue of the action for a free relativistic point particle:

$$S_{\text{point-particle}} = -m(\text{length of worldline}) = -m \int d\tau \sqrt{-\frac{dX^\mu}{d\tau} \frac{dX_\mu}{d\tau}}. \quad (1.37)$$

The action for a point particle is proportional to the length of the worldline, the curve it sweeps out through spacetime. The length of the worldline is also known as the particle’s proper time. Similarly, the Nambu–Goto action is proportional to the area of the string’s worldsheet, the surface it sweeps out through spacetime. The constant of proportionality is the string tension T , which is frequently exchanged for either the Regge slope parameter α' or the string length ℓ_s via

$$T = \frac{1}{2\pi\alpha'} \quad \alpha' = \ell_s^2. \quad (1.38)$$

Note that the literature frequently uses different definitions for ℓ_s , but we use the above throughout this document. The string length ℓ_s is the natural length scale of string theory. The Regge slope parameter gets its name from the linear relation between the squared-mass m^2 and spin J of the quantized string excitations [41]:

$$J = \alpha' m^2. \quad (1.39)$$

As one can see from Equation (1.36), the action is defined in terms of a two-dimensional integral and thus can be thought of as a two-dimensional field theory. One can make the action look more like a conventional two-dimensional field theory by writing it in the form

$$S_{\text{Polyakov}} = -\frac{1}{4\pi\alpha'} \int d\tau d\sigma \sqrt{-\det \gamma} \gamma^{ab} \partial_a X^\mu \partial_b X_\mu, \quad (1.40)$$

the Polyakov action for the string.⁵ Note that we have introduced an auxiliary variable γ_{ab} , which acts as the metric on the two-dimensional worldsheet (also called the base space). One can integrate out γ_{ab} and recover Equation (1.36). This looks like the action for free

⁵The action was found by Brink, Di Vecchia, and Howe [54] and independently by Deser and Zumino [55]; however, Polyakov [56] “popularized” it [43].

scalars X^μ in a two-dimensional space with background metric γ_{ab} . The action has worldsheet diffeomorphism and Weyl symmetry. The diffeomorphism invariance gives us the ability to define new worldsheet coordinates,

$$(\sigma, \tau) \mapsto (\sigma'(\sigma, \tau), \tau'(\sigma, \tau)) \quad (1.41)$$

with the X^μ transforming as scalars and γ_{ab} as a two-index tensor. The Weyl symmetry allows us to make position dependent rescalings of the worldsheet metric,

$$\gamma_{ab} \mapsto e^{2\omega(\sigma, \tau)} \gamma_{ab} \quad (1.42)$$

with arbitrary $\omega(\sigma, \tau)$ and X^μ not transforming. Rescaling the metric changes the distance between distinct points in the two-dimensional base space. This symmetry can be thought of as a reflection of the fact that the string is fundamental, and not composed of any smaller objects—thus, it looks the same on all scales.

Let us focus our attention on the closed string, that is, we demand $X^\mu(\sigma = 0) = X^\mu(\sigma = 2\pi)$. When one quantizes the Polyakov action with these boundary conditions one finds that the vacuum state of the two-dimensional theory corresponds to a tachyon in the ambient spacetime. The tachyon is a problem, which we address later. The first excited states form a massless two-index tensor. We can break the tensor into a symmetric traceless part $h_{\mu\nu}$, an antisymmetric part $b_{\mu\nu}$, and the trace ϕ . The fact that we have a massless spin-2 particle $h_{\mu\nu}$ suggests that this is a theory of gravity, since general relativity is essentially the unique theory resulting from a field theory of massless spin-2 particles [2, 57–62]. By computing the scattering cross-section of gravitons, for instance, we can fix the 10-dimensional Newton’s constant in terms of the string coupling [41–44, 51]:

$$16\pi G_N^{(10)} = (2\pi)^7 \alpha'^4 g_s^2. \quad (1.43)$$

Since we have massless bosonic fields in spacetime, it is reasonable to assume that they can condense and acquire a vacuum expectation value. The essentially unique way to generalize Equation (1.40) to this case is [41, 43]⁶

$$S = \frac{1}{4\pi\alpha'} \int d\tau d\sigma \sqrt{-\det \gamma} \left[(\gamma^{ab} G_{\mu\nu}(X) + i\epsilon^{ab} B_{\mu\nu}(X)) \partial_a X^\mu \partial_b X^\nu + \alpha' \Phi(X) R \right], \quad (1.44)$$

where $G_{\mu\nu}$ is the background metric from $h_{\mu\nu}$, $B_{\mu\nu}$ is the background field from $b_{\mu\nu}$, Φ is the background from ϕ , and R is the Ricci scalar curvature of the two-dimensional metric γ^{ab} . The last term controls how difficult it is for the string to split apart or join together. For instance, consider the case that Φ is a constant Φ_0 , then the last term can be evaluated

⁶The overall minus sign is from an analytic continuation to Euclidean signature.

using the Gauss–Bonnet theorem:⁷

$$S_{\Phi_0} = \frac{\Phi_0}{4\pi} \int d\tau d\sigma \sqrt{-\det \gamma} R = \Phi_0 \chi, \quad (1.45)$$

where χ is the Euler characteristic of the worldsheet. The Euler characteristic is determined

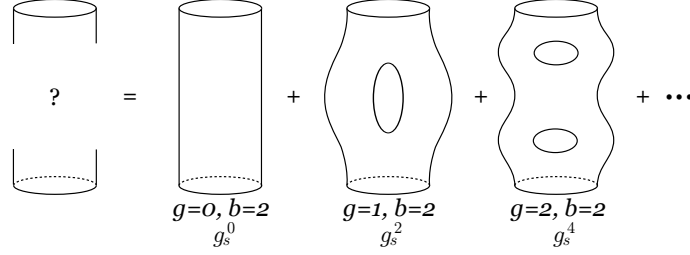


Figure 1.4: A cartoon illustrating the sum over all possible topologies of the interacting string.

by the total number of initial and final states b (boundaries of the worldsheet) and the number of loops g (the genus of the worldsheet) via

$$\chi = 2 - 2g - b. \quad (1.46)$$

Thus we can expand the partition function in topology as

$$Z = \sum_{\chi} (e^{\Phi_0})^{-\chi} Z_{\chi}(\alpha'), \quad (1.47)$$

which suggests that we identify the string coupling constant as $g_s = \exp \Phi_0$. The terms $Z_{\chi}(\alpha')$ are sums over all intermediate excitations of the string with fixed topology. In perturbative string theory, we expand both in α' , which controls the intermediate string states, and in g_s , which controls the worldsheet topology. The topological expansion is illustrated in Figure 1.4. For each topology shown, we perform a sum over all α' corrections to the shape.

Now, let us return to the action in Equation (1.44). As mentioned above the classical string has a Weyl rescaling symmetry; however, this symmetry is anomalous in the quantum theory. As it turns out, we must demand that the quantum theory be Weyl invariant,

⁷We have cheated slightly here. There is an additional boundary term that goes into χ . We have implicitly assumed here that the worldsheet is a closed manifold, but the Euler characteristic dependence we find applies more generally. See [41–44] for the correct treatment.

which means that the following beta functions must vanish [43]:

$$\beta_{\mu\nu}^G = \alpha' R_{\mu\nu} + 2\alpha' \nabla_\mu \nabla_\nu \Phi - \frac{\alpha'}{4} H_{\mu\lambda\omega} H_\nu{}^{\lambda\omega} + O(\alpha'^2) \quad (1.48a)$$

$$\beta_{\mu\nu}^B = -\frac{\alpha'}{2} \nabla^\omega H_{\omega\mu\nu} + \alpha' \nabla^\omega \Phi H_{\omega\mu\nu} + O(\alpha'^2) \quad (1.48b)$$

$$\beta^\Phi = \frac{D-26}{6} - \frac{\alpha'}{2} \nabla^2 \Phi + \alpha' \nabla_\omega \Phi \nabla^\omega \Phi - \frac{\alpha'}{24} H_{\mu\nu\lambda} H^{\mu\nu\lambda} + O(\alpha'^2), \quad (1.48c)$$

where $H_{\mu\nu\lambda}$ is the field strength of $B_{\mu\nu}$. Notice that requiring β^G to vanish gives Einstein's equations, β^B gives $B_{\mu\nu}$'s equations of motion, and β^Φ fixes the (bosonic string theory) spacetime dimension D to be 26 and gives Φ 's equations of motion. Consistency demands that the background field $G_{\mu\nu}$, which the string travels through, must obey Einstein's equation. This is another way in which we see gravity emerging from string theory, and a beautiful result of string theory.

The worldsheet theory we have discussed so far describes bosonic string theory. The theory has two problems: it only has bosonic degrees of freedom and it has a tachyon in its spectrum. Both of these problems can be cured by adding fermions to the two-dimensional field theory in Equation (1.40) in such a way to make the theory supersymmetric [41–44].

When one adds fermions one must carefully specify the boundary conditions. Firstly, we can consider closed or open strings: strings whose ends join to form closed curves in space, or strings with free endpoints. A closed string implies that $X(\sigma = 0) = X(\sigma = 2\pi)$. On the other hand, for open strings we need to specify Dirichlet or Neumann boundary conditions for the ends. Additionally, one needs to consider the fermions. For the closed string there are antiperiodic, called Neveu–Schwarz (NS), boundary conditions; and periodic, called Ramond (R), boundary conditions around the loop. For the open string, there are analogous conditions one can impose on the fermions. The Hilbert space of the worldsheet naturally breaks up into left-moving modes and right-moving modes, and we can specify the boundary conditions on the left- and right-moving modes separately.

While the string we are describing is a one-dimensional extended object, if its size is very small it looks like a point particle with mass that depends on the internal state of the string. The size of the string is on the order of the string length. Since we have not yet observed stringy behavior in any experiments, we must assume that the string length is much smaller than the smallest distances probed so far. Furthermore, it is natural to assume that the string length is close to the Planck length.⁸ Thus, we restrict our attention to the massless modes and think about what kinds of particles they look like from the perspective of the ambient spacetime. The massless NS–NS sector of the closed string is the same as that of the closed bosonic string described above. We list the rest of the

⁸Although there are many exceptions.

bosonic massless degrees of freedom for the two type II strings⁹ in Table 1.1. The NS–R and R–NS sectors of the string give fermionic degrees of freedom, which do not form condensates. If one analyzes the superstring instead of the bosonic string, one finds that the low-energy limit is 10-dimensional supergravity. In particular, the IIA and IIB string theories give IIA and IIB supergravity, with the massless spectrum of the closed string forming the supergravity multiplet.

Looking at Table 1.1, let us discuss the physics of the R–R gauge fields. The C fields are gauge fields that arise from the R–R sector; the superscript index indicates what kind of form (antisymmetric tensor) the gauge field is. For instance $C^{(0)}$ is a Lorentz scalar, while $C^{(2)}$ has two antisymmetrized Lorentz indices. The corresponding field strength for the gauge field is the exterior derivative of the form. The plus on $C^{(4)+}$ is a reminder that the corresponding field strength $dC^{(4)+}$ should be self-(Hodge star)-dual. This is possible since the exterior derivative of a 4-form is a 5-form, which can be self-dual in 10 dimensions.

1.3.2 D-branes

| | | | IIB | IIA |
|-------|------------------------------|------------------------|------------------------------|------------------------------|
| NS–NS | g_{MN}, ϕ, B_{MN} | g_{MN}, ϕ, B_{MN} | $D(-1) \rightarrow C^{(0)}$ | $D0 \rightarrow C^{(1)}$ |
| | | | $D1 \rightarrow C^{(2)}$ | $D2 \rightarrow C^{(3)}$ |
| R–R | $C^{(0)}, C^{(2)}, C^{(4)+}$ | $C^{(1)}, C^{(3)}$ | $D3 \rightarrow C^{(4)+}$ | $D4 \rightarrow C^{(3)} [M]$ |
| | | | $D5 \rightarrow C^{(2)} [M]$ | $D6 \rightarrow C^{(1)} [M]$ |
| | | | $D7 \rightarrow C^{(0)} [M]$ | $D8$ |
| | | | $D9$ | |

Table 1.1: The left table is a summary of the bosonic field content of types IIA and IIB supergravity, which describe the corresponding string theories in the low-energy and small string coupling limit. On the right, is a summary of the D-brane content of the theories and what gauge field the D-brane primarily couples to. The [M] indicates a magnetic type coupling and the + superscript is a reminder that the corresponding field strength is constrained to be self-dual.

We saw above how the NS–NS sector couples to the string worldsheet. One may wonder what the R–R C fields couple to when they acquire a vacuum expectation value (vev). If we have these gauge fields living in the 10-dimensional spacetime, it is natural to ask

⁹The roman numeral ‘II’ refers to two Weyl supersymmetries of the spacetime theory. The ‘A’ and ‘B’ label different choices for the chirality of the worldsheet fermions. For our purposes here, one can take Table 1.1 as defining the differences.

what couples to them and how. Supergravity has solitonic solutions which are $(p + 1)$ -dimensional (including time) extended (but very localized in the $10 - p$ dimensions) objects, which we call Dp -branes. These objects couple to the R-R gauge fields as shown in the table on the right [44, 51]. A '[M]' indicates that the Dp -brane couples to the gauge field magnetically. If supergravity has these solutions, then how do they generalize to string theory?

So far, we have restricted our discussion to closed strings—strings that form closed loops. One could also consider open strings with free ends, with Neumann or Dirichlet boundary conditions. If one uses Dirichlet boundary conditions, then one breaks Poincare invariance; an unhappy state of affairs, *unless* the Dirichlet boundary condition is on some other object in the theory. In this case, Poincare invariance is only broken spontaneously. The Dp -branes are precisely objects on which open strings may end with Dirichlet boundary conditions, which is the origin of the letter 'D' (for Dirichlet). Since the D-branes are solitons of some form of string field theory, one expects their mass to go like one over the string coupling, and indeed for a Dp -brane one finds [51]

$$T_p = \frac{\text{mass}}{p\text{-volume}} = \frac{1}{(2\pi)^p \alpha'^{\frac{p+1}{2}} g_s}. \quad (1.49)$$

Thus, when the string's excitations are light and weakly interacting, the D-branes are heavy and vice-versa.

In string perturbation theory, the defining quality of Dp -branes is that they are p -spatial dimensional objects that open strings can have endpoints fixed to; moreover, open strings may *only* end on D-branes. For example, if an open string has Neumann boundary conditions in all $9 + 1$ dimensions, then there must be a spacetime-filling D9-brane [43, 44, 51].

Since D-branes are solitonic objects with mass proportional to the inverse of the string coupling, they never arise directly in perturbation theory: one cannot scatter two closed strings and produce a D-brane; however, if a D-brane is already present in our spacetime, then we can do a perturbative expansion around this new background. How does the presence of a D-brane change the perturbation theory?

Well, for one, the perturbation theory now includes open strings. The open strings can have both endpoints fixed to the same D-brane or to two different D-branes. The open strings also have discrete oscillator modes, and a similar mass spectrum to the closed strings. As with the closed strings, we focus on the massless ground states of the open string. In contradistinction to the closed string, the open string's ground state polarization only has one Lorentz index [43, 44, 51]. These different configurations are shown in Figure 1.5.

An open string with both ends on the same D-brane can join its ends together forming a closed string that leaves the D-brane. This process has a coupling of $\sqrt{g_s}$. Of course,

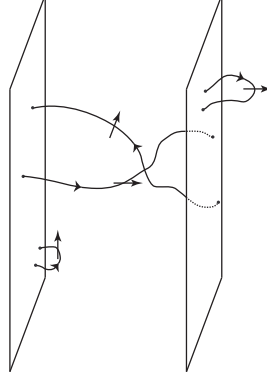


Figure 1.5: An illustration of the different ways that open strings can be configured on D-branes. The long arrows indicate the polarization of the open string, *not* its velocity, which has been suppressed.

the opposite process can happen as well—a closed string can bump into a D-brane and become an open string with end points fixed to the D-brane. Other types of processes can occur: two correctly oriented open strings connecting to the same D-brane can meet up and form one open string. In Figure 1.6, cartoons of these processes are shown.

How are these various processes reflected in the low-energy supergravity description? Is there some effective field theory description of the D-brane that captures these dynamics? As it happens, there is: the Dirac–Born–Infeld (DBI) action with R–R gauge field couplings [51]

$$\begin{aligned}
 S_{DBI} = & -T_p \int d^{p+1}\xi \, e^{-\Phi} \sqrt{-\det \left(G^{(\text{ind.})} + B^{(\text{ind.})} + 2\pi\alpha' F_p \right)} \\
 & + iT_p \int C^{(p+1)} + iT_p \int C^{(p-1)} \wedge F_p \cdots,
 \end{aligned} \tag{1.50}$$

where $G^{(\text{ind.})}$ and $B^{(\text{ind.})}$ are the induced metric and R–R gauge field; F_p is a gauge field strength of a $U(1)$ gauge field living in the world-volume of the Dp brane; the last two and the omitted terms depend slightly on what p is, but they are the coupling of the Dp -brane to the R–R gauge fields. This action is a good approximation when $\alpha'^{3/2} \partial_a F_{bc} \ll 1$, i.e. when the D-brane varies slowly in time and space [43, 44, 51, 53]. If one expands the square root and determinant for small F and B about the metric induced from flat Minkowski spacetime, then one finds a standard $U(1)$ gauge theory action. This action only describes the D-brane dynamics, there is still a full 10-dimensional bulk supergravity action, as well.

How can we see the string processes described above in Equation (1.50)? The emission of closed strings from the D-brane is described by the coupling of the various closed string gauge fields (and gravity) to the D-brane. The open string excitations of the D-brane can

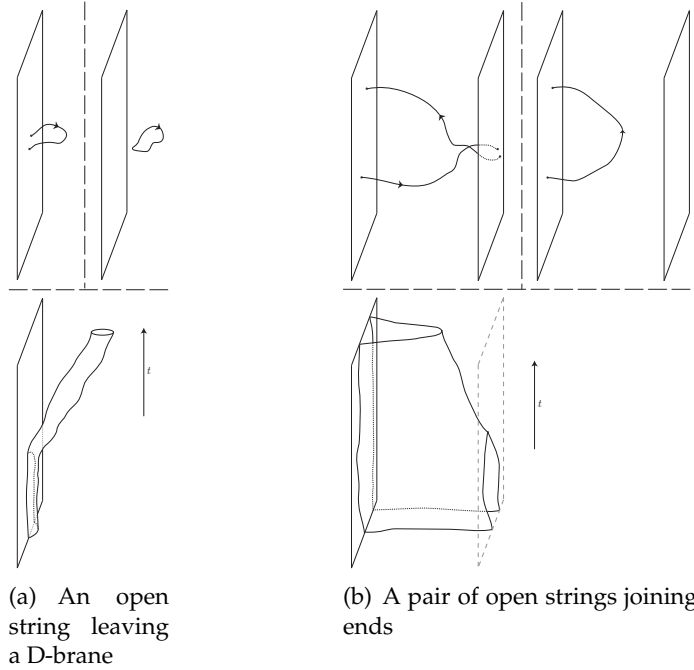


Figure 1.6: The top figures are before and after picture of open strings interacting at order $\sqrt{g_s}$, and the bottom figures represent the worldsheets for the same processes. The arrowheads indicate the orientation of the string.

be broken into two classes: those polarized along the brane and those perpendicular to the brane. The excitations polarized along the D-brane are described by a $U(1)$ gauge field living in the Dp -brane's $(p+1)$ -dimensional worldvolume, while the excitations polarized perpendicular to the brane are described by waves in the position of the brane in the $(10-p)$ transverse dimensions [43, 44, 51].

Open strings connecting two D-branes are not included in the DBI action, since they will have mass proportional to the separation of the D-branes and thus are suppressed. This is true unless the separation between D-branes, in some limit, is zero. If we consider, for instance, a stack of N parallel, coincident Dp -branes, then the open strings that have endpoints on the same D-brane form a $U(1)$ gauge field as before. If that was all we had then the overall gauge group would just be $U(1)^N$; however, there can now also be open strings connecting different D-branes, which will connect the $U(1)$ s to each other in non-trivial ways. This leads to a $U(N)$ gauge group in $(p+1)$ dimensions, with those $U(1)$ s embedded as noncommuting subgroups [43, 44, 51, 53].

There is a diagonal $U(1)$ degree of freedom which describes all of the Dp -branes moving together in the same way, and transforming all of the $U(1)$ s in the same way. Typically, we are not interested in this trivial type of motion, and therefore focus on only the $SU(N)$ gauge group left after modding out the diagonal $U(1)$. D-branes, as it turns out

are $1/2$ -BPS¹⁰ objects, spontaneously breaking one-half of the 32 components of the $9 + 1$ -dimensional $\mathcal{N} = 2$ supersymmetry [53].¹¹ Therefore, we expect the effective field theory describing the D-brane to have 16 supercharges and an $SU(N)$ gauge group.

A summary of the total low-energy action would be

$$S = S_{\text{bulk}} + S_{\text{branes}} + S_{\text{brane-bulk interaction}}, \quad (1.51)$$

where S_{bulk} is the supergravity action, S_{branes} is the $SU(N)$ gauge theory, and the last term is the coupling of the R–R gauge fields in the bulk supergravity to the $SU(N)$ field strength of the brane action.

We know roughly what S_{branes} and $S_{\text{brane-bulk}}$ look like from Equation (1.50), but we have not discussed what happens to the supergravity action. In particular, the proposed stack of D-branes is quite massive in the limits where supergravity is valid, since α' and g_s are small, which suggests that the metric should be distorted by the mass. Since the D-brane’s mass is homogeneously spread over its volume, we make an ansatz for the metric of the D-branes,

$$ds^2 = f_1(r)dx_{\parallel}^2 + f_2(r)(dr^2 + r^2 d\Omega_{10-p-2}^2), \quad (1.52)$$

where r is a radial coordinate in the perpendicular space, measuring how far one is from the stack, and the $d\Omega^2$ is the metric for the constant radius sphere in the perpendicular space. By dx_{\parallel}^2 , we mean a Minkowski dot product of the one-forms living along the brane directions. We also expect the C -field to which the D-brane primarily couples to be sourced by the D-brane. For instance, for a stack of N D3 brane [45, 65]

$$\frac{1}{f_1(r)} = f_2(r) = \sqrt{1 + \frac{4\pi N g_s \alpha'^2}{r^4}}. \quad (1.53)$$

Note that if one takes an appropriate limit in which the 1 in $f_2(r)^2$ can be dropped, then the resulting metric is that of $\text{AdS}_5 \times S^5$.

1.3.3 The AdS–CFT Correspondence

From the above considerations, one can arrive at one of the most remarkable results in string theory. The AdS–CFT correspondence, or the statement that string theory in $d + 1$ -dimensional anti-de Sitter (AdS) space is *dual* to the physics of a d -dimensional conformal field theory, is one of the most important recent ideas to arise in theoretical physics. The duality is the most explicit and powerful instance of gravitational holography. For more comprehensive treatments, see [65, 66].

¹⁰They saturate a Bogomol’nyi–Prasad–Sommerfield (BPS) bound [63, 64] for an object breaking half of the supersymmetry charges.

¹¹The ‘II’ in IIA/B refers to the there being two Majorana–Weyl supersymmetries.

The most heuristic argument for the existence of gravitational holography was made prior to AdS–CFT [67, 68]. Consider a gravitational theory, and suppose you want to pack as much information as possible into as small a volume as possible, i.e. you want to make the perfect hard drive. For typical physical systems the amount of information one can store grows with the volume and the energy. So if one wants to store more information in a fixed volume, then one ends up making an increasingly massive hard drive; however, we know that once one packs enough energy into a given volume one ends up with a black hole. Since the entropy (and therefore the information one could store) of a black hole scales with the *area* of the black hole and the black hole has the maximum entropy a gravitational system can contain in a fixed volume, one might guess that a $d + 1$ -dimensional gravitational system should admit a d -dimensional *non*gravitational description.

A second reason to believe the correspondence arises from considering the large N limit of $SU(N)$ gauge theory. If one takes $N \rightarrow \infty$ while holding the 't Hooft coupling $\lambda = g_{YM}^2 N$ fixed, then one gets a nontrivial theory [69, 70]. One can do a double perturbative expansion in $1/N$ and in λ . When one organizes the perturbative series using 't Hooft double line notation, one finds that the $1/N$ expansion corresponds to an expansion in the topology of the diagram. The expansion, then, takes a remarkably similar form to the string perturbative expansion in Equation (1.47). The extra dimension arises as an energy scale of the gauge theory.

The above considerations are indirect and quite broad. We can precisely state the correspondence by treating the most studied case. Consider a stack of N D3-branes in IIB string theory such as we described in Section 1.3.2. As we discussed, the open string modes give rise to a $SU(N)$ 3+1-dimensional gauge theory. On the other hand, the closed string modes give rise to an $\text{AdS}_5 \times S^5$ spacetime with N units of $C^{(4)+}$ flux on the S^5 . On the third hand, in string theory there is open–closed string duality: a string Feynman diagram can be viewed as either a closed string diagram *or* a higher order open string diagram. Calculating in both ways gives the same answer.

As an example, we consider a closed string scattering off of a D-brane. To leading order in g_s , the relevant diagram is shown in Figure 1.7. In the right half of the figure, we interpret the interaction as the D-brane emitting a closed string and joining up with a second closed string. This is a tree-level process, with three external legs. In the left half of the figure if we run time into the page, we interpret the interaction as a pair of open strings popping out of the vacuum, one of the legs splitting and rejoining, and finally the remaining two open strings popping back into the vacuum. This is a two loop vacuum bubble, requiring a sum over all possible intermediate open string states. The distinction is easier to see if one conformally shrinks the external legs and looks at the two processes as a sphere with holes in it, and as a disk with holes in it. Examining Figure 1.8, we can imagine stretching the top hole in the sphere and smoothing the sphere into the disk with

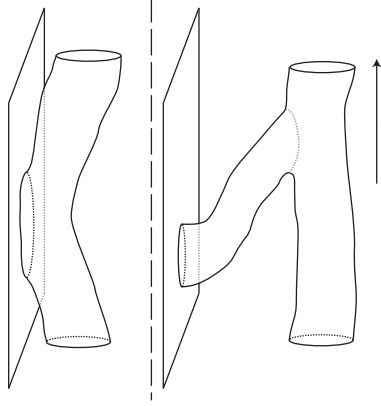


Figure 1.7: Two different ways of picturing a closed string scattering off of a D-brane

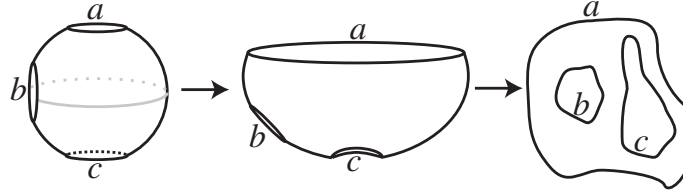


Figure 1.8: A cartoon of transforming a closed string tree-level Feynman diagram into a two-loop open string diagram. We have not been careful to represent the conformal nature of the transformation in the figure.

two holes in it.

We see that tree-level closed string processes are equivalent to open string loop diagrams, since the same argument can equally well apply for an interaction with a large number of closed string legs from the D-brane, as long as the closed string worldsheet does not have any loops. In string perturbation theory it seems quite natural that the same diagram can be viewed as a closed string process and as an open string process; however, if we ask how this duality manifests itself in the effective field theory description, we become quite confused. The closed string process should correspond to tree-level supergravity from S_{bulk} , while the open string process should correspond to the $SU(N)$ SYM from S_{branes} ; but they are both included in the total action. Is the action in Equation (1.51) actually *double-counting* in some sense? Are S_{bulk} and S_{branes} dual to each other? Maldacena conjectured that, at least some of the time, the answer is yes [45].

Defining the Correspondence

Let us now describe the correspondence for the best studied case, which arises when considering a stack of N D3-branes. The statement is that type IIB superstring theory in an $\text{AdS}_5 \times S^5$ background with string coupling g_s , both manifolds having radius R and $F^{(5)+}$ satisfying $\int_{S^5} F^{(5)+} = N$, and four-dimensional $\mathcal{N} = 4$ $SU(N)$ SYM with coupling constant g_{YM} , are dual to each other [45, 65]. Moreover, we identify

$$2\pi g_s = g_{\text{YM}}^2 \quad R^4 = 4\pi g_s N \alpha'^2 \quad \langle C^{(0)} \rangle = \theta_I, \quad (1.54)$$

where θ_I is the instanton angle. The above identifications are part of what is called the dictionary of the correspondence.

By duality, we mean that there exists a well-defined one-to-one and onto mapping of states, operators, and correlation functions in both theories. The duality is best understood in the large N limit, when string loops are suppressed. When the 't Hooft coupling $g_{\text{YM}}^2 N$ is large, the string theory is weakly coupled and well-approximated by supergravity, while the field theory is strongly coupled. It is sometimes helpful to write the dictionary in a slightly different form:

$$\left(\frac{R}{\ell_s}\right)^4 = \lambda \quad \left(\frac{R}{\ell_{\text{pl}}^{(10)}}\right)^4 = \frac{\sqrt{2}}{\pi^2} N. \quad (1.55)$$

We see that the 't Hooft coupling is the AdS radius measured in string units and N is the AdS radius measured in 10-dimensional Planck units. This makes the role played by N and λ clearer in the string theory description. While a complete proof remains to be found, the AdS–CFT conjecture is extremely useful and is supported by a large body of evidence [52, 53, 66].

In the large N limit, we can elucidate more precisely the nature of the duality by considering the Laplace equation for fields living in the AdS. For appropriate boundary conditions, one can bijectively map the behavior of the field at the boundary of AdS onto the corresponding field configuration in the bulk of AdS. This suggests, then, that we associate with a field ϕ in AdS which has boundary value ϕ_0 a local operator in the dual field theory \mathcal{O} . Then the duality becomes the identification [47]

$$\left\langle e^{\int_{S^4} \phi_0 \mathcal{O}} \right\rangle_{\text{CFT}} = Z_S(\phi_0), \quad (1.56)$$

where the classical supergravity partition function is

$$Z_S(\phi_0) = e^{-S_{\text{sugra}}(\phi)}. \quad (1.57)$$

We see that the boundary value of ϕ acts as a classical source for \mathcal{O} in the CFT partition

function. The field theory’s Minkowski space has been written as S^4 , since we are stating the Euclidean version of the correspondence.

In this discussion, we focused on the $\text{AdS}_5\text{--CFT}_4$ correspondence that comes from considering D3-branes since it is the most widely studied; however, there are many other incarnations of AdS–CFT duality [66]. While there are many important differences between the different versions of the duality, there are several features that are universal; most importantly, the identification (1.56) and the strong–weak nature of the duality. The AdS–CFT correspondence is expected to hold more generally. For instance, [71] conjectures that every CFT satisfying certain basic requirements should have a dual AdS description.

In this dissertation, we treat the $\text{AdS}_3\text{--CFT}_2$ version of the correspondence that arises when one considers a bound state of D1 and D5 branes. The two-dimensional CFT is the “D1D5 CFT” of the title. In Chapter 2, we describe both the gravity and the field theory description of this system. Another important point is that the majority of interest in AdS–CFT is in using weakly coupled gravity calculations to understand strongly coupled field theory. Here, the primary motivation is to use the two-dimensional CFT to understand strongly coupled gravity.

1.4 The Fuzzball Proposal

Having introduced string theory, which is claimed to be a consistent theory of quantum gravity, we should return to the issues discussed in Section 1.1 and see what string theory can tell us. String theory has had some success in addressing both the issues of spacetime singularities and the information paradox. The AdS–CFT correspondence has proved a useful tool in a number of these studies. Some classes of singularities are resolved and others are much better understood within string theory, but a complete theory remains elusive [8, 72–74].

In this dissertation we are more concerned with the information paradox and the structure of black holes within string theory. The AdS–CFT proposal and more generally the study of D-branes has proved invaluable in understanding black holes. For our treatment, we adopt the fuzzball proposal, which we review below. For more thorough treatment of the proposal see [75–80].

Let us begin our discussion not with the information paradox but with the entropy puzzle of black holes. We return to the information paradox later. Recall that in Equation (1.27), we associate an entropy with a black hole that is proportional to its horizon area. It is a little unusual to associate an entropy with a classical solution of a fundamental theory. If we take this entropy seriously (and Hawking’s calculation certainly suggests we should), then we are immediately forced to ask: where/what are the $e^{S_{\text{BH}}}$ microstates? This is the entropy puzzle. In a typical thermodynamical system, say a gas of molecules,

the entropy is the logarithm of the number of microstates that have the same macroscopic properties which define the system's macrostate. What are the analogous statements for the black hole?

One of string theory's greatest triumphs addresses this question. One can consider forming a black hole from a collection of D-branes. When the gravitational coupling is weak, the D-branes can be described via a worldvolume gauge theory. On the other hand, when the coupling is strong, the gauge theory is strongly coupled, but there is a gravity description as a black hole. One can count the degrees of freedom at weak coupling and compare to the Bekenstein–Hawking entropy at strong coupling. In general, one would not expect a weak and strong coupling answer to agree; however, for certain supersymmetric black holes, these counts are “protected”¹² from changes in coupling. When one performs this calculation, one finds exact agreement in the limit of large macroscopic charges (see [82–84] for early calculations and [81] for a recent review). Within string theory, then, we see the appearance of $e^{S_{\text{BH}}}$ microstates; however, the counting we described leaves us with the question of how the microstates manifest themselves at strong coupling when there is a black hole. For instance, we can take a single microstate of the weakly coupled gauge theory, and ask what happens to that state as we turn up the coupling. Do these microstates of the gauge theory give rise to a phase space of solutions when the black hole is a good description?

It appears at first that there is no phase space for the black hole. We only have the black hole solution and there are various “no hair” results [85, 86] that limit the number of alternative solutions one could consider—certainly one would not be able to find $e^{S_{\text{BH}}}$ states by considering perturbations to the black hole solution. Even if one could find such perturbations, it would be difficult to interpret them: each of those “microstates” would also have a horizon, and therefore an entropy. Microstates are pure states and should not have an entropy.

One might also conclude that all of the microstates must be quantum mechanical, approaching the naive black hole metric in the classical limit. After all, dimensional analysis suggests that the microstates should be variations of the black hole geometry when the curvature becomes Planck scale near the singularity; however, as mentioned in Section 1.1.2, this dimensional reasoning does not seem to allow the information paradox to be resolved. Also, this scenario seems a bit unphysical since it requires packing a large amount of phase space into a small physical volume. In fact, one can show that if we wish to retain quantum mechanics and locality, the state at the horizon must depend, in a significant way, on the microstate that the black hole is in [22, 23].

¹²Typically, it is not directly the number of microstates that is protected but an “index.” See [81] for more on this point.

The fuzzball proposal [87, 88] states that the black hole solution is an effective coarse-grained description that results from averaging over $e^{S_{\text{BH}}}$ horizon-free nonsingular microstates that have nontrivial structure differing from the “naive” black hole solution up to (at least) the horizon scale. If one starts considering very stringy states where causality is not well-defined, the notion of “horizon-free” becomes ill-defined, and it is currently an open problem how to precisely formulate this aspect of the fuzzball proposal for very stringy microstates. Qualitatively, however, the statement is simply that *the microstates have nontrivial structure up to the horizon* of the corresponding naive black hole solution. This fact resolves the information paradox: the radiation leaves from the surface and carries information about the state of the system. This is just the way any other thermal body radiates. From this point of view, we can define the fuzzball proposal as the statement that the state at the horizon is almost orthogonal to the vacuum [22].

For certain extremal black holes, one can explicitly construct solutions of supergravity that form a phase space of black hole microstates, which account for the entropy of the black hole (see [89–92] and the reviews [75–80]). The solutions are nonsingular, horizon-free, and differ from each other up to the horizon scale. Asymptotically they approach the black hole solution. Furthermore, there is an explicit mapping between solutions and states of the D1D5 CFT. Of course the solutions receive g_s and α' corrections, which are more or less important for different microstates. It remains an open question whether nonextremal black holes’ phase space is completely captured by a corresponding phase space of supergravity solutions; see [93] and [94] for recent, differing perspectives on this issue. Let us emphasize, however, that the fuzzball proposal does not require the microstates to be well-described by supergravity. We only need the microstates to differ from the naive black hole solution and each other up to the would-be horizon. In fact, we expect generic states of the black hole not to have a well-defined geometric description; however, there may still be certain special states that have nice classical descriptions.

Finally, let us comment on the relationship of AdS–CFT duality and more generally gravitational holography to the fuzzball proposal. One might wonder why we insist on using a gravitational description if we expect to have a (strongly coupled) field theory description. Are we not just using the wrong variables to think about the problem? We know that the field theory is unitary. Since all of the issues with black holes and gravity arise when considering the geometrical description, it is important to resolve those issues in the same language. For instance, if one is to resolve the Hawking information paradox, one must show what aspect of the argument fails. Otherwise, we are faced with the specter of giving up quantum mechanics, and therefore string theory and the AdS–CFT correspondence. That is to say, using AdS–CFT to solve the information paradox with no other explanation of what breaks in Hawking’s calculation *begs the question*. More generally, we need an answer to when and why general relativity breaks down. Since one can make

the curvature arbitrarily weak at the horizon of the naive black hole by considering very massive black holes (see Equation (1.2)) and locally there does not seem to be anything interesting happening at the horizon; it is difficult to introduce new physics at the horizon without contradicting existing experimental evidence that supports general relativity. See [22, 95] for more on this point, and its connection to the fuzzball proposal.

1.5 Outline

This dissertation focuses on using the CFT description of the D1D5 system to understand black holes and the fuzzball proposal. Some of the calculations, however, have more general applications. In particular, we show how to relax the decoupling limit and allow some excitations to leak out of the near-horizon AdS/CFT. This is the content of Chapter 3. In Chapter 4, we compute emission out of particular nonextremal microstate geometries. One of the important results that we learn along the way is that many different physical processes in the gravity description are related to the same CFT process. This proves a computational boon for the immediate goal of finding the emission. The results of these two chapters demonstrate some interesting aspects of the AdS–CFT correspondence that have not been extensively studied. In Chapter 5 we compute the effect of a marginal deformation operator in the D1D5 CFT. This operator is believed to be important for understanding the dynamical physics of black holes: thermalization, formation, and in-falling observer. While we do not find concrete answers to these questions, we do see hints. In particular, we find that states with a few high-energy excitations have an amplitude to “fragment” into many low-energy excitations.

We now outline the remaining chapters of this dissertation in detail.

In Chapter 2, we describe the D1D5 system in detail. It leads to an $\text{AdS}_3\text{--CFT}_2$ correspondence, and we describe both the gravitational theory and the conformal field theory. Of particular importance is the 20-dimensional moduli space, and the orbifold point where the CFT is particularly simple. The rest of the calculations presented in this dissertation are in the orbifold CFT.

In Chapter 3, we describe how to set up a scattering problem using AdS–CFT from asymptotic flat space *outside* of the AdS space. This is different from most AdS–CFT calculations that do not discuss any asymptotically flat space outside of the AdS. Here, we are perturbatively relaxing the decoupling limit.

In Chapter 4, we discuss emission from a particular class of geometries. We introduce the geometries and argue that as per the fuzzball proposal they should be considered classical approximations to microstates of the corresponding black hole. The geometries are unstable and decay in a calculable way. We reproduce the gravity spectrum for the emission using the methods in Chapter 3 and a detailed CFT calculation. We explain the

significance of the calculation for understanding black holes within the fuzzball proposal.

In Chapter 5, we introduce a marginal deformation operator to the orbifold CFT at first order in perturbation theory. We introduce a number of tools to calculate the effect of the operator. In particular we find the effect of the operator on the vacuum is to produce a squeezed state, and that excitations may be moved across the operator with Bogolyubov-like coefficients.

Finally, in Chapter 6, we present some concluding remarks. We discuss opportunities for future work and our hopes for greater understanding of black holes through continued study of the D1D5 system.

Chapter 2

THE D1D5 SYSTEM

| | 0 | 1 | 2 | 3 | 4 | 5 | 6 | 7 | 8 | 9 |
|----|---|---|---|---|---|---|---|---|---|---|
| D5 | – | • | • | • | • | – | – | – | – | – |
| D1 | – | • | • | • | • | – | • | • | • | • |

Table 2.1: Diagram showing the D1D5 brane configuration. The \bullet 's indicate that the object is “pointlike” in the corresponding direction and the $-$'s indicate that the object is extended in the corresponding direction. The ‘0’ direction is time; the ‘5’ direction is the S^1 ; the ‘1’–‘4’ directions are the noncompact spatial part of $M^{4,1}$; and the ‘6’–‘9’ directions are the string scale T^4 .

In this chapter we discuss the “D1D5 system” in generality, quoting relevant results from the literature and providing the reader with some necessary background. The basic setup is IIB string theory compactified on $T^4 \times S^1$ with a bound state of D5-branes wrapping the whole compact space and D1-branes wrapping the circle, S^1 .¹³ The configuration is summarized in Table 2.1. The S^1 direction is distinguished from the T^4 because we want to consider the S^1 to be much larger than the T^4 .

Just as for the D3-brane system, there are two dual descriptions of the D1D5 system. Depending on the coupling, one can consider either an open string (field theory) description of the brane configuration or a closed string (gravitational) description. In this dissertation, we focus primarily on the field theory description. One can think about the field theory in several different ways. Most fundamentally, perhaps, one can think about the effective theory that arises from the zero modes of the open strings and its flow into the

¹³More generally, we should consider compactifications on compact hyperkähler four-dimensional manifolds, M^4 , crossed with a large S^1 . There are two compact hyperkähler four-dimensional manifolds: T^4 and $K3$. For this dissertation, we restrict our attention to T^4 .

IR [66, 96]; however, it turns out that the the description one arrives at by considering open strings has a limited regime of validity. Alternatively, one can consider starting with the D5-brane worldvolume gauge theory in which the D1-branes are realized as strings of instantons [97, 98]. In the IR, one need only describe the behavior of the instantons. Finally, there is a specific proposed CFT, the symmetric product CFT that is believed to describe the IR of a specific point in moduli space [66, 98–107]. Much of this chapter’s material can be found in the review [96].

2.1 IIB on a Torus

As mentioned, we are interested in compactifying string theory on a small T^4 down to a six-dimensional theory. In the six-dimensional theory, the D1 and D5 branes appear as strings wrapping the large S^1 . Before thinking about the D1D5 system specifically, let us first turn our attention to IIB string theory on $T^4 \times S^1$.

2.1.1 IIB on T^5

For the moment, let us follow [103] and consider the circle S^1 as part of a five-torus, T^5 . We then consider how the physics compactified on the T^4 is embedded in the T^5 physics. This approach proves useful in organizing the content of the theories.

The massless, bosonic field content of IIB string theory is summarized in Table 1.1. When we compactify on T^5 we get a set of $U(1)$ gauge fields, A_μ in the resulting five-dimensional theory. For this section, we use lower-case Greek indices for the noncompact five-dimensional Minkowski space, $M^{4,1}$ and capital Latin indices for the compact T^5 . We get a $U(1)$ gauge field by considering any of the fields with only one index in the noncompact space:

$$g_{\mu A} (5) \quad B_{\mu A} (5) \quad C_{\mu A}^{(2)} (5) \quad C_{\mu ABC}^{(4)} (10), \quad (2.1)$$

which gives us 25 $U(1)$ gauge fields (the number of degrees of freedom for each field is shown in parentheses). There are two more that we missed. If one takes the Hodge star of the exterior derivative of one of the two-forms, $B_{\mu\nu}^{NS}$ or $C_{\mu\nu}^{(2)}$, then one gets a two-index field strength. These correspond to two “magnetic” $U(1)$ gauge fields. Thus, we have a total of 27 $U(1)$ gauge fields. They couple to 27 different charges: 5 Kaluza–Klein (KK) momenta, 5 F1 winding modes, 1 NS5 brane wrapping T^5 , 5 D1 winding modes, 10 D3 modes, and 1 D5 brane wrapping T^5 . They source, respectively, the metric, the NS B-field, the magnetic NS B-field, the RR 2-form, the RR 4-form, and the magnetic RR 2-form gauge fields.

| $SO(5, 1)_E$ rep | $SO(5, 5)$ rep | charges | gauge field | mass |
|------------------|----------------------|--|--|--------------|
| tensor | vector (10) | $\{n_5, d_5, f_1, d_1, D^{5ij}\}$ | $\{B_{\mu 5}^M, C_{\mu 5}^M, B_{\mu 5}, C_{\mu 5}, C_{5ij\mu}\}$ | $1/\ell_s^2$ |
| vector | spinor (16) | $\{\vec{w}_{F1}, \vec{w}_{D1}, D_{ijk}, \vec{p}\}$ | $\{B_{\mu i}, C_{\mu i}, C_{\mu ijk}, g_{\mu i}\}$ | $1/\ell_s$ |
| scalar | scalar (1) | p_5 | $g_{\mu 5}$ | ℓ_s^0 |

Table 2.2: Type IIB string theory compactified on T^5 has 27 U(1) charges in the fundamental representation of the $E_{6(6)}$ duality group. This **27** transforms as a **10**, **16**, and **1** of the $SO(5, 5)$ subgroup that is preserved when we take the near-horizon limit. The 27 gauge fields and their corresponding sources are shown in the above table along with their transformation properties. The M superscript indicates magnetic coupling. The mass column shows the scaling as we take ℓ_s small, which corresponds to the near-horizon limit.

How many scalars do we get? We get 42 scalars from

$$g_{AB} (15) \quad B_{AB} (10) \quad \phi (1) \quad C_{ABCD} (5) \quad C_{AB} (10) \quad C^{(0)} (1), \quad (2.2)$$

where we have suppressed the differential form superscript on the Ramond–Ramond fields. The 42 scalars parameterize the 42-dimensional moduli space of the 5-dimensional theory compactified on T^5 . The moduli space has the local geometry of the 42-dimensional coset manifold [44, 51, 103, 108]

$$\frac{E_{6(6)}}{Sp(4)}, \quad (2.3)$$

where $E_{6(6)}$ is a noncompact version of E_6 with 6 “sign flips.” It has the same *complexified* Lie algebra as E_6 , and is 78-dimensional. The symplectic group $Sp(4)$ is 36-dimensional, so the coset space is 42-dimensional as advertised. This is not a global description of moduli space since we must mod out by a discrete duality group to avoid redundant descriptions.

Type IIB supergravity has a continuous $E_{6(6)}$ symmetry which gets broken to a discrete $E_{6(6)}(\mathbb{Z})$ U-duality group in full string theory [44, 51, 103, 108]. The U-duality group is generated by S and T -duality transformations that mix the 27 charges. For instance, S -duality exchanges F1 and D1 winding charges, NS5 and D5 charges. D3-branes are self-dual, and KK-momenta are invariant under S -duality. The 27 charges transform as a fundamental vector of $E_{6(6)}(\mathbb{Z})$.

2.1.2 Relationship with IIB on T^4

We have described the structure of the 5-dimensional theory that results from compactifying IIB string theory on T^5 . What happens when we take one of the S^1 ’s to be large and consider the 6-dimensional theory? We keep the T^4 at the string scale. The $E_{6(6)}$ structure gets broken to $SO(5, 5)$, and the **27** of $E_{6(6)}$ gets broken into a **10** (vector), a **16** (spinor), and a **1** (singlet) of $SO(5, 5)$. Each representation has a different mass scaling with ℓ_s [103].

The way the different charges break up is summarized in Table 2.2. The U-duality group $E_{6(6)}(\mathbb{Z})$ gets broken to a subgroup $SO(5, 5; \mathbb{Z}) \leq E_{6(6)}(\mathbb{Z})$.

The moduli space of the 6-dimensional theory is 25-dimensional, and locally is [44, 51, 102, 103, 108]

$$\frac{SO(5, 5)}{SO(5) \times SO(5)}. \quad (2.4)$$

The moduli space is parameterized by (we now use lower-case Latin for indices in the T^4 and ‘5’ for the large S^1) the 25 fields:

$$g_{ij}(10) \quad B_{ij}(6) \quad \phi(1) \quad C_{ijkl}(1) \quad C_{ij}(6) \quad C^{(0)}(1). \quad (2.5)$$

Having given some generalities, let us now more precisely specify the D1D5 system. Of the heavy $SO(5, 5)$ vector charges we want only to have d_1 and d_5 charges, so $n_5 = f_1 = D^{5ij} = 0$. Similarly, we want the spinor to vanish. Note that we want D1 winding charge only on the S^1 , d_1 , and not winding charge on the T^4 , \vec{w}_{D1} . At times, we do want to consider some p_5 charge. This is sometimes referred to as the D1D5P system. Thus we restrict our attention to a three-dimensional subspace of the 27 possible charges. As explained in [103], one can use U-duality to rotate d_1 and d_5 into each other, preserving the product $d_1 d_5$.

2.2 Supergravity Description

We now turn to the closed string description of the D1D5 system. As the gravity description, is not our primary interest in this paper, so our treatment is appropriately brief. See [51, 96] for more thorough treatments.

2.2.1 The Two-charge Extremal Black Hole

There is a black hole solution that is asymptotically

$$M^{4,1} \times S^1 \times T^4, \quad (2.6)$$

and has only D1 and D5 charge. The geometry can be found by using the “harmonic superposition rule” [109] and T -duality¹⁴ to get to the appropriate duality frame (see [96],

¹⁴[110] may come in handy.

e.g.). The solution can be written down in the form [51]¹⁵

$$\begin{aligned} \left(\frac{H_1}{H_5}\right)^{\frac{1}{4}} ds_E^2 &= \frac{1}{\sqrt{H_1 H_5}} (-dt^2 + dy^2) + \sqrt{H_1 H_5} (dr^2 + r^2 d\Omega_3^2) + \sqrt{V_{T^4}} \sqrt{\frac{H_1}{H_5}} ds_{T^4}^2 \\ e^\phi &= g_s^\infty \sqrt{\frac{H_1}{H_5}} \\ F^{(3)} &= dC^{(2)} \quad F_{rty}^{(3)} = \partial_r H_1^{-1} \quad F_{\theta\phi\chi}^{(3)} = 2Q_5 \sin^2 \theta \sin \phi, \end{aligned} \quad (2.7)$$

where

$$H_1 = 1 + \frac{Q_1}{r^2} \quad H_5 = 1 + \frac{Q_5}{r^2}, \quad (2.8)$$

and r is the radius in the noncompact space; θ , ϕ and χ are the angular coordinates of Ω_3 ; and g_s^∞ is the string coupling at infinity. We coordinatize the S^1 with y and the $ds_{T^4}^2$ is the metric on T^4 with unit volume. The solution is more precisely termed a black ring, since the S^1 direction is large. This is the extremal 2-charge black ring solution. The horizon coincides with the singularity at $r = 0$. We find it convenient to write the volume of the T^4 at infinity as

$$V_{T^4} = (2\pi\ell_s)^4 v_\infty, \quad (2.9)$$

where $\ell_s^2 = \alpha'$. The charges Q_1 and Q_5 are related to the integer-valued charges d_1 and d_5 via

$$Q_1 = \frac{g_s^\infty \ell_s^2}{v_\infty} d_1 \quad Q_5 = g_s^\infty \ell_s^2 d_5. \quad (2.10)$$

The solution preserves one-fourth of the supersymmetry of IIB string theory, as expected for a two-charge solution.

This is the “naive” black hole solution, which we discuss in Chapters 1 and 3. The fuzzball proposal suggests that this solution results from some form of coarse-graining over nonsingular, horizonless microstates. For the 2-charge extremal black ring, all of these solutions have been found [89, 90, 111, 112]. They are exact solutions of supergravity that are smooth, horizonless and asymptotically look the same as the naive solution—they have the same charge and mass. Geometric quantization of the space of solutions [113] reproduces the entropy of the black hole as computed, for instance from the brane description [114, 115].¹⁶

Let us investigate the asymptotic behavior of the solution. For very large r , H_1 and H_5 become unity and the solution is flat 5-dimensional Minkowski with an S^1 and a T^4 as advertised. The RR 2-form flux is appropriate for the D1 and D5 charges. The string coupling is g_s^∞ .

¹⁵The metric is written in the Einstein frame.

¹⁶We would be remiss if we did not note that [116] gives a discussion of potential problems with the interpretation of these results within the fuzzball proposal.

We can also consider the small r limit when we drop the ‘1’ in H_1 and H_5 . Then, the solution takes the form

$$ds_S^2 = \left(\frac{Q_1}{Q_5}\right)^{\frac{1}{4}} ds_E^2 = \frac{r^2}{\sqrt{Q_1 Q_5}} (-dt^2 + dy^2) + \sqrt{Q_1 Q_5} \frac{dr^2}{r^2} + \sqrt{Q_1 Q_5} d\Omega_3^2 + \sqrt{V_{T^4} \frac{Q_1}{Q_5}} ds_{T^4}^2$$

$$e^\phi = g_s^\infty \sqrt{\frac{Q_1}{Q_5}}.$$
(2.11)

We see that both the T^4 volume and the string coupling get scaled by Q_1/Q_5 ; the S^3 gets a fixed size; and the r , t and y coordinates form an AdS_3 space. Both the AdS_3 and the S^3 have radius $(Q_1 Q_5)^{\frac{1}{4}}$. These facts are for the string frame metric. One can study the Einstein metric and see that the event horizon at $r = 0$ has vanishing surface gravity and area. The vanishing surface gravity means that the black hole has zero temperature and therefore does not Hawking radiate—this is expected for an extremal hole. The geometry receives α' higher derivative corrections, which give the geometry (in other duality frames, at least) a nonzero area and therefore entropy [81, 83, 84, 117, 118]. The (r, t, y) part of the metric in (2.11) is an extremal BTZ black hole [119, 120], so we can think of the near-horizon geometry as $\text{BTZ} \times S^3 \times T^4$.

In order for classical supergravity to be a good description we need the curvature to be small (radius of the AdS_3 to be large) with respect to the string scale. We also need the string coupling to be small so that we do not need to consider loops. These requirements translate into a large-charge limit [66, 96]

$$d_1, d_5 \gg \frac{1}{g_s} \gg 1. \quad (2.12)$$

In the large-charge limit the entropy can be computed using a CFT description and agreement is found [82–84].

2.2.2 Generalizations

One can similarly construct a 3-charge D1D5P extremal black hole solution and look for corresponding microstate geometries [91, 92, 121–123]. The extremal black holes are where the fuzzball proposal is best tested; however, extremal black holes are peculiar. They have an infinitely long AdS throat that can nevertheless be traversed in a finite proper time by massless particles and they saturate a BPS bound. They have the minimum amount of mass for the amount of charge they have, so they do not Hawking radiate. It is interesting, therefore, to consider the fuzzball proposal for nonextremal black holes. This is the subject of Chapter 4.

The solution in Equation (2.7) and its 3-charge extremal generalization have none of the 25 moduli listed in Equation (2.5) turned on. This point in moduli space is “marginally

bound” [51, 96, 102, 103, 124], which means that the D1 and D5 branes can separate with no additional energy. One can also construct solutions that are not marginally bound by adding, for example, NS B-field on the torus [125, 126]. In fact, one can show that the branes may split apart with no additional energy if and only if both the appropriate linear combination of the RR scalar $C^{(0)}$ and the RR 4-form $C_{6789}^{(4)}$, as well as the NS B-field vanish [99, 103].

For reviews of progress in the fuzzball proposal, we refer the reader to [75–80]. For a review of accounting for the entropy of black holes by performing weak coupling microscopic counting, see [81].

2.2.3 The Near-Horizon Limit

In order for us to make use of the AdS–CFT correspondence, we must take a near-horizon limit that decouples the asymptotic flat physics from the AdS physics [45, 66]. This decoupling limit corresponds to going to the IR fixed point of the D-brane description, and is in effect a low-energy limit. As demonstrated above, in this limit, the supergravity description becomes $\text{AdS}_3 \times S^3 \times T^4$. One might expect that by appropriately tuning the 25 moduli in Equation (2.5) at asymptotic infinity one could attain any value of the moduli in the AdS-space. If this were the case, the near-horizon geometry would have a 25-dimensional moduli space. In fact, this is *not* the case: The 25-dimensional moduli space at infinity gets “attracted” to a certain submanifold in the near-horizon limit that depends only on the charges [127–130]. The attractor mechanism results from the extremality of the system and does not require supersymmetry [128, 131–133].

For the D1D5 system, the 25-dimensional moduli space (at infinity) is attracted to a 20-dimensional subspace in the near-horizon limit—five of the scalars get “fixed,” and excitations around the preferred value acquire a mass. One can find the near-horizon moduli space by minimizing the mass of the bound state¹⁷ with respect to the moduli [130], in which case one finds the constraints [103]:

$$v B_{ij} g^{ik} g^{jl} = \frac{1}{2} B_{ij} \epsilon^{ijkl} \quad (2.13a)$$

$$v C^{(0)} = C_{6789}^{(4)} - \frac{1}{8} \epsilon^{ijkl} B_{ij} C_{kl}^{(2)} \quad (2.13b)$$

$$v + \frac{1}{8} \epsilon^{ijkl} B_{ij} B_{kl} = \frac{d_1}{d_5}, \quad (2.13c)$$

where v is the near-horizon analog of v_∞ in Equation (2.9). It is worth emphasizing that the moduli in Equation (2.13) are the *near-horizon* moduli. If we set all of the moduli to zero, then we find

$$v = \frac{d_1}{d_5} = v_\infty \frac{Q_1}{Q_5} \quad (2.14)$$

¹⁷More generally the critical points of the central charge.

after using Equation (2.10). This is consistent with the solution in Equation (2.7).

Equation (2.13a) gives a self-duality constraint on the NS B-field; Equation (2.13b) fixes a linear combination of the RR scalar and the RR 4-form; Equation (2.13c) fixes the volume of the T^4 , v , at the horizon. Note that the metric in Equations (2.13) is the string metric, and that we treat the volume of the T^4 as a separate modulus, v . Then, we see that Equation (2.13a) forces the NS B-field to be self-dual (under the Hodge star). The 3 component anti-self-dual part gets set to zero, and perturbations about that point are massive.

We would like to find a basis for the 20-dimensional near-horizon moduli space that solves the constraints (2.13). The basis that we find convenient to use is listed in Table 2.3. The scalar Ξ is the linear combination of $C^{(0)}$ and $C_{6789}^{(4)}$ that remains massless (ie. is tangent to the constraint surface defined by (2.13b)). The rightmost column counts the degrees of freedom, which one sees sum to 20 as claimed. As mentioned, the near-horizon geometry is $AdS_3 \times S^3 \times T^4$. It is helpful to identify the fields in terms of their representation under the $SO(4)_E$ isometry of the S^3 and also the $SO(4)_I$ symmetry of the T^4 tangent space. The $SO(4)_I$ symmetry is broken by the compactification, but it is still useful as an organizing principle [96, 104]. The two $SO(4)$ algebras are more naturally thought of in terms of $SU(2) \times SU(2)$ for later connection with the CFT description.

| Field | $SO(4)_E \simeq SU(2)_L \times SU(2)_R$ | $SO(4)_I \simeq SU(2)_1 \times SU(2)_2$ | DOF |
|---|---|---|-----|
| $g_{ij} - \frac{1}{4}\delta_{ij}g_{kk}$ | (1, 1) | (3, 3) | 9 |
| B_{ij}^+ | (1, 1) | (3, 1) | 3 |
| $C_{ij}^{(2)}$ | (1, 1) | $(3, 1) \oplus (1, 3)$ | 6 |
| Ξ | (1, 1) | (1, 1) | 1 |
| ϕ | (1, 1) | (1, 1) | 1 |
| | | | 20 |

Table 2.3: Table of the gravitational near-horizon moduli. These fields do not have any preferred value at the horizon. 5 of the 25 moduli at infinity get “fixed” in the near-horizon limit—these are the 20 remaining near-horizon moduli. Note that they are all singlets of the $SO(4)_E$ isometry of S^3 .

Having lost 5 of the 25 fields that parameterize the moduli space at infinity, it is natural to ask what happens to $SO(5, 5)/SO(5) \times SO(5)$ local geometry of moduli space. The 20-dimensional near-horizon moduli space is locally the coset space [102, 103]

$$\mathcal{K}_{\text{sugra}}^* = \frac{SO(5, 4)}{SO(5) \times SO(4)} \subset \frac{SO(5, 5)}{SO(5) \times SO(5)}, \quad (2.15)$$

where again we must mod out by a discrete duality group that preserve the background charges, $\Gamma_{\vec{q}} \leq SO(5, 5; \mathbb{Z})$. One can easily check that $\mathcal{K}_{\text{sugra}}^*$ is 20-dimensional, as claimed. We call the full moduli space

$$\mathcal{M}_{\text{sugra}, q}^* = \Gamma_{\vec{q}} \backslash \mathcal{K}_{\text{sugra}}^* \quad (2.16)$$

for later use.

2.3 The Brane Description

Classical supergravity, as discussed above, is a good description of the D1D5 system in the large-charge limit (with large $g_s d_1$ and $g_s d_5$) in Equation (2.12). From the D-brane tension (1.49) and the DBI action (1.50), we see that $\sqrt{g_s}$ plays the role of field theory coupling for the brane description. This is consistent with the interpretation of $\sqrt{g_s}$ as the open string coupling constant. In the large-charge limit, then we want to keep the 't Hooft couplings small. Thus the brane description should be weakly coupled when

$$1 \ll d_1, d_5 \ll \frac{1}{g_s}. \quad (2.17)$$

We wish to find a description in this limit, which should be dual to the above supergravity description.

As before, we wish to emphasize that AdS–CFT arises from open–closed string duality. The supergravity description arises from the low-energy behavior of the closed string modes. We now wish to find the CFT description that arises from the low-energy behavior of the open string modes. In fact, the behavior of the open string modes should first give rise to a nonconformal field theory. We then RG flow to the IR fixed point CFT. This should (loosely) correspond to taking the near-horizon limit of the gravity description. Just as there is a 20-dimensional near-horizon moduli space for the gravity description, there is a 20-dimensional moduli space of CFTs. At the orbifold point, for instance, one can explicitly identify 20 exactly marginal perturbations that move one in 20 different directions in CFT space, and further relate them to the 20 supergravity moduli in Table 2.3. In fact, one can do more—one can even find 5 irrelevant perturbations that correspond to the 5 directions in moduli space that got fixed in the near-horizon limit. This helps make the connection between RG flow and the near-horizon limit more precise. For more on these points see [134].

Following [96], we give two descriptions of the open string modes. First, we explicitly consider the gauge theory that results from considering open strings that begin and end on either the D1 or the D5 branes. This model makes a lot of comments about the D1D5 system and its moduli space more explicit (see e.g. [96, 100, 135, 136]). We then recognize that we can use a “branes within branes” description [97, 98], where the D1s are realized as

instanton configurations within the D5-brane worldvolume gauge theory. This description has a larger regime of validity, and more directly connects with the orbifold model of the D1D5 CFT.

2.3.1 Gauge Theory Description

The effective field theory description of D-branes results from the open string zero modes. Working within perturbative string theory, the D-branes define boundary conditions for the open strings. There are three types of strings we may consider: 5–5 strings with both endpoints on D5 branes; 1–1 strings with both endpoints on D1 branes; and 1–5 and 5–1 strings with one endpoint on a D1 and one endpoint on a D5.

The 5–5 Strings

Let us first consider the 5–5 strings. If we just had a stack of $d_5 = N_5$ D5-branes, then the open string modes give rise to a 5+1-dimensional $U(N_5)$ gauge theory with 16 supercharges. This is precisely what the 5–5 open strings give. Let us recall the heuristic picture of how the bosonic degrees of freedom arise. The open strings with polarization parallel to the branes have Neumann boundary conditions and give rise to a $U(N_5)$ gauge field. The open strings with polarization perpendicular to the branes have Dirichlet boundary conditions and give adjoint scalars of the 5+1-dimensional theory. The adjoint scalars describe the transverse oscillations of the D-branes. When the scalars acquire a vev it corresponds to some of the D-branes separating in the corresponding direction. If the branes separate in some direction then the $U(N_5)$ gauge group is broken. When all of the D-branes are coincident, the gauge theory is said to be in the Higgs phase, and when some of the D-branes have separated the gauge theory is said to be in the Coulomb phase.

The gauge theory should have 16 supercharges, since a stack of D-branes breaks half of the 32 supercharges of IIB string theory. In 5+1-dimensions, the 16 supercharges break into $\mathcal{N} = 2$ Weyl spinors. One can find the Lagrangian for the 5–5 open string modes by dimensionally reducing $\mathcal{N} = 1$ 9+1-dimensional $U(N_5)$ super–Yang–Mills theory to 5+1 dimensions. One can see this from T-duality of a space-filling D9-brane, for instance. The coupling constant for the worldvolume gauge theory of a Dp-brane can be identified as [51]

$$(g_{\text{YM},p})^2 = g_s (2\pi)^{p-2} \alpha'^{\frac{p-3}{2}} \longrightarrow g_{\text{YM},5} = g_s (2\pi)^3 \ell_s. \quad (2.18)$$

Recall that we are taking the size of T^4 to be on the string scale. Therefore, we should dimensionally reduce the 5+1 dimensional theory down to 1+1 dimensions parameterized by time and the S^1 coordinates, t and y . The KK momentum modes should be dropped, since they are very massive, and we are interested in the low-energy theory. The coupling in the 1+1-dimensional theory gets a factor of v from the dimensional reduction.

The literature (e.g. [51, 66, 96, 135, 136]) frequently organizes the field content of the theory according to a four-dimensional $\mathcal{N} = 2$ classification. In four-dimensions, $\mathcal{N} = 2$ corresponds to 8 supercharges (either two four-component Majorana spinors or two (complex) two-component Weyl spinors). There are two massless supersymmetry representations that are relevant to us: a vector multiplet and a hypermultiplet. The vector multiplet (on-shell) consists of a vector field, two spin-half Weyl fermions, and a complex scalar. The off-shell multiplet has three additional auxiliary real scalars (usually called D). The hypermultiplet consists of two complex scalars, two Weyl spinors, and two complex auxiliary scalars (usually called F). The $\mathcal{N} = 2$ four-dimensional supersymmetry has an $SU(2)_R$ symmetry. In the vector multiplet, the vector field and complex scalars are singlets, the Weyl spinors transform as two doublets, and the three auxiliary D -fields transform as a triplet. In the hypermultiplet, the fermions transform as singlets, the two complex scalars transform as a doublet, as do the two complex F -fields. See e.g. [137, 138].

We can organize the bosonic field content that comes from the 5–5 strings as follows [96, 136]:

$$\begin{aligned} \text{vector:} & \quad A_t^{(5)}, A_y^{(5)}, \vec{\Phi}^{(5)} \\ \text{hyper:} & \quad \Phi_i^{(5)} \end{aligned} \tag{2.19}$$

where the vector symbol is used to denote a vector in the four-dimensional spatial part of $M^{4,1}$. The Φ 's are the scalars resulting from open strings polarized perpendicular to the t – y space, and the A 's are the two-components of the gauge field. All of the above are adjoints of the $U(N_5)$ gauge group. Note that we must take two degrees of freedom from $\vec{\Phi}$ along with the two gauge field components to form a *four*-dimensional vector of the vector multiplet—the remaining two components of $\vec{\Phi}$ are the two scalars.

The 1–1 Strings

The 1–1 strings in actuality differ very little from the 5–5 strings. If we have $d_1 = N_1$ D1 strings, then the opens strings must give rise to a $U(N_1)$ gauge theory in 1+1 dimensions that has 16 supercharges. The interpretation of the open string modes parallel and perpendicular to the branes is the same as above, of course. One can derive the Lagrangian by dimensionally reducing $\mathcal{N} = 1$ 9+1-dimensional $U(N_1)$ super–Yang–Mills down to 1+1 dimensions. Notice that is precisely what we ended up doing for the 5–5 open string modes, replacing N_1 with N_5 . The $U(N_1)$ Yang–Mills coupling is

$$g_{\text{YM},1} = \frac{g_s}{2\pi\ell_s^2}. \tag{2.20}$$

We organize the 1–1 field content analogously to Equation (2.19),

$$\begin{aligned} \text{vector:} & \quad A_t^{(1)}, A_y^{(1)}, \vec{\Phi}^{(1)} \\ \text{hyper:} & \quad \Phi_i^{(1)} \end{aligned} \quad (2.21)$$

The fields are labeled in the same fashion as for the 5–5 strings, and they all take values in the adjoint of $U(N_1)$.

The 5–1 and 1–5 Strings

The 5–1 and 1–5 strings are the most important for many of our purposes. Note that both the 1–1 and the 5–5 theories have 16 supercharges ($\mathcal{N} = 4$ in 3+1), but we expect that the bound state should have 8 supercharges. The 5–1 and 1–5 strings break the supersymmetry down to 8 supercharges.

Let us first consider 5–1 strings. These strings are bifundamental, fundamental under $U(N_5)$ and antifundamental under $U(N_1)$. The behavior of the string depends on the polarization. In particular, the NN and DD directions behave differently from the ND or DN directions.¹⁸ For 5–1 strings, the NN directions are time and the S^1 while the DD directions are the noncompact space. The ND directions are the T^4 , and there are no DN directions. There are two sectors for the open string, NS and R. In the NS sector, the ground states consist of four zero modes ψ_0^i in the DN direction (the T^4)—GSO projection cuts that down to two bosonic degrees of freedom. The excitations polarized in the NN and DD directions are massive in the NS sector. In the R sector, only the excitations in the NN and DD are massless, and give rise to two on-shell fermionic degrees of freedom after GSO projection [51, 96, 136].

The 1–5 strings work out very similarly: we get two bosonic degrees of freedom from the NS sector and two fermionic degrees of freedom from the R sector. All of the bosonic degrees of freedom are polarized in the T^4 directions, while the fermionic degrees of freedom are polarized in the time, S^1 , and noncompact directions. Combining the 5–1 string massless excitations with the 1–5 massless excitations to form a bifundamental hypermultiplet. As above, we focus on the bosonic content [51, 96, 136]:

$$\text{hyper:} \quad \chi^A, \quad (2.22)$$

a spinor of $SU(2)_1$, where recall $SO(4)_I = SU(2)_1 \times SU(2)_2$. We also have its complex conjugate, χ^\dagger .

¹⁸N and D refer to Neumann and Dirichlet boundary conditions on the end points. Since the string has an orientation ND is distinct from DN. Note that for 1–1 or 5–5 strings we can only have NN or DD boundary conditions.

The Potential and Moduli Space

For this section, let us call the bosonic part of the vector multiplets $Y_a^{(1)}$ and $Y_a^{(5)}$, with a running over the noncompact \mathbb{R}^4 as well as the t and y coordinates. The Lagrangian for the theory we have outlined can be deduced by dimensionally reducing $d = 6$ $\mathcal{N} = 1$ field theory with $U(N_1)$ and $U(N_5)$ gauge groups. Of primary importance for our discussion here, is the potential on the bosonic field content.

We quote the result from [96]; the potential may be written as the sum of four terms:

$$V_1 = -\frac{1}{4g_1^2} \sum_{a,b} \text{Tr}_1[Y_a^{(1)}, Y_b^{(1)}]^2 - \frac{1}{4g_5^2} \sum_{a,b} \text{Tr}_5[Y_a^{(5)}, Y_b^{(5)}]^2 \quad (2.23a)$$

$$V_2 = -\frac{1}{4g_1^2} \sum_{i,a} \text{Tr}_1[\Phi_i^{(1)}, Y_a^{(1)}]^2 - \frac{1}{g_5^2} \sum_{i,a} \text{Tr}_5[\Phi_i^{(5)}, Y_a^{(5)}]^2 \quad (2.23b)$$

$$V_3 = \frac{1}{4} \sum_a \text{Tr}_1(\chi Y_a^{(5)} - Y_a^{(1)} \chi)(Y_a^{(5)} \chi^\dagger - \chi^\dagger Y_a^{(1)}) \quad (2.23c)$$

$$V_4 = \frac{1}{4} \text{Tr}_1 \left(\chi i\Gamma_{ij}^T \chi^\dagger + i[\Phi_i^{(1)}, \Phi_j^{(1)}]^+ - \frac{\zeta_{ij}^+}{N_1} \right)^2 + \frac{1}{4} \text{Tr}_5 \left(\chi^\dagger i\Gamma_{ij} \chi + i[\Phi_i^{(5)}, \Phi_j^{(5)}] - \frac{\zeta_{ij}^+}{N_5} \right)^2, \quad (2.23d)$$

where the ‘+’ superscript indicates the self-dual part of an antisymmetric matrix. We use i, j as indices in the compact T^4 and a, b as indices in the noncompact space parameterized by \vec{x} . The ζ_{ij} are Fayet–Iliopoulos (FI) parameters, and the $\Gamma_{ij} = \frac{1}{2}[\Gamma_i, \Gamma_j]$ are the spinor rotation matrices of $SO(4)_I$. Note that the above expressions may use slightly different conventions than the above and following discussion, but this does not affect any of our conclusions.

Since we want to discuss the IR limit, we are interested in supersymmetric minima satisfying $V = V_1 + V_2 + V_3 + V_4 = 0$. The space of solutions to $V = 0$ are the moduli space of the theory—different possible vev’s that the fields can have. Note that we are discussing a two-dimensional theory, and one usually expects IR fluctuations to restore any continuous symmetry breaking (see e.g. [139]), and therefore we should not be speaking of fields acquiring vevs; however, we use this language with the understanding that we end up with the correct description with the space of solutions to $V = 0$ becomes the *target space* of a two-dimensional sigma model [140].

The Higgs and Coulomb Phase

There are two classes of minima to the potential in Equation (2.23): those where hypermultiplets are zero and those where the vector multiplets are zero. The first is called the

Coulomb branch and the second is called the Higgs branch. When the Y_a acquire a nonzero vev that corresponds to some of the branes separating in the noncompact space and breaking the gauge group down. In the most extreme case we only have $U(1)$ gauge theories when all of the branes are widely separated, hence the name Coulomb branch. When the Y_a are zero, in the Higgs branch, the branes all sit at the origin of the noncompact space, but the hypermultiplets may have a nonzero vev. We are interested in describing the physics of the Higgs branch when we truly have a bound state. When all of fields vanish, we are at the “intersection” of the Higgs and Coulomb branches.

On the Higgs branch, then, $V_1 = V_2 = V_3 = 0$ by definition. Thus, we are only left with the condition that V_4 vanish (which can be interpreted as two D -flatness conditions). The Higgs branch is parameterized by $\Phi_i^{(1)}, \Phi_i^{(5)}$, and the hypermultiplet χ . What role is played by the FI parameters, ζ ? One can show that they are proportional to the amount of NS B-field turned on in the supergravity description [96, 135]. Thus one can see that when the NS B-field is non-vanishing we must lie on the Higgs branch in order for $V = 0$, and thus the branes cannot separate. For a more careful treatment of these issues, see [99, 102, 103].

Since V_4 is the sum of two positive definite terms, we must demand that both terms vanish individually. Let us write out the components of the doublet as

$$\chi = \begin{pmatrix} A \\ B^\dagger \end{pmatrix}. \quad (2.24)$$

If one carefully analyzes the solutions to $V_4 = 0$ modulo gauge invariance, then one finds that χ must satisfy

$$\text{Tr}_5(A^\dagger A) - \text{Tr}_1(B^\dagger B) = \zeta_{69}^+ \quad (2.25a)$$

$$\text{Tr}_5(AB^T) = \zeta_{67}^+ + i\zeta_{68}^+, \quad (2.25b)$$

the traceless parts of the Φ_i 's are completely fixed, and the traces are free. The 8 degrees of freedom associated with $\text{Tr}_1 \Phi_i^{(1)}$ and $\text{Tr}_5 \Phi_i^{(5)}$ are the center of mass degrees of freedom of the D1 branes and the D5 branes, respectively, in the T^4 . This entire analysis was performed in [135] and reviewed in [96].

The CFT Limit

We should now take the extreme IR limit, which should correspond to taking the near-horizon limit in the closed string description. Before thinking about what we get from the above gauge theory, let us ask: What are our basic expectations for the IR theory from the dual supergravity description? First, we expect the theory to be a CFT, since it is an IR fixed point and since it should be dual to anti-de Sitter space whose isometries generate a Virasoro algebra [66]. Second, since it should live on the boundary of the near-horizon

$AdS_3 \times S^3 \times T^4$, it should be a two-dimensional conformal field theory. Furthermore it should have 8 supercharges. Finally, one can work out the central charges of the CFT_2 by calculating the classical Poisson brackets of the generators of diffeomorphisms that preserve the asymptotic AdS space; under an infinitesimal transformations ξ_μ the metric transforms as $g_{\mu\nu} \mapsto g_{\mu\nu} + \xi_{\mu;\nu} + \xi_{\nu;\mu}$. In fact this analysis for AdS_3 was performed in 1986 [141], over a decade before AdS–CFT! In any case, one finds that the central charge is

$$c = \frac{3R_{AdS_3}}{2G_N^{(3)}}, \quad (2.26)$$

where $G_N^{(3)}$ is the three dimensional Newton’s constant and R_{AdS_3} is the AdS radius. If one plugs in with the solution in Equation (2.11), then one finds

$$c = 6N_1N_5 + (\text{subleading}), \quad (2.27)$$

where the subleading corrections come from an expansion in N_1N_5 —we only expect the calculation to be correct in the large charge limit when supergravity is a good description.

Now, let us follow [96, 135] and think about what the IR theory for the $U(N_5) \times U(N_1)$ gauge theory outlined above should be. Note that we already discussed how to dimensionally reduce to a two-dimensional theory, and the theory has the right number of supersymmetries. We should expect that the lowest energy excitations should correspond to moving in “flat” directions of the potential. Since we are interested in a description of the Higgs branch, these excitations correspond to moving around in the moduli space defined by $V_4 = 0$ with the vector multiplets having zero vev. Thus, we expect to describe collectively a collective mode for A and B subject to the constraint (2.25), as well as the traces $\text{Tr}_1 \Phi_i^{(1)}$ and $\text{Tr}_5 \Phi_i^{(5)}$. The bosonic part of the conformally invariant point is

$$\int dt dy \text{Tr} \left[\partial_\alpha A^\dagger \partial^\alpha A + \partial_\alpha B^\dagger \partial^\alpha B \right], \quad (2.28)$$

where the index α runs over t and y ; we also have the center of mass degrees of freedom. The A and B of χ are constrained to live on the target space defined by (2.25). The manifold defined by (2.25) is hyper-Kähler, which is required for $\mathcal{N} = (4, 4)$ supersymmetry of a two-dimensional sigma model [99]. From the above field content (along with the fermions that we have neglected slightly) the central charge is

$$c = \bar{c} = 6(N_1N_5 + 1), \quad (2.29)$$

where the extra 6, comes from the center of mass degrees of freedom in the torus: $\text{Tr}_1 \Phi_i^{(1)}$ and $\text{Tr}_5 \Phi_i^{(5)}$, and the superpartners. In this description, the gauge group $U(N_5) \times U(N_1)$ gets broken down to the discrete subgroup $S_{N_5} \times S_{N_1}$ [96, 135].

Regime of Validity

The gauge theory derivation we outlined above has many elements of the final orbifold CFT that we settle on, as we see in what follows; however, its regime of validity is limited and is believed to be less accurate than the orbifold CFT. As mentioned, the theory has the same supersymmetry as $\mathcal{N} = 2$ in four dimensions (or $\mathcal{N} = 1$ in six dimensions) so we used the same multiplet language. Recall that the bosonic content of the hypermultiplets should transform as a doublet under the $SU(2)$ R-symmetry of four-dimensional $\mathcal{N} = 2$ theory. Thus we identify $SU(2)_1$ of the torus as the R -symmetry of the four-dimensional theory; however, David, Mandal, and Wadia [96] argue that it is not consistent to have compact hypermultiplets. Therefore, we must be working in a decompactifying limit in which the hypermultiplets effectively see a noncompact space and not the small T^4 . This means, they argue, that the expectation values of the hypermultiplets must be much less than the string scale—ie., we are near the origin of the Higgs branch that connects with the Coulomb branch [96]. If one decompactifies the torus by taking $v \rightarrow \infty$, then one finds the theory discussed in [124].

Let us emphasize the key points that we learn from the above description before we abandon it. The first point is that D1D5 system has a rich moduli space that we can explore quite explicitly via Equation (2.23). In particular it has two branches: a Coulomb branch where the branes can separate and a Higgs branch where the branes are bound. Recall that the supergravity description with no RR fields or NS B-field turned on is marginally bound and can fragment with no additional energy cost. The correct description of the intersection of the Coulomb and Higgs branches was investigated in [102, 142]. In particular, one finds that although classically the two branches meet, in the CFT description the two branches are infinitely far away and one cannot get from one to the other [102].

The second aspect of the gauge theory description that is worth emphasizing is the qualitative nature of the effective IR CFT we find. It is a two-dimensional $\mathcal{N} = (4, 4)$ sigma model with hyper-Kähler target space and central charge $c = 6(N_1 N_5 + 1)$. All of these facts remain essentially unchanged in our ultimate description. Let us make one further comment. Conformal field theories have a moduli space whose tangent space is spanned by a set of exactly marginal operators—perturbing the CFT with one of these operators gives a new CFT with different properties. Moreover, in the case of two-dimensional $\mathcal{N} = (4, 4)$ supersymmetric CFTs (SCFTs) the local structure of the moduli space is completely determined by supersymmetry to be of the form [143, 144]

$$\frac{SO(4, n)}{SO(4) \times SO(n)}, \quad (2.30)$$

where n is fixed by the number of marginal operators. See also [134] for a review of the moduli space of these SCFTs. Let us clarify: so far we have discussed three moduli spaces.

First we discussed the moduli space of supergravity compactified on $T^4 \times S^1$ and its near-horizon subset. Then, we showed that the open strings give rise to a $U(N_5) \times U(N_1)$ gauge theory with a moduli space defined by the vanishing of Equation (2.23). When we went to the effective IR CFT, the gauge theory moduli space became the *target* space of a two-dimensional sigma model. Now, we just introduced the moduli space of that two-dimensional sigma model. Since the near-horizon supergravity should be dual to the IR sigma model, we should expect that their respective moduli spaces agree. Indeed, we see that Equation (2.15) is of the form in Equation (2.30) with $n = 5$.

2.3.2 Instanton Description

We now switch to an alternative, more accurate treatment of the D1D5 bound state. Let us begin our discussion with only the N_5 D5-branes wrapping $T^4 \times S^1$. The ground state excitations of the open strings living on the D5-branes give rise, as discussed above, to a 5+1-dimensional $U(N_5)$ with 16 supercharges. In six dimensions, this corresponds to $\mathcal{N} = 2$ Weyl self-conjugate super-spinors. One can derive this theory by dimensionally reducing $\mathcal{N} = 1$ $U(N_5)$ gauge theory in ten dimensions on a four-torus. At this point in our previous discussion we dimensionally reduced on the string scale T^4 , arguing that the KK modes are too heavy to excite in the low-energy description of interest. There are other, non-perturbative, excitations; however, that one might consider on the T^4 .

Recall that Yang–Mills theory in four dimensions has instanton solutions: classical solutions of the Euclidean equations of motion with finite action. The field strength of these configurations satisfy a self-duality condition

$$F^{(2)} = \pm * F^{(2)} \quad \longrightarrow \quad F_{ij} = \pm \frac{1}{2} \epsilon_{ijkl} F^{kl}, \quad (2.31)$$

and have nontrivial winding number or Pontryagin index $\nu \in \mathbb{Z}$ defined by

$$32\pi^2\nu = \text{Tr} \left[\int F^{(2)} \wedge F^{(2)} \right] = \frac{1}{2} \text{Tr} \left[\int d^4x \epsilon_{ijkl} F^{ij} F^{kl} \right]. \quad (2.32)$$

The superscripted ‘2’ indicates that F is a 2-form. The solutions are localized in time and but otherwise are similar to solitons, hence the name. Instantons are treated in many different places in the literature (see e.g. [69, 145, 146]).

There are analogous solutions to the D5-brane worldvolume theory with field strength self-dual with respect to the T^4 directions. From the perspective of the full six-dimensional theory these solutions are dynamical strings wrapping S^1 that are localized in T^4 . Following the literature, we term these solutions instantons even though they are not localized in time. These solutions break half of the 5-brane worldvolume theory’s supersymmetries.

The 5-brane field theory contains a term

$$\int C^{(2)} \wedge \text{Tr}[F \wedge F], \quad (2.33)$$

and therefore the instantons source the RR 2-form in quantized units from (2.32). All of these facts suggest that we interpret these strings of instantons as D1-branes wrapping S^1 [97, 98].

From this discussion, we conclude that we are interested in N_1 strings of instantons in the D5-brane worldvolume theory. In particular, we want an effective IR CFT description of this theory. There are a set of fermionic and bosonic zero modes associated with the instanton solutions [69, 147, 148]. The IR limit of the theory should be just these zero modes. Put another way, the N_1 strings of instantons of the $U(N_5)$ gauge theory have a moduli space of solutions that have the same D1-brane charge. Let us call this space $\mathcal{W}_{\text{inst.}}$.¹⁹ From our above discussion, we see that the IR dynamics of the D1D5 system should be a two-dimensional $\mathcal{N} = (4, 4)$ sigma model with target space $\mathcal{W}_{\text{inst.}}$ [97–99]. One can show that this moduli space is hyper-Kähler, and that the SCFT has the same local geometry as the near-horizon geometry in Equation (2.15) and central charge $c = 6N_1N_5$ [66, 96, 99, 102]. The center of mass zero modes are separate degrees of freedom as in Section 2.3.1. They do not play a role in any of the physics we describe here, so we do not mention them further. This SCFT has a moduli space $\mathcal{M}_{\text{SCFT}}$ that one can show exactly coincides with $\mathcal{M}_{\text{sugra}}^*$ [99]. This description, as before, is on the Higgs branch. The intersection with the Coulomb branch manifests itself as points in $\mathcal{M}_{\text{sugra}}^*$ where there is a “small instanton singularity,” which correspond to a D1 brane being emitted, for example [51, 102, 103].

In [98, 124], it is argued that the instanton moduli space $\mathcal{W}_{\text{inst.}}$ is a smooth deformation of a symmetric product of a four-torus \tilde{T}^4

$$\text{Sym}_{N_1N_5}(\tilde{T}^4) = \frac{(\tilde{T}^4)^{N_1N_5}}{S_{N_1N_5}}, \quad (2.34)$$

where S_n is the symmetric group of degree n ; and furthermore, that there is a point in the moduli space, $\mathcal{M}_{\text{SCFT}}$ or equivalently $\mathcal{M}_{\text{sugra}}^*$, where $\mathcal{W}_{\text{inst.}}$ takes this form. Heuristically, we can motivate this description. Consider the case of $N_5 = 1$, in which case, we have N_1 strings of instantons wrapping S^1 . The low-energy theory describes the instanton dynamics inside the D5-brane worldvolume. Thus we must specify their position within the T^4 ; however, there is no physical distinction between permutations of the instanton labels 1 to N_1 and so we should mod out by all possible permutations, S_{N_1} . Of course, this argument is too simplistic to be rigorous since among other things the instantons have finite size. Moreover, as emphasized in [96], the \tilde{T}^4 can be different from the compactification torus,

¹⁹We choose this notation so that the target moduli space \mathcal{W} is clearly distinct from the CFT moduli space.

T^4 . Since we do not use the detailed structure of either of the tori, we drop the distinguishing tilde for the rest of the dissertation. The connection between the two tori is discussed in [100].

The point in moduli space where $\mathcal{W}_{\text{inst.}}$ takes the form (2.34) is referred to as the “symmetric product point” or the “orbifold point,” interchangeably. Arguments for its existence and location within moduli space are advanced in [96, 99, 100, 102, 103]. In particular, Larsen and Martinec [103] identify the orbifold point with canonical charges where $d_5 = N_5 = 1$ is $g_s = 0$ and $C^{(0)} = 1/2$. One can see that this far away from the regime of validity for supergravity (2.12).

The SCFT with target space $(T^4)^{N_1 N_5} / S_{N_1 N_5}$, we call the “orbifold model” or “orbifold CFT.” All of the calculations in the chapters that follow are in this CFT. We describe the details of the orbifold CFT in Section 2.5.

2.4 The Correspondence

Before describing the orbifold CFT in detail, let us pause to explicitly state the proposed $\text{AdS}_3\text{--CFT}_2$ correspondence that is being proposed, filling in some parts of the dictionary and addressing some subtleties. The claim is that type IIB string theory compactified on T^4 in $\text{AdS}_3 \times S^3$ is dual to two-dimensional $\mathcal{N} = (4, 4)$ SCFT with central charge $c = \bar{c} = 6N_1 N_5$ and target space $\mathcal{W}_{\text{inst.}}$.²⁰ The CFT lives at the two-dimensional boundary of AdS_3 . The fermions of the CFT derive their periodicity from the AdS space. If we have global AdS space, then the CFT is in the NS sector (anti-periodic boundary conditions) since global AdS has a contractible cycle and going around the S^1 at the boundary looks like a 2π rotation at a point in AdS space. See Figure 2.1(b) for a depiction of global AdS_3 . The CFT also has a R sector (periodic boundary conditions) that can be related to the NS sector via *spectral flow* [149] (see Section A.9). The NS vacuum is dual to global AdS_3 , whereas the R vacuum is dual to the two-charge extremal black hole in Equation (2.11). This is consistent since the geometry does not have a contractible cycle [66].

In our discussion so far we have focused on the moduli spaces of the SCFT and the supergravity, emphasizing the role of the near-horizon/low-energy limit. We have not been careful to discuss and show the agreement of the symmetries of the two theories. Recall that the D1D5 system is 1/4-BPS, and therefore supergravity solutions have 8 Killing spinors, ie. eight supersymmetries. When one takes the near-horizon limit, however, one goes to a more symmetric space $\text{AdS}_3 \times S^3$ which preserves 16 supersymmetries [66]. This doubling of the supersymmetry in the near-horizon limit also happens for the D3-brane case, for instance. The $\mathcal{N} = (4, 4)$ superalgebra; however, only has 8 (real) supersymmetries. Fortunately, when we take the IR limit, we end up with a $\mathcal{N} = (4, 4)$ *superconformal*

²⁰As discussed, there is also the center of mass degrees of freedom, which we suppress.

symmetry that has twice the number of fermionic symmetries. This illustrates again the connection between the near-horizon limit of the gravity description and the IR limit of the field theory description. The commutator of the special conformal operator with the supercharges gives new fermionic symmetries, usually denoted S . The S 's are not supercharges since they anticommute to give a special conformal transformation and not a translation. Thus, the $\mathcal{N} = (4, 4)$ superconformal algebra has 16 fermionic symmetries, of which 8 are supersymmetries.

The $\text{AdS}_3 \times S^3 \times T^4$ has an $SO(2, 2) \simeq SL(2, \mathbb{R}) \times SL(2, \mathbb{R})$ isometry of the AdS_3 , an $SO(4)_E$ isometry of S^3 , and $SO(4)_I$ of the torus which is broken by the compactification. The conformal group in two dimensions is infinite-dimensional with Virasoro generators L_n and \bar{L}_n for all $n \in \mathbb{Z}$; however, only the subalgebra spanned by $n = -1, 0, 1$ are well-behaved symmetries globally [150]. This subalgebra generates an $SL(2, \mathbb{R}) \times SL(2, \mathbb{R})$ group of transformations that can be identified with the isometries of AdS_3 . These are the transformations under which the vacuum is invariant in the SCFT [66]. The $\mathcal{N} = (4, 4)$ superconformal algebra has an $SO(4)$ R -symmetry which is identified with the $SO(4)_E$ isometry of S^3 . The $\mathcal{N} = (4, 4)$ superconformal algebra also has an $SO(4)$ outer automorphism (see e.g. [134, 149]) that we identify with $SO(4)_I$ of the torus. As discussed above, both the geometry and the SCFT have the same number of fermionic symmetries; putting the bosonic and fermionic symmetries together, one can show that both the geometry and the SCFT have the same supergroup, $SU(1, 1|2) \times SU(1, 1|2)$ [66, 96].

2.5 The Orbifold Model of the D1D5 CFT

In this section we explicitly describe the orbifold model of the D1D5 CFT. For a quick summary of our conventions, see Appendix A. As already mentioned, this is a two-dimensional $\mathcal{N} = (4, 4)$ superconformal sigma model with target space $(T^4)^{N_1 N_5} / S_{N_1 N_5}$. The orbifold model is the analog of free super Yang–Mills in the more familiar $\text{AdS}_5\text{--CFT}_4$ duality. The base space of the sigma model is the cylinder parameterized by (t, y) (the S^1 and time of the supergravity). We take y to have periodicity $2\pi R$; R is the radius of the S^1 .

2.5.1 The Symmetries and Action

The symmetries of our theory are $SO(4)_E \simeq SU(2)_L \times SU(2)_R$ and the $SO(4)_I \simeq SU(2)_1 \times SU(2)_2$ rotations of the torus. Indices correspond to the following representations

| | | | |
|-----------------|----------------------|-----------------------------|-----------------------|
| α, β | doublet of $SU(2)_L$ | $\dot{\alpha}, \dot{\beta}$ | doublet of $SU(2)_R$ |
| A, B | doublet of $SU(2)_1$ | \dot{A}, \dot{B} | doublet of $SU(2)_2$ |
| i, j | vector of $SO(4)_I$ | a, b | vector of $SO(4)_E$. |

Note that these conventions differ slightly from what we use above. The two-dimensional theory can be written in terms of bosons $X_{(r)}^i(t, y)$ and two-component Majorana-Weyl fermions $\Psi_{(r)}^{aA}(t, y)$.²¹ The subscripted parenthetical index is a “copy” index. Since the target space is the symmetric product of $N_1 N_5$ T^4 s, we have $N_1 N_5$ copies of a sigma model with target space T^4 which we symmetrize. The symmetrization $S_{N_1 N_5}$ we can think of as a discrete gauge symmetry. Each copy has four real bosons and eight real fermions. Once these are broken into left and right sectors of a CFT, we get $c = \bar{c} = 6$ central charge from each copy which is consistent with our previous discussion. We frequently suppress the copy index in our discussion and calculations.

The action can be written roughly in the form (up to numerical factors)

$$S \sim \sum_{r=1}^{N_1 N_5} \int dt \int_0^{2\pi R} dy \left[\partial_\rho X_{(r)}^i \partial^\rho X_{(r)}^i + i \epsilon_{\dot{A}\dot{B}} \bar{\Psi}_{(r)}^{a\dot{A}} \gamma^\rho \partial_\rho \Psi_{(r)}^{a\dot{B}} \right], \quad (2.35)$$

where ρ runs over t and y , and γ^ρ is the Dirac gamma matrix. We mention this only to make contact with our previous discussion. We find it more convenient to Wick rotate to Euclidean time and map the cylinder to a dimensionless complex plane, breaking the theory into left and right-movers. We define dimensionless Euclidean coordinates via

$$\tau = \frac{it}{R} \quad \sigma = \frac{y}{R}, \quad (2.36)$$

and map to the complex plane with coordinates z and \bar{z} via

$$z = e^{\tau + i\sigma} \quad \bar{z} = e^{\tau - i\sigma}. \quad (2.37)$$

Holomorphic functions of z are the “left-movers” and anti-holomorphic functions are the “right-movers.”

We also break the two-component fermions into single-component left-moving and right-moving fermions, $\psi_{(r)}^{\alpha\dot{A}}(z)$ and $\bar{\psi}_{(r)}^{\dot{\alpha}A}(\bar{z})$, satisfying a reality constraint

$$\psi_{\alpha\dot{A}}^\dagger = -\epsilon_{\alpha\beta} \epsilon_{\dot{A}\dot{B}} \psi^{\beta B} \quad \bar{\psi}_{\dot{\alpha}A}^\dagger = -\epsilon_{\dot{\alpha}\dot{\beta}} \epsilon_{AB} \bar{\psi}^{\beta\dot{B}}. \quad (2.38)$$

We can also break the vector of $SO(4)_I$ into doublets of $SU(2)_1$ and $SU(2)_2$, writing the bosons as

$$X_{A\dot{A}(r)}(z, \bar{z}). \quad (2.39)$$

The action for a single copy in this notation can be written as

$$S = \frac{1}{4\pi} \int d^2 z \left[\partial X^i(z) \bar{\partial} X^i(\bar{z}) - \psi^{\alpha\dot{A}} \partial \psi_{\alpha\dot{A}} - \bar{\psi}^{\dot{\alpha}A} \bar{\partial} \bar{\psi}_{\dot{\alpha}A} \right], \quad (2.40)$$

²¹Each two-component Ψ (with fixed i , A , and (r)) has one real degree of freedom once we demand that Ψ satisfy a reality condition (Majorana) and have positive chirality (Weyl).

where the conventions for raising and lowering indices is in Appendix A. The action is not particularly interesting since it is a free theory in two dimensions. The theory has an OPE current algebra. On the left sector (the right sector is analogous) we have the stress–energy current, the supercurrents, and the $SU(2)_L$ currents which are give by $T(z)$, $G^{\alpha A}(z)$, and $J^a(z)$ respectively. Note that $a = 1, 2, 3$ or $a = +, -, 3$ is an $SU(2)_L$ triplet index. The currents have modes labeled by L_n , $G_m^{\alpha A}$, and J_n^a respectively. All of these currents and modes have an implicit copy index; however, since we mod out by $S_{N_1 N_5}$ it is only the diagonal sum over all copies that survives as a symmetry of the full theory.

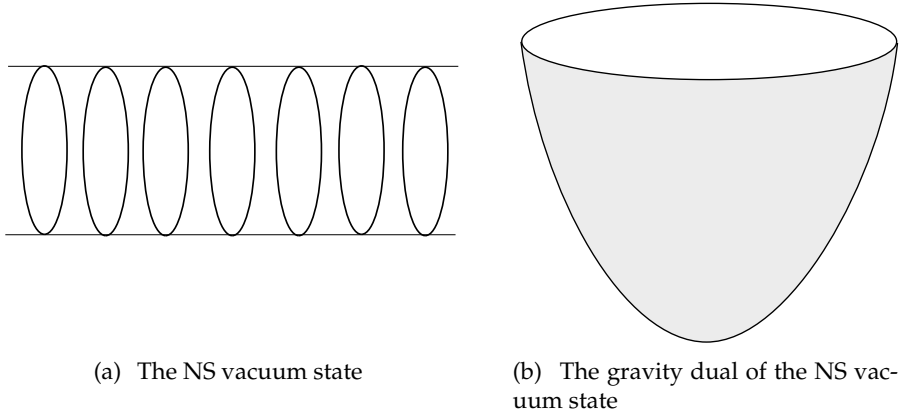


Figure 2.1: (a) The NS vacuum state in the CFT and (b) its gravity dual, which is global AdS . The NS vacuum is the simplest possible state having no twists, no excitations, and no base spin.

As we discuss in Section 2.4, while the L_n , $G_n^{\alpha A}$, and J_n^a span an infinite-dimensional algebra; only a finite subalgebra generate globally defined symmetries. These are the generators that annihilate the NS vacuum: $\{L_{\pm 1}, L_0, G_{\pm \frac{1}{2}}^{\alpha A}, J_0^a\}$. These generators also form a basis for the anomaly-free subalgebra. Note that the NS sector corresponds to anti-periodic boundary conditions for the fermions on the *cylinder*; when one maps to the complex plane, there is a Jacobian factor that switches the sign so that periodic fermions in the z -plane correspond to anti-periodic fermions on the cylinder and vice-versa. In the NS sector, then, the fermions and supersymmetry generators have half-integer modes and integer modes in the R sector. The Cartan subalgebra is spanned by $\{L_0, J_0^3\}$. A state's eigenvalue of L_0 is its conformal weight or scaling dimension usually denoted h or Δ . Since J_0^a are the generators of $SU(2)_L$, we have the usual $SU(2)$ representation theory. In particular, we can label states by their Casimir $(J_0^a)^2$ in addition to their J_0^3 eigenvalues, which we generally

denote by j and m , respectively. Of course, there are the analogous eigenvalues on the right sector, which have bars on top, as usual.

2.5.2 Twist Operators

Since we orbifold by the symmetric group $S_{N_1 N_5}$, we generate “twist sectors,” which can be obtained by acting with “twist operators” σ_n on an untwisted state. Suppose we insert a twist operator at a point z in the base space. As we circle the point z , different copies of T^4 get mapped into each other. Let us denote the copy number by a subscript $a = 1, 2, \dots, n$. The twist operator is labeled by the permutation it generates. For instance, every time one circles the twist operator

$$\sigma_{(123\dots n)}, \quad (2.41)$$

the fields $X_{(r)}^i$ get mapped as

$$X_{(1)}^i \rightarrow X_{(2)}^i \rightarrow \dots \rightarrow X_{(n)}^i \rightarrow X_{(1)}^i, \quad (2.42)$$

and the other copies of $X_{(a)}^i$ are unchanged. More explicitly, if we insert $\sigma_{(123\dots n)}(z_0)$, then the bosons have boundary conditions

$$\begin{aligned} X_{(r)}^i(z_0 + ze^{2\pi i}) &= X_{(r+1)}^i(z_0 + z) & r = 1, \dots, n-1 \\ X_{(n)}^i(z_0 + ze^{2\pi i}) &= X_{(1)}^i(z_0 + z), \end{aligned} \quad (2.43)$$

with copies $r = n+1$ through $N_1 N_5$ unaffected. We have a similar action on the fermionic fields. We depict this twisting in Fig. 2.2. Each set of linked copies of the CFT is called one “component string.” Because of the altered boundary conditions, in n -twisted sector there are new $1/n$ -moded excitations. These fractional modes are important for black hole physics and are in the background of much of the work presented in this dissertation.

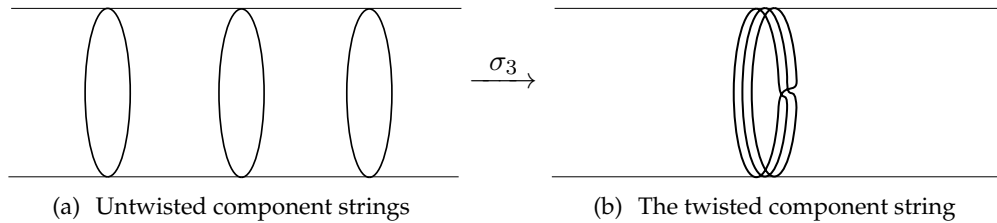


Figure 2.2: The twist operator σ_3 . Each loop represents a copy of the CFT wrapping the S^1 . The twist operator joins these copies into one single copy of the CFT living on a circle of three times the length of the original circle.

We often abbreviate a twist operator like the one in Equation (2.41) with σ_n for simplicity (we have to give the indices involved in the permutation explicitly when we use σ_n in a correlator). We call these operators, σ_n , “bare twists” to distinguish them from operators which have additional $SU(2)_L$ charge added to the bare twist forming operators that are chiral primaries for the supersymmetric CFT. See Appendix D (or for the original references [151, 152]) for how to compute correlators of twist operators. By calculating the difference in Casimir energy, one can show that the bare twist operators, σ_n , have weight [151]

$$\Delta_n = \bar{\Delta}_n = \frac{c}{24} \left(n - \frac{1}{n} \right), \quad (2.44)$$

where for us $c = 6$, the central charge of a *single* copy, *not* the total central charge, $c_{\text{tot.}} = 6N_1N_5$.

2.5.3 Chiral Primaries and Short Multiplets

Let us discuss some representation theory of the NS sector of the $\mathcal{N} = (4, 4)$ algebra. The theory is very similar to the $\mathcal{N} = (2, 2)$ case [134, 153]. We call a state a *Virasoro primary* if it is killed by all the positive Virasoro generators. Virasoro primaries are a useful concept since they correspond to operators that transform nicely under general conformal transformations. If we just use the word *primary*, this is the sense in which we mean it. Finally, we call a state $|\phi\rangle$ a *global primary* if it is killed by all of the positive modes of the anomaly-free subalgebra:

$$L_{+1} |\phi\rangle = G_{+\frac{1}{2}}^{\alpha A} |\phi\rangle = 0. \quad (2.45)$$

The global primaries are useful because they are killed by all of the positive modes of the subalgebra that corresponds to the symmetries of the supergravity. We are interested in exploring the representation theory of the anomaly-free subalgebra. Note that the literature does not typically distinguish between these two concepts.²²

Let us now consider the anti-commutator of the fermionic symmetry generators $G_{\pm 1/2}^{\alpha A}$ from Appendix A:

$$\{G_{+\frac{1}{2}}^{-A}, G_{-\frac{1}{2}}^{+B}\} = \epsilon^{AB} (J_0^3 - L_0) \quad (2.46a)$$

$$\{G_{+\frac{1}{2}}^{+A}, G_{-\frac{1}{2}}^{-B}\} = \epsilon^{AB} (J_0^3 + L_0). \quad (2.46b)$$

²²The $\mathcal{N} = (2, 2)$ literature (e.g. [134]) sometimes define a superconformal primary as a state that is annihilated by all of the positive modes of the chiral algebra. We do not find such a concept useful here.

From these one can show that for any state $|\psi\rangle$ with weight h and J_0^3 charge m

$$\sum_B |G_{-\frac{1}{2}}^{+B} |\psi\rangle|^2 + \sum_B |G_{\frac{1}{2}}^{-B} |\psi\rangle|^2 = 2(h - m) \quad (2.47a)$$

$$\sum_B |G_{-\frac{1}{2}}^{-B} |\psi\rangle|^2 + \sum_B |G_{\frac{1}{2}}^{+B} |\psi\rangle|^2 = 2(h + m). \quad (2.47b)$$

Since in any unitary theory the left-hand sides of Equations (2.47a) and (2.47b) are the sum of positive definite quantities, we immediately derive a bound on all physical states of the theory,

$$h \geq |m| \quad \longrightarrow \quad h \geq j. \quad (2.48)$$

We call a state $|\chi\rangle$ *chiral* if it satisfies

$$G_{-\frac{1}{2}}^{+A} |\chi\rangle = 0 \quad A = 1, 2. \quad (2.49)$$

The chiral (Virasoro) primary states are of especial importance. They are the analog of the highest weight state for $SU(2)$ [153], their energies as well as their two and three-point functions are protected as one moves in moduli space [66, 134], and they are used to identify the duals of supergravity particles in the bulk. Furthermore, under spectral flow chiral primary operators map to Ramond vacua.

Chiral primary states are precisely the states that saturate the $h \geq m$ bound. That is, chiral primary implies $h = m$, and $h = m$ implies chiral primary. In fact, $h = m$ implies both (Virasoro) primary and global primary. That $h = m$ implies chiral, can be seen from Equation (2.47a). Thus, chiral global primary, chiral (Virasoro) primary, and $h = m$ are all equivalent. From the bound we immediately see that chiral primaries are also the highest weight states of the $SU(2)_L$ multiplet, $h = j = m$. The $G_{\pm\frac{3}{2}}^{\alpha A}$ anti-commutator can be used to derive a bound on the weight h of chiral primaries:

$$h_{\text{c.p.}} \leq \frac{c_{\text{tot.}}}{6} = N_1 N_5. \quad (2.50)$$

In fact, we can make a much stronger statement for the orbifold model. By looking at general G anticommutators in the n -twisted sector, where there are $1/n$ -fractional modes, one can show that chiral primaries in the n -twisted sector must have weight bounded by

$$\frac{n-1}{2} \leq h_{\text{c.p.}} \leq \frac{n+1}{2}. \quad (2.51)$$

Indeed, this is precisely what is demonstrated quite explicitly below. Note that the maximum twist is $n = N_1 N_5$, which gives a much tighter bound than Equation (2.50).

Of importance later in the dissertation, is that supergravity particles can be identified as the anomaly-free subalgebra descendants of chiral primaries; that is, chiral primary operators which are acted upon only by L_{-1} , J_0^- , or $G_{-\frac{1}{2}}^{-A}$. The other generators of the

| state | $h = j = m$ | degeneracy |
|--|-----------------|------------|
| $ c_0\rangle$ | $\frac{n-1}{2}$ | 1 |
| $\psi_{-\frac{1}{2}}^{+\dot{A}} c_0\rangle$ | $\frac{n}{2}$ | 2 |
| $J_{-1}^+ c_0\rangle$ | $\frac{n+1}{2}$ | 1 |

Table 2.4: In the n -twisted sector there are four chiral primaries. Their structure is summarized above. The lowest and highest weight chiral primaries saturate the bound in Equation (2.51). Each of the four chiral primaries gives a short multiplet and can be mapped to a distinct R ground state by spectral flow.

anomaly-free subalgebra annihilate the state since $h = m$ implies global primary.

In the singly twisted sector, there are four chiral primaries,

$$|\emptyset\rangle_{NS} \quad \psi_{-\frac{1}{2}}^{+\dot{A}} |\emptyset\rangle_{NS} \quad J_{-1}^+ |\emptyset\rangle_{NS} \propto \psi_{-\frac{1}{2}}^{+\dot{1}} \psi_{-\frac{1}{2}}^{+\dot{2}} |\emptyset\rangle_{NS}, \quad (2.52)$$

one with $h = j = 0$, two with $h = j = \frac{1}{2}$, and one with $h = j = 1$. The last one saturates the bound for the singly twisted sector. To make more chiral primaries we must look at twist operators. This structure is repeated for the twisted chiral primaries; there is a minimal charge chiral primary to which we can apply two fermion operators to get a total of four chiral primaries in each twist sector. See Figure 2.3 to see the chiral primaries (red dots) of the 3-twisted sector in the weight–charge plane.

Let us also introduce the supermultiplets of the theory, the representations of the anomaly-free subalgebra. Consider a global primary state—a state annihilated by $G_{+\frac{1}{2}}^{\alpha A}$ and L_1 . We can generate new states by acting with combinations of the four $G_{-\frac{1}{2}}^{\alpha A}$. This gives $1 + 4 + 6 + 4 + 1 = 16$ states (each term in the sum corresponds to a different number of $G_{-\frac{1}{2}}$ s being applied). On each of these states we can act with L_{-1} an arbitrary number of times to increase the weight. These are the supermultiplets.

There are also *short multiplets*, for which some of the $G_{-\frac{1}{2}}^{\alpha A}$'s annihilate the state. These are precisely the chiral primaries, and their descendents under the anomaly-free subalgebra, which we identify as the duals of supergravity particles. We can only act with half of the $G_{-\frac{1}{2}}$'s, so we can generate four states by acting with $G_{-\frac{1}{2}}^{-A}$. The chiral primary must be the top member of its $SU(2)_L$ multiplet from the bound (2.48). One can show that the two Virasoro primaries created by a single application of $G_{-\frac{1}{2}}^{-A}$ on a chiral primary $|c\rangle$ must be annihilated by J_0^+ . This can easily be seen from the commutator of J_0^+ and $G_{-\frac{1}{2}}^{-A}$:

$$J_0^+ G_{-\frac{1}{2}}^{-A} |c\rangle = G_{-\frac{1}{2}}^{-A} |c\rangle + G_{-\frac{1}{2}}^{-A} J_0^+ |c\rangle = 0, \quad (2.53)$$

where the two terms separately vanish from the chirality of $|c\rangle$ and it being the highest

weight state of $SU(2)_L$. One can also demonstrate that both states are annihilated by all the positive Virasoro generators. Thus, both descendants of a chiral primary by a single susy charge are the top members of the $SU(2)_L$ multiplet and are Virasoro primaries. These states are not chiral and they are not global primaries.

Let us now consider the state with both applications of $G_{-\frac{1}{2}}^{-A}$. One can show that

$$\begin{aligned} L_1 J_0^+ (G_{-\frac{1}{2}}^{-1} G_{-\frac{1}{2}}^{-2} |c\rangle) &= L_1 \left(G_{-\frac{1}{2}}^{+1} G_{-\frac{1}{2}}^{-2} |c\rangle + G_{-\frac{1}{2}}^{-1} J_0^+ G_{-\frac{1}{2}}^{-2} |c\rangle \right) \\ &= -L_1 L_{-1} |c\rangle \\ &= -2h |c\rangle. \end{aligned} \tag{2.54}$$

Thus we see that *part* of two applications $G_{-\frac{1}{2}}^{-A}$ on $|c\rangle$ is equivalent to $J_0^- L_{-1} |c\rangle$. For a chiral primary with weight $h = j = m$, we take the combination

$$G_{-\frac{1}{2}}^{-1} G_{-\frac{1}{2}}^{-2} |c\rangle + \frac{1}{2h} J_0^- L_{-1} |c\rangle, \tag{2.55}$$

which one can show is the top member of a spin- $(c-1)$ $SU(2)_L$ multiplet and is killed by L_{+1} . This state is only $SL(2, \mathbb{R})$ primary.

See Figure 2.3 for a depiction of the 3-twisted short multiplets in the $h-m$ and $h-j$ plane. Each point in the $h-j$ plane in Figure 2.3(b) is the top member of a $SU(2)_L$ multiplet that can be filled out by repeated application of J_0^- . We can also act with L_{-1} an arbitrary number of times to generate a new state which will also be the top member of its $SU(2)_L$ multiplet.

We can summarize the discussion as follows. In each twist sector there is a minimal weight chiral primary. We can apply two different fermion modes or both to generate 3 more chiral primaries. Each of those four chiral primaries gives a distinct short multiplet. Each short multiplet has four states that are annihilated by L_1 and are the top member of their $SU(2)_L$ multiplet: a chiral primary $|c\rangle$, $G_{-\frac{1}{2}}^{-1} |c\rangle$, $G_{-\frac{1}{2}}^{-2} |c\rangle$, and the state in Equation (2.55). To each of those four states we can apply L_{-1} an arbitrary number of times and fill out the rest of the $SU(2)_L$ multiplets by repeated application of J_0^- . See Tables 2.5 and 2.4. There are also special ultra-short multiplets with chiral primaries of weight less than or equal to $h = 1/2$. For these multiplets, the state in Equation (2.55) is missing.

See [66, 134, 153, 154] for more details. Let us emphasize that we are only discussing the left sector here, but there are parallel statements for the right sector.

The Basic Chiral Primary Operators σ_{l+1}^0

Let us recall the construction of chiral primary operators introduced in [152]. Start with the NS vacuum state $|\emptyset\rangle_{NS}$, which is in the completely untwisted sector, where all the component strings are “singly wound.” The gravity dual is global AdS.

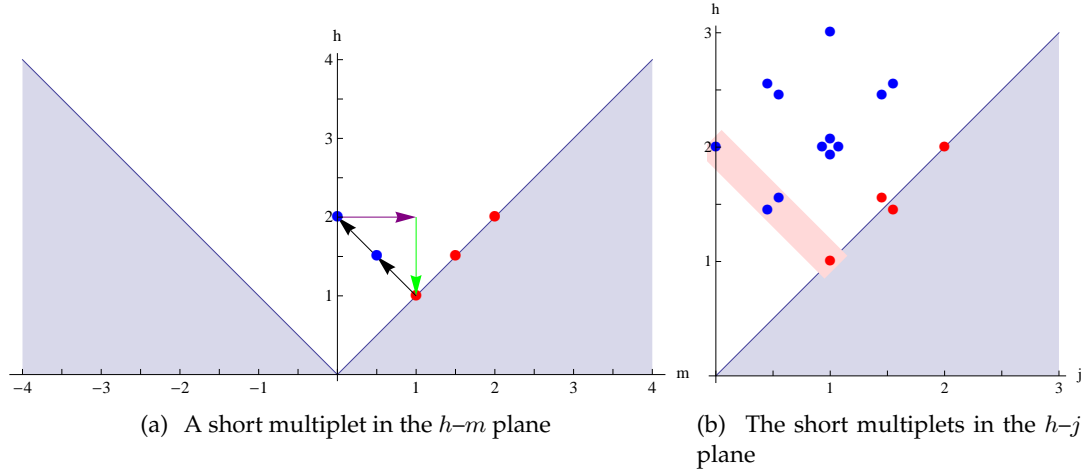


Figure 2.3: On the left, we show the h - m plane for the NS sector. Unitarity excludes the shaded region. The red dots are the chiral primary states of the 3-twisted sector. The middle red dot corresponds to two distinct chiral primaries. The blue dots represent states one attains by acting with $G_{-1/2}^{-A}$ on the $h = j = 1$ chiral primary. There are two at $h = m = 1/2$. The purple arrow represents the action of J_0^+ and the green arrow represents the action of L_1 . As discussed in the text, this gives the same state with $h = 1$ and $m = 2$, which must be projected out. The h - j plane on the right, shows the states of the short multiplets (up to application of J_0^- and L_{-1}). The dots are displaced slightly off the vertices to show the degeneracy. One of the short multiplets is highlighted in light red.

Now suppose in this gravity dual we want to add one supergravity quantum carrying angular momentum $\frac{l}{2}$ in each of the two factors of $SU(2)_L \times SU(2)_R$ (scalars must have $j = \bar{j}$). We take a set of $l + 1$ copies of the CFT and join them by using a twist operator σ_{l+1} into one “multiply wound” component string. Let us take the lowest energy state in this twist sector. This state has dimensions [152]

$$h = \bar{h} = \frac{c}{24} \left[(l + 1) - \frac{1}{(l + 1)} \right], \quad (2.56)$$

but it does not yet have any charge, so it is not a chiral primary; it has more dimension than charge. The current operator J^+ carries positive charge, and we can apply contour integrals of J^+ to our state to raise its charge. Since all operators in the theory have $h > |m|$, one might think that we cannot reach a chiral primary with $h = j = m$ if we start with the state (2.56); however, on the twisted component string we can apply *fractional* modes $J_{\frac{k}{l+1}}^a$ of the current operators, because any contour integral around the twist operator insertion has to close only after going around the insertion $l + 1$ times.

Before we apply these fractionally-moded current operators, there is one more point

| | state | h | j | m |
|----|--|-------------------|-------------------|-------------------|
| CP | $ c\rangle$ | h | h | h |
| P | $G_{-\frac{1}{2}}^{-A} c\rangle$ | $h + \frac{1}{2}$ | $h - \frac{1}{2}$ | $h - \frac{1}{2}$ |
| S | $G_{-\frac{1}{2}}^{-1} G_{-\frac{1}{2}}^{-2} c\rangle + \frac{1}{h} J_0^- L_{-1} c\rangle$ | $h + 1$ | $h - 1$ | $h - 1$ |

Table 2.5: We illustrate the basic structure of a short multiplet. One can start with a chiral primary (CP) $|c\rangle$, apply two different supercharges to get two Virasoro primaries (P), and finally apply both supercharges to a $SL(2, \mathbb{R})$ primary (S) (after projecting out). Each of those four states is the top member of an $SU(2)_L$ multiplet and has lowest conformal weight with respect to $SL(2, \mathbb{R})$. One can apply L_{-1} an arbitrary number of times and apply J_0^- to fill out the $SU(2)_L$ multiplet. This completes the short multiplet.

to note. For the case of $l + 1$ even one finds that the twist operator σ_n yields anti-periodic boundary conditions for the fermion field when we traverse around the twist insertion $l + 1$ times. Since we wanted the fermion field to return to itself after going $l + 1$ times around the insertion, we must insert a spin field to change the periodicity of these fermions. The construction of these spin fields was explained in detail in [152], but for now we just denote the twist with spin field insertions (for both left and right fermions) as $(S_{l+1}^+ \bar{S}_{l+1}^+ \sigma_{l+1})$. With this notation we find that the chiral primaries are given by

$$\sigma_{l+1}^0 = \begin{cases} J_{-\frac{l-1}{l+1}}^+ J_{-\frac{l-3}{l+1}}^+ \cdots J_{-\frac{1}{l+1}}^+ \bar{J}_{-\frac{l-1}{l+1}}^+ \bar{J}_{-\frac{l-3}{l+1}}^+ \cdots \bar{J}_{-\frac{1}{l+1}}^+ \sigma_{l+1} & (l+1) \text{ odd} \\ J_{-\frac{l-1}{l+1}}^+ J_{-\frac{l-3}{l+1}}^+ \cdots J_{-\frac{2}{l+1}}^+ \bar{J}_{-\frac{l-1}{l+1}}^+ \bar{J}_{-\frac{l-3}{l+1}}^+ \cdots \bar{J}_{-\frac{2}{l+1}}^+ (S_{l+1}^+ \bar{S}_{l+1}^+ \sigma_{l+1}) & (l+1) \text{ even.} \end{cases} \quad (2.57)$$

This construction generates chiral primaries with dimensions and charges

$$\sigma_{l+1}^0 : \quad h = m = \frac{l}{2}, \quad \bar{h} = \bar{m} = \frac{l}{2}. \quad (2.58)$$

Note that $J^+ \sim \psi^{+\dot{1}} \psi^{+\dot{2}}$, and the current operators in (2.57) fill up the left and right moving “Fermi seas” up to a Fermi level (here we write only the left sector)

$$\sigma_{l+1}^0 \sim \begin{cases} \psi_{-\frac{l-1}{2(l+1)}}^{+\dot{1}} \psi_{-\frac{l-1}{2(l+1)}}^{+\dot{2}} \psi_{-\frac{l-3}{2(l+1)}}^{+\dot{1}} \psi_{-\frac{l-3}{2(l+1)}}^{+\dot{2}} \cdots \psi_{-\frac{1}{2(l+1)}}^{+\dot{1}} \psi_{-\frac{1}{2(l+1)}}^{+\dot{2}} \sigma_{l+1} & (l+1) \text{ odd} \\ \psi_{-\frac{l-1}{2(l+1)}}^{+\dot{1}} \psi_{-\frac{l-1}{2(l+1)}}^{+\dot{2}} \psi_{-\frac{l-3}{2(l+1)}}^{+\dot{1}} \psi_{-\frac{l-3}{2(l+1)}}^{+\dot{2}} \cdots \psi_{-\frac{1}{2(l+1)}}^{+\dot{1}} \psi_{-\frac{1}{2(l+1)}}^{+\dot{2}} (S_{l+1}^+ \sigma_{l+1}) & (l+1) \text{ even.} \end{cases} \quad (2.59)$$

Additional Chiral Primaries

Above we described the construction of the simplest chiral primary σ_{l+1}^0 . We can make additional chiral primaries as follows:

1. The next available fermion level for the fermion $\psi^{+\dot{1}}$ in (2.59) is $\psi^{+\dot{1}}_{-\frac{1}{2}}$. If we fill this level, we raise both dimension and charge by $\frac{1}{2}$, so we get another chiral primary.
2. We can do the same with the fermion $\psi^{+\dot{2}}$.
3. We can add both fermions $\psi^{+\dot{1}}, \psi^{+\dot{2}}$, which is equivalent to an application of J_{-1}^+ .

Of course we can make analogous excitations to the right sector as well. This gives a total of $4 \times 4 = 16$ chiral primaries (more precisely chiral primary–chiral primary) in a given twist sector. This exhausts all the possible chiral primaries for this system.

Anti-chiral Primaries

We define anti-chiral primaries as states with

$$h = -m, \quad \bar{h} = -\bar{m}. \quad (2.60)$$

To construct these states, we again start with a twist operator σ_{l+1} and then apply modes of J^- instead of J^+ . Proceeding in the same way as for chiral primaries, we get the anti-chiral primary (denoted with a tilde over the σ) as

$$\tilde{\sigma}_{l+1}^0 = \begin{cases} J_{-\frac{l-1}{l+1}}^- J_{-\frac{l-3}{l+1}}^- \cdots J_{-\frac{1}{l+1}}^- \bar{J}_{-\frac{l-1}{l+1}}^- \bar{J}_{-\frac{l-3}{l+1}}^- \cdots \bar{J}_{-\frac{1}{l+1}}^- \sigma_{l+1} & (l+1) \text{ odd} \\ J_{-\frac{l-1}{l+1}}^- J_{-\frac{l-3}{l+1}}^- \cdots J_{-\frac{2}{l+1}}^- \bar{J}_{-\frac{l-1}{l+1}}^- \bar{J}_{-\frac{l-3}{l+1}}^- \cdots \bar{J}_{-\frac{2}{l+1}}^- (S_{l+1}^- \bar{S}_{l+1}^- \sigma_{l+1}) & (l+1) \text{ even.} \end{cases} \quad (2.61)$$

We can construct additional anti-chiral primaries just as in the case of chiral primaries. A chiral primary has a nonvanishing 2-point function with its corresponding anti-chiral primary. The chiral and anti-chiral twist operators are normalized such that the 2-point function is unity at unit separation.

2.5.4 Marginal Deformations

The orbifold point in moduli space does not have a good supergravity description [66, 96, 99, 103]. Since we are interested in using the CFT description to study black hole physics, we need gravity to be a reasonable description so that the concept of black hole is well-defined. We have two options to deal with this problem. We can compute quantities in the orbifold CFT, and hope that the quantities are protected by a non-renormalization theorem so that they are not affected by changes in the moduli; or, alternatively, we can add marginal deformations to the orbifold CFT that move one toward points in moduli space that do have a good supergravity description. The calculations of Chapter 4 are of the first kind. In Chapter 5, we consider the effect of a single application of a marginal deformation. This corresponds to first order in perturbation theory. Since the orbifold

point is far from a good supergravity description, we do not expect perturbation theory to be sufficient for getting to a supergravity point. We hope, however, that such analysis may give some insight. Much of that analysis remains to be completed, at the time of this writing.

We want to find the exactly marginal deformation to the orbifold CFT that preserve the $\mathcal{N} = (4, 4)$ supersymmetry. To be marginal, the operator should have weight $h = \bar{h} = 1$. If we take any state with weight $h = \bar{h} = 1$; however, there is no guarantee that its weight won't get renormalized as we change the moduli. Therefore it should be in a short multiplet. If it is to preserve the $\mathcal{N} = (4, 4)$ supersymmetry then it must be a singlet of the R -symmetry, $SO(4)_E = SU(2)_L \times SU(2)_R$. These requirements imply that we should look for chiral primary–chiral primaries (CP–CP) with weight $\bar{h} = \bar{j} = \bar{m} = h = j = m = 1/2$, and apply $G_{-1/2}^{-A} \bar{G}_{-1/2}^{\dot{B}}$ to form a $SO(4)_E$ singlet [96, 134, 155].

There are exactly five CP–CP operators with weight $h = \bar{h} = 1/2$:

$$\psi^{+A} \bar{\psi}^{+\dot{B}} \quad \sigma_2^{++}. \quad (2.62)$$

Each of the five CP–CP operators gives four deformation operators following our discussion of short multiplets. Note that applying $G_{-1/2}^{-A} \bar{G}_{-1/2}^{\dot{B}}$ to the fermion CP–CP operators just gives

$$\partial X^{A\dot{A}} \bar{\partial} X^{B\dot{B}} \sim \partial X^i \bar{\partial} X^j. \quad (2.63)$$

These may be broken into irreducible representations of $SO(4)_I$. There is the trace, the antisymmetric part, and the symmetric traceless part. There are four twist deformations [96, 155]

$$\mathcal{T}^{AB} = G_{-1/2}^{-A} \bar{G}_{-1/2}^{\dot{B}} \sigma_2^{++} \quad (2.64)$$

which can be broken into a singlet and a triplet of $SU(2)_1$ of $SO(4)_I$ that we call \mathcal{T}^0 and \mathcal{T}^1 , respectively. In total, then, there are 20 exactly marginal deformations that preserve the $\mathcal{N} = (4, 4)$ superconformal symmetry, which gives a 20 dimensional moduli space, as expected. From their basic properties, the 20 deformations can be identified with the 20 supergravity moduli in Table 2.3 [96, 103]. The deformations are listed in Table 2.6 with their corresponding supergravity field. We are particularly interested in the 4 twist deformations that move the theory away from the orbifold point—individual twist sectors are no longer eigenstates of the Hamiltonian. These are the object of study in Chapter 5.

One can also identify the fixed supergravity moduli in the CFT [134, 156]. These are operators that preserve the $\mathcal{N} = (4, 4)$ supersymmetry and the $SO(4)_E$ R -symmetry but break conformal invariance. To make the irrelevant operators that satisfy these conditions, one starts with $h = \bar{h} = 1$ CP–CP states and applies both supercharges on the left and the right (and projects out to the irreducible part). These states have weight $h = \bar{h} = 2$, and so

| CFT | SUGRA | $SO(4)_I \simeq SU(2)_1 \times SU(2)_2$ | DOF |
|---|---|--|-----|
| $\partial X^{(i} \bar{\partial} X^{j)} - \frac{1}{4} \delta^{ij} \partial X^i \bar{\partial} X_i$ | $g_{ij} - \frac{1}{4} \delta_{ij} g_{kk}$ | $(\mathbf{3}, \mathbf{3})$ | 9 |
| \mathcal{T}^1 | B_{ij}^+ | $(\mathbf{3}, \mathbf{1})$ | 3 |
| $\partial X^{[i} \bar{\partial} X^{j]}$ | $C_{ij}^{(2)}$ | $(\mathbf{3}, \mathbf{1}) \oplus (\mathbf{1}, \mathbf{3})$ | 6 |
| \mathcal{T}^0 | Ξ | $(\mathbf{1}, \mathbf{1})$ | 1 |
| $\partial X^i \bar{\partial} X_i$ | ϕ | $(\mathbf{1}, \mathbf{1})$ | 1 |
| | | | 20 |

Table 2.6: Table of the marginal deformation operators of the orbifold CFT along with the corresponding near-horizon supergravity moduli.

break the conformal symmetry. There are 6 CP–CP states with $h = \bar{h} = 1$:

$$J_{-1}^+ \bar{J}_{-1}^+ |\emptyset\rangle_{NS} \quad \psi_{-\frac{1}{2}}^+ \bar{\psi}_{-\frac{1}{2}}^+ |\sigma_2^0\rangle \quad |\sigma_3^0\rangle. \quad (2.65)$$

Each of the corresponding 6 CP–CP operators gives rise to one $h = \bar{h} = 2$ irrelevant deformation. These correspond to the 5 fixed moduli and the fixed size of the S^3 [134].

2.5.5 Spectral Flow

Spectral flow [149] maps amplitudes in the CFT to amplitudes in another CFT; under this map dimensions and charges of the left sector change as (we write only the left sector)

$$h' = h + \alpha j + \frac{c\alpha^2}{24} \quad m' = m + \frac{c\alpha}{12}, \quad (2.66)$$

for spectral flow parameter $\alpha \in \mathbb{R}$. We can also separately spectral flow the right sector with spectral flow parameter $\bar{\alpha}$ (where the bar is not indicating complex conjugation). Spectral flow with odd α (in the singly twisted sector) exchanges NS and R boundary conditions of the left fermions, and spectral flow with even α preserves the boundary conditions. In the singly twisted sector, spectral flow by non-integer units gives more general fermion boundary conditions that are not useful to consider here.

For a single copy, the center Al charge is $c = 6$. Setting $\alpha = -1$ gives

$$|0_R^-\rangle : \quad h = \frac{1}{4} \quad m = -\frac{1}{2} \quad (2.67)$$

which is one of the Ramond ground states of the singly wound component string. For more on spectral flow, see Section A.9 in the Appendix.

2.5.6 The Ramond Sector

Most of our discussion of the orbifold CFT so far is in the NS sector. The NS sector is a bit simpler to treat in some ways since the fermions are periodic *in the complex plane*, but the black hole physics of interest is in the R sector. Fortunately, we can use spectral flow to map problems in the NS sector to problems in the R sector. We make use of this technique in Chapter 4. Thus, we do not need to use the details of the R sector most of the time. Let us comment, however, that each CP–CP in the NS sector spectral flows to a distinct R ground state. Thus each component string in the R sector has a $16 = 4 \cdot 4$ degeneracy from four left and four right fermion zero modes. Moreover, one sees that twisting does not cost any additional energy. We see, then, that the R ground state has a large degeneracy. This corresponds to the microstates of the corresponding extremal black hole. See Appendix A for more details on the Ramond sector.

2.6 Overview

In this chapter, we have described the D1D5 CFT on T^4 . Throughout our discussion, we have emphasized the role of the moduli space. We introduced the supergravity description and its asymptotic and near-horizon moduli spaces. We then went through several descriptions of the open string degrees of freedom. We looked at the ground states of open strings connecting the different branes, which with the symmetries of the theory suffice to give the low-energy effective action. This action has a potential with two branches. The Coulomb branch corresponds to some of the branes separating and it is not of interest in this dissertation. This description has a limited regime of validity. We then transitioned to a description in which the D1s are realized as instantons in the D5 worldvolume theory. Finally we argued that at some point in moduli space, the low-energy effective theory should be the orbifold CFT.

The whole discussion serves to motivate the orbifold CFT, which we then summarized. Most of the calculations presented in this dissertation are in the orbifold CFT. The fact that the orbifold CFT has twist sectors, results in most of the nontrivial physics. Of importance, is the identification of the 20 marginal deformation operators that correspond to the 20 directions in the tangent space of the moduli space.

Chapter 3

COUPLING THE CFT TO FLAT SPACE

In this short chapter, we show how to use AdS–CFT to relate CFT amplitudes to the emission or absorption by a collection of branes into the asymptotic flat space. In essence, we are perturbatively relaxing the decoupling limit by adding an irrelevant operator to the CFT that couples to flat space degrees of freedom. A similar calculation was performed in [157]; however, we demonstrate a much more general construction—taking into account the effect of the “neck” and considering general AdS_{d+1} – CFT_d . This material was developed in [158].

Constructing the desired formalism requires two main steps. For the first, note that the CFT describes only the physics in the “near-horizon region” of the branes; vertex operators in the CFT create excitations that must travel through the “neck” of the D-brane geometry and then escape to infinity as traveling waves. Thus we set up a general formalism that relates CFT amplitudes to absorption/emission rates observed from infinity.

Traditionally, one uses AdS–CFT to compute correlation functions in the CFT and compare them to quantities computed in the AdS geometry, but we are interested in finding the interactions of the brane system with quanta coming in from or leaving to *flat* infinity. Thus we must consider the full metric of the branes, where at large r the *AdS* region changes to a “neck” and finally to flat space.

In Section 3.1, we review the structure of the geometric description of branes in string theory. Then, in Section 3.2 we fix the coupling between gravity fields and operators in the CFT; first fixing the normalization of the fields and operators, then demanding the two-point functions agree. In Sections 3.3 and 3.4, we discuss the behavior of minimal scalars in the asymptotic flat space and the intermediate transition to AdS, respectively. Finally, in Section 3.5 we write down the interacting action that couples modes in the asymptotic flat space to the CFT dual to the inner AdS region. We apply the interaction to case of particle emission in Section 3.6, deriving a formula which we use in Chapter 4.

3.1 The Geometry

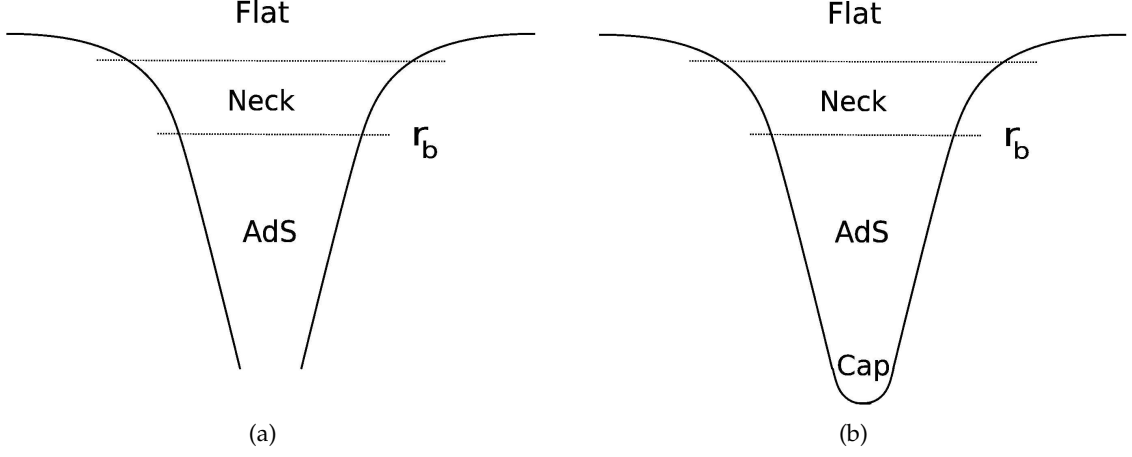


Figure 3.1: (a) The geometry of branes is flat at infinity, then we have a “neck”, and further in the geometry takes the form $AdS_{d+1} \times S^p$. (b) Still further in, the geometry ends in a “fuzzball cap” whose structure is determined by the choice of microstate. For the simple state that we choose for the D1D5 system, the Cap and AdS regions together are just a part of global AdS .

Consider the geometry traditionally written down for branes that have a near-horizon $AdS_{d+1} \times S^p$ region. This geometry has the form

$$ds^2 = H^{-\frac{2}{d}} \left[-dt^2 + \sum_{i=1}^{d-1} dy_i dy_i \right] + H^{\frac{2}{p-1}} [dr^2 + r^2 d\Omega_p^2]. \quad (3.1)$$

If there is only one kind of brane producing the metric (and hence only one length scale) the function H is given by

$$H = 1 + \frac{Q}{r^{p-1}}. \quad (3.2)$$

The BPS black holes studied in string theory are constructed from \mathcal{B} sets of mutually BPS branes. In these cases H is given by

$$H = \prod_{i=1}^{\mathcal{B}} \left(1 + \frac{Q_i}{r^{p-1}} \right)^{\frac{1}{\mathcal{B}}}. \quad (3.3)$$

(This reduces to (3.2) for $\mathcal{B} = 1$.) Let Q_{\max} be the largest of the Q_i and Q_{\min} the smallest. It is convenient to define the length scale

$$R_s = \left(\prod_{i=1}^{\mathcal{B}} Q_i \right)^{\frac{1}{\mathcal{B}(p-1)}}. \quad (3.4)$$

For small r the angular directions give a sphere with radius R_s .

We picture such a geometry in Figure 3.1(a). The geometry has three regions:

1. *The outer region:* For large r ,

$$r \gg Q_{\max}^{\frac{1}{p-1}}, \quad (3.5)$$

we have essentially flat space.

2. *The intermediate region:* For smaller r we find a “neck,” which we write as

$$CQ_{\min}^{\frac{1}{p-1}} < r < DQ_{\max}^{\frac{1}{p-1}}; \quad (C \ll 1, \quad D \gg 1). \quad (3.6)$$

3. *The inner region:* For

$$r < CQ_{\min}^{\frac{1}{p-1}}, \quad (3.7)$$

we can replace the harmonic function by a power:

$$H \rightarrow \left(\frac{R_s}{r} \right)^{p-1}. \quad (3.8)$$

The directions y_i join up with r to make an AdS space, and the angular directions become a sphere of constant radius:

$$ds^2 \approx \left[\left(\frac{r}{R_s} \right)^{\frac{2(p-1)}{d}} \left(-dt^2 + \sum_{i=1}^{d-1} dy_i dy_i \right) + R_s^2 \frac{dr^2}{r^2} \right] + R_s^2 d\Omega_p^2, \quad (3.9)$$

which is $AdS_{d+1} \times S^p$. We introduce a new radial coordinate \tilde{r} ,

$$\left(\frac{\tilde{r}}{R_s} \right) = \left(\frac{r}{R_s} \right)^{\frac{p-1}{d}}, \quad (3.10)$$

which makes the AdS physics more apparent. In terms of this new radial coordinate one has the inner region metric,

$$ds^2 \approx \left[\left(\frac{\tilde{r}}{R_s} \right)^2 \left(-dt^2 + \sum_{i=1}^{d-1} dy_i dy_i \right) + \left(R_s \frac{d}{p-1} \right)^2 \frac{d\tilde{r}^2}{\tilde{r}^2} \right] + R_s^2 d\Omega_p^2. \quad (3.11)$$

We can scale t, y_i to put the AdS into standard form, but it is more convenient to leave it as above, since the coordinates t, y_i are natural coordinates at infinity and we need to relate the AdS physics to physics at infinity. The radius of AdS_{d+1} and the sphere S^p are given by

$$R_{AdS_{d+1}} = R_s \frac{d}{p-1}, \quad R_{S^p} = R_s. \quad (3.12)$$

In region (iii), we can put a boundary at

$$\tilde{r} = \tilde{r}_b, \quad (3.13)$$

which we regard as the boundary of the AdS space. We can then replace the space at $\tilde{r} < \tilde{r}_b$ by a dual CFT. Let us note that \tilde{r}_b plays the role of a UV cutoff for the dual field theory, via the usual correspondence. Thus, traditional AdS/CFT calculations are carried out only with the region $\tilde{r} < \tilde{r}_b$. Our interest, however, is in the emission and absorption of quanta between the AdS region and asymptotic infinity. Thus we need a formalism to couple quanta in region (i) to the CFT.

Next, we note that this “traditional” AdS geometry cannot be completely right. In the case of the D1D5 system, we know that the ground state has a large degeneracy $\sim \exp[2\sqrt{2}\pi\sqrt{N_1 N_5}]$. At sufficiently large r , all these states have the form (3.1). But at smaller r these states differ from each other. None of the states has a horizon; instead each ends in a different “fuzzball cap” [75–79, 87, 88, 90, 121, 122, 159–174]. We can choose special states where this cap is given by a classical geometry. In the simplest case the cap is such that the entire region $\tilde{r} < \tilde{r}_b$ has the geometry of $global\ AdS_3 \times S^3$. We picture the full geometry for this state in Figure 3.1(b).

The geometry without the cap (Figure 3.1(a)) needs to be supplemented with boundary conditions for the gravity fields at $\tilde{r} = 0$. But since the actual states of the system (e.g. Figure 3.1(b)) have “caps,” we do have a well defined duality between the physics of the region $\tilde{r} < \tilde{r}_b$ and the CFT at \tilde{r}_b .

3.2 The Coupling between Gravity Fields and CFT Operators

Let us start with region (iii), where we have the AdS–CFT duality map. This map says that the partition function of the CFT, computed with sources ϕ_b , equals the partition function for gravity in the AdS, with field values at the boundary equal to ϕ_b [47]:

$$\int D[X] e^{-S_{CFT}[X] + \mu \int d^d y \sqrt{g_d} \phi_b(y) \mathcal{V}(y)} = \int D[\phi] e^{-S_{AdS}[\phi]} \Big|_{\phi(\tilde{r}_b) = \phi_b}. \quad (3.14)$$

Here we have rotated to Euclidean spacetime, setting $t = y_d$. The symbol ϕ denotes fields in gravity, and $\hat{\mathcal{V}}$ are CFT operators (depending on X) coupling to the gravity fields. Our first task is to determine the coupling constant μ , for the normalizations of ϕ_b and $\hat{\mathcal{V}}$ that

we choose.

Let us discuss the angular dependence in more detail. On S^p the fields $\phi(\tilde{r}, y, \Omega)$ can be decomposed into spherical harmonics,

$$\phi(\tilde{r}, y, \Omega) = \sum_{l, \vec{m}} \tilde{\phi}_{l, \vec{m}}(\tilde{r}, y) Y_{l, \vec{m}}(\Omega). \quad (3.15)$$

For the remainder of this discussion we consider a fixed l mode. Note that the reality of ϕ imposes the condition

$$\tilde{\phi}_{l, \vec{m}}^* = \tilde{\phi}_{l, -\vec{m}}. \quad (3.16)$$

Thus if we expand field in the usual spherical harmonics then we should write Equation (3.14) as

$$\int D[X] \exp \left(-S_{\text{CFT}}[X] + \mu \sum_{\vec{m}} \int d^d y \sqrt{g_d} \tilde{\phi}_{b, \vec{m}} \mathcal{V}_{\vec{m}} \right) = \int D[\phi] e^{-S_{\text{AdS}}} \Big|_{\tilde{\phi}_{\vec{m}}(\tilde{r}_b, y) \equiv \tilde{\phi}_{b, \vec{m}}(y)}. \quad (3.17)$$

Reality of the action requires

$$\hat{\mathcal{V}}_{\vec{m}}^\dagger(y) = \hat{\mathcal{V}}_{-\vec{m}}(y). \quad (3.18)$$

At leading order we can replace the gravity path integral by the classical action evaluated with the given boundary values of the gravity fields,

$$\int D[\phi] e^{-S_{\text{AdS}}[\phi]} \Big|_{\phi(r_b) = \phi_b} = e^{-S_{\text{AdS}}[\phi^{\text{cl.}}]}. \quad (3.19)$$

Then the 2-point function in the CFT is given by

$$\langle \hat{\mathcal{V}}_{\vec{m}}(y_1) \hat{\mathcal{V}}_{\vec{m}'}(y_2) \rangle = \frac{1}{\mu^2} \frac{\delta}{\delta \tilde{\phi}_{b, \vec{m}}(y_1)} \frac{\delta}{\delta \phi_{b, \vec{m}'}(y_2)} (-S_{\text{AdS}}). \quad (3.20)$$

Let us now define the normalizations of ϕ and $\hat{\mathcal{V}}$. We consider a minimal scalar field for concreteness, though our computations should be extendable to other supergravity fields with no difficulty. The gravity action is

$$S_{\text{AdS}} = \frac{1}{16\pi G_D} \int d^D x \sqrt{g} \left(\frac{1}{2} \partial \phi \partial \phi \right), \quad (3.21)$$

where $D = d + 1 + p$ is the dimension of the spacetime ($D = 10$ for string theory, $D = 11$ for M theory, and we have $D = 6$ for the D1D5 system after we reduce on a compact T^4). In region (iii), the spacetime has the form

$$AdS_{d+1} \times S^p \times \mathcal{M}. \quad (3.22)$$

For cases like the D1D5 system we have the additional compact 4-manifold $\mathcal{M} = T^4$ or

$\mathcal{M} = K3$. We take ϕ to be a zero mode on \mathcal{M} and dimensionally reduce on \mathcal{M} , so that we again have a space $AdS_3 \times S^3$, with G now the 6-d Newton's constant.

If the spherical harmonics are normalized such that,

$$\int d\Omega |Y_{l,\vec{m}}(\Omega)|^2 = 1, \quad (3.23)$$

then dimensionally reducing on S^p yields

$$S_{\text{AdS}} = \frac{R_s^p}{16\pi G_D} \sum_{\vec{m}} \int d^{d+1}y \sqrt{g_{d+1}} \left[\frac{1}{2} |\partial \tilde{\phi}_{\vec{m}}|^2 + \frac{1}{2} m^2 |\tilde{\phi}_{\vec{m}}|^2 \right]. \quad (3.24)$$

The l -dependent mass, m , comes from

$$m^2 = \frac{\Lambda}{R_s^2}, \quad \Delta_p Y(\Omega) = -\Lambda Y(\Omega), \quad \Lambda = l(l+p-1). \quad (3.25)$$

The CFT lives on the surface $\tilde{r} = \tilde{r}_b$. The metric on this surface is (from (3.11))

$$ds^2 = \left(\frac{\tilde{r}_b}{R_s} \right)^2 \sum_{i=1}^d dy_i dy_i. \quad (3.26)$$

We choose the normalization of the operators $\hat{\mathcal{V}}$ by requiring the 2-point function to have the short distance expansion $\sim \frac{1}{(\text{distance})^{2\Delta}}$:

$$\langle \hat{\mathcal{V}}_{\vec{m}}(y_1) \hat{\mathcal{V}}_{\vec{m}'}(y_2) \rangle = \frac{\delta_{\vec{m}+\vec{m}',0}}{\left[\left(\frac{\tilde{r}_b}{R_s} \right) |y_1 - y_2| \right]^{2\Delta}}. \quad (3.27)$$

Following [47], we define the boundary-to-bulk propagator which gives the value of ϕ in the AdS region given its value on the boundary at r_b :

$$\tilde{\phi}_{\vec{m}}(\tilde{r}, y) = \int K(\tilde{r}, y; y') \tilde{\phi}_{b,\vec{m}}(y') \sqrt{g_d} d^d y', \quad (3.28)$$

where $\sqrt{g_d} d^d y'$ is the volume element on the metric (3.26) on the boundary. We have

$$K(\tilde{r}, y; y') = \frac{R_{\text{AdS}}^{2\Delta-d}}{\tilde{r}_b^\Delta \pi^{\frac{d}{2}}} \frac{\Gamma(\Delta)}{\Gamma(\Delta - \frac{d}{2})} \left[\frac{\tilde{r}}{R_{\text{AdS}}^2 + \frac{\tilde{r}^2}{R_s^2} |y - y'|^2} \right]^\Delta, \quad (3.29)$$

where

$$\Delta = \frac{1}{2} (d + \sqrt{d^2 + 4m^2 R_{\text{AdS}}^2}) = (l+p-1) \frac{d}{p-1}. \quad (3.30)$$

We then have

$$\frac{\delta}{\delta \tilde{\phi}_{b,\tilde{m}}(y_1)} \frac{\delta}{\delta \phi_{b,\tilde{m}'}(y_2)} (-S_{\text{AdS}}) = -\frac{R_s^p}{16\pi G_D} \delta_{\tilde{m}+\tilde{m}',0} \left(\frac{2\Delta-d}{\Delta} \right) \partial_{\tilde{r}} K(\tilde{r}, y_1; y_2) \left(\sqrt{g^{\tilde{r}\tilde{r}}} \Big|_{\tilde{r}=\tilde{r}_b} \right), \quad (3.31)$$

where the extra factor $\frac{2\Delta-d}{\Delta}$ comes from taking care with the limit $\tilde{r}_b \rightarrow \infty$ when using the kernel (3.29) [175].

Putting (3.27) and (3.31) into (3.20) we get

$$\mu = \left[\frac{R_s^{2\Delta-(d+1)+p} \left(\frac{d}{p-1} \right)^{2\Delta-(d+1)}}{16\pi G_D} \frac{(2\Delta-d)}{\pi^{\frac{d}{2}}} \frac{\Gamma(\Delta)}{\Gamma(\Delta-\frac{d}{2})} \right]^{\frac{1}{2}}. \quad (3.32)$$

3.3 The Outer Region

The wave equation for the minimal scalar is

$$\square \phi = 0. \quad (3.33)$$

We write

$$\phi = h(r) Y(\Omega) e^{-iEt} e^{i\vec{\lambda} \cdot \vec{y}}, \quad (3.34)$$

getting the solution

$$h = \frac{1}{r^{\frac{p-1}{2}}} \left[C_1 J_{l+\frac{p-1}{2}} \left(\sqrt{E^2 - \lambda^2} r \right) + C_2 J_{-l-\frac{p-1}{2}} \left(\sqrt{E^2 - \lambda^2} r \right) \right]. \quad (3.35)$$

Note that we can define a CFT in the *AdS* region only if the excitations in the *AdS* region decouple to leading order from the flat space part of the geometry [45]. Such an approximate decoupling happens for quanta with energies $E \ll 1/R_s$: waves incident from infinity with wavelengths much longer than the *AdS* curvature scale almost completely reflect off the ‘neck’ region and there is only a small probability of absorption into the *AdS* part of the geometry. Correspondingly, waves with such energies trapped in the *AdS* region have only a small rate of leakage to flat space. Thus we work throughout this paper with the assumption

$$E \ll \frac{1}{R_s}. \quad (3.36)$$

With this, we find that to leading order the wave in the outer region has the $C_2 \approx 0$ [176]:

$$h \approx C_1 \frac{1}{\Gamma(l+\frac{p+1}{2})} \left[\frac{\sqrt{E^2 - \lambda^2}}{2} \right]^{l+\frac{p-1}{2}} r^l. \quad (3.37)$$

A general wave is a superposition of different modes of the form (3.34). We wish to extract a given spherical harmonic from this wave, so that we can couple it to the appropriate

vertex operator of the CFT. Define

$$[\partial^l \phi]^{l, \vec{m}} = Y_{l, \vec{m}}^{k_1 k_2 \dots k_l} \partial_{k_1} \partial_{k_2} \dots \partial_{k_l} \phi, \quad (3.38)$$

where the above differential operator is normalized such that²³

$$Y_{l, \vec{m}}^{k_1 k_2 \dots k_l} \partial_{k_1} \partial_{k_2} \dots \partial_{k_l} [r^{l'} Y_{l', \vec{m}'}(\Omega)] = \delta_{ll'} \delta_{\vec{m}, \vec{m}'}. \quad (3.39)$$

Thus the required angular component of ϕ at small r satisfies

$$\phi \approx [\partial^l \phi] \Big|_{r \rightarrow 0}^{l, \vec{m}} r^l Y_{l, \vec{m}}(\Omega). \quad (3.40)$$

3.4 The Intermediate Region

In the “neck” region we can set E and λ to zero in solving the wave equation, since we assume that we are at low energies and momenta so the wavelength is large compared to the size of the intermediate region. Thus the E and λ terms do not induce oscillations of the waveform in the limited domain of the intermediate region.

With this approximation we now have to solve the wave equation in the intermediate region. From this solution, we need the following information to construct our full solution. Suppose in the outer part of the intermediate region $r \sim Q_{\max}^{\frac{1}{p-1}}$ we have the solution

$$\phi \approx r^l. \quad (3.41)$$

Evolved to the inner part of the intermediate region $r \ll Q_{\max}^{\frac{1}{p-1}}$, we have a form given by AdS physics:

$$\phi \approx b_l \tilde{r}^{\Delta-d}. \quad (3.42)$$

These two numbers, b_l , Δ , give the information we need about the effect of the intermediate region on the wavefunction. Δ is known from the CFT, while the number b_l appears in our final expression for the emission amplitude as representing the physics of the intermediate region which connects the AdS region to flat infinity. In essence, b_l is a tunneling coefficient telling us if we start with a unit amount of ϕ in the outer region how much makes it through to the inner region.

We now note that for the case that we work with, the minimally coupled scalar, we can in fact write down the values of b_l and Δ . The wave equation for a minimally coupled scalar in the background (3.1) with the ansatz (3.34) takes the form

$$H^{\frac{2(d+p-1)}{d(p-1)}} (E^2 - \lambda^2) r^2 h(r) + \frac{1}{r^{p-2}} \partial_r (r^p \partial_r h(r)) - l(l+p-1) h(r) = 0. \quad (3.43)$$

²³See Appendix B for more details and some examples.

The term

$$H^{\frac{2(d+p-1)}{d(p-1)}} r^2 \quad (3.44)$$

is bounded in the “neck” region (3.6). Therefore, assuming small E, λ , the wave equation in the neck is

$$\frac{1}{r^{p-2}} \partial_r (r^p \partial_r h(r)) - l(l+p-1)h(r) = 0. \quad (3.45)$$

This has the solution

$$h(r) = Ar^l + Br^{-l-p+1}. \quad (3.46)$$

Thus we see that if we use the coordinate r throughout the intermediate region, then there is no change in the functional form of ϕ as we pass through the intermediate region. We are interested in the r^l solution, so we set $B = 0$. We must now write this in terms of the coordinate \tilde{r} appropriate for the AdS region. First consider the case $d = p - 1$ which holds for the D3 and D1D5 cases. Then we see that

$$\tilde{r} = r, \quad b_l = 1. \quad (3.47)$$

Now consider $d \neq p - 1$. From (3.10) and (3.30) we get

$$b_l = R_s^{l(1-\frac{d}{p-1})}. \quad (3.48)$$

In general the scalars are not “minimal;” i.e., they can have couplings to the gauge fields present in the geometry. Then b_l needs to be computed by looking at the appropriate wave equation. Examples of such non-minimal scalars are “fixed” scalars discussed in [177].

To summarize, we find that the change of the waveform through the intermediate region is given by b_l, Δ . The wave at the boundary $\tilde{r} = \tilde{r}_b$ is then

$$\tilde{\phi}_{b,\vec{m}}(y) = b_l \tilde{r}_b^{\Delta-d} [\partial^l \phi(y)] \Big|_{r=0}^{l,\vec{m}}. \quad (3.49)$$

3.5 The Interaction

We can break the action of the full problem into three parts

$$S_{\text{total}} = S_{\text{CFT}} + S_{\text{outer}} + S_{\text{int}}, \quad (3.50)$$

where the contribution of the interaction between the CFT and the outer asymptotically flat region, S_{int} , vanishes in the strict decoupling limit. We work in the limit where the interaction is small but nonvanishing, to first order in the interaction.

The coupling of the external wave at r_b to the CFT is given by the interaction

$$S_{\text{int}}^l = -\mu \sum_{\vec{m}} \int \sqrt{g_d} d^d y \tilde{\phi}_{b,\vec{m}}(y) \hat{\mathcal{V}}_{l,\vec{m}}(y). \quad (3.51)$$

If we want to *directly* couple to the modes in the *outer region*, then we can incorporate the intermediate region physics into S_{int} by writing

$$S_{\text{int}}^l = -c_l \sum_{\vec{m}} \int \sqrt{g_d} d^d y [\partial^l \phi(y)] \Big|_{r=0}^{l, \vec{m}} \hat{\mathcal{V}}_{l, \vec{m}}(y), \quad (3.52)$$

where

$$c_l = \mu b_l \tilde{r}_b^{\Delta-d}. \quad (3.53)$$

This is the general action connecting modes in the AdS/CFT with the modes in the asymptotically flat space. We focus specifically on (first-order) emission processes, but one can consider more general interactions (absorption, scattering, etc.).

3.6 Emission

Suppose we have an excited state in the “cap” region, $|i\rangle$, and the vacuum in the outer region, $|\emptyset\rangle_{\text{outer}}$. Because of the coupling (3.53), a particle can be emitted and escape to infinity, changing the state in the cap to a lower-energy state $|f\rangle$, and leaving a 1-particle state in the outer region, $|E, l, \vec{m}, \vec{\lambda}\rangle_{\text{outer}}$. We wish to compute the rate for this emission, Γ . We can write the total amplitude for this process as

$$\mathcal{A} = \left({}_{\text{outer}} \langle E, l, \vec{m}, \vec{\lambda} | \langle f | \right) i S_{\text{int}} \left(|i\rangle |\emptyset\rangle_{\text{outer}} \right). \quad (3.54)$$

We quantize the field ϕ in the outer region as

$$\begin{aligned} \hat{\phi} = \sqrt{\frac{16\pi G_D}{2V_y}} \sum_{\vec{\lambda}, l, \vec{m}} \int_0^\infty dE \frac{J_{l+\frac{p+1}{2}}(\sqrt{E^2-\lambda^2} r)}{r^{\frac{p-1}{2}}} \Big[\hat{a}_{E, l, \vec{m}, \lambda} Y_{l, \vec{m}} e^{i(\vec{\lambda} \cdot \vec{y} - Et)} \\ + (\hat{a}_{E, l, \vec{m}, \lambda})^\dagger Y_{l, \vec{m}}^* e^{-i(\vec{\lambda} \cdot \vec{y} - Et)} \Big], \end{aligned} \quad (3.55)$$

where

$$[\hat{a}_{E, l, \vec{m}, \lambda}, (\hat{a}_{E', l', \vec{m}', \lambda'})^\dagger] = \delta_{ll'} \delta_{\vec{m}, \vec{m}'} \delta_{\lambda \lambda'} \delta(E - E'). \quad (3.56)$$

Using the asymptotic behavior,

$$J_\nu(z) \approx \frac{1}{\Gamma(\nu+1)} \left(\frac{z}{2}\right)^\nu, \quad (3.57)$$

we find that

$$[\partial^l \hat{\phi}]_{r=0}^{\vec{m}} = \sqrt{\frac{16\pi G_D}{2V_y}} \sum_{\vec{\lambda}} \int_0^\infty dE \frac{(\frac{\sqrt{E^2 - \lambda^2}}{2})^{l + \frac{p-1}{2}}}{\Gamma(l + \frac{p+1}{2})} \left[\hat{a}_{E,l,\vec{m},\lambda} e^{i(\vec{\lambda} \cdot \vec{y} - Et)} + (\hat{a}_{E,l,-\vec{m},\lambda})^\dagger e^{-i(\vec{\lambda} \cdot \vec{y} - Et)} \right]. \quad (3.58)$$

Using the coupling c_l from (3.53) we get the interaction Lagrangian

$$S_{\text{int}} = -\mu b_l \tilde{r}_b^{\Delta-d} \sqrt{\frac{16\pi G_D}{2V_y}} \sum_{\vec{\lambda}, \vec{m}} \int \sqrt{g_d} d^d y \int_0^\infty dE \frac{(\frac{\sqrt{E^2 - \lambda^2}}{2})^{l + \frac{p-1}{2}}}{\Gamma(l + \frac{p+1}{2})} \left[\hat{a}_{E,l,\vec{m},\lambda} e^{i(\vec{\lambda} \cdot \vec{y} - Et)} + (\hat{a}_{E,l,-\vec{m},\lambda})^\dagger e^{-i(\vec{\lambda} \cdot \vec{y} - Et)} \right] \hat{\mathcal{V}}_{l,\vec{m}}(t, \vec{y}). \quad (3.59)$$

We can pull out the (t, \vec{y}) dependence of the CFT part of the amplitude by writing

$$\langle f | \hat{\mathcal{V}}(t, \vec{y}) | i \rangle = e^{-iE_0 t + i\vec{\lambda}_0 \cdot \vec{y}} \langle f | \hat{\mathcal{V}}(t=0, \vec{y}=0) | i \rangle, \quad (3.60)$$

where E_0 and λ_0 can be determined from the initial and final states of the CFT, $|i\rangle$ and $|f\rangle$. We also work in the case where the initial and final CFT states select out a single l, m mode in the interaction, whose indices have been suppressed. The CFT lives on a space of (coordinate) volume V_y . When computing CFT correlators we work in a “unit-sized” space with volume $(2\pi)^{d-1}$. Scaling the operator $\hat{\mathcal{V}}$ we have

$$\langle f | \hat{\mathcal{V}}(t=0, \vec{y}=0) | i \rangle = \left[\frac{(2\pi)^{d-1}}{(\frac{\tilde{r}_b}{R_s})^{d-1} V_y} \right]^{\frac{\Delta}{d-1}} \langle f | \hat{\mathcal{V}}(t=0, \vec{y}=0) | i \rangle_{\text{unit}}. \quad (3.61)$$

Rotating back to Lorentzian signature, the amplitude for emission of a particle from an excited state of the CFT is

$$\mathcal{A} = -i\mu b_l \tilde{r}_b^{\Delta-d} \sqrt{\frac{16\pi G_D}{2V_y}} \frac{(\frac{\sqrt{E^2 - \lambda^2}}{2})^{l + \frac{p-1}{2}}}{\Gamma(l + \frac{p+1}{2})} \left[\frac{(2\pi)^{d-1}}{(\frac{\tilde{r}_b}{R_s})^{d-1} V_y} \right]^{\frac{\Delta}{d-1}} \langle f | \hat{\mathcal{V}}_{l,-\vec{m}}(t=0, \vec{y}=0) | i \rangle_{\text{unit}} \times \int_0^T dt \int (\frac{\tilde{r}_b}{R_s})^d d^{d-1} y e^{-i(E_0 - E)t} e^{i(\vec{\lambda}_0 - \vec{\lambda}) \cdot \vec{y}}. \quad (3.62)$$

The amplitude gives the emission rate in a straightforward calculation:

$$\begin{aligned} \frac{d\Gamma}{dE} &= \lim_{T \rightarrow \infty} \frac{|\mathcal{A}|^2}{T} \\ &= (2\pi)^{2\Delta+1} \frac{R_s^{4\Delta-3d+p-1} \left(\frac{d}{p-1} \right)^{2\Delta-(d+1)}}{V_y^{\frac{2\Delta-d+1}{d-1}}} \left[\frac{(2\Delta-d)}{2\pi^{\frac{d}{2}}} \frac{\Gamma(\Delta)}{\Gamma(\Delta - \frac{d}{2})} \right] |b_l|^2 \left[\frac{1}{\Gamma(l + \frac{p+1}{2})} \right]^2 \end{aligned}$$

$$\times \left(\frac{E^2 - \lambda^2}{4} \right)^{l + \frac{p-1}{2}} \left| \langle 0 | \hat{\mathcal{V}}_{l, -\vec{m}}(0) | 1 \rangle_{\text{unit}} \right|^2 \delta_{\vec{\lambda}, \vec{\lambda}_0} \delta(E - E_0). \quad (3.63)$$

From this expression, we see that in the strict decoupling limit where $ER_s \rightarrow 0$ this rate vanishes as expected.

We have derived the above result for a general CFT and its corresponding brane geometry. In Chapter 4 we work with the D1D5 system. For a minimal scalar in the D1D5 geometry we have

$$d = 2, \quad p = 3 \quad \Delta_{\text{tot.}} = l + 2 \quad b_l = 1 \quad R_s = (Q_1 Q_5)^{\frac{1}{4}} \quad V_y = 2\pi R. \quad (3.64)$$

Plugging in, we reduce the decay rate formula to the form

$$\frac{d\Gamma}{dE} = \frac{2\pi}{2^{2l+1} l!^2} \frac{(Q_1 Q_5)^{l+1}}{R^{2l+3}} (E^2 - \lambda^2)^{l+1} \left| \langle 0 | \hat{\mathcal{V}} | 1 \rangle_{\text{unit}} \right|^2 \delta_{\lambda, \lambda_0} \delta(E - E_0), \quad (3.65)$$

which we use directly in Chapter 4. Do not confuse the radius of the S^3 , R_s , with the radius of the boundary, R . Note that most previous treatments would only have a proportionality, but using our formalism we have completely fixed the equality.

Chapter 4

EMISSION FROM JMART GEOMETRIES

In this chapter, we apply the formalism developed in Chapter 3 to the emission from a particular family of smooth, horizon-free three-charge nonextremal geometries. In the fuzzball proposal, they are candidate microstates of a three-charge non-extremal black hole. The particular family of geometries was found by Jejjala, Madden, Ross, and Titchener [168], so they are prosaically called JM(a)RT geometries. In [178], it was shown that the JMART geometries have a classical instability associated with the ergoregion in the geometry: one solves the classical wave equation for a minimal scalar in these JMART background, and finds solutions that are exponentially growing in time. Eventually, back-reaction becomes important and the geometry decays. Initially, this seemed problematic for the fuzzball interpretation [178, 179]: black holes are only unstable *semi*-classically due to Hawking radiation—the JMART geometries decay much faster. In [180–182], using heuristic CFT computations for some special cases, it was argued that the ergoregion emission is the Hawking radiation from this subset of microstates for the D1D5 black hole. In the CFT, one observes that the states dual to the JMART geometry are nongeneric, having many copies in the same state. The Hawking process, then, gets a large Bose enhancement.

Here, we outline work done in [158, 183], which closes some of the holes in [180–182]. We reproduce the *entire* spectrum and rate of emission for *all* of the JMART geometries using rigorous CFT calculations. We also note that the previous calculations could only normalize the action of the vertex operator by demanding agreement with Hawking radiation. Using the results in Chapter 3, we can fix the coupling from the two-point function in AdS, which makes the argument a bit more satisfying. One of the main upshots of the calculations presented in this chapter is that seemingly diverse gravitational processes are realized in essentially the same way in the CFT via spectral flow and Hermitian conjugation.

In Section 4.1, we briefly review the JMART geometries and their ergoregion instability. In Section 4.2, we perform the CFT calculation that reproduces the emission for a subset of the JMART geometries with $\kappa = 1$. Using spectral flow, the calculation is ultimately

reduced to computing a two-point function of the vertex operator. In Section 4.3, we generalize to $\kappa > 1$, which gives the emission spectra for all of the JMaRT geometries. The calculation for $\kappa > 1$ cannot be reduced to a two-point function via spectral flow. To complete the calculation, it is necessary to use the technology developed in [151, 152] for computing correlation functions of twist operators. The technique is reviewed in Appendix D. Finally in Section 4.4, we interpret the results and explain why the ergoregion emission is Hawking radiation from the microstates. We also discuss what lessons one might hope to apply to the fuzzball proposal in general.

4.1 JMaRT Geometries

For a fixed amount of D1 charge, D5 charge, and S^1 -momentum, [168] found a three-parameter family of geometries that have the following properties. At infinity they are asymptotically flat, then as one goes radially inward one encounters a “neck” region. After passing through the neck, one finds an AdS throat which terminates in an ergoregion cap. The fuzzball proposal interprets these smooth, horizonless geometries as classical approximations to microstates of a black hole with the same mass and charges.

The presence of ergoregions renders these geometries unstable [178, 180, 182]. The instability is exhibited by emission of particles at infinity, with exponentially increasing flux, carrying energy and angular momentum out of the geometry. In [180–182], using heuristic CFT computations for some special cases, it was argued that the ergoregion emission is the Hawking radiation from this subset of microstates for the D1D5 black hole. Figure 4.1 depicts the emission process in the gravity and CFT descriptions.

These geometries are dual to CFT states parameterized by three integers n , \bar{n} , and κ . In [158], the spectrum and rate of emission from the geometries with $\kappa = 1$ was exactly reproduced with a CFT computation. The parameter κ (called k in [182]), controls a conical defect in the geometry. For $\kappa = 1$, there is no conical defect or orbifold singularity.

4.1.1 Features of the Geometries

The D1D5 system we work with lives in a ten-dimensional geometry compactified on $T^4 \times S^1$. We wrap N_5 D5 branes on the full compact space, $T^4 \times S^1$; and we wrap N_1 D1 branes on the circle, S^1 . This gives rise to an $AdS_3 \times S^3$ throat in the noncompact space, which is dual to a two-dimensional CFT [45, 99, 102–104, 107, 184–186]. The core AdS region has radius $(Q_1 Q_5)^{\frac{1}{4}}$, where the D1 and D5 charges Q_1 and Q_5 are given by

$$Q_1 = \frac{g\alpha'^3}{V} N_1 \quad Q_5 = g\alpha' N_5, \quad (4.1)$$

with string coupling g and T^4 volume $(2\pi)^4 V$.

The JMaRT solutions are found as special cases of nonextremal three-charge black holes in [187, 188]. The three charges come from the D1-branes wrapping S^1 , the D5-branes wrapping $T^4 \times S^1$, and momentum on S^1 . These solutions have (string-frame) metric [168]

$$\begin{aligned}
ds^2 = & -\frac{f}{\sqrt{\tilde{H}_1 \tilde{H}_5}}(dt^2 - dy^2) + \frac{M}{\sqrt{\tilde{H}_1 \tilde{H}_5}}(s_p dy - c_p dt)^2 \\
& + \sqrt{\tilde{H}_1 \tilde{H}_5} \left(\frac{r^2 dr^2}{(r^2 + a_1^2)(r^2 + a_2^2) - Mr^2} + d\theta^2 \right) \\
& + \left(\sqrt{\tilde{H}_1 \tilde{H}_5} - (a_2^2 - a_1^2) \frac{(\tilde{H}_1 + \tilde{H}_5 - f) \cos^2 \theta}{\sqrt{\tilde{H}_1 \tilde{H}_5}} \right) \cos^2 \theta d\psi^2 \\
& + \left(\sqrt{\tilde{H}_1 \tilde{H}_5} - (a_2^2 - a_1^2) \frac{(\tilde{H}_1 + \tilde{H}_5 - f) \sin^2 \theta}{\sqrt{\tilde{H}_1 \tilde{H}_5}} \right) \sin^2 \theta d\phi^2 \\
& + \frac{M}{\sqrt{\tilde{H}_1 \tilde{H}_5}} (a_1 \cos^2 \theta d\psi + a_2 \sin^2 \theta d\phi)^2 \\
& + \frac{2M \cos^2 \theta}{\sqrt{\tilde{H}_1 \tilde{H}_5}} [(a_1 c_1 c_5 c_p - a_2 s_1 s_5 s_p) dt + (a_2 s_1 s_5 c_p - a_1 c_1 c_5 s_p) dy] d\psi \\
& + \frac{2M \sin^2 \theta}{\sqrt{\tilde{H}_1 \tilde{H}_5}} [(a_2 c_1 c_5 c_p - a_1 s_1 s_5 s_p) dt + (a_1 s_1 s_5 c_p - a_2 c_1 c_5 s_p) dy] d\phi \\
& + \sqrt{\frac{\tilde{H}_1}{\tilde{H}_5}} \sum_{i=1}^4 dz_i^2,
\end{aligned} \tag{4.2}$$

where

$$\tilde{H}_i = f + M \sinh^2 \delta_i \quad f = r^2 + a_1^2 \sin^2 \theta + a_2^2 \cos^2 \theta \quad c_i = \cosh \delta_i \quad s_i = \sinh \delta_i \quad i = 1, 5, p. \tag{4.3}$$

The D1 and D5 branes also source the RR 2-form, as expected. The nonzero RR 2-form and dilaton may be found in [168]. They are not relevant for our purposes here. The metric in Equation (4.2) is the ten-dimensional string frame metric; however, if we omit the T^4 part, dz_i^2 , then it is the six-dimensional Einstein frame metric. Our interest is mostly in this six-dimensional space.

The constants δ_i determine the asymptotic charges via

$$\begin{aligned}
Q_1 &= M \sinh \delta_1 \cosh \delta_1 = \frac{M}{2} \sinh 2\delta_1 \\
Q_5 &= M \sinh \delta_5 \cosh \delta_5 = \frac{M}{2} \sinh 2\delta_5 \\
Q_p &= M \sinh \delta_p \cosh \delta_p = \frac{M}{2} \sinh 2\delta_p.
\end{aligned} \tag{4.4}$$

For given asymptotic charges, Q_i , we can change the parameters a_1 , a_2 , and M subject to the above constraint. The geometry has ADM mass and angular momentum given by

$$\begin{aligned} M_{\text{ADM}} &= \frac{M}{2} (\cosh 2\delta_1 + \cosh 2\delta_5 + \cosh 2\delta_p) \\ J_\psi &= -M (a_1 \cosh \delta_1 \cosh \delta_5 \cosh \delta_p - a_2 \sinh \delta_1 \sinh \delta_5 \sinh \delta_p) \\ J_\phi &= -M (a_2 \cosh \delta_1 \cosh \delta_5 \cosh \delta_p - a_1 \sinh \delta_1 \sinh \delta_5 \sinh \delta_p), \end{aligned} \quad (4.5)$$

from which it is clear that we must choose $M \geq 0$ [168].

The Asymptotic Flat Space

Let us first note that in the large r limit the geometry takes the form of $M^{4,1} \times S^1 \times T^4$, as desired:

$$ds^2 \xrightarrow[r^2 \gg M]{} -dt^2 + dy^2 + dr^2 + r^2 (d\theta^2 + \cos^2 \theta d\psi^2 + \sin^2 \theta d\phi^2) + dz_i^2, \quad (4.6)$$

where y is the S^1 coordinate; z_i are coordinates on the T^4 ; and θ , ψ and ϕ are angular coordinates of S^3 . We can relate them to the usual Cartesian coordinates (at infinity) via

$$\begin{aligned} x_1 &= r \sin \theta \sin \psi \\ x_2 &= r \sin \theta \cos \psi \\ x_3 &= r \cos \theta \sin \phi \\ x_4 &= r \cos \theta \cos \phi. \end{aligned} \quad (4.7)$$

We see then that J_ψ and J_ϕ are the angular momenta associated with rotation in the 1–2 and 3–4 planes, respectively.

Horizon Removal

The simplest way to ascertain whether the geometry has a horizon or singularity is to examine the rr component of the inverse metric,

$$g^{rr} = \frac{1}{r^2 \sqrt{\tilde{H}_1 \tilde{H}_5}} [(r^2 + a_1^2)(r^2 + a_2^2) - Mr^2] \equiv \frac{1}{r^2 \sqrt{\tilde{H}_1 \tilde{H}_5}} [(r^2 - r_+^2)(r^2 - r_-^2)]. \quad (4.8)$$

This vanishes for $r = r_\pm$, where

$$r_\pm^2 = \frac{1}{2} \left[(M - a_1^2 - a_2^2) \pm \sqrt{(M - a_1^2 - a_2^2)^2 - 4a_1^2 a_2^2} \right]. \quad (4.9)$$

In order for r_\pm^2 to be real we must have

$$M \geq (a_1 + a_2)^2 \quad \text{OR} \quad M \leq (a_1 - a_2)^2. \quad (4.10)$$

Thus there are three different regions of parameter space that we can consider [168, 178]:

$$M \leq (a_1 - a_2)^2 \implies r_+^2 < 0 \quad (4.11a)$$

$$(a_1 - a_2)^2 < M < (a_1 + a_2)^2 \implies r_+^2 \notin \mathbb{R} \quad (4.11b)$$

$$M \geq (a_1 + a_2)^2 \implies r_+^2 > 0. \quad (4.11c)$$

We are interested in the first case, Equation (4.11a), where r_+^2 is negative. This case corresponds to the JMaRT solution, which has no horizon. The second and third case give a naked singularity and black hole, respectively.

Having $r^2 < 0$ may seem strange, but we can in essence analytically continue by defining a new radial coordinate

$$\rho^2 = r^2 - r_+^2. \quad (4.12)$$

We can then look at what happens near $\rho^2 = 0$ or $r^2 = r_+^2$. The determinant of the metric is proportional to

$$\det g \propto (r^2 - r_+^2)(r^2 - r_-^2), \quad (4.13)$$

and thus vanishes at this point. This vanishing can signal either an event horizon or a degeneration of the coordinate system, as happens at the origin of a polar coordinate system. To have a fuzzball, we want a horizonless solution and so we want the second case. This means that at $r^2 = r_+^2$ a circle in the geometry must pinch off to zero size. This story will be familiar to anyone who has studied the Euclidean Schwarzschild solution, for instance. A general Killing vector pointing in a circular direction can be written in the form

$$\xi = \partial_y - \alpha \partial_\psi - \beta \partial_\phi. \quad (4.14)$$

So we must require that ξ^2 vanishes at $r^2 = r_+^2$ for some choice of α and β . A necessary condition being that the determinant of the metric at fixed r and t , $\det_{y\theta\phi\psi} g$, must vanish at $r^2 = r_+^2$.

Working through these requirements, one finds [168]

$$M = a_1^2 + a_2^2 - a_1 a_2 \frac{c_1^2 c_5^2 c_p^2 + s_1^2 s_5^2 s_p^2}{s_1 c_1 s_5 c_5 s_p c_p} \implies r_+^2 = -a_1 a_2 \frac{s_1 s_5 s_p}{c_1 c_5 c_p}, \quad (4.15)$$

and the Killing vector that degenerates is given by

$$\alpha = -\frac{s_p c_p}{a_1 c_1 c_5 c_p - a_2 s_1 s_5 s_p} \quad \beta = -\frac{s_p c_p}{a_2 c_1 c_5 c_p - a_1 s_1 s_5 s_p}. \quad (4.16)$$

This suggests that the natural angular coordinates in the interior of the solution,

$$\tilde{\psi} = \psi + \alpha y \quad \tilde{\phi} = \phi + \beta y, \quad (4.17)$$

are shifted with respect to the natural angular coordinates at infinity. We choose the y coordinate to have range $y \in [0, 2\pi R)$. Thus, it would be natural to demand that the geometry be $2\pi R$ -periodic where the geometry pinches off, so that there is no conical singularity; however, in string theory it is consistent to consider orbifold singularities, since the worldsheet theory is well-defined on these backgrounds. We therefore introduce an integer parameter, $\kappa \in \mathbb{Z}^+$, and demand that the geometry be $2\pi\kappa R$ -periodic at $r^2 = r_+^2$. This implies [168]²⁴

$$\alpha R = -\hat{n} \quad \beta R = \hat{m} \quad \hat{m}, \hat{n} \in \mathbb{Z}, \quad (4.18)$$

and

$$R = \frac{M}{\kappa\sqrt{a_1 a_2}} \frac{s_1 c_1 s_5 c_5 \sqrt{s_1 c_1 s_5 c_5 s_p c_p}}{c_1^2 c_5^2 c_p^2 - s_1^2 s_5^2 s_p^2}. \quad (4.19)$$

Thus for fixed Q_1 , Q_5 , and R , we have three integer parameters that give distinct JMaRT geometries: κ , \hat{m} , and \hat{n} . The requirement that M be nonnegative implies that $\hat{m} > \hat{n} \geq 0$, after making some choices that do not result in loss of generality [168].

Let us note that the JMaRT solitons have mass and rotation outside of the “black hole bound.” Thus, there is no nonextremal black hole with the JMaRT conserved charges. This does not pose a major problem for our interpretation for several reasons. Part of the fuzzball proposal is identifying states in the CFT that are dual to geometries (in the appropriate limits). We are certainly testing and exploring that identification here. Within the CFT, there is no sharp distinction between states that are in the black hole bound and states that are not—they are all perfectly good states. Moreover, if one works in a canonical ensemble, rather than a microcanonical ensemble, then the CFT states considered here (and therefore the JMaRT geometries) do enter as “microstates” in any calculation of thermodynamic quantities. It is expected based on this discussion, however, that the JMaRT solutions will be nongeneric and may have properties that differ significantly from more generic geometries.

The Near-Horizon Geometry

Of importance to our considerations is that the geometry has a near-horizon (κ -orbifolded) $AdS_3 \times S^3$. We take the near-horizon limit by taking $Q_1, Q_5 \gg M, a_1^2, a_2^2$ and $r^2 \ll Q_1, Q_5$,

²⁴We use hats to distinguish these parameters from variables we use later.

which results in [168]

$$\begin{aligned}
ds^2 = & - \left(\frac{\rho^2}{L^2} + 1 \right) d\tau^2 + \left(\frac{\rho^2}{L^2} + 1 \right)^{-1} d\rho^2 + \rho^2 d\varphi^2 \\
& + L^2 \left[d\theta^2 + \sin^2 \theta \left(d\phi + \hat{m} d\varphi - \frac{\hat{n}}{L} d\tau \right)^2 \right. \\
& \left. + \cos^2 \theta \left(d\psi - \hat{n} d\varphi + \frac{\hat{m}}{L} d\tau \right)^2 \right],
\end{aligned} \tag{4.20}$$

where

$$L^2 = \sqrt{Q_1 Q_5} \quad \varphi = \frac{y}{R} \quad \tau = \frac{tL}{R} \quad \rho^2 = \frac{R^2}{L^2} \left[r^2 + (M - a_1^2 - a_2^2) s_p^2 + a_1 a_2 \sinh 2\delta_p \right]. \tag{4.21}$$

We see then that \hat{m} and \hat{n} give shifts to the angular coordinates. This shifting of the angular coordinates corresponds to spectral flow in the dual CFT.

The Ergoregion

The geometry also has an *ergoregion*. If we start with a timelike Killing vector at asymptotic infinity, it necessarily becomes spacelike in the cap of the geometry—the lightcones tip over into an angular direction. Let us note that this is different from an event horizon, in which the lightcones tip over in a radial direction and nothing can escape. In this case, if one is in the ergoregion, then one must rotate with respect to the asymptotic flat space; however, one can still exit an ergoregion.

The most general causal Killing field at infinity, can be written as²⁵

$$\zeta = \partial_t + \gamma \partial_y, \tag{4.22}$$

for $\gamma^2 < 1$. The norm may be written in the form

$$\begin{aligned}
\zeta^2 &= g_{tt} + 2\gamma g_{ty} + \gamma^2 g_{yy} \\
&= \frac{1}{\sqrt{\tilde{H}_1 \tilde{H}_5}} \left[-(1 - \gamma^2) f + M(c_p - \gamma s_p)^2 \right].
\end{aligned} \tag{4.23}$$

The “most” timelike choice is $\gamma = s_p/c_p = \tanh \delta_p$, but ζ still becomes spacelike for this choice in the region defined by [168]

$$\text{ergoregion: } f = r^2 + a_1^2 \sin^2 \theta + a_2^2 \cos^2 \theta < M, \tag{4.24}$$

where recall that M is fixed by Equation (4.15). Let us emphasize that *there is* a global time-like Killing vector and hence no ergoregion within the asymptotic AdS geometry in

²⁵Please do not confuse γ here with the notation of [182].

Equation (4.20). It is only when comparing the *asymptotic flat space* notion of time and the interior space notion of time that we see an ergoregion. The lightcones starting in the asymptotic AdS do not tip over completely when going deep into the cap. This point is important since it means that we can only see the physical effects of the ergoregion, namely ergoregion emission, if *we relax the strict decoupling limit* and re-attach the asymptotic flat space.

Identification in the CFT

In order to perform a calculation with the CFT, we must identify the CFT state dual to the JMaRT geometry. We can identify the weight and charge of the state from the corresponding charges of the geometric description. For instance, the energy of the state in the CFT, the sum of the left and right conformal weight, is given by the (ADM) mass of the geometry *above extremality*, ΔM_{ADM} . The S^1 -momentum gives the difference between the left and right weights. Thus, we can identify h and \bar{h} of the state. The angular momenta J_ψ and J_ϕ give the left and right J^3 charges, m and \bar{m} . This exercise gives [168]

$$\begin{aligned} h &= N_1 N_5 \frac{1}{4\kappa^2} (\kappa^2 - 1 + (\hat{m} + \hat{n})^2) & m &= N_1 N_5 \frac{\hat{m} + \hat{n}}{2\kappa} \\ \bar{h} &= N_1 N_5 \frac{1}{4\kappa^2} (\kappa^2 - 1 + (\hat{m} - \hat{n})^2) & \bar{m} &= N_1 N_5 \frac{\hat{m} - \hat{n}}{2\kappa}. \end{aligned} \quad (4.25)$$

The periodicity of the fermions is determined by the parity of $\hat{m} + \hat{n}$: if the sum is odd, then we are in the R–R sector; if the sum is even we are in the NS–NS sector [168]. We are interested in the R–R sector that is relevant for black hole physics.

Let us note the special case when $\hat{m} = \hat{n} + 1$ and $\kappa = 1$. In this case, we see that $\bar{h} = \frac{1}{4} N_1 N_5$ and $\bar{m} = \frac{1}{2} N_1 N_5$. The weight and charge of the right sector uniquely determine the right part of the state to be the Ramond vacuum with all of the “base spins” up. These are the three-charge supersymmetric (extremal, BPS) geometries studied in [122, 172, 189]. In general the weight and charge of a state do not suffice to identify it in the CFT; however, we can identify the JMaRT states since the angular shifts in the boundary of the AdS region correspond to spectral flow in the left and right sectors by $2n$ units on the left and $2\bar{n}$ units on the right, where

$$\frac{\hat{m} + \hat{n}}{\kappa} = 2n + \frac{1}{\kappa} \quad \frac{\hat{m} - \hat{n}}{\kappa} = 2\bar{n} + \frac{1}{\kappa}. \quad (4.26)$$

We find it more convenient to parameterize the geometries with n , \bar{n} , and κ for calculations in the CFT. When n and \bar{n} both vanish, then $\hat{m} = 1$ and $\hat{n} = 0$ and both the left and right sectors of the CFT are in the R ground state with all base spins up. Thus, the JMaRT geometries correspond to an even number of units of left and right spectral flow of the Ramond ground state. The states where $n = 0$ or $\bar{n} = 0$ are extremal and have no ergoregion or ergoregion emission. Therefore, we see that the existence of an ergoregion and

therefore ergoregion emission is tied to the nonextremality of the geometry. In [180–182], it was suggested that this may hold for more general nonextremal microstates: perhaps generic nonextremal microstates do not have a global timelike Killing vector. This would tie in nicely with the interpretation of the ergoregion emission as the Hawking radiation process.

4.1.2 Ergoregion Emission

Ergoregions are usually encountered in geometries that also have a horizon, i.e. black holes. For instance, outside the event horizon of a Kerr black hole there is an ergoregion that has the same rotational sense as the black hole. This is an example of frame-dragging. Because there is no global timelike Killing vector, and therefore no global notion of time-translation, one can have energies in the ergoregion that are negative with respect to asymptotic infinity.

For ergoregions in the presence of a horizon, one gets the phenomenon of superradiance. If one sends a wave at the ergoregion and black hole, a greater amplitude wave can be reflected off. In this way, one can mine energy and angular momentum out of the black hole geometry until the ergoregion disappears. If one places a “mirror” outside the ergoregion, then the reflected wave cannot vanish and one gets repeated amplification until the mirror breaks. This is the “black hole bomb” scenario [190].

Since the JMaRT geometries do not have a horizon, they are not superradiant, but they suffer from another instability which we call the ergoregion instability [178, 179, 191–193]. The instability is associated with the ability to form bound states in the negative energy region. This produces a large classical instability to decay. More specifically, if one solves the classical wave equation of a minimal scalar in this background, one finds modes with frequency, ω , that have positive imaginary part—the solution grows exponentially in time until back-reaction becomes important and the geometry decays [178, 179]. This process happens very rapidly. One can interpret this process as pair production: negative energy particles with angular momentum canceling out the ergoregion’s condense in the ergoregion, while their positive energy cousins carry energy and angular momentum out of the geometry to asymptotic flat space [181].

Our goal in this chapter is to reproduce the spectrum and rate of the ergoregion instability by using a CFT description. We work in the large-charge limit where the AdS space is large and the ergoregion emission has been computed analytically via the method of matched asymptotic expansions [178]. We also require the radius of S^1 be large so that the AdS space is “deep” enough for the CFT to be a good description. Previous calculations in [180, 182] could only reproduce the spectrum for certain special cases. The full spectrum was found in [158, 183].

4.2 Reproducing $\kappa = 1$ Emission using the Orbifold CFT

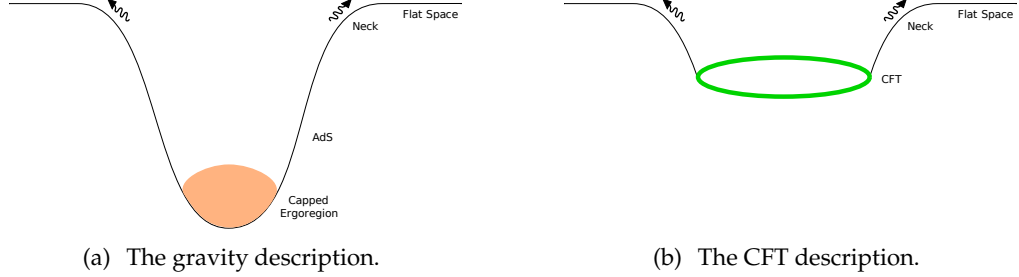


Figure 4.1: A depiction of the emission process we consider. In the cap region of the geometry, there is an ergoregion (shown in orange), which leads to the emission of particles into the flat space. In the CFT description particles are emitted by the CFT (shown in green) directly into the “neck” region of the geometry.

Early computations of radiation [84, 194–198] used the somewhat heuristic picture of an “effective string” to describe the D1D5 bound state. We construct states and vertex operators in the orbifold CFT, setting up notation and tools that allow us to compute amplitudes with ease. We apply these steps to compute the emission rate of supergravity scalars from particular D1D5 states. In particular we can compute emissions in cases where it was unclear how to proceed with the effective string model. The CFT amplitudes, converted to radiation rates by our general formalism, show exact agreement with the emission rates in the dual gravitational geometry.

Specifically, we perform the following steps:

1. As an example of our CFT techniques we consider minimal scalars in the D1D5 geometry. An example of such scalars is given by the graviton with indices along the compact torus directions. We construct the correctly normalized vertex operators for these scalars, which are obtained by starting with a twist operator in the CFT and dressing it with appropriate modes of the chiral algebra.
2. We use the notion of “spectral flow” to map states from the Ramond sector (which describes the D1D5 bound state) to the NS sector (which has the vacuum $|\emptyset\rangle_{NS}$). This map helps us in two ways. First, it is not clear which states in the Ramond sector correspond to supergravity excitations (as opposed to string excitations). In the NS sector there *is* a simple map: the supergravity excitations are given by chiral primaries and their descendants under the anomaly-free subalgebra of the chiral

algebra. Thus the spectral flow map allows us to find the initial and final states of our emission process, given the quantum numbers of these states. Second, for the process of interest the final state turns out to be the *vacuum* in the NS description; thus we do not need an explicit vertex operator insertion to create this state when computing amplitudes after spectral flowing to the NS sector.

3. We consider a simple decay process where an excited state of the CFT decays to the ground state and emits a supergravity quantum. We compute the CFT amplitude for this emission process. As mentioned above, the final state in the amplitude is nontrivial in the Ramond sector, but maps to the NS vacuum $|\emptyset\rangle_{NS}$ under spectral flow. This converts a 3-point correlator in the Ramond sector to a 2-point correlator in the NS sector. With this amplitude, we use the result in (i) to compute Γ , the rate of emission to flat space.
4. In the above computations we take the initial state to contain a few excitations above the ground state, and we compute the decay rate for these excitations. Alternatively, we can choose to start with the initial state having *no* excitations in the NS sector, and then perform a spectral flow on this state. This spectral flow adds a large amount of energy to the state, giving a configuration which is described in the dual gravity by a *nonextremal* classical metric [168]. This metric is known to emit radiation by ergoregion emission [178], and in [180–182] it was shown that for a subset of possible supergravity emissions the CFT rate agreed exactly with the gravity emission rate. We can now extend this agreement to all allowed emissions of supergravity quanta by using the orbifold CFT. It turns out that the simple decay process computed in steps (iii) and (iv) can be used to give the emission rate from this highly excited initial state. This is because using spectral flow the initial state can be mapped to the vacuum, and in fact the entire amplitude maps under spectral flow to a time reversed version of the decay amplitude computed above. We find exact agreement with the radiation rate in the dual gravity description.

4.2.1 The Initial State, the Final State, and the Vertex Operator

Our main computation addresses the following physical process. Consider a bound state of N_1 D1 branes and N_5 D5 branes, sitting at the origin of asymptotically flat space. As mentioned above, the CFT describing this bound state is in the Ramond sector, which has a number of degenerate ground states. We pick a particular Ramond ground state. Instead of describing this choice directly in the Ramond sector, we note that all Ramond sector ground states are obtained by one unit of spectral flow from chiral primary states of the NS sector. We pick the Ramond ground state that arises from the simplest chiral primary: the NS vacuum $|\emptyset\rangle_{NS}$. The gravity dual of this state can be described as follows [87, 89,

111, 112]: there is flat space at infinity, then a “neck,” then an AdS region, and then a “cap,” as pictured in Fig. 3.1(b). While the structure of the “cap” depends on the choice of Ramond ground state, in the present case the structure is particularly simple: below r_b in Fig. 3.1(b) the geometry is a part of global $AdS_3 \times S^3$.

By itself such a D1D5 state is stable, and does not radiate energy. We therefore add an excitation to the D1D5 brane state. In the supergravity dual, the excitation we choose corresponds to adding a supergravity quantum sitting in the “cap.” The supergravity field we choose is a scalar ϕ_{ij} , where $i, j = 1, \dots, 4$ are vector indices valued in the compact T^4 . These scalars arise from the following fields:

1. A symmetric traceless matrix h_{ij} with $i, j = 1, \dots, 4$ giving the transverse traceless gravitons with indices in the T^4 .
2. An antisymmetric matrix B_{ij}^{RR} giving the components of the Ramond-Ramond B field with indices in the torus.
3. The dilaton, which is a scalar in the full 10-dimensional theory.

We can put all these scalars together into a 4×4 matrix ϕ_{ij} , with the symmetric traceless part coming from h_{ij} , the antisymmetric part from B_{ij}^{RR} and the trace from the dilaton. (Such a description was used for example in [87, 196]. But we may need to scale the above fields by some function. For instance, it is not the graviton, h_{ij} , but $(H_5/H_1)^{\frac{1}{4}} h_{ij}$ which behaves as a minimal scalar in the 6-d space obtained by dimensional reduction on T^4 .

The supergravity particle is described by its angular momenta in the S^3 directions given by $SU(2)_L \times SU(2)_R$ quantum numbers $(\frac{l}{2}, m), (\frac{l}{2}, \bar{m})$; and a “radial quantum number,” N , where $N = 0$ gives the lowest energy state with the given angular momentum, and $N = 1, 2, \dots$ give successively higher energy states.

Adding this quantum to the $r < r_b$ region of the geometry corresponds to making an excitation of the D1D5 CFT. Since we compute all processes after spectral flowing to the NS sector, we should describe this excitation in the NS sector. In the NS sector, the excitation is a supersymmetry descendant of a chiral primary state, which is acted on N times with L_{-1} to further raise the energy. We describe the construction of this initial state in more detail below.

The process of interest is the emission of this supergravity particle from the cap out to infinity. The final state is thus simple: in the Ramond sector description we return to the Ramond ground state that we started with. In the spectral flowed NS sector description that we compute with, the final state is just the NS vacuum $|\emptyset\rangle_{NS}$.

The emission is caused by the interaction Lagrangian in Equation (3.52) which couples excitations in the CFT to modes at infinity; the general structure of this coupling was discussed in Chapter 3. We write down the vertex operator $\hat{\mathcal{V}}$ which leads to the emission of the quanta ϕ_{ij} , and compute the emission amplitude $\langle f | \hat{\mathcal{V}} | i \rangle$.

We now describe the initial state, the final state, and the vertex operator in detail.

The Initial State in the NS Sector

Let us first write the state, and then explain its structure. The left and right parts of the state have similar forms, so we only write the left part (indicated by the subscript L):

$$|\phi_{N+1}^{\frac{l}{2}, \frac{l}{2}-k}\rangle_L^{A\dot{A}} = \mathcal{C}_L L_{-1}^N (J_0^-)^k G_{-\frac{1}{2}}^{-A} \psi_{-\frac{1}{2}}^{+\dot{A}} \sigma_{l+1}^0 |\emptyset\rangle_{NS}, \quad (4.27)$$

where the normalization constant \mathcal{C}_L is determined in Appendix C:

$$\mathcal{C}_L = \sqrt{\frac{(l-k)!(l-\bar{k})!}{N!\bar{N}!(N+l+1)!(\bar{N}+l+1)!k!\bar{k}!(l+1)^2}}. \quad (4.28)$$

The normalization is chosen such that

$${}_{A\dot{A}}^L \langle \phi_{N+1}^{\frac{l}{2}, \frac{l}{2}-k} | \phi_{N+1}^{\frac{l}{2}, \frac{l}{2}-k} \rangle_L^{B\dot{B}} = \delta_A^B \delta_{\dot{A}}^{\dot{B}}. \quad (4.29)$$

Let us describe the structure of this state starting with the elements on the rightmost end:

1. We start with the NS vacuum $|\emptyset\rangle_{NS}$. In this state each copy of the CFT is “singly wound,” and each copy is unexcited. In the supergravity dual, we have global AdS space with no particles in it.
2. We apply the chiral primary σ_{l+1}^0 , thereby twisting together $l+1$ copies of the CFT into one “multiply wound” component string. It also adds charge, so that we get a state with

$$h = m = \bar{h} = \bar{m} = \frac{l}{2}. \quad (4.30)$$

In the gravity dual, we have one supergravity quantum, with angular momenta (m, \bar{m}) .

3. We act with $\psi_{-\frac{1}{2}}^{+\dot{A}}$. This increases both h and m by $\frac{1}{2}$, and so gives another chiral primary. We do the same for the right movers, so that overall the new state created is again bosonic. In the supergravity dual, it corresponds to a different bosonic quantum in the AdS.
4. We act with elements of the “anomaly-free subalgebra” of the chiral algebra:
 - (a) The $G_{-\frac{1}{2}}^{-A}$ changes the chiral primary to a supersymmetry descendant of the chiral primary, corresponding to a different supergravity particle in the gravity dual. Again, because we apply this supersymmetry operator on both left and

right movers, the new supergravity quantum is bosonic. We now find that the indices carried by this quantum are those corresponding to a minimal scalar with both indices along the T^4 in the gravity description. Thus we have finally arrived at the supergravity quantum that we wanted to consider.

- (b) The $(J_0^-)^k$ rotate the quantum in the S^3 directions. Before this rotation, the quantum numbers (m, \bar{m}) were the highest allowed for the given supergravity particle state. The application of the $(J_0^-)^k, (\bar{J}_0^-)^k$ give us other members of the $SU(2)_L \times SU(2)_R$ multiplet.
- (c) The L_{-1}^N move and boost the quantum around in the AdS , thus increasing its energy and momentum.

5. Finally, we have the normalization constant. We derive this in detail in Appendix C. The final expression for the radiation rate involves factors appearing in this normalization.

In the gravity description it is natural to write the field as ϕ_{ij} , with vector indices ij of the internal symmetry group $SO(4)_I$ of the T^4 directions. For CFT computations it is more useful to use indices $A\dot{A}$ for $SU(2)_1 \times SU(2)_2$, as we do above. The conversion is achieved by

$$|\phi_{N+1}^{\frac{l}{2}, \frac{l}{2}-k}\rangle_L^i = \frac{1}{\sqrt{2}} (\sigma^i)^{A\dot{A}} \epsilon_{AB} \epsilon_{\dot{A}\dot{B}} |\phi_{N+1}^{\frac{l}{2}, \frac{l}{2}-k}\rangle_L^{B\dot{B}}. \quad (4.31)$$

We then have

$${}_L^i \langle \phi_{N+1}^{\frac{l}{2}, \frac{l}{2}-k} | \phi_{N+1}^{\frac{l}{2}, \frac{l}{2}-k} \rangle_L^j = \delta^{ij}. \quad (4.32)$$

Similarly, one typically labels the angular momentum eigenstates in terms of (l, m_ψ, m_ϕ) , instead of (l, m, \bar{m}) . The two bases are related via

$$\begin{aligned} m_\psi &= -(m + \bar{m}) \\ m_\phi &= m - \bar{m}, \end{aligned} \quad (4.33)$$

where the values on the right-hand side are the angular momenta of the initial state in the NS sector.

The Final State

In the supergravity description the initial state had one quantum in it. The emission process of interest leads to the emission of this quantum. Thus the final state has no quanta, and in the NS description is just the vacuum

$$|f\rangle = |\emptyset\rangle_{NS}. \quad (4.34)$$

The Vertex Operator

We need the vertex operator that emits the supergravity quantum described by the initial state $|i\rangle$. Vertex operators describing supergravity particles are given by chiral primaries and their descendants under the anomaly-free part of the chiral algebra.

For the process of interest the emission vertex must have appropriate charges to couple to the supergravity field under consideration. Thus, one naturally concludes that the vertex operator has essentially the same structure as the state $|i\rangle$, with two differences. First, the operator has charges that are opposite to the charges carried by the state. (We get a nonvanishing inner product between $|i\rangle$ and the Hermitian *conjugate* of $|i\rangle$.) Second, the operator does not have the L_{-1} modes present in the description of the CFT state. This is because applying an L_{-1} mode is equivalent to translating the location of the vertex insertion, and we have already chosen the insertion to be the point (σ, τ) . Note that after applying the supercurrent to give the operator the correct $SO(4)_I$ index structure, one finds that the operator already has the correct weight to couple to a minimal scalar in Equation (3.52) and form a scale invariant action.

The vertex operator, then, is given by (we drop the hat on the vertex operator from now on)

$$\tilde{\mathcal{V}}_{l,l-k-\bar{k},k-\bar{k}}^{A\dot{A}B\dot{B}}(\sigma, \tau) = \sqrt{\frac{(l-k)!(l-\bar{k})!}{(l+1)^2(l+1)!^2 k! \bar{k}!}} (J_0^+)^k (\bar{J}_0^+)^{\bar{k}} G_{-\frac{1}{2}}^{+A} \psi_{-\frac{1}{2}}^{-\dot{A}} \bar{G}_{-\frac{1}{2}}^{+B} \bar{\psi}_{-\frac{1}{2}}^{-\dot{B}} \tilde{\sigma}_{l+1}^0(\sigma, \tau). \quad (4.35)$$

The subscript on the vertex operator $\mathcal{V}_{l,m_\psi,m_\phi}$ are the $SO(4)_E$ angular momenta labels. Again the normalization is a crucial part of the final amplitude, so we perform it in more detail below.

Note that for $l = 0$, the vertex operator reduces to $[\partial X]^{A\dot{A}}[\bar{\partial} X]^{B\dot{B}}$, the old “effective string” coupling found by expanding the DBI action [196].

We map the operator from the cylinder onto the complex plane via

$$z = e^{\tau+i\sigma} \quad \bar{z} = e^{\tau-i\sigma}. \quad (4.36)$$

The vertex operator has weight $\frac{l}{2} + 1$ on both the left and the right, so we get

$$\begin{aligned} \tilde{\mathcal{V}}_{l,l-k-\bar{k},k-\bar{k}}^{A\dot{A}B\dot{B}}(\sigma, \tau) &= |z|^{l+2} \sqrt{\frac{(l-k)!(l-\bar{k})!}{(l+1)^2(l+1)!^2 k! \bar{k}!}} \\ &\quad \times \left((J_0^+)^k (\bar{J}_0^+)^{\bar{k}} G_{-\frac{1}{2}}^{+A} \psi_{-\frac{1}{2}}^{-\dot{A}} \bar{G}_{-\frac{1}{2}}^{+B} \bar{\psi}_{-\frac{1}{2}}^{-\dot{B}} \tilde{\sigma}_{l+1}^0(z, \bar{z}) \right)_{z, \bar{z}} \\ &= |z|^{l+2} \mathcal{V}_{l,l-k-\bar{k},k-\bar{k}}^{A\dot{A}B\dot{B}}(z, \bar{z}). \end{aligned} \quad (4.37)$$

The normalization of the vertex operator in the complex plane is chosen such that

$$\begin{aligned}\langle \mathcal{V}_{l,-m_\psi,-m_\phi}^{A\dot{A}B\dot{B}}(z) \mathcal{V}_{l,m_\psi,m_\phi}^{C\dot{C}D\dot{D}}(0) \rangle &= \frac{\epsilon^{AC} \epsilon^{\dot{A}\dot{C}} \epsilon^{BD} \epsilon^{\dot{B}\dot{D}}}{|z|^{l+2}} \\ \langle \mathcal{V}_{l,-m_\psi,-m_\phi}^{ij}(z) \mathcal{V}_{l,m_\psi,m_\phi}^{kl}(0) \rangle &= \frac{\delta^{ik} \delta^{jl}}{|z|^{l+2}}.\end{aligned}\tag{4.38}$$

Note that this is the normalization of the operator corresponding to one particular way of permuting $l+1$ copies of the CFT. As mentioned earlier, the actual vertex operator coupling to ϕ_{ij} is a symmetrized sum over all possible ways of permuting $l+1$ copies from the $N_1 N_5$ available copies. We discuss the combinatorics of this choice in Section 4.2.4 below, and at that time note the extra normalization factor which is needed to agree with (3.27).

4.2.2 Using Spectral Flow

We wish to relate a CFT amplitude computed in the NS sector,

$$\mathcal{A}' = \langle f' | \mathcal{V}(z, \bar{z}) | i' \rangle, \tag{4.39}$$

to an amplitude in the Ramond sector, since the physical D1D5 system has its fermions periodic around the y circle. In this section, we show how to spectral flow [149, 153, 199] the computation in the NS sector to the physical problem in the R sector. Furthermore, we find that we can relate this NS sector computation to a whole family of Ramond sector amplitudes, and each member of the family describes a different physical emission process.

If spectral flowing the states $|i'\rangle$ and $|f'\rangle$ by α units is given by

$$|i'\rangle \mapsto |i\rangle = \mathcal{U}_\alpha |i'\rangle \quad \langle f' | \mapsto \langle f | = \langle f' | \mathcal{U}_{-\alpha}, \tag{4.40}$$

then we can compute the amplitude in the Ramond sector by using

$$\mathcal{A}_{\text{Ramond}} = \langle f | \mathcal{V}(z, \bar{z}) | i \rangle = (\langle f | \mathcal{U}_\alpha) (\mathcal{U}_{-\alpha} \mathcal{V} \mathcal{U}_\alpha) (\mathcal{U}_{-\alpha} | i \rangle) = \langle f' | \mathcal{V}'(z, \bar{z}) | i' \rangle. \tag{4.41}$$

Note that one finds \mathcal{V}' by spectral flowing \mathcal{V} by $-\alpha$ units.

We need to determine how the vertex operator transforms under spectral flow. First, we demonstrate that the $G\psi$ part is unaffected, since

$$\begin{aligned}\left(G_{-\frac{1}{2}}^{+A} \psi_{-\frac{1}{2}}^{-\dot{A}} \right)_z &= \oint_z \frac{dz_1}{2\pi i} \oint_z \frac{dz_2}{2\pi i} \frac{G^{+A}(z_1) \psi^{-\dot{A}}(z_2)}{z_2 - z} \\ &= - \oint_z \frac{dz_1}{2\pi i} \oint_z \frac{dz_2}{2\pi i} \frac{[\partial X(z_2)]^{\dot{A}A}}{(z_2 - z)(z_1 - z_2)}\end{aligned}\tag{4.42}$$

and the bosons are unaffected by spectral flow.

Therefore, we need only spectral flow the k J_0^+ 's and the chiral primary. The effect of spectral flow by *negative* α units on chiral ($h = m$) and anti-chiral primaries ($h = -m$) is very simple:

$$\mathcal{O}'_{\text{c.p.}}(z) = z^{\alpha m} \mathcal{O}_{\text{c.p.}}(z) \quad \mathcal{O}'_{\text{a.c.p.}}(z) = z^{\alpha m} \mathcal{O}_{\text{a.c.p.}}(z). \quad (4.43)$$

One can see this most directly after bosonizing the fermions; see Appendix A.9 for details.

Under spectral flow by $-\alpha$ units the J^\pm transform as

$$J^\pm(z) \mapsto z^{\pm\alpha} J^\pm(z), \quad (4.44)$$

from which we see that

$$(J_0^+)_z = \oint_z \frac{dz'}{2\pi i} J^+(z') \mapsto \oint_z \frac{dz'}{2\pi i} J^+(z') z'^\alpha = z^\alpha (J_0^+)_z + \alpha z^{\alpha-1} (J_1^+)_z + \dots \quad (4.45)$$

Only the first term contributes since the positive modes annihilate a chiral primary. Therefore, we conclude that spectral flowing the vertex operator by $-\alpha$ units has the effect of

$$\mathcal{V}'_{l,l-k-\bar{k},k-\bar{k}}(z, \bar{z}) = z^{-\alpha(\frac{l}{2}-k)} \bar{z}^{-\bar{\alpha}(\frac{l}{2}-\bar{k})} \mathcal{V}_{l,l-k-\bar{k},k-\bar{k}}(z, \bar{z}). \quad (4.46)$$

Thus we observe that we can spectral flow the initial and final states, keep the vertex operator unchanged, and compute the amplitude

$$\mathcal{A}' = \langle f' | \mathcal{V}(z, \bar{z}) | i' \rangle. \quad (4.47)$$

The result we want, $\mathcal{A}_{\text{Ramond}}$, is then given by

$$\mathcal{A}_{\text{Ramond}} = z^{-\alpha(\frac{l}{2}-k)} \bar{z}^{-\bar{\alpha}(\frac{l}{2}-\bar{k})} \langle f' | \mathcal{V}(z, \bar{z}) | i' \rangle = z^{-\alpha(\frac{l}{2}-k)} \bar{z}^{-\bar{\alpha}(\frac{l}{2}-\bar{k})} \mathcal{A}'. \quad (4.48)$$

Here α is chosen to have a value that spectral flows from the NS to the Ramond sector, but this can be achieved by *any* odd integral value of α :

$$\alpha = (2n + 1) \quad \bar{\alpha} = (2\bar{n} + 1) \quad n, \bar{n} \in \mathbb{Z}. \quad (4.49)$$

For these values of α the initial and final states have weight and charge

$$\begin{aligned} h &= h' + (2n + 1)m' + (2n + 1)^2 \frac{c_{\text{tot.}}}{24} \\ m &= m' + (2n + 1) \frac{c_{\text{tot.}}}{12}, \end{aligned} \quad (4.50)$$

where $c_{\text{tot.}}$ is $c = 6$ times the number of copies being spectral flowed. A similar relation holds on the right sector.

In our present computation in the NS sector, we have

$$\begin{aligned} h'_i &= \frac{l}{2} + N + 1 & h'_f &= 0 \\ m'_i &= \frac{l}{2} - k & m'_f &= 0. \end{aligned} \quad (4.51)$$

In the next section we look at the Ramond sector process for $\alpha = \bar{\alpha} = 1$. In this case the weights and charges of the Ramond sector states are

$$\begin{aligned} h_i &= \frac{l}{2} + N + 1 + \left(\frac{l}{2} - k \right) + \frac{l+1}{4} & h_f &= (l+1) \frac{1}{4} \\ m_i &= \frac{l}{2} - k + \frac{l+1}{2} & m_f &= (l+1) \frac{1}{2}. \end{aligned} \quad (4.52)$$

We see that the final state has the weight and charge of the “spin-up” Ramond vacuum, while the initial state has the correct weight and charge above the Ramond vacuum. Although the current calculation is $\alpha = 1$, we leave α as an explicit parameter in following calculations for later use and illustration.

In section 4.2.6, the full α and $\bar{\alpha}$ dependence is of physical interest, since how big α and $\bar{\alpha}$ are roughly corresponds to how nonextremal the initial state is.

4.2.3 Evaluating the CFT Amplitude

Let us now compute the amplitude

$$\mathcal{A}'^{A\dot{A}}(\sigma, \tau) = \langle f' | \tilde{\mathcal{V}}(\sigma, \tau) | i' \rangle = |z|^{l+2} \langle f' | \mathcal{V}(z, \bar{z}) | i' \rangle. \quad (4.53)$$

We choose the charges of the initial state and the vertex operator so that we get a nonvanishing amplitude. The nonvanishing amplitude is

$$\mathcal{A}'^{A\dot{A}}_L = \frac{1}{\sqrt{2}} (\sigma^{\bar{i}})_{B\dot{B}} z^{\frac{l}{2}+1} {}_{NS} \langle \emptyset | \mathcal{V}_{L;l,k}^{A\dot{A}}(z) | \phi_{N+1}^{\frac{l}{2}, \frac{l}{2}-k} \rangle_L^{B\dot{B}} \quad (4.54)$$

where A, \dot{A} and \bar{i} are free indices. The \bar{i} is the index of the initial state excitation and A, \dot{A} are the indices on the vertex operator.

Let us note that

$$| \phi_{N+1}^{\frac{l}{2}, \frac{l}{2}-k} \rangle_L^{B\dot{B}} = (-1)^k \sqrt{\frac{(l+1)!}{N!(N+l+1)!}} L_{-1}^N \mathcal{V}_{L;l,2l-k}^{B\dot{B}}(0) | \emptyset \rangle_{NS} \quad (4.55)$$

and that the action of L_{-1} on a primary field \mathcal{O} is

$$L_{-1} \mathcal{O}(0) = \oint \frac{dz}{2\pi i} T(z) \mathcal{O}(0) = \partial \mathcal{O}(0). \quad (4.56)$$

Therefore, we may write

$$\langle \mathcal{V}_{L;l,k}^{A\dot{A}}(z) L_{-1}^N \mathcal{V}_{L;l,2l-k}^{B\dot{B}} \rangle = \epsilon^{AB} \epsilon^{\dot{A}\dot{B}} \lim_{v \rightarrow 0} \partial_v^N \frac{1}{(z-v)^{l+2}} = \frac{(N+l+1)!}{(l+1)!} \frac{1}{z^{\frac{l}{2}+N+1}} \quad (4.57)$$

and one finds the left amplitude reduces to the simple form

$$\mathcal{A}'_L^{A\dot{A}} = (-1)^k \frac{1}{\sqrt{2}} (\sigma^{\bar{i}})^{A\dot{A}} \frac{1}{z^{\frac{l}{2}+N+1}} \sqrt{\binom{N+l+1}{N}}. \quad (4.58)$$

From Equation (4.48), we find that the left part of the CFT amplitude in the Ramond sector is given by

$$\begin{aligned} \mathcal{A}_L^{A\dot{A}} &= z^{-\alpha(\frac{l}{2}-k)} \mathcal{A}'_L \\ &= (-1)^k \frac{1}{\sqrt{2}} (\sigma^{\bar{i}})^{A\dot{A}} \frac{1}{z^{(1+\alpha)\frac{l}{2}-\alpha k+N+1}} \sqrt{\binom{N+l+1}{N}}. \end{aligned} \quad (4.59)$$

Finally, converting back to $SO(4)$ indices for the vertex operator, one gets in the Ramond sector

$$\begin{aligned} \mathcal{A}_L^{\bar{i}}(z) &= \frac{1}{\sqrt{2}} (\sigma^{\bar{i}})_{A\dot{A}} \mathcal{A}_L^{A\dot{A}} \\ &= (-1)^{k+1} \frac{1}{z^{(1+\alpha)\frac{l}{2}-\alpha k+N+1}} \sqrt{\binom{N+l+1}{N}}, \end{aligned} \quad (4.60)$$

The free index \bar{i} and a similar index from the right movers \bar{j} correspond to the indices ϕ_{ij} for the field coupling to the emission vertex.

4.2.4 Combinatorics

The full CFT has $N_1 N_5$ copies of the basic $c = 6$ CFT. In the above section, we took a set of $l+1$ copies twisted together, and look at an emission process where the emission vertex untwists these copies. Now, we must put this computation in its full CFT context, by doing the following:

1. We must compute the combinatorics of how we pick the particular way of twisting $l+1$ copies in the initial state from all $N_1 N_5$ copies.
2. We must similarly consider all the ways that the vertex operator can twist copies. This allows us to normalize the vertex operator in the full theory so that we reproduce (3.27).
3. We can take the limit $N_1 N_5 \rightarrow \infty$ to get the “classical limit” of the D1D5 system; the result in this limit should agree with the computation in the dual supergravity theory.

In fact we start with something a little more general. We assume that the initial state has ν quanta of the same kind, and let the emission process lead to the final state with $\nu - 1$ quanta. We then observe a Bose enhancement of the emission amplitude by a factor $\sqrt{\nu}$, which agrees with the enhancement observed in both CFT and dual gravity computations in [180].

The Initial State

We wish to have ν excitations, each of which involve twisting together $l + 1$ copies of the $c = 6$ CFT. We can pick the needed copies in any way from the full set of $N_1 N_5$ copies, and because of the orbifold symmetry between these copies the state must be a symmetrized sum over these possibilities:

$$|\Psi_\nu\rangle = \mathcal{C}_\nu \left[|\psi_\nu^1\rangle + |\psi_\nu^2\rangle + \dots \right], \quad (4.61)$$

where \mathcal{C}_ν is the overall normalization and each $|\psi_\nu^i\rangle$ is individually normalized. To understand what we are doing better, note that the state $|\psi_\nu^1\rangle$ can be written schematically as

$$|\psi_\nu^1\rangle = |[12 \cdots (l+1)] [(l+2) \cdots 2(l+1)] \cdots [(\nu(l+1) - l) \cdots \nu(l+1)]\rangle, \quad (4.62)$$

where the numbers in the square brackets are indicating particular ways of twisting individual strands corresponding to particular cycles of the permutation group. For instance,

$$|[1234]\rangle, \quad (4.63)$$

indicates that we twist strand 1 into strand 2 into strand 3 into strand 4 into strand 1 and leave strands 5 through $N_1 N_5$ untwisted.

Our first task is to determine the number of terms in Equation (4.61) and thereby its normalization \mathcal{C}_ν . To count the number of states we imagine constructing one of these states and see how many choices we have along the way. First, we choose $\nu(l+1)$ of the total $N_1 N_5$ strands that are going to be twisted in some way. The remaining strands are untwisted. Those $\nu(l+1)$ strands must now be broken into sets of $l+1$. To do this, we first choose $l+1$ of the $\nu(l+1)$, then the next set of $l+1$ from the remaining $(\nu-1)(l+1)$, and so on. Note that $|[12][34]\rangle = |[34][12]\rangle$, and so there is no sense in talking about the “first” set versus the “second set.” Therefore we should divide by the number of ways to rearrange the ν sets of $l+1$. Finally, we should choose a particular cycle for each set of $(l+1)$; since it does not matter where we start on the final cycle, this gives a factor $l!$ for each twisted cycle. Putting all of these factors together yields the number of terms in Equation (4.61),

$$N_{\text{terms}} = \binom{N_1 N_5}{\nu(l+1)} \times \binom{\nu(l+1)}{l+1} \binom{(\nu-1)(l+1)}{l+1} \cdots \binom{l+1}{l+1} \times \frac{1}{\nu!} \times (l!)^\nu$$

$$= \frac{(N_1 N_5)!}{(l+1)^\nu \nu! [N_1 N_5 - \nu(l+1)]!}. \quad (4.64)$$

Without loss of generality, let us choose \mathcal{C}_ν to be real, which gives

$$\mathcal{C}_\nu = \left[\frac{(N_1 N_5)!}{(l+1)^\nu \nu! [N_1 N_5 - \nu(l+1)]!} \right]^{-\frac{1}{2}}. \quad (4.65)$$

The Final State

The final state is simply $|\Psi_{\nu-1}\rangle$, with its corresponding normalization $\mathcal{C}_{\nu-1}$.

The Vertex Operator

The vertex operator can twist together any $l+1$ copies of the CFT with any $l+1$ -cycle, and it should be written as a symmetrized sum over these possibilities:

$$\mathcal{V}_{\text{sym}} = \mathcal{C} \sum_i \mathcal{V}_i. \quad (4.66)$$

Since the joined copies form a single long loop, the order of copies matters but not which copy is the “first one” in the loop. Thus the number of terms in the sum is

$$\binom{N_1 N_5}{l+1} l! = \frac{(N_1 N_5)!}{(l+1) [N_1 N_5 - (l+1)]!}. \quad (4.67)$$

This gives the normalization

$$\mathcal{C} = \left[\frac{(N_1 N_5)!}{(l+1) [N_1 N_5 - (l+1)]!} \right]^{-\frac{1}{2}}. \quad (4.68)$$

The Amplitude

To compute the amplitude

$$\langle \Psi_{\nu-1} | \mathcal{V}_{\text{sym}} | \Psi_\nu \rangle, \quad (4.69)$$

we have to count the different ways that terms in the initial state can combine with terms in the vertex operator and terms in the final state to produce a nonzero amplitude. For a given initial state term $|\psi_\nu^i\rangle$, there are exactly ν vertex operators \mathcal{V}_i that can de-excite it into a final state. There is only one final state that works, obviously. Thus the number of ways that we can get a nonzero amplitude is simply

$$\nu N_{\text{terms}} = \frac{\nu}{\mathcal{C}_\nu^2}.$$

Let

$$\langle \psi_{\nu-1}^1 | \mathcal{V}_1 | \psi_\nu^1 \rangle \quad (4.70)$$

be the amplitude obtained by using only one allowed initial state $|\psi_\nu^1\rangle$ from the set in Equation (4.61) and one allowed vertex operator \mathcal{V}_1 from the set in Equation (4.66). Then we have

$$\begin{aligned}\langle\Psi_{\nu-1}|\mathcal{V}_{\text{sym.}}|\Psi_\nu\rangle &= \mathcal{C}\mathcal{C}_\nu\mathcal{C}_{\nu-1} \cdot \frac{\nu}{\mathcal{C}_\nu^2} \langle\psi_{\nu-1}^1|\mathcal{V}_1|\psi_\nu^1\rangle \\ &= \sqrt{\nu} \sqrt{\frac{[N_1N_5 - (\nu-1)(l+1)]![N_1N_5 - (l+1)]!}{[N_1N_5 - \nu(l+1)]!(N_1N_5)!}} \langle\psi_{\nu-1}^1|\mathcal{V}_1|\psi_\nu^1\rangle\end{aligned}\quad (4.71)$$

The Large N_1N_5 Limit

We are ultimately interested in the limit of large N_1N_5 . Then we have

$$\frac{[N_1N_5 - (\nu-1)(l+1)]!}{[N_1N_5 - \nu(l+1)]!} \longrightarrow (N_1N_5)^{l+1} \quad \frac{[N_1N_5 - (l+1)]!}{(N_1N_5)!} \longrightarrow (N_1N_5)^{-(l+1)}, \quad (4.72)$$

which gives

$$\langle\Psi_{\nu-1}|\mathcal{V}_{\text{sym.}}|\Psi_\nu\rangle \longrightarrow \sqrt{\nu} \langle\psi_{\nu-1}^1|\mathcal{V}_1|\psi_\nu^1\rangle. \quad (4.73)$$

The prefactor $\sqrt{\nu}$ gives a “Bose enhancement” effect which tells us that if we start with ν quanta, the amplitude to emit another quantum is amplified by a factor $\sqrt{\nu}$ (compared to the case when there was only one quantum). This gives an enhancement ν in the probability, which just tells us that if we start with ν quanta in the initial state, then the rate of emission is proportional to ν .

4.2.5 The Rate of Emission

We now put together all the computations of the above sections to get the emission rate for a quantum from the excited CFT state. We need to do the following:

1. We use (4.73) to relate the decay amplitude for one $(l+1)$ -permutation to the amplitude with all the required symmetrizations put in

$$\langle\Psi_0|\mathcal{V}_{\text{sym.}}|\Psi_1\rangle = \sqrt{\nu} \langle\psi_0^1|\mathcal{V}_1|\psi_1^1\rangle. \quad (4.74)$$

2. From Equation (4.60), we have the decay amplitude for a given $l+1$ -permutation (we put the right sector back in now):

$$\begin{aligned}\langle\psi_0^1|\mathcal{V}_1|\psi_1^1\rangle &= \mathcal{A}^{\bar{i}\bar{j}}(z, \bar{z}) \\ &= (-1)^{k+\bar{k}} \sqrt{\binom{N+l+1}{N} \binom{\bar{N}+l+1}{\bar{N}}} z^{-(\alpha+1)\frac{l}{2}+\alpha k-N-1} \bar{z}^{-(\bar{\alpha}+1)\frac{l}{2}+\bar{\alpha}\bar{k}-\bar{N}-1}.\end{aligned}\quad (4.75)$$

We now rotating back to Lorentzian signature and replacing τ, σ by the physical (t, y) coordinates. Note that we are still working with a CFT with spatial section of “unit size” where the spatial circle has length (2π) . The “unit-sized” amplitude is thus

$$\mathcal{A}_{\text{unit}}^{\bar{i}\bar{j}}(t, y) = (-1)^{k+\bar{k}} \sqrt{\binom{N+l+1}{N} \binom{\bar{N}+l+1}{\bar{N}}} \times e^{\frac{i}{R}(-(\alpha+1)\frac{l}{2}+\alpha k-N-1)(y+t)} e^{-\frac{i}{R}(-(\bar{\alpha}+1)\frac{l}{2}+\bar{\alpha}\bar{k}-\bar{N}-1)(y-t)}. \quad (4.76)$$

3. From Equation (4.76) or by comparing the initial and final states, we can read off

$$\begin{aligned} E_0 &= \frac{1}{R} [(\alpha + \bar{\alpha} + 2)\frac{l}{2} - \alpha k - \bar{\alpha}\bar{k} + N + \bar{N} + 2] = \frac{1}{R} [2l - k - \bar{k} + N + \bar{N} + 2] \\ \lambda_0 &= \frac{1}{R} [-(\alpha - \bar{\alpha})\frac{l}{2} + \alpha k - \bar{\alpha}\bar{k} - N + \bar{N}] = \frac{1}{R} [k - \bar{k} - N + \bar{N}], \end{aligned} \quad (4.77)$$

where we have set $\alpha = \bar{\alpha} = 1$ for the physical process of interest. We also can determine the “unit-sized” amplitude with the position dependence removed,

$$\langle f | \mathcal{V} | i \rangle_{\text{unit}} = \mathcal{A}_{\text{unit}}^{\bar{i}\bar{j}}(0, 0) = (-1)^{k+1} \sqrt{\nu} \sqrt{\binom{N+l+1}{N} \binom{\bar{N}+l+1}{\bar{N}}}. \quad (4.78)$$

Putting this into Equation (3.65), one finds the final emission rate

$$\frac{d\Gamma}{dE} = \nu \frac{2\pi}{2^{2l+1}l!^2} \frac{(Q_1 Q_5)^{l+1}}{R^{2l+3}} (E^2 - \lambda^2)^{l+1} \binom{N+l+1}{N} \binom{\bar{N}+l+1}{\bar{N}} \delta_{\lambda, \lambda_0} \delta(E - E_0). \quad (4.79)$$

This is the emission rate for one of ν excitations in the CFT to de-excite and emit a super-gravity particle with energy E_0 , S^1 -momentum λ_0 , and angular momentum

$$\begin{aligned} m_\psi &= -(m + \bar{m}) = -l + k + \bar{k} \\ m_\phi &= m - \bar{m} = \bar{k} - k. \end{aligned} \quad (4.80)$$

The angular momentum can be read off from the angular momentum of the NS sector initial state, or the difference in angular momentum between the initial and final physical states.

The expression for the emission rate obtained above matches the one obtained in [122] where it is given in a slightly different form. There the expression for a minimally coupled scalar to be absorbed into the geometry and re-emerge is given in Equation (5.34) along with the time of travel in Equation (5.33). The total probability is the product of the probabilities to be absorbed and to re-emerge, which are equal. Therefore, the rate of emission is the square root of the total probability, with the energy and other quantum numbers taking the corresponding values for excitations in the background, divided by the time of travel.

This expression is seen to match the emission rate obtained above.

4.2.6 Emission from Nonextremal Microstates

From a physics point of view the emission computed above corresponds to a very simple process. We take an extremal 2-charge D1D5 microstate, excite it by adding a quantum, and compute the rate at which the state de-excites by emitting this quantum.

But this same computation can be slightly modified to obtain the emission rate for a more interesting physical process. We start with a nonextremal D1D5 microstate which has a large energy above extremality. This particular microstate is obtained by taking an extremal D1D5 microstate and performing a spectral flow on both the left and right moving sectors. Such a spectral flow adds fermionic excitations to *every* component string. Thus we get a large energy above extremality, not just the energy of one nonextremal quantum as was the case with our earlier computations [121, 122, 168].

This nonextremal state emits radiation, and we wish to compute the rate of emission after ν quanta have been emitted. We again get the “Bose enhancement” like that in (4.73), so that the rate of emission keeps increasing as more quanta are emitted. In [180] it was shown that the resulting decay behavior is exactly the Hawking radiation expected from this particular microstate. But the computation of [180] was restricted to certain choices of spins and excitation level $N = 0$ for the emitted quantum; now we are able to get a general expression for all values of spins and N .

The CFT Process

As discussed earlier, the physical D1D5 system is in the Ramond sector. We can relate Ramond sector states to NS sector states by spectral flow. Recall that under spectral flow the dimensions and charges change as follows:

$$\begin{aligned} h' &= h + \alpha m + \frac{c\alpha^2}{24} \\ m' &= m + \frac{c\alpha}{12}. \end{aligned} \tag{4.81}$$

If we start with the NS vacuum $|\emptyset\rangle_{NS}$ and spectral flow by $\alpha = 1$, we reach the Ramond vacuum state with $h = \frac{c}{24}$. But we can also reach a Ramond state by spectral flow by $\alpha = 3, 5, \dots$, which are excited states with energy more than the energy of the Ramond vacua. Let us take our initial state in the Ramond sector to be the state obtained by spectral flow of $|\emptyset\rangle_{NS}$ by $\alpha = 2n + 1$ on the left and $\bar{\alpha} = 2\bar{n} + 1$ on the right. The spectral flow adds fermions to the left and right sectors, raising the level of the Fermi sea on both these sectors. Thus we get an excited state of the D1D5 system, which we depict in Fig. 4.2(b).

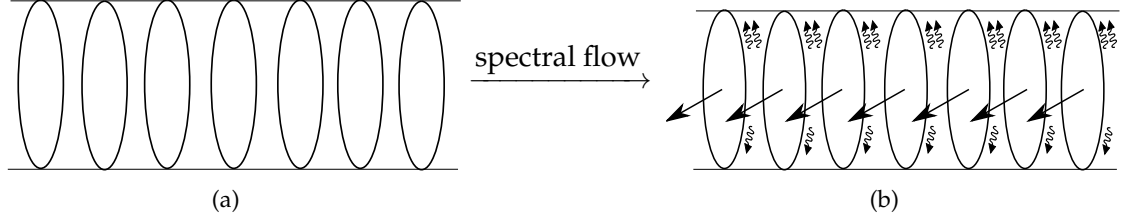


Figure 4.2: (a) The NS vacuum state in the CFT and (b) the CFT state after spectral flow. The arrows at the center of the circle indicate the “base spin” of component strings in the Ramond sector. The wavy arrows on top (bottom) of the strands represent fermionic excitations in the left (right) sector.

The vertex operator we have constructed can twist together $l + 1$ copies of the CFT. In our earlier computation, we started with a set of twisted copies, and the vertex operator “untwisted” these, leading to a final state with no twists. This time the initial state has all copies of the CFT “untwisted,” but these copies are all in an excited state. The vertex operator can therefore twist together $l + 1$ copies, leading to a twisted component string in the final state. Even though twisting a set of strings increases the energy, this component string in the final state can have lower energy than the strings in the initial state because of the fermionic excitations present on the initial component strings. The energy difference between the initial and final states is the energy of the emitted supergravity particle.

Let us now set up the CFT computation needed for this process. We observe that the amplitude can be obtained in a simple way from the amplitude that we have already computed.

The Initial State

As before, we do all our computations in the NS sector. If we spectral flow the starting state depicted in Fig. 4.2(b) by $-(2n + 1)$ units, we arrive at the NS vacuum $|\emptyset\rangle_{NS}$ depicted in Fig. 4.2(a). It may appear that this vacuum state cannot lead to any emission, but recall that we have used spectral flow only as a technical trick; the actual initial state has a much higher energy, and indeed leads to emission.

If we wanted to start with this state and proceed with the computation we would set $|i'\rangle = |\emptyset\rangle_{NS}$. But we instead look at a slightly more general situation where $\nu - 1$ quanta have already been emitted. In this case, the initial state looks like the one depicted in Fig. 4.4(c), where $\nu - 1$ sets of $l + 1$ copies have already been twisted together.

This may look like a complicated initial state, but we look only at a specific amplitude: the amplitude for emission of a further quantum of the same kind as the quanta already present. This process therefore requires us to take $l + 1$ of the *untwisted* copies of the

CFT, and use the vertex operator to twist them together. The other copies of the CFT are unaffected by the vertex operator. Thus, for the purposes of computing the amplitude, the initial state of the $l + 1$ copies of interest is

$$|i'\rangle = |\emptyset\rangle_{NS}. \quad (4.82)$$

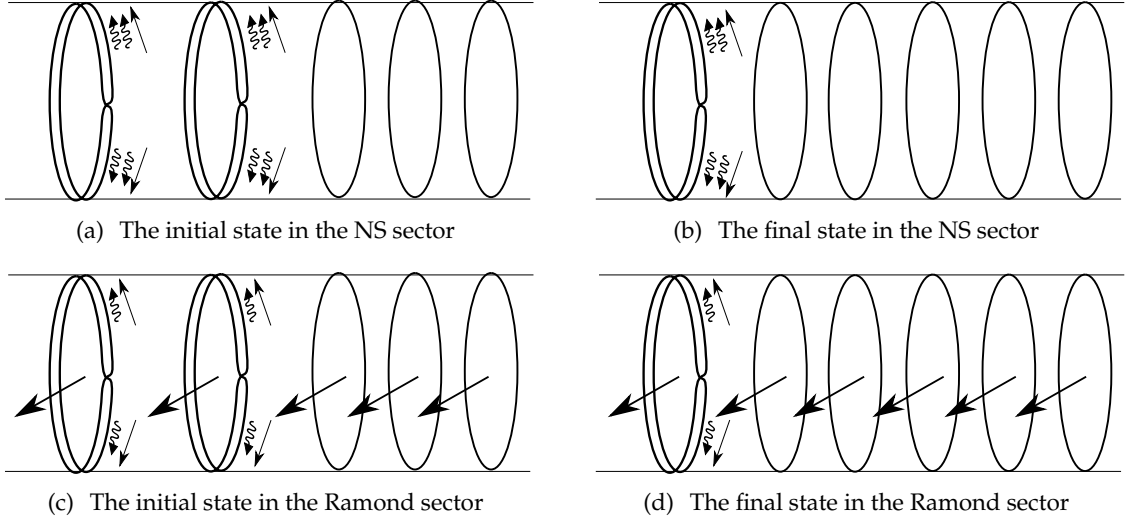


Figure 4.3: The initial and final states for the emission process discussed in Sections 4.2.1, 4.2.3, and 4.2.5. The pictures correspond to $\nu = 2$ and $l = 1$ emission. The straight arrows pointing up (down) on the loops indicate bosonic excitations in the left (right) sector.

The Final State

The final state is determined by the fact that we are looking for the amplitude to transition to a supergravity state, and we have a unique supergravity excitation with given twist and angular quantum numbers. Working again in the NS sector, arrived at by spectral flow by $-(2n + 1)$ units, we get

$$|f'\rangle = |\phi_{N+1}^{\frac{l}{2}, \frac{l}{2}-k}\rangle; \quad (4.83)$$

the initial state of our previous calculation.

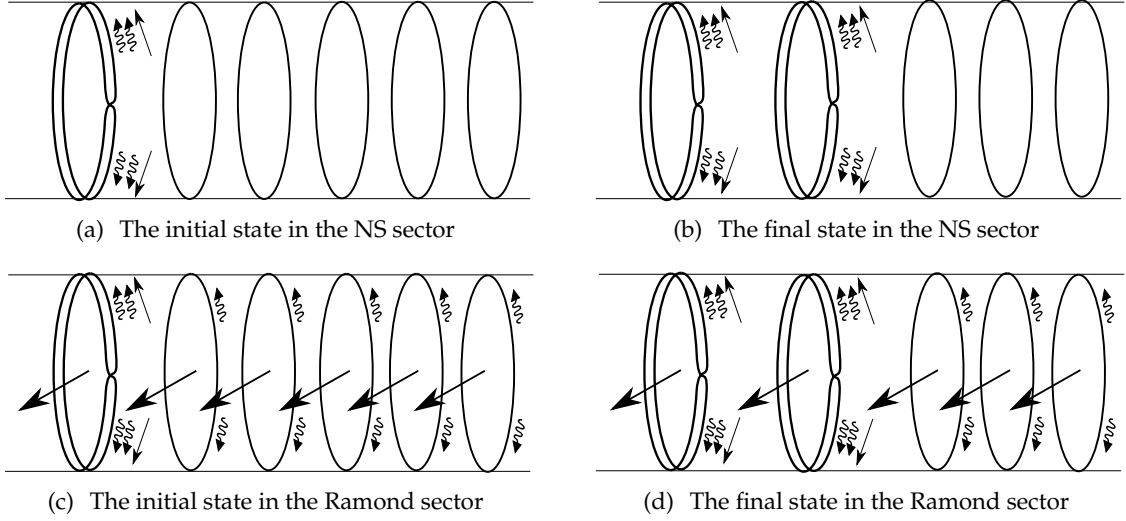


Figure 4.4: The initial and final states for the nonextremal emission process discussed in Section 4.2.6. The specific case depicted is $\nu = 2$ and $l = 1$.

The Vertex Operator

The vertex operator is independent of the states it acts on. It is completely determined by the supergravity scalar to which it couples in Equation (3.52).

We now see that the present process is similar to the amplitude we computed earlier if we reverse the direction of time τ . That is, the initial state now is untwisted, while in our earlier computation the *final* state was untwisted. The vertex operator then leads to a final twisted state, and since there is a unique supergravity state with given quantum numbers, we can write down this state.

Relating the Emission Amplitude to the Earlier Computed Amplitude

We term the supergravity excitation emission in the previous sections “untwisting” emission since a twisted component string in the initial state “untwists” under the action of the vertex operator and leads to a final state with no twists. We call the emission of the present section “twisting” emission since the initial state has no twists, and the vertex operator leads to a twisted component string in the final state.

By comparing the initial and final states of the two process, we immediately see that the current NS sector twisting amplitude is simply the Hermitian conjugate of the previous NS sector untwisting amplitude,

$$\mathcal{A}_{l,m_\psi,m_\phi}^{\text{twisting}}(t,y) = [\mathcal{A}_{l,-m_\psi,-m_\phi}^{\text{untwisting}}(-t,y)]^\dagger, \quad (4.84)$$

with flipped $SO(4)_E$ charges and reversed time. In the complex plane, this statement becomes

$$\mathcal{A}'_{l,m_\psi,m_\phi}{}^{\text{twisting}}(z,\bar{z}) = [\mathcal{A}'_{l,-m_\psi,-m_\phi}{}^{\text{untwisting}}(\frac{1}{\bar{z}},\frac{1}{z})]^\dagger. \quad (4.85)$$

To see the above relation explicitly, consider the Hermitian conjugate of the previous, untwisting amplitude:

$$\begin{aligned} [\mathcal{A}'_{l,m_\psi,m_\phi}{}^{\text{untwisting}}(z,\bar{z})]^\dagger &= [|z|^{l+2} \langle f' | \mathcal{V}_{l,m_\psi,m_\phi}(z,\bar{z}) | i' \rangle]^\dagger \\ &= |z|^{l+2} \langle i' | [\mathcal{V}_{l,m_\psi,m_\phi}(z,\bar{z})]^\dagger | f' \rangle \\ &= \frac{1}{|z|^{l+2}} \langle i' | \mathcal{V}_{l,-m_\psi,-m_\phi}(\frac{1}{\bar{z}},\frac{1}{z}) | f' \rangle, \end{aligned} \quad (4.86)$$

where the i' and f' are from the previous calculation. The amplitude we now wish to compute is (in terms of the previous calculation's states)

$$\mathcal{A}'_{l,m_\psi,m_\phi}{}^{\text{twisting}}(z,\bar{z}) = |z|^{l+2} \langle i' | \mathcal{V}_{l,m_\psi,m_\phi}(z,\bar{z}) | f' \rangle \quad (4.87)$$

Comparing these two expressions, one arrives at Equation (4.85).

From Equation (4.60), we have

$$\mathcal{A}'^{\text{untwisting}}(z,\bar{z}) = (-1)^{k+\bar{k}} \sqrt{\binom{N+l+1}{N} \binom{\bar{N}+l+1}{\bar{N}}} z^{-\frac{l}{2}-N-1} \bar{z}^{-\frac{l}{2}-\bar{N}-1}, \quad (4.88)$$

and so using Equation (4.85) gives

$$\mathcal{A}'^{\text{twisting}} = (-1)^{k+\bar{k}} \sqrt{\binom{N+l+1}{N} \binom{\bar{N}+l+1}{\bar{N}}} z^{\frac{l}{2}+N+1} \bar{z}^{\frac{l}{2}+\bar{N}+1}. \quad (4.89)$$

Note that this amplitude is in the NS sector, and before we can use it to get emission we have to spectral flow it to the Ramond sector. Spectral flowing by $\alpha = 2n + 1$ units to the Ramond sector gives

$$\begin{aligned} \mathcal{A}_{\text{twisting}}^{(\alpha,\nu)} &= z^{-\alpha(\frac{l}{2}-k)} \bar{z}^{-\bar{\alpha}(\frac{l}{2}-\bar{k})} \mathcal{A}'^{\nu}_{\text{twisting}} \\ &= (-1)^{k+\bar{k}} \sqrt{\nu} \sqrt{\binom{N+l+1}{N} \binom{\bar{N}+l+1}{\bar{N}}} z^{\frac{l}{2}+N+1-\alpha(\frac{l}{2}-k)} \bar{z}^{\frac{l}{2}+\bar{N}+1-\bar{\alpha}(\frac{l}{2}-\bar{k})} \end{aligned} \quad (4.90)$$

where we have put the combinatoric factor in as well. Note that the combinatorics work out the same as before since the combinatorics cannot be affected by Hermitian conjugation; however, the interpretation is different. The initial state starts with $\nu - 1$ sets of $(l + 1)$ -twisted component strings, while the final state has ν $(l + 1)$ -twisted component strings. Therefore, if at some initial time all of the strands were untwisted and each twist corresponds to an emitted supergravity particle, then the above is the amplitude for the

emission of the ν th particle.

Comparing Equation (4.90) with Equation (4.75), we see that the amplitudes agree except for the power of z , which is different because of the different energies of the concerned states in the two processes. Thus we can immediately write down the emission rate for the ν th particle from the cap into the flat space

$$\frac{d\Gamma}{dE} = \nu \frac{2\pi}{2^{2l+1}l!^2} \frac{(Q_1 Q_5)^{l+1}}{R^{2l+3}} (E^2 - \lambda^2)^{l+1} \binom{N+l+1}{N} \binom{\bar{N}+l+1}{\bar{N}} \delta_{\lambda, \lambda_0} \delta(E - E_0) \quad (4.91)$$

where

$$\begin{aligned} E_0 &= \frac{1}{R} [(\alpha + \bar{\alpha} - 2)\frac{l}{2} - \alpha k - \bar{\alpha} \bar{k} - N - \bar{N} - 2] \\ \lambda_0 &= \frac{1}{R} [-(\alpha - \bar{\alpha})\frac{l}{2} + \alpha k - \bar{\alpha} \bar{k} + N - \bar{N}]. \end{aligned} \quad (4.92)$$

For sufficiently large α or $\bar{\alpha}$, E_0 is positive and the physical process is emission and not absorption. In taking the hermitian conjugate we have flipped the the angular momentum of the emitted particle from that in Equation (4.80); therefore, the above emission rate is for

$$m_\psi = l - k - \bar{k} \quad m_\phi = k - \bar{k}. \quad (4.93)$$

One can check that the emission rate above agrees with the emission rate from the gravity dual [178, 180]. Such a check was carried out in [180] only for states with excitation level $N = 0$, because it was not clear how to construct the initial state for $N > 0$ in the effective string description of the D1D5 bound state. With our present construction of states and vertex operators in the orbifold CFT, we can compute amplitudes for emission of supergravity quanta from all initial states containing supergravity excitations.

4.3 Reproducing $\kappa > 1$ Emission

In this section, we extend the results by computing the emission from a broader class of D1D5 states; those with $\kappa > 1$. The above calculation only reproduces the supergravity emission and spectrum for the JMaRT geometries with $\kappa = 1$.

The calculation may be broken into the following steps:

1. In Section 4.3.1, we set up the physical emission problem from the geometries of [168] for $\kappa > 1$, in the CFT language developed in [158]. Specifically, we describe the initial excited state and the final state that go into the CFT amplitude, which when plugged into Equation (3.65) give the emission rate of the minimal scalars. Evaluating the CFT amplitude is a nontrivial exercise, to which the majority of Section 4.3 is dedicated. The initial state is parameterized by three integers n , \bar{n} , and κ . The positive integer κ , called k in [182], controls a conical defect in the AdS region. The spectrum and rate

of emission found in the previous section are for $\kappa = 1$. We extend those calculations to $\kappa > 1$.

2. We do not directly compute the physical CFT amplitude of interest. Instead, we compute a CFT amplitude that does *not* correspond to a physical gravitational process, and then map this “unphysical” amplitude onto the physical problem using spectral flow and hermitian conjugation. This route avoids some subtleties and allows us to use some results from the previous section (first derived in [158]) in the calculation. In Section 4.3.2, we precisely set up the unphysical CFT amplitude to be computed.
3. In Section 4.3.3, we show how to relate the unphysical amplitude to the physical problem using spectral flow and Hermitian conjugation.
4. Before starting the calculation of the unphysical CFT amplitude, in Section 4.3.4 we explain the specific method used to compute it. The unphysical amplitude, we explain, can be lifted to a covering space, where it becomes an amplitude computed in Section 4.2.6. The Jacobian factors that arise in mapping to the covering space, however, are highly nontrivial. Additionally there are some important combinatoric factors, which come in from symmetrizing over all $N_1 N_5$ copies of the CFT.
5. In Section 4.3.5, we compute the Jacobian factors that arise from mapping the twist operators to the covering space. We use the methods for evaluating correlation functions of twist operators developed in [151]. For details, see Appendix D.
6. In Section 4.3.6, we compute the Jacobian factors produced by the non-twist operator insertions in the unphysical amplitude.
7. In Section 4.3.8, we compute the combinatoric factors that come from symmetrizing over all $N_1 N_5$ copies of the CFT. The result simplifies in the large $N_1 N_5$ limit that is physically relevant.
8. Finally in Section 4.3.9, we use Section 4.3.3 to relate the computed unphysical amplitude to the final amplitude for emission. We then plug the amplitude into Equation (3.65) to find the rate of emission. The explicit κ -dependence comes in the form of a power, κ^{-2l-3} , multiplying the rate for $\kappa = 1$; the spectrum is also affected. The spectrum and rate exactly match the gravity calculation in [182].

We take some results from the previous section.

4.3.1 Emission from κ -orbifolded Geometries

Below, we first describe the initial state of the physical CFT problem, which is dual to the unperturbed background geometry. Then, we roughly describe the final state of the

physical CFT amplitude that the initial state decays to. We do not precisely give these states since we do not directly compute with them. In Section 4.3.2, we give the precise states used in the “unphysical” CFT amplitude, which in Section 4.3.3 we relate to the physically relevant states of this section.

The CFT Initial State

The physical initial state is the background geometry described in [168] and [182]. The decoupled AdS-part of the geometry can be obtained by spectral flowing κ -orbifolded $AdS_3 \times S^3$ by $\alpha = 2n + \frac{1}{\kappa}$ units on the left-moving sector and by $\bar{\alpha} = 2\bar{n} + \frac{1}{\kappa}$ units on the right-moving sector. The fractional spectral flow may seem strange; however, it arises because of the conical defect. In [111, 112, 122] geometries were constructed which had a decoupled AdS part which can be understood in this context as spectral flow by $\alpha = 2n + \frac{1}{\kappa}$ and $\bar{\alpha} = \frac{1}{\kappa}$. However these geometries are BPS and do not have an ergoregion and thus do not radiate. We discuss fractional spectral flow in the CFT context in Section 4.3.3.

The κ -orbifolded AdS_3 is described, after a left and right spectral flow by $\frac{1}{\kappa}$, as twisting the $N_1 N_5$ strands into κ -length component strings in the R sector. This geometry is stable and does not emit anything. Performing further spectral flow, however, adds fermionic excitations to all of the component strings and allows for the possibility of emission.

The κ -twisted component string in the Ramond vacuum has weight $\kappa/4$. The Ramond vacuum also has “base spin” coming from the fermion zero modes. Let us start with the “spin up” κ -twisted Ramond vacuum with weight and charge

$$h = \bar{h} = \frac{\kappa}{4} \quad m = \bar{m} = \frac{1}{2}. \quad (4.94)$$

We then add energy and charge to this state by spectral-flowing by $2n$ units, where spectral flow by α units affects the weight and charge of a state by [149]

$$\begin{aligned} h &\mapsto h + \alpha m + \frac{\alpha^2 c_{\text{tot.}}}{24} \\ m &\mapsto m + \frac{\alpha c_{\text{tot.}}}{12}. \end{aligned} \quad (4.95)$$

Spectral flowing the κ -twisted Ramond vacuum by $2n$ units corresponds to filling all fermion energy levels up to the “Fermi sea level” $n\kappa$. Keep in mind that there are two complex fermions which have spin up and spectral flow fills fermion levels with both fermions. This gives the initial state’s weight and charge [182]

$$h_i = \kappa \left(n^2 + \frac{n}{\kappa} + \frac{1}{4} \right) \quad m_i = n\kappa + \frac{1}{2} \quad (4.96)$$

and similarly for the right sector replacing n by \bar{n} . Compare this to Equation (4.25). This state is depicted in Figure 4.5(a).

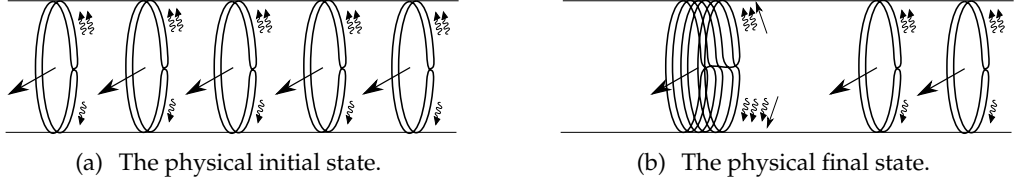


Figure 4.5: A depiction of the initial and final states of the physical amplitude for $\kappa = l = 2$.

The CFT Final State

In emitting a particle of angular momentum (l, m_ψ, m_ϕ) the initial state is acted on by the supergravity vertex operator $\mathcal{V}_{l, -m_\psi, -m_\phi}$ from Equation (4.35).

We consider the process where the $(l+1)$ -twist operator acts on $l+1$ distinct component strings of the background forming one long $\kappa(l+1)$ -twisted component string. The final state, then, is in the $\kappa(l+1)$ -twisted R sector. In principle there are other ways that the vertex operator may twist the initial state; however, we work in the limit where $N_1 N_5 \gg \kappa$, in which case this process dominates. Processes in which the vertex operator twists more than one strand of the same κ -length component string have probabilities suppressed by factors of $1/(N_1 N_5)$.

The charge/angular momentum of the vertex operator $\mathcal{V}_{l, l-k-\bar{k}, k-\bar{k}}$ is given by

$$\begin{aligned}
 m_v &= -\left(\frac{l}{2} - k\right) & m_\psi^{\text{vertex}} &= -m_\psi = l - k - \bar{k} \\
 \bar{m}_v &= -\left(\frac{l}{2} - \bar{k}\right) & m_\phi^{\text{vertex}} &= -m_\phi = k - \bar{k}.
 \end{aligned} \tag{4.97}$$

From the charge of the vertex operator and the initial state it is easy to deduce the charge of the final state:

$$m_f = (l+1) \left(n\kappa + \frac{1}{2}\right) - \left(\frac{l}{2} - k\right) = (l+1)n\kappa + k + \frac{1}{2}. \tag{4.98}$$

There can be different final states with the same charge corresponding to different harmonics of the emitted quanta. Since we derive the amplitude using spectral flowed states it is not important to write down the weights of the states here. However they are found easily by using the charge and weight of the spectral flowed states. The final state, which we call $|f\rangle$, is shown in Figure 4.5(b).

The Physical CFT Amplitude

From the initial and final states, the CFT amplitude which we use to find the emission spectrum and rate is given by

$$\mathcal{A}_{l,m_\psi,m_\phi} = \langle f | \tilde{\mathcal{V}}_{l,m_\psi,m_\phi}(\sigma, \tau) | i \rangle. \quad (4.99)$$

We prefer to calculate on the complex plane with z coordinates instead of on the cylinder. Mapping the vertex operator to the plane using Equation (4.36) gives a Jacobian factor, $|z|^{l+2}$, from its conformal weight. Thus, the physical CFT amplitude that we ultimately wish to find is written as

$$\mathcal{A}_{l,m_\psi,m_\phi}(z) = |z|^{l+2} \langle f | \mathcal{V}_{l,m_\psi,m_\phi}(z, \bar{z}) | i \rangle. \quad (4.100)$$

The majority of the calculation is expended in finding this amplitude. The tilde on the vertex operator in Equation (4.99) is to distinguish it from the operator in the complex plane.

4.3.2 The “Unphysical” Amplitude

We do not directly compute the amplitude of interest with the initial and final states described above. Instead we compute an amplitude, described below, that is related to the physical problem by spectral flow and Hermitian conjugation. In this other amplitude, the calculation is simpler and we have a better understanding of what the initial and final states should be. In Section 4.2, the same technique was used.

In this section we describe the initial and final states of the unphysical amplitude, $|i'\rangle$ and $|f'\rangle$, that we use to calculate

$$\mathcal{A}' = \langle f' | \mathcal{V}(z) | i' \rangle. \quad (4.101)$$

Later, we relate this process to the physical problem by spectral flow and Hermitian conjugation. Before we can give the states, we must describe the notation we use, specifically addressing the fermions’ periodicity.

Fermion Periodicities

First, let us emphasize what the R and NS sectors *mean* in the twisted sector. We define two parameters β_+ and β_- , which specify the periodicity of the fermions in the theory:

$$\psi^{\pm\dot{A}}(ze^{2\pi i}) = e^{i\pi\beta_\pm} \psi^{\pm\dot{A}}(z). \quad (4.102)$$

Obviously, β_\pm are only defined modulo two under addition.

The R sector means $\beta_{\pm} \equiv 1$, whereas the NS sector means $\beta_{\pm} \equiv 0$. Spectral flow by α units has the effect of taking

$$\beta_{\pm} \mapsto \beta_{\pm} \pm \alpha. \quad (4.103)$$

In the p -twisted sector, the boundary conditions are

$$\psi_{(j)}^{\pm\dot{A}}(ze^{2\pi i}) = e^{i\pi\beta_{\pm}} \psi_{(j+1)}^{\pm\dot{A}}(z), \quad (4.104)$$

where (j) indexes the different copies of the target space. This implies that

$$\psi_{(j)}^{\pm\dot{A}}(ze^{2p\pi i}) = e^{ip\pi\beta_{\pm}} \psi_{(j)}^{\pm\dot{A}}(z). \quad (4.105)$$

In the base space, over each point z , there are p different copies of each field. To calculate, it is convenient to map to a covering space where these p copies become a single-valued field. When one goes to a covering space the periodicity of the total single-valued field $\Psi(t)$, then is given by

$$\Psi^{\pm\dot{A}}(te^{2\pi i}) = \exp[i(p\beta_{\pm} + (p-1))\pi] \Psi^{\pm\dot{A}}(t), \quad (4.106)$$

where the extra factor of $(p-1)$ in the exponent comes from the Jacobian of the weight-half fermion, under a map of the form $z \propto t^p$. We label the periodicity in the cover by

$$\beta_{\pm}^{(\text{cover})} = p(\beta_{\pm} + 1) - 1. \quad (4.107)$$

In the untwisted sector, we use the natural definition of the fermions, $\psi(z)$, as being periodic, without branch cut. Thus, application of a spin field operator is necessary to give antiperiodic boundary conditions. In the twisted sector, the periodicity of fermions in the base space is neither “naturally” periodic nor antiperiodic since there is a hole and branch cut from the twist operator; however, in the covering space, the fields are, again, naturally periodic.

We denote “bare twists” which insert the identity in the cover as

$$\sigma_p(z, \bar{z}) \xrightarrow[\text{cover}]{\text{to the}} \mathbb{1}(t, \bar{t}) \quad h = \bar{h} = \Delta_p = \frac{c}{24} \left(p - \frac{1}{p} \right). \quad (4.108)$$

After the above discussion, we see that one should always use

$$(\text{NS Sector}) \implies \begin{cases} \sigma_p(z, \bar{z}) & p \text{ odd} \\ S_p^{\alpha}(z) \bar{S}_p^{\dot{\alpha}}(\bar{z}) \sigma_p(z, \bar{z}) & p \text{ even} \end{cases}, \quad (\text{R Sector}) \implies S_p^{\alpha}(z) \bar{S}_p^{\dot{\alpha}}(\bar{z}) \sigma_p(z, \bar{z}). \quad (4.109)$$

The S_p 's indicate that one should insert a spin field in the p -fold covering space at the image of the point z . In the above statement, one could equally well choose $SU(2)_2$ indices instead of $SU(2)_{L/R}$ indices for the spin fields.

The CFT amplitude we compute uses the bare twists, which for odd twist order correspond to the NS sector and for even twist order correspond to neither the NS nor the R sector. Even though this amplitude is not physically relevant, we can use spectral flow to relate it to the R sector process of physical interest. Below, we give the initial and final states of the unphysical amplitude, starting with the simpler final state.

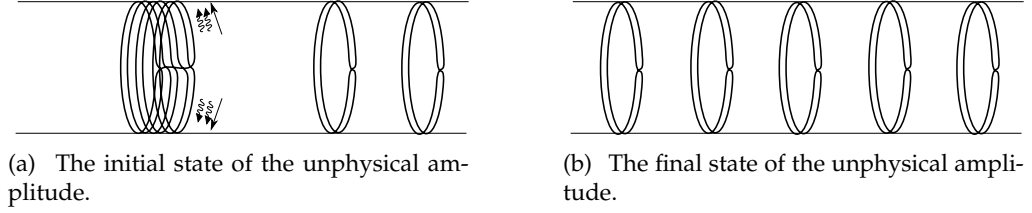


Figure 4.6: The initial and final states of the unphysical amplitude for $\kappa = l = 2$. The initial state spectral flows to the physical final state, and the final state spectral flows to the physical initial state.

The Final State

The *final* state²⁶ spectral flows to the *initial* state of the physical problem. All of the excitations and spin fields of the physical state can be acquired via spectral flow, so we use bare twists for the unphysical amplitude final state:

$$|f'\rangle = \underbrace{\sigma_\kappa \sigma_\kappa \cdots \sigma_\kappa}_{l+1} |\emptyset\rangle_{NS}. \quad (4.110)$$

This state has weight and charge

$$h_f = \bar{h}_f = \frac{1}{4}(l+1) \left(\kappa - \frac{1}{\kappa} \right) \quad m_f = \bar{m}_f = 0. \quad (4.111)$$

Note that for odd κ this state corresponds to the NS sector, but for κ even it corresponds to neither the NS nor the R sector. This state, which we call $|i\rangle$, is shown in Figure 4.6(b).

The Initial State

The *initial* state spectral flows to the physical final state, and therefore consists of excitations in the $\kappa(l+1)$ -twisted sector, as shown in Figure 4.6(a). Below, modulo normalization,

²⁶Here, we just discuss the $\kappa(l+1)$ strands that are involved in the nontrivial part of the correlator. Later, we introduce the combinatoric factors which result from symmetrizing over all $N_1 N_5$ copies of the CFT.

we give the left part of the state

$$|i'\rangle = (J_0^-)^k G_{-\frac{1}{2\kappa}}^{-A} (L_{-\frac{1}{\kappa}})^N \psi_{-\frac{1}{2\kappa}}^{\dot{A}} \begin{cases} J_{-\frac{l-1}{\kappa(l+1)}}^+ J_{-\frac{l-3}{\kappa(l+1)}}^+ \cdots J_{-\frac{1}{\kappa(l+1)}}^+ \sigma_{\kappa(l+1)} |\emptyset\rangle_{NS} & (l+1) \text{ odd} \\ J_{-\frac{l-1}{\kappa(l+1)}}^+ J_{-\frac{l-3}{\kappa(l+1)}}^+ \cdots J_{-\frac{2}{\kappa(l+1)}}^+ S_{\kappa(l+1)}^+ \sigma_{\kappa(l+1)} |\emptyset\rangle_{NS} & (l+1) \text{ even.} \end{cases} \quad (4.112)$$

The normalization of the state is κ -dependent, which plays an important role in the calculation as discussed in Section 4.3.6.

This state has weight and charge

$$h_i = \frac{1}{\kappa} \left(\frac{l}{2} + N + 1 \right) + \frac{1}{4} (l+1) \left(\kappa - \frac{1}{\kappa} \right) \quad m_i = \frac{l}{2} - k, \quad (4.113)$$

and similarly for the right sector. We conjecture the above form for the initial state based on the $\kappa = 1$ case in Section 4.2 and work done in [182] for $\kappa > 1$. The excited initial state should be dual to a supergravity excitation of the orbifolded-AdS background. In global AdS, one identifies the supergravity duals as the descendants of chiral primary states under the anomaly-free subalgebra; here, we propose the above modification for the κ -orbifolded background. This is motivated, in part, by the action of the vertex operator for absorption of supergravity particles on κ -orbifolded AdS.

The Amplitude

The amplitude we compute, then, is

$$\mathcal{A}'^\kappa = \langle f' | \mathcal{V}_{l,l-k-\bar{k},k-\bar{k}}(z_2) | i' \rangle. \quad (4.114)$$

Note that if we map to the κ -cover, then these states are the initial and final states of the $\kappa = 1$ calculation in Section 4.2. In mapping to a κ -covering space the final state's twist operators are removed, and the initial state's twist operator becomes an $(l+1)$ -twist. The J^+ modes acting on the initial state, along with the spin field for even $l+1$, act on the $(l+1)$ -twist in the κ -cover in precisely the correct way to form the lowest weight chiral primary twist operator of [152]:

$$J_{-\frac{l-1}{\kappa(l+1)}}^+ J_{-\frac{l-3}{\kappa(l+1)}}^+ \cdots \begin{cases} J_{-\frac{1}{\kappa(l+1)}}^+ \sigma_{\kappa(l+1)} \\ J_{-\frac{2}{\kappa(l+1)}}^+ S_{\kappa(l+1)}^+ \sigma_{\kappa(l+1)} \end{cases} \xrightarrow[\kappa\text{-cover}]{\text{to}} J_{-\frac{l-1}{l+1}}^+ J_{-\frac{l-3}{l+1}}^+ \cdots \begin{cases} J_{-\frac{1}{l+1}}^+ \sigma_{l+1} \\ J_{-\frac{2}{l+1}}^+ S_{l+1}^+ \sigma_{l+1} \end{cases} = \sigma_{l+1}^0. \quad (4.115)$$

We follow the notation of [158] by denoting the lowest weight chiral primary $(l+1)$ -twist operator, introduced in [152], as σ_{l+1}^0 . The above equation does not include Jacobian factors, computed in Sections 4.3.5 and 4.3.6, which are introduced in going to the κ -covering space.

The specific covering space to which we map preserves the form of the $(l+1)$ -twist vertex operator. The fact that going to a κ covering space gives the $\kappa = 1$ amplitude

along with the gravity description of the emission process, is precisely the motivation for introducing the specific form of the state $|i'\rangle$.

4.3.3 Relating the Computed CFT Amplitude to the Physical Problem

There are two steps needed to map the physical problem onto the unphysical CFT computation. First, we use spectral flow to map the physical states, $|i\rangle$ and $|f\rangle$, to the “primed states,” $|f'\rangle$ and $|i'\rangle$. Second, we use Hermitian conjugation to reverse the initial and final primed states.

Using Spectral Flow

We wish to relate a CFT amplitude computed with the unphysical “primed states,”

$$\mathcal{A}' = \langle f' | \mathcal{V}(z, \bar{z}) | i' \rangle, \quad (4.116)$$

to the physical amplitude in the Ramond sector. In this section, we show how to spectral flow [149, 153, 199] the physical problem in the R sector to the actual CFT amplitude we compute.

If spectral flowing the states $|i'\rangle$ and $|f'\rangle$ by α units is given by

$$|f'\rangle \mapsto |i\rangle = \mathcal{U}_\alpha |f'\rangle \quad \langle i' | \mapsto \langle f | = \langle i' | \mathcal{U}_{-\alpha}, \quad (4.117)$$

then we can compute the physical Ramond sector amplitude for emission of a particle with angular momentum (l, m_ψ, m_ϕ) by using

$$\begin{aligned} \mathcal{A}_{l, m_\psi, m_\phi} &= |z|^{l+2} \langle f | \mathcal{V}_{l, -m_\psi, -m_\phi}(z, \bar{z}) | i \rangle \\ &= |z|^{l+2} (\langle f | \mathcal{U}_\alpha) (\mathcal{U}_{-\alpha} \mathcal{V}_{l, -m_\psi, -m_\phi} \mathcal{U}_\alpha) (\mathcal{U}_{-\alpha} | i \rangle) \\ &= |z|^{l+2} \langle i' | \mathcal{V}'_{l, -m_\psi, -m_\phi}(z, \bar{z}) | f' \rangle. \end{aligned} \quad (4.118)$$

Note that one finds \mathcal{V}' by spectral flowing \mathcal{V} by $-\alpha$ units.

In [158], it was shown that the vertex operator transforms under spectral flow as

$$\mathcal{V}'_{l, l-k-\bar{k}, k-\bar{k}}(z, \bar{z}) = z^{-\alpha(\frac{l}{2}-k)} \bar{z}^{-\bar{\alpha}(\frac{l}{2}-\bar{k})} \mathcal{V}_{l, l-k-\bar{k}, k-\bar{k}}(z, \bar{z}). \quad (4.119)$$

We can use the vertex operator’s transformation to write

$$\mathcal{A}_{l, k+\bar{k}-l, \bar{k}-k} = z^{-\alpha(\frac{l}{2}-k)} \bar{z}^{-\bar{\alpha}(\frac{l}{2}-\bar{k})} |z|^{l+2} \langle i' | \mathcal{V}_{l, l-k-\bar{k}, k-\bar{k}}(z, \bar{z}) | f' \rangle. \quad (4.120)$$

Note that the primed states are reversed from what one would like.

The spectral flow parameter, α , is chosen to have a value that spectral flows the primed states to the physical states, which is achieved by

$$\alpha = 2n + \frac{1}{\kappa} \quad \bar{\alpha} = 2\bar{n} + \frac{1}{\kappa} \quad n, \bar{n} \in \mathbb{Z}. \quad (4.121)$$

Spectral flowing by non-integer units may seem strange, however, one can show that this results from the peculiar bare twist operators. Consider spectral flowing the bare twist σ_κ by $\frac{1}{\kappa}$ units, and recall that under spectral flow by α units

$$\beta_\pm \mapsto \beta_\pm \pm \alpha, \quad (4.122)$$

and

$$\beta_\pm^{(\text{cover})} = \kappa(\beta_\pm + 1) - 1. \quad (4.123)$$

The bare twist has $\beta_\pm^{(\text{cover})} = 0$, which after spectral flowing by $1/\kappa$ units becomes $\beta_\pm^{(\text{cover})} = 1$ consistent with the R boundary conditions in the base space. Similarly, one finds that the fermion periodicity of $|i'\rangle$ becomes correct for the R sector after spectral flowing by $1/\kappa$ units. After spectral flowing by $1/\kappa$ units to get to the R sector, we spectral flow by an even number of units to build up the fermionic excitations of the state $|i\rangle$.

Hermitian Conjugation

Having related the physical amplitude to

$$\langle i' | \mathcal{V}_{l, m_\psi, m_\phi}(z, \bar{z}) | f' \rangle, \quad (4.124)$$

we now wish to switch the initial and final primed states by Hermitian conjugation.

On the cylinder, the vertex operator Hermitian conjugates as

$$\left[\tilde{\mathcal{V}}_{l, m_\psi, m_\phi}(\tau, \sigma) \right]^\dagger = \tilde{\mathcal{V}}_{l, -m_\psi, -m_\phi}(-\tau, \sigma), \quad (4.125)$$

and therefore

$$\langle i' | \tilde{\mathcal{V}}_{l, m_\psi, m_\phi}(\tau, \sigma) | f' \rangle = \left[\langle f' | \tilde{\mathcal{V}}_{l, -m_\psi, -m_\phi}(-\tau, \sigma) | i' \rangle \right]^\dagger. \quad (4.126)$$

In the complex plane, this statement translates to

$$|z|^{l+2} \langle i' | \mathcal{V}_{l, m_\psi, m_\phi}(z, \bar{z}) | f' \rangle = |z|^{-(l+2)} \left[\langle f' | \mathcal{V}_{l, -m_\psi, -m_\phi}\left(\frac{1}{z}, \frac{1}{\bar{z}}\right) | i' \rangle \right]^\dagger. \quad (4.127)$$

Applying this result to Equation (4.120), we may write the physical CFT amplitude for emission of a particle with angular momentum $(l, k + \bar{k}, \bar{k} - k)$ as

$$\mathcal{A}_{l, k + \bar{k} - l, \bar{k} - k} = z^{-\alpha(\frac{l}{2} - k)} \bar{z}^{-\bar{\alpha}(\frac{l}{2} - \bar{k})} |z|^{-(l+2)} \left[\langle f' | \mathcal{V}_{l, k + \bar{k} - l, \bar{k} - k}\left(\frac{1}{z}, \frac{1}{\bar{z}}\right) | i' \rangle \right]^\dagger$$

$$= z^{-\frac{l}{2}-1-\alpha(\frac{l}{2}-k)} \bar{z}^{-\frac{l}{2}-1-\bar{\alpha}(\frac{l}{2}-\bar{k})} \left[\mathcal{A}'_{l, k+\bar{k}-l, \bar{k}-k} \left(\frac{1}{z}, \frac{1}{\bar{z}} \right) \right]^\dagger. \quad (4.128)$$

Thus, we compute the unphysical amplitude $\mathcal{A}'(z, \bar{z})$, and use the above relation to find the physical amplitude \mathcal{A} . The unphysical amplitude \mathcal{A}' is independent of k and \bar{k} , so we suppress the subscripts.

4.3.4 Method of Computation

The way we compute the CFT amplitude \mathcal{A}'^κ is by noting that if one were to lift to the κ -cover, the amplitude becomes $\mathcal{A}'^{\kappa=1}$ computed in Section 4.2.6. Specifically, if we transform to a coordinate u via the map

$$z = bu^\kappa \quad b = \frac{z_2}{u_2^\kappa}, \quad (4.129)$$

where u_2 is the image of the point z_2 ; then, the operators left in the correlator are exactly those for $\mathcal{A}'^{\kappa=1}$. In lifting to the cover, however, we do get some nontrivial “Jacobian factors” from the various operators in the correlator transforming under the map. Therefore, we write

$$\mathcal{A}'^\kappa = \left(\frac{\mathcal{A}'^\kappa}{\mathcal{A}'^{\kappa=1}} \right) \mathcal{A}'^{\kappa=1} = TM \mathcal{A}'^{\kappa=1}, \quad (4.130)$$

where we have written the Jacobian factors as the product of two contributions: one from the twists, T , and one from the modes, M .

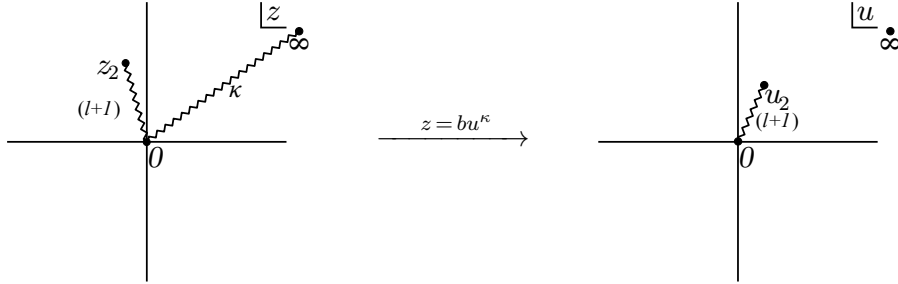


Figure 4.7: In the z -plane, there is a twist operator of order $\kappa(l+1)$ at the origin, a twist of order $l+1$ at a point we call z_2 , and $l+1$ κ -twists at infinity. The diagram on the left depicts the branch cuts connecting the three points. The number next to the branch cut depicts its “order.” One can remove the $l+1$ branch cuts of order κ between the origin and infinity by mapping to the u -coordinate, as shown in the figure on the right.

We begin with the lengthier calculation of the nontrivial factor T that comes from the twist operators transforming. One can see that T is given by the ratio

$$T = \lim_{z_3 \rightarrow \infty} |z_3|^{4(l+1)\Delta_\kappa} \frac{\langle \sigma_\kappa \dots \sigma_\kappa(z_3) \sigma_{l+1}(z_2) \sigma_{\kappa(l+1)}(0) \rangle}{\langle \sigma_{l+1}(u_2) \sigma_{l+1}(0) \rangle}, \quad (4.131)$$

where all of the above twists are “bare” twists which give *no* insertions in total $\kappa(l+1)$ -covering space. The z_3 prefactor ensures that in the limit as $z_3 \rightarrow \infty$ the $l+1$ twists at infinity make a normalized bra.

After computing T , we compute the mode Jacobian factor M , which is given by the product of all of the Jacobian factors that the modes circling the origin and the point z_2 acquire.

4.3.5 Computing the Twist Jacobian Factor T

Since the *effect* of the twist operators is inherently nonlocal, they do not transform in a simple local way when lifting to a covering space. The simplest way to compute the numerator of Equation (4.131), is by lifting to the total covering space and then computing the Liouville action that comes in conformally transforming the induced metric on the covering space to a fiducial metric. This is the method developed in [151]. Recently, [200, 201] developed new technology for correlators of $S_{N_1 N_5}$ -twist operators; however, we do not use those techniques here.

The denominator of Equation (4.131) is just the two-point function of some normalized twist operators, and so we know the answer:

$$\langle \sigma_{l+1}(u_2) \sigma_{l+1}(0) \rangle = \frac{1}{|u_2|^{\frac{c}{6}(l+1-\frac{1}{l+1})}} = \frac{1}{|u_2|^{4\Delta_{l+1}}}. \quad (4.132)$$

From the weights of the twist operators and $SL(2, \mathbb{C})$ invariance of the correlator, we know that any three-point function of quasi-primary fields must be given by

$$\begin{aligned} & \langle \mathcal{O}_3(z_3) \mathcal{O}_2(z_2) \mathcal{O}_1(z_1) \rangle \\ &= \frac{|C_{123}|^2}{(|z_1 - z_2|^{\Delta_1 + \Delta_2 - \Delta_3} |z_2 - z_3|^{\Delta_2 + \Delta_3 - \Delta_1} |z_3 - z_1|^{\Delta_3 + \Delta_1 - \Delta_2})^2}. \end{aligned} \quad (4.133)$$

In the present case where $z_3 = \infty$ and $z_1 = 0$, this gives (after regularizing the divergence which corresponds to correctly normalizing the final state)

$$\lim_{z_3 \rightarrow \infty} |z_3|^{4(l+1)\Delta_\kappa} \langle \sigma_\kappa \dots \sigma_\kappa(z_3) \sigma_{l+1}(z_2) \sigma_{\kappa(l+1)}(0) \rangle = \frac{|C|^2}{|z_2|^{2(\Delta_{\kappa(l+1)} + \Delta_{l+1} - (l+1)\Delta_\kappa)}}. \quad (4.134)$$

It is the constant C which is nontrivial and is determined in the calculation that follows. From the above, one sees that the twist Jacobian factor is completely determined by the

constant C :

$$T = |C|^2 \frac{|u_2|^{4\Delta_{l+1}}}{|z_2|^{2(\Delta_{\kappa(l+1)} + \Delta_{l+1} - (l+1)\Delta_{\kappa})}}. \quad (4.135)$$

To compute C in Equation (4.134) and thereby the twist Jacobian factor, T , we undertake the following steps:

1. We find the map to the total covering space, $z = z(t)$, that has the required properties.
2. We compute the Liouville action that comes from conformally mapping the induced metric of the total covering space to the fiducial form in Equation (D.7).
3. The above correlators are all of normalized twist operators. The normalization is such that the two-point function has unit correlator at unit separation, as determined in [151]. We put in the normalization factors, which cancel out the ε -dependence of the correlator.
4. Finally, we put all of the pieces together to determine C , and thereby T .

The Map to the Total Covering Space

The first step in the calculation of T , then, is to find the map to the total covering space. We have an $SL(2, \mathbb{C})$ symmetry of the covering space that allows us to fix three points. We fix the image of the origin of the z -plane to the origin of the t -plane, the image of z_2 ²⁷ to the point $t = 1$, and one image of $z = \infty$ to $t = \infty$. Having expended the $SL(2, \mathbb{C})$ symmetry, we do not have freedom to fix the locations of the other images of infinity in the covering space. We call the other images of infinity $t_{\infty}^{(j)}$, where $j = 1, \dots, l$.

Thus, we require our map to behave as

$$\begin{aligned} z &\sim t^{\kappa(l+1)} & z &\approx 0, \quad t \approx 0 \\ z - z_2 &\sim (t - 1)^{l+1} & z &\approx z_2, \quad t \approx 1 \\ z &\sim t^{\kappa} & z &\rightarrow \infty, \quad t \rightarrow \infty \\ z &\sim (t - t_{\infty}^{(j)})^{-\kappa} & z &\rightarrow \infty, \quad t \rightarrow t_{\infty}^{(j)}, \end{aligned} \quad (4.136)$$

and be regular at all other points. Here, \sim means proportional to at leading order. Generically, one expects $\kappa(l + 1)$ images of infinity. However, in this case there should only be $l + 1$ images of infinity since there are only $l + 1$ disconnected strings at $z \rightarrow \infty$. A priori, we do not know the $t_{\infty}^{(j)}$; this is part of the output in finding the map.

From the above conditions and requiring regularity everywhere but the above special points, we see that $\frac{dz}{dt}$ may have zeroes only at $t = 0$ (of degree $\kappa(l + 1) - 1$) and $t = 1$ (of

²⁷We should point out that there are other images of z_2 , but only $t = 1$ corresponds to where the vertex operator acts. The fact that there are other images of z_2 corresponds to the fact that the vertex operator only acts on $l + 1$ strands of the $\kappa(l + 1)$ initial strands.

degree l). The meromorphic map we want can be written as the ratio of two polynomials,

$$z = \frac{f_1(t)}{f_2(t)}, \quad (4.137)$$

where f_1 must be of degree $\kappa(l+1)$ and f_2 must be of degree κl , from the number of sheets and the behavior at infinity. Furthermore, near the origin we know that f_1 must behave as $t^{\kappa(l+1)}$ and f_2 a constant. Thus, we already have determined that

$$f_1 \propto t^{\kappa(l+1)}. \quad (4.138)$$

From familiarity with the two-point function map in [151] and consideration of the above requirements, one can immediately write down the correct map:

$$z = z_2 \frac{t^{\kappa(l+1)}}{[t^{l+1} - (t-1)^{l+1}]^\kappa}. \quad (4.139)$$

Note that when $\kappa = 1$, the map reduces to the usual two-point map between 0 and z_2 ; and when $l = 0$, the map reduces to

$$z = z_2 t^\kappa, \quad (4.140)$$

which is the correct map for a two-point function between 0 and infinity. Furthermore, that the map is simply raising the two-point function map to the κ power makes sense, since when one goes to the κ -cover the correlator should become just the order $(l+1)$ two-point function as depicted in Figure 4.7. The derivative of the map is

$$\frac{dz}{dt} = \frac{\kappa(l+1)z_2}{[t^{l+1} - (t-1)^{l+1}]^{\kappa+1}} t^{\kappa(l+1)-1} (t-1)^l, \quad (4.141)$$

which has zeroes at the correct points. One can see from the map that it only has $l+1$ distinct images of infinity, as required.

The behavior of the map near the irregular points is needed for the computation. Near the origin

$$z \approx (-1)^{\kappa l} z_2 t^{\kappa(l+1)} \quad \frac{dz}{dt} \approx (-1)^{\kappa l} \kappa(l+1) z_2 t^{\kappa(l+1)-1}. \quad (4.142)$$

Near $t = 1$,

$$z \approx z_2 + z_2 \kappa (t-1)^{l+1} \quad \frac{dz}{dt} \approx z_2 \kappa (l+1) (t-1)^l. \quad (4.143)$$

For large t ,

$$z \approx \frac{z_2}{(l+1)^\kappa} t^\kappa \quad \frac{dz}{dt} \approx \frac{z_2 \kappa}{(l+1)^\kappa} t^{\kappa-1}. \quad (4.144)$$

The images of infinity at finite t are the same as for the $l+1$ order two-point map, that is

$$t_\infty^{(j)} = \frac{1}{1 - \alpha_j} \quad (\alpha_j)^{l+1} = 1, \quad (4.145)$$

where the α_j are the $(l+1)$ roots of unity:

$$\alpha_j = e^{2\pi i \frac{j}{l+1}}. \quad (4.146)$$

Note that $\alpha_0 = 1$, which corresponds to $t \rightarrow \infty$; the case we already covered. Therefore, the images of infinity at finite t correspond to $j = 1, \dots, l$. If we let

$$t = \frac{1}{1 - \alpha_j} + x, \quad (4.147)$$

for small $x \in \mathbb{C}$, then near the images of infinity the map behaves as

$$z \approx (-1)^\kappa z_2 \left[\frac{\alpha_j}{(l+1)(1 - \alpha_j)^2} \frac{1}{x} \right]^\kappa. \quad (4.148)$$

Plugging back in with t , one finds the behavior of the map near the finite images of infinity:

$$\begin{aligned} z &\approx (-1)^\kappa z_2 \left[\frac{\alpha_j}{(l+1)(1 - \alpha_j)^2} \right]^\kappa \frac{1}{(t - t_\infty^{(j)})^\kappa} \\ \frac{dz}{dt} &\approx (-1)^{\kappa+1} \kappa z_2 \left[\frac{\alpha_j}{(l+1)(1 - \alpha_j)^2} \right]^\kappa \frac{1}{(t - t_\infty^{(j)})^{\kappa+1}}. \end{aligned} \quad (4.149)$$

The map is regular at all other points not considered above.

The Twist Jacobian Factor T

In Appendix D, we use the local behavior of the map given above to compute the various contributions to the Liouville action. In the notation used there, the quantities which define the correlator are

$$\begin{aligned} M &= 2 & F &= N = l + 1 & s &= \kappa(l + 1) \\ z_1 &= 0 & z_2 &= z_2 \\ t_1 &= 0 & t_2 &= 1 \\ p_1 &= \kappa(l + 1) & p_2 &= l + 1 & q_j &\equiv \kappa, \end{aligned} \quad (4.150)$$

and the local behavior of the map one needs is encoded in the coefficients

$$\begin{aligned} a_1 &= (-1)^{\kappa l} z_2 \\ a_2 &= z_2 \kappa \\ b_0 &= \frac{z_2}{(l+1)^\kappa} \\ b_j &= (-1)^\kappa z_2 \left[\frac{\alpha_j}{(l+1)(1 - \alpha_j)^2} \right]^\kappa \quad j = 1, \dots, l. \end{aligned} \quad (4.151)$$

Plugging in with these values, we find that [183]

$$Z = \delta^{4(l+1)\Delta_\kappa} \kappa^{-\frac{c}{12} \frac{l(l+2)}{l+1}}, \quad (4.152)$$

where we use the identity

$$\prod_{j=1}^l \alpha_j^l (1 - \alpha_j)^2 = (l+1)^2. \quad (4.153)$$

We normalize the twists at infinity in the same way as those in the finite z -plane: at unit separation in their local coordinates they should have unit correlator with themselves. From Appendix D, we see that if we normalize the twists at infinity in this way, then [183]

$$\langle \sigma_\kappa(\infty) \sigma_\kappa(0) \rangle_\delta = \delta^{4\Delta_\kappa}. \quad (4.154)$$

To ensure that the final state corresponds to a normalized bra, then, we should use

$$\lim_{z_3 \rightarrow \infty} |z_3|^{4\Delta_\kappa} \sigma_\kappa(z_3) = \delta^{-4\Delta_\kappa} \sigma_\kappa(\infty). \quad (4.155)$$

Thus, the δ dependence cancels out.

The constant C , then, is given as a power of κ :

$$|C|^2 = \kappa^{-\frac{c}{12} \frac{l(l+2)}{l+1}}. \quad (4.156)$$

The power of κ may seem mysterious, until one realizes that

$$\Delta_{l+1} = \frac{c}{24} \left(l+1 - \frac{1}{l+1} \right) = \frac{1}{4} \frac{l(l+2)}{l+1},$$

and so we write

$$|C|^2 = \kappa^{-2\Delta_{l+1}}. \quad (4.157)$$

Plugging in the value of C into Equation (4.135), one finds the twist Jacobian factor,

$$T = \kappa^{-2\Delta_{l+1}} \frac{|u_2|^{4\Delta_{l+1}}}{|z_2|^{2\frac{\kappa+1}{\kappa}\Delta_{l+1}}}. \quad (4.158)$$

Note that this Jacobian factor cannot naturally be thought of as the product of Jacobian factors from the different twist operators. This fact makes correlation functions of twist operators nontrivial.

4.3.6 Computing the Mode Jacobian Factor M

To compute the mode Jacobian factor, M , we first illustrate how modes transform under the map $z = bu^\kappa$. Then, we compute the mode Jacobian factor from the initial state modes, followed by the mode Jacobian factor from the vertex operator modes. The final state does

not have any modes, and therefore does not contribute to M . In discussing the initial state, we find that we must also consider the κ -dependence of the normalization of the state.

Transformation Law for Modes

First, let us examine how the different modes transform under the map,

$$z = bu^\kappa. \quad (4.159)$$

Modes that circle the origin get opened up by a factor of κ , and also get a Jacobian factor. They transform as

$$\mathcal{O}_m^{(z)} = b^m \kappa^{1-\Delta} \mathcal{O}_{m\kappa}^{(u)}, \quad (4.160)$$

where Δ is the weight of the *field* $\mathcal{O}(z)$. One can see this from the definition of modes in the $\kappa(l+1)$ -twisted sector [152]:

$$\mathcal{O}_{\frac{m}{\kappa(l+1)}}^{(z)} = \oint \frac{dz}{2\pi i} \sum_{j=1}^{\kappa(l+1)} \mathcal{O}_{(j)}(z) e^{2\pi i \frac{m}{\kappa(l+1)}(j-1)} z^{\Delta-1+\frac{m}{\kappa(l+1)}}. \quad (4.161)$$

The subscripted parenthetical index on the field $\mathcal{O}_{(j)}$ denotes the copy the field lives on.

Modes which circle z_2 , where there is no branching point, transform as

$$\mathcal{O}_m^{(z)} = \left(\frac{dz}{du} \Big|_{u_2, z_2} \right)^m \mathcal{O}_m^{(u)}. \quad (4.162)$$

Near the point u_2 , the map behaves as

$$\begin{aligned} z &\approx z_2 + \kappa b u_2^{\kappa-1} (u - u_2) \\ &= z_2 + \kappa \frac{z_2}{u_2} (u - u_2). \end{aligned} \quad (4.163)$$

Therefore, we see that, under this map, modes which circle the point z_2 transform as

$$\mathcal{O}_m^{(z)} = \left(\kappa \frac{z_2}{u_2} \right)^m \mathcal{O}_m^{(u)}. \quad (4.164)$$

Since the spectral flowed final state does not have any modes, we can write M as a product of Jacobian factors from the initial state and Jacobian factors from the vertex operator,

$$M = M_i M_v. \quad (4.165)$$

The Mode Jacobian Factor from the Initial State

For the initial state, we need to be a little careful about the normalization. Consider an initial state defined in the base space as

$$|\psi^{(z)}\rangle = \mathcal{C} \mathcal{O}_m^{(z)} |\sigma_{\kappa(l+1)}\rangle. \quad (4.166)$$

The norm of this state is given by

$$\begin{aligned} \langle \psi^{(z)} | \psi^{(z)} \rangle &= |\mathcal{C}|^2 \langle \sigma_{\kappa(l+1)} | \mathcal{O}_{-m}^{\dagger(z)} \mathcal{O}_m^{(z)} | \sigma_{\kappa(l+1)} \rangle \\ &= |\mathcal{C}|^2 \langle \sigma_{l+1} | \left(b^{-m} \kappa^{1-\Delta} \mathcal{O}_{-m\kappa}^{\dagger(u)} \right) \left(b^m \kappa^{1-\Delta} \mathcal{O}_{m\kappa}^{(u)} \right) | \sigma_{l+1} \rangle \\ &= |\mathcal{C}|^2 \kappa^{2(1-\Delta)} \langle \sigma_{l+1} | \mathcal{O}_{-m\kappa}^{\dagger(u)} \mathcal{O}_{m\kappa}^{(u)} | \sigma_{l+1} \rangle. \end{aligned} \quad (4.167)$$

On the other hand, suppose one were to define the state directly in the cover as

$$|\psi^{(u)}\rangle = \mathcal{C}_{\text{cover}} \mathcal{O}_{m\kappa}^{(u)} |\sigma_{l+1}\rangle, \quad (4.168)$$

then its norm is given by

$$\langle \psi^{(u)} | \psi^{(u)} \rangle = |\mathcal{C}_{\text{cover}}|^2 \langle \sigma_{l+1} | \mathcal{O}_{-m\kappa}^{\dagger(u)} \mathcal{O}_{m\kappa}^{(u)} | \sigma_{l+1} \rangle. \quad (4.169)$$

Requiring that both $|\psi^{(z)}\rangle$ and $|\psi^{(u)}\rangle$ be normalized, means

$$\mathcal{C} = \frac{\mathcal{C}_{\text{cover}}}{\kappa^{1-\Delta}}. \quad (4.170)$$

Thus, using Equation (4.160) with Equation (4.166), one finds

$$|\psi^{(z)}\rangle = b^m |\psi^{(u)}\rangle. \quad (4.171)$$

From this we see that the κ factor in Equation (4.160) gets cancelled out by the κ s one gets in normalizing the state in the covering space. This argument easily generalizes to all of the modes acting in the initial state.

The only contributions to M_i , therefore, come from the factors b^m . Because of the way they come in, we see that the the total factor we get (from the left) is

$$b^{-h_i^{\text{modes}}}, \quad (4.172)$$

where h_i^{modes} is the weight of all of the modes in the initial state. This is simply the total weight of the initial state minus the weight of the bare twist:

$$\begin{aligned} h_i^{\text{modes}} &= h'_i - \Delta_{\kappa(l+1)} \\ &= \frac{l+1}{4} \left(\kappa - \frac{1}{\kappa} \right) + \frac{1}{\kappa} \left(\frac{l}{2} + 1 \right) + \frac{N}{\kappa} - \frac{1}{4} \left(\cancel{\kappa(l+1)} - \frac{1}{\kappa(l+1)} \right) \end{aligned}$$

$$= \frac{1}{\kappa} \left[\frac{l}{2} + N + 1 - \Delta_{l+1} \right]. \quad (4.173)$$

Therefore, the total contribution (including both the left and right sectors) to the mode Jacobian factor from the initial state is given by

$$\begin{aligned} M_i &= |b|^{-\frac{2}{\kappa}[\frac{l}{2}+1-\Delta_{l+1}]} b^{-\frac{N}{\kappa}} \bar{b}^{-\frac{\bar{N}}{\kappa}} \\ &= \frac{|u_2|^{2[\frac{l}{2}+1-\Delta_{l+1}]} u_2^N \bar{u}_2^{\bar{N}}}{|z_2|^{\frac{2}{\kappa}[\frac{l}{2}+1-\Delta_{l+1}]} z_2^{\frac{N}{\kappa}} \bar{z}_2^{\frac{\bar{N}}{\kappa}}}. \end{aligned} \quad (4.174)$$

The Mode Jacobian Factor from the Vertex Operator

The vertex operator, we can see from

$$\mathcal{O}_m^{(z)} = \left(\kappa \frac{z_2}{u_2} \right)^m \mathcal{O}_m^{(t)},$$

contributes a factor of

$$M_v = \left(\kappa \frac{z_2}{u_2} \right)^{-h_v^{\text{modes}}} \left(\kappa \frac{\bar{z}_2}{\bar{u}_2} \right)^{-\bar{h}_v^{\text{modes}}}, \quad (4.175)$$

where h_v^{modes} is the weight of the vertex operator less the weight of the bare $(l+1)$ -twist, that is,

$$h_v^{\text{modes}} = \bar{h}_v^{\text{modes}} = \frac{l}{2} + 1 - \Delta_{l+1}. \quad (4.176)$$

Therefore, we see that the contribution to the mode Jacobian factor from the vertex operator is given by

$$M_v = \kappa^{2\Delta_{l+1}-(l+2)} \left(\frac{|u_2|}{|z_2|} \right)^{l+2-2\Delta_{l+1}}. \quad (4.177)$$

4.3.7 The CFT Amplitude

Multiplying the mode Jacobian factor,

$$M = M_i M_v = \kappa^{2\Delta_{l+1}-(l+2)} \frac{|u_2|^{2(l+2)-4\Delta_{l+1}} u_2^N \bar{u}_2^{\bar{N}}}{|z_2|^{\frac{\kappa+1}{\kappa}[l+2-2\Delta_{l+1}]} z_2^{\frac{N}{\kappa}} \bar{z}_2^{\frac{\bar{N}}{\kappa}}}, \quad (4.178)$$

with the twist Jacobian factor,

$$T = \kappa^{-2\Delta_{l+1}} \frac{|u_2|^{4\Delta_{l+1}}}{|z_2|^{2\frac{\kappa+1}{\kappa}\Delta_{l+1}}},$$

one finds

$$TM = \kappa^{-(l+2)} \frac{|u_2|^{2(l+2)} u_2^N \bar{u}_2^{\bar{N}}}{|z_2|^{\frac{\kappa+1}{\kappa}(l+2)} z_2^{\frac{N}{\kappa}} \bar{z}_2^{\frac{\bar{N}}{\kappa}}}. \quad (4.179)$$

Finally, from Section 4.2 we take the $\kappa = 1$ CFT amplitude (before spectral flow and without Jacobian prefactor $|z|^{l+2}$ from mapping from the cylinder to the complex plane), which can be deduced from Equation (4.60):

$$\mathcal{A}'^{\kappa=1} = (-1)^{k+\bar{k}} \sqrt{\binom{N+l+1}{N} \binom{\bar{N}+l+1}{\bar{N}}} \frac{1}{|u_2|^{2(l+2)} u_2^N \bar{u}_2^{\bar{N}}}. \quad (4.180)$$

We use the Jacobian factor TM to find

$$\mathcal{A}'^\kappa(z_2, \bar{z}_2) = \kappa^{-(l+2)} \sqrt{\binom{N+l+1}{N} \binom{\bar{N}+l+1}{\bar{N}}} \frac{1}{|z_2|^{\frac{\kappa+1}{\kappa}(l+2)} z_2^{\frac{N}{\kappa}} \bar{z}_2^{\frac{\bar{N}}{\kappa}}}, \quad (4.181)$$

which reduces to Equation (4.180) for $\kappa = 1$.

4.3.8 Combinatorics

As in Section 4.2, we want to consider an initial state with ν excitations that de-excites into a final states with $\nu - 1$ excitations (shown in Figure 4.8); however, the background geometry now consists of κ -twisted component strings. We assume, therefore, that κ divides $N_1 N_5$. Because the theory is orbifolded by $S_{N_1 N_5}$, the initial state, the final state, and the vertex operator must all be symmetrized over the $N_1 N_5$ copies.

We relate the full symmetrized states and operator to the amplitude computed above, in which we do not worry about these combinatoric factors. The combinatorics for this problem are quite similar to and for $\kappa = 1$ reduce to the combinatorics in Section 4.2.4.

The Initial State

We write the initial state as a sum over all the symmetric permutations:

$$|\Psi_\nu\rangle = \mathcal{C}_\nu \left[|\psi_\nu^1\rangle + |\psi_\nu^2\rangle + \dots \right], \quad (4.182)$$

where \mathcal{C}_ν is the overall normalization and each $|\psi_\nu^i\rangle$ is individually normalized. The initial state for $\nu = 2$, $\kappa = 2$, and $l = 2$ is shown in Figure 4.8(a).

To understand what we are doing better, note that the state $|\psi_{\nu=2}^1\rangle$ with $\kappa = 2$ and $l + 1 = 3$ can be written schematically as

$$|\psi_\nu^1\rangle = |[1 \cdots 6] [7 \cdots 12] [12, 13] [14, 15] \cdots\rangle \quad (4.183)$$

where the numbers in the square brackets are indicating particular ways of twisting individual strands corresponding to particular cycles of the permutation group. For instance,

$$|[1234]\rangle, \quad (4.184)$$

indicates that we twist strand 1 into strand 2 into strand 3 into strand 4 into strand 1 and leave strands 5 through $N_1 N_5$ untwisted. In Equation (4.183), the first two 6-twists are the two $\kappa(l+1)$ -twists which indicate the two excitations; the remaining $(\kappa = 2)$ -twists correspond to the background.

To determine the normalization \mathcal{C}_ν , we need to count the number of distinct terms in Equation (4.182). To count the number of states, we imagine constructing one of the terms and count how many choices we have. First, of the $N_1 N_5$ strands we must pick $\nu\kappa(l+1)$ of them to make into the ν excited states. Next, we must break the $\nu\kappa(l+1)$ strands into sets of $\kappa(l+1)$ to be twisted together. Then, we must pick a way of twisting together each set of $\kappa(l+1)$. Finally, we must make similar choices for the $N_1 N_5 - \nu\kappa(l+1)$ strands that are broken into the κ -twists of the background. Putting these combinatoric factors together, one finds

$$\begin{aligned}
N_{\text{terms}} &= \binom{N_1 N_5}{\nu\kappa(l+1)} \\
&\quad \times \binom{\nu\kappa(l+1)}{\kappa(l+1)} \binom{(\nu-1)\kappa(l+1)}{\kappa(l+1)} \cdots \binom{\kappa(l+1)}{\kappa(l+1)} \frac{1}{\nu!} \times ([\kappa(l+1) - 1]!)^\nu \\
&\quad \times \binom{N_1 N_5 - \nu\kappa(l+1)}{\kappa} \cdots \binom{\kappa}{\kappa} \frac{1}{[\frac{N_1 N_5}{\kappa} - \nu(l+1)]!} \times ((\kappa - 1)!)^{\frac{N_1 N_5}{\kappa} - \nu(l+1)} \\
&= \frac{(N_1 N_5)!}{[\kappa(l+1)]^\nu \kappa^{\frac{N_1 N_5}{\kappa} - \nu(l+1)} (\frac{N_1 N_5}{\kappa} - \nu(l+1))! \nu!}. \tag{4.185}
\end{aligned}$$

Choosing \mathcal{C}_ν to be real, one finds

$$\mathcal{C}_\nu = \frac{1}{\sqrt{N_{\text{terms}}}} = \left[\frac{(N_1 N_5)!}{[\kappa(l+1)]^\nu \kappa^{\frac{N_1 N_5}{\kappa} - \nu(l+1)} (\frac{N_1 N_5}{\kappa} - \nu(l+1))! \nu!} \right]^{-\frac{1}{2}}. \tag{4.186}$$

The Final State

The final state is simply $|\Psi_{\nu-1}\rangle$ with its corresponding normalization $\mathcal{C}_{\nu-1}$. This state is shown for $\nu = 2$, $\kappa = 2$, and $l = 2$ in Figure 4.8(b).

The Vertex Operator

The normalization of the *full* vertex operator is determined in Section 4.2.4. The full symmetrized vertex operator is written

$$\mathcal{V}_{\text{sym}} = \mathcal{C} \sum_i \mathcal{V}_i, \tag{4.187}$$

where

$$\mathcal{C} = \left[\frac{(N_1 N_5)!}{(l+1)[N_1 N_5 - (l+1)]!} \right]^{-\frac{1}{2}}. \tag{4.188}$$

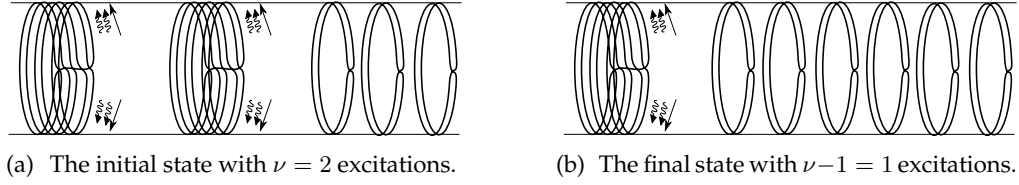


Figure 4.8: The initial and final states of the unphysical amplitude with some excitations present in the background. An $l = 2$ transition from $\nu = 2$ excitations to 1 excitation of the $\kappa = 2$ background is shown.

The Amplitude

The full amplitude of interest is

$$\langle \Psi_{\nu-1} | \mathcal{V}_{\text{sym}} | \Psi_{\nu} \rangle, \quad (4.189)$$

which we wish to relate to a “single” unsymmetrized amplitude. Having the normalization of the initial state, the final state, and the vertex operator, all that remains is to determine which terms in the symmetrized states and operator combine to give a nonzero amplitude. For each initial state there are ν excitations that a term in the vertex operator can de-excite. We are left with the question, how many $(l + 1)$ -twists can untwist a given $\kappa(l + 1)$ -twist into $l + 1$ κ -twists? In fact, there are κ such twist operators, which brings the number of nonzero amplitudes to

$$N_{\text{terms}} \nu \kappa = \kappa \frac{\nu}{\mathcal{C}_{\nu}^2}. \quad (4.190)$$

To illustrate, consider the initial state in Equation (4.183) for $\nu = 2$, $\kappa = 2$, and $l + 1 = 3$. First, there are two different excitations to untwist. Consider untwisting the first excitation [123456]. There are exactly two 3-twist vertex operators that untwist the excitation into three sets of 2-twists: [531] and [642]. The [531] vertex operator breaks the initial state into [12][34][56], while the [642] vertex operator breaks the initial state into [61][23][45].

Using Equation (4.190) and the normalizations, we can relate the total symmetrized amplitude to the amplitude computed with only one term from the initial state, the final state, and the vertex operator:

$$\begin{aligned} \langle \Psi_{\nu-1} | \mathcal{V}_{\text{sym}} | \Psi_{\nu} \rangle &= \mathcal{C}_{\nu-1} \mathcal{C}_{\nu} \kappa \frac{\nu}{\mathcal{C}_{\nu}^2} \langle \psi_{\nu-1}^1 | \mathcal{V}_1 | \psi_{\nu}^1 \rangle \\ &= \sqrt{\kappa^{l+2} \nu \frac{[\frac{N_1 N_5}{\kappa} - (\nu - 1)(l + 1)]! [N_1 N_5 - (l + 1)]!}{[\frac{N_1 N_5}{\kappa} - \nu(l + 1)]! (N_1 N_5)!}} \langle \psi_{\nu-1}^1 | \mathcal{V}_1 | \psi_{\nu}^1 \rangle. \end{aligned} \quad (4.191)$$

The Large $N_1 N_5$ Limit

While the expression in Equation (4.191) is complicated, it simplifies considerably in the large $N_1 N_5$ limit of ultimate interest. We take both $N_1 N_5$ and $N_1 N_5 / \kappa$ to be large,

$$\frac{\left[\frac{N_1 N_5}{\kappa} - (\nu - 1)(l + 1)\right]!}{\left[\frac{N_1 N_5}{\kappa} - \nu(l + 1)\right]!} \longrightarrow \left(\frac{N_1 N_5}{\kappa}\right)^{(l+1)} \quad \frac{[N_1 N_5 - (l + 1)]!}{(N_1 N_5)!} \longrightarrow (N_1 N_5)^{-(l+1)}, \quad (4.192)$$

in which case Equation (4.191) reduces to

$$\langle \Psi_{\nu-1} | \mathcal{V}_{\text{sym}} | \Psi_{\nu} \rangle = \sqrt{\kappa \nu} \langle \psi_{\nu-1}^1 | \mathcal{V}_1 | \psi_{\nu}^1 \rangle. \quad (4.193)$$

The $\sqrt{\nu}$ prefactor can be thought of as a “Bose enhancement” effect.

4.3.9 The Rate of Emission

We now can put all of the pieces together to find the spectrum and rate of emission. Plugging Equation (4.181) into Equation (4.128) along with the combinatoric factors from Equation (4.193), one finds the amplitude for emission with angular momentum $(l, k + \bar{k} - l, \bar{k} - k)$

$$\mathcal{A}_{l, k + \bar{k} - l, \bar{k} - k} = \sqrt{\nu \kappa} \kappa^{-(l+2)} \sqrt{\binom{N + l + 1}{N} \binom{\bar{N} + l + 1}{\bar{N}}} \times \kappa^{\frac{1}{\kappa}(\frac{l}{2} + N + 1) - \alpha(\frac{l}{2} - k)} \bar{\kappa}^{\frac{1}{\kappa}(\frac{l}{2} + \bar{N} + 1) - \bar{\alpha}(\frac{l}{2} - \bar{k})}. \quad (4.194)$$

Plugging back in with the physical cylindrical coordinates,

$$z = e^{\frac{i}{R}(y+t)} \quad \bar{z} = e^{-\frac{i}{R}(y-t)}, \quad (4.195)$$

we can read off the spectrum for emission,

$$\begin{aligned} E_0 &= \frac{1}{\kappa R} \left[(\kappa \alpha + \kappa \bar{\alpha} - 2) \frac{l}{2} - \kappa(\alpha k + \bar{\alpha} \bar{k}) - N - \bar{N} - 2 \right] \\ \lambda_0 &= \frac{1}{\kappa R} \left[-\kappa(\alpha - \bar{\alpha}) \frac{l}{2} + \kappa(\alpha k - \bar{\alpha} \bar{k}) + N - \bar{N} \right], \end{aligned} \quad (4.196)$$

where recall that $\alpha = 2n + 1/\kappa$ and $\bar{\alpha} = 2\bar{n} + 1/\kappa$. For there to be emission the energy of the emitted particle must be positive, meaning that $E_0 > 0$.

The unit amplitude with the (σ, τ) dependence removed is

$$\mathcal{A}_{\text{unit}}(0) = \sqrt{\nu \kappa}^{-l - \frac{3}{2}} \sqrt{\binom{N + l + 1}{N} \binom{\bar{N} + l + 1}{\bar{N}}}. \quad (4.197)$$

Section 4.3.8, where ν is defined, calculates the combinatorics for the *unphysical* amplitude. For the *physical* amplitude, the combinatorics are the same except that the emission process

is a transition from $\nu - 1$ to ν $\kappa(l + 1)$ -twists. Thus, the above is the amplitude for emission of the ν th particle. Plugging into Equation (3.65), one finds the emission rate for the ν th particle,

$$\frac{d\Gamma}{dE} = \nu \kappa^{-2l-3} \frac{2\pi}{2^{2l+1} l!^2} \frac{(Q_1 Q_5)^{l+1}}{R^{2l+3}} (E^2 - \lambda^2)^{l+1} \binom{N+l+1}{N} \binom{\bar{N}+l+1}{\bar{N}} \delta_{\lambda, \lambda_0} \delta(E - E_0), \quad (4.198)$$

with energy and momentum in Equation (4.196) and angular momentum $(l, k + \bar{k} - l, \bar{k} - k)$. This answer exactly matches the gravity calculation in [182].

4.4 Discussion

We reproduced the full spectrum and emission rate of supergravity minimal scalars from the geometries found in [168] by using a CFT formalism. In [180–182], using a heuristic picture of the CFT process the spectrum and rate was found, but only for special cases ($N = \bar{N} = 0$ and $k = \bar{k} = 0$) and the normalization of the heuristic vertex operator was determined only indirectly. In Section 4.2, the full rate and spectrum was found as a rigorous calculation for $\kappa = 1$ with a vertex operator whose coupling to flat space and normalization was determined directly from the AdS–CFT correspondence.

The new feature of Section 4.3 is the κ -dependence. Using the old effective string description, the κ -dependence in Equations (4.196) and (4.198) could have been guessed via a heuristic argument that we now describe. Taking higher values of κ corresponds to twisting the background strings by κ . The process, then, looks the same as for $\kappa = 1$ but taking $R \mapsto \kappa R$. This reproduces the explicit κ dependence of Equation (4.198), but the spectrum is slightly more complicated. In the spectrum, we also should take $R \mapsto \kappa R$, since the energy level spacing becomes reduced by a factor of κ ; however, things are complicated by the parameters n and \bar{n} . Why does the n and \bar{n} part of the spectrum get multiplied by κ with respect to the rest of the contributions to the energy? The parameters n and \bar{n} control the Fermi level of the physical initial state. In the κ -cover, the fermions fill up to energy level κn and not n ; thus, the extra factor of κ .

With the final answer and CFT computation in front of us, this heuristic argument seems compelling indeed; however, we argue that it is not completely obvious a priori that the effective string reasoning works for this calculation. Certainly, the way that the κ -dependence works out in the rigorous CFT calculation seems quite nontrivial and nonobvious. That the action of the vertex operator so simply gets “divided by” κ does not seem obvious. In any case, one of the goals in this chapter is to demonstrate the formalism in Chapter 3 and put the reasoning in [180–182] on a firmer footing. Along the way, we found (conjectured?) the form of supergravity excitations on the orbifolded-AdS background; it would be nice to better understand the identification of the supergravity multiplet in

orbifolded-AdS.

That the rate of emission computed in this class of geometries can be reproduced via a CFT calculation may seem insignificant in the face of so many AdS–CFT successes. There are two reasons why this calculation is of interest. First, most AdS–CFT calculations use a gravity calculation in the AdS to compute a CFT correlator, whereas we use the methods of Chapter 3 to compute the rate of emission *out of the* CFT or AdS. This demonstrates the formalism of Chapter 3 [158], which hearkens back to and puts a firmer footing on the “effective string” calculations of [84, 194–198]. Second, as explained in [180–182], the CFT calculation justifies interpreting the ergoregion emission as Hawking radiation from these, albeit nongeneric, microstates of a black hole. This may help us better understand black holes in string theory and thereby quantum gravity.

If one computes the CFT amplitude for emission from a thermally distributed initial state and sums over all possible final states, then one reproduces the full Hawking radiation spectrum. The calculation was performed in [80], using precisely the formalism developed in Chapter 3. The usual thermal field theory technique of compactifying time was used, putting the CFT on a torus. The answer precisely matched the gravity calculation. The important point being that it is the *same* vertex operator \mathcal{V} in the CFT for Hawking radiation and for the ergoregion emission described above. The only difference being whether one considers a particular nongeneric state of the CFT, or a thermal distribution. This strongly suggests that the naive nonextremal black hole and its Hawking radiation is the result of thermally averaging over microstates. Some of which, at least, allow a geometric description.

All of the calculation were performed on the “orbifold point” of the D1D5 CFT. The emission process described in the gravity side should be dual to the CFT off of the orbifold point, and so it is an open question why this and many other calculations on the orbifold point so accurately reproduce the gravitational physics. Although, some calculations should agree due to established non-renormalization theorems [96, 134]. In Chapter 5, we discuss how to move off of the orbifold point.

Chapter 5

MOVING OFF THE ORBIFOLD POINT

As discussed in Chapter 2, the point in moduli space where the orbifold CFT is a good description does not coincide with points in moduli space where supergravity is a good description. If one wants to understand black holes better, then one needs a CFT description at points in moduli space where one also has black hole physics. In Section 2.5.4, we introduced the marginal deformations of the orbifold CFT that move the CFT in its 20-dimensional moduli space. Of the 20 marginal deformations, we are interested in the 4 twist deformations that correspond to blow-up modes of the orbifolded target space. While the supergravity is far from the orbifold point in moduli space, we take a perturbative approach and study the effect of a single application of the deformation operator. This work was performed in [202–204]. It is hoped that these results will provide some qualitative and maybe even quantitative answers to questions about black holes. Most of the analysis is deferred to later work.

In Section 5.1, we recall the structure of the marginal deformation operator of interest and make its structure more explicit. In Section 5.2, we find the state created by the application of the deformation operator to the vacuum. The state is a “squeezed state” with a long power-law “tail” [202]. In Section 5.3, we show how to calculate the state created by the marginal deformation on excited states [203]. In Section 5.4, we show an alternative method for computing the state created by the marginal deformation on excited states. This alternative method may be preferable because it comes in the form of intertwining relations for individual modes [204]. These can loosely be thought of as Bogolyubov coefficients for bosonic and fermionic modes. Unfortunately, this second method suffers from ambiguous multidimensional series—the ambiguity is resolved via a physically motivated prescription. In Section 5.5 we use the results from Section 5.4 in two different ways, demonstrating the techniques. In Section 5.6, we briefly recapitulate the chapter, and outline some future directions for which these results may be useful.

Before proceeding, let us alert the careful reader to some notational changes made in this chapter. Since the entire discussion focuses on going from two singly-wound copies

to a single doubly-wound copy, we find it convenient to use parenthetical superscripts to indicate the copy number “before the twist” and no corresponding notation for modes and fields “after the twist.” Furthermore, modes in the twisted sector are defined with a factor of 2 with respect to previous chapters. So α_n in this chapter corresponds to $\alpha_{\frac{n}{2}}$ in previous chapters.

5.1 The Deformation Operator

The deformation operator of interest, \mathcal{T} , is introduced in Section 2.5.4. Recall that the deformation is a singlet under $SU(2)_L \times SU(2)_R$. To obtain such a singlet we apply $G_{A,-\frac{1}{2}}^\mp$ to σ_2^\pm . A singlet under $SU(2)_L \times SU(2)_R$ can be made as (writing both left and right moving sectors) [155, 157, 205]

$$\mathcal{T}_{AB} \propto \frac{1}{4} \epsilon_{\alpha\beta} \epsilon_{\dot{\alpha}\dot{\beta}} \left[\int_{w_0} \frac{dw}{2\pi i} G_A^\alpha(w) \right] \left[\int_{\bar{w}_0} \frac{d\bar{w}}{2\pi i} \bar{G}_B^{\dot{\alpha}}(\bar{w}) \right] \sigma_2^{\beta\dot{\beta}} \quad (5.1)$$

In Section 2.5.3, we demonstrate that $G_{-\frac{1}{2}}^-$ acting on a chiral primary gives the top member of $SU(2)_L$. In this case, that means that $\mathcal{T}_{A\dot{B}}$ is a singlet—a fact pointed out in Section 2.5.4. Thus we can write the deformation operator as (we choose its normalization at this stage)

$$\mathcal{T}_{AB} = \left[\int_{w_0} \frac{dw}{2\pi i} G_A^-(w) \right] \left[\int_{\bar{w}_0} \frac{d\bar{w}}{2\pi i} \bar{G}_B^-(\bar{w}) \right] \sigma_2^{++}(w_0) \quad (5.2)$$

The normalization of σ_2^{++} is specified below. The indices \dot{A} and \dot{B} can be contracted to rewrite the above four operators as a singlet and a triplet of $SU(2)_1$.²⁸

5.1.1 Normalization of σ_2^+

Now we describe the normalization of σ_2^{++} . Let us focus on the left moving part of the operator, which we denote by σ_2^+ . Let the conjugate operator be called $\sigma_{2,+}$, and normalize these operators so that they have the OPE

$$\sigma_{2,+}(z') \sigma_2^+(z) \sim \frac{1}{z' - z} \quad (5.3)$$

On the cylinder this implies

$$\lim_{\tau' \rightarrow \infty} \lim_{\tau \rightarrow -\infty} {}^{(1)}\langle 0 | {}^{(2)}\langle 0 | e^{\frac{1}{2}(\tau' + i\sigma)} \sigma_{2,+}(\tau' + i\sigma) e^{-\frac{1}{2}(\tau + i\sigma)} \sigma_2^+(\tau + i\sigma) | 0 \rangle^{(1)} | 0 \rangle^{(2)} = 1 \quad (5.4)$$

where $|0\rangle^{(1)}|0\rangle^{(2)}$ is the (untwisted) NS vacuum.

²⁸Since we can write the deformation operator in terms of $G^- \sigma_2^+$ or in terms of $G^+ \sigma_2^-$, it provides a good check on the results that we get the same final state each way.

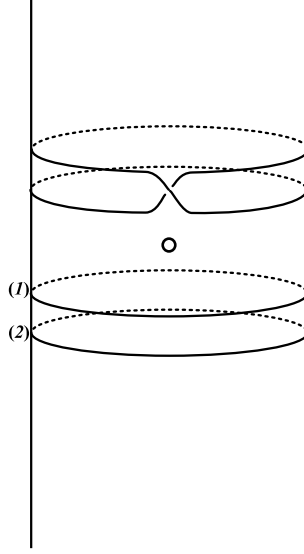


Figure 5.1: The effect of the twist contained in the deformation operator: two circles at earlier times get joined into one circle after the insertion of the twist.

Let us perform a spectral flow (2.66) with parameter $\alpha = -1$. This changes the untwisted NS vacuum as

$$|0\rangle^{(1)} |0\rangle^{(2)} \rightarrow |0_R^-\rangle^{(1)} |0_R^-\rangle^{(2)} \quad (5.5)$$

We also have to ask what happens to the twist operator $\sigma_2^+(w_0)$ under this spectral flow. As discussed in Section 4.2.2, the action of spectral flow is simple for operators where the fermion content can be expressed as a simple exponential in the language where we bosonize the fermions. For such operators with charge j , spectral flow with parameter α leads to a multiplicative factor [158]

$$\mathcal{O}_j(w) \rightarrow e^{-\alpha j w} \mathcal{O}_j(w) \quad (5.6)$$

The operator σ_2^+ is indeed of this simple form [152], so we just get a multiplicative factor under spectral flow. Its charge is $q = \frac{1}{2}$, so we get

$$\sigma_2^+(w) \rightarrow e^{-\alpha \frac{1}{2} w} \sigma_2^+(w_0) = e^{\frac{1}{2}(\tau + i\sigma)} \sigma_2^+(\tau + i\sigma) \quad (5.7)$$

The operator $\sigma_{2,+}$ has charge $-\frac{1}{2}$, so we get

$$\sigma_{2,+}(w') \rightarrow e^{\alpha \frac{1}{2} w'} \sigma_{2,+}(w') = e^{-\frac{1}{2}(\tau' + i\sigma)} \sigma_{2,+}(\tau' + i\sigma) \quad (5.8)$$

Thus under spectral flow the relation (5.4) gives

$$\lim_{\tau' \rightarrow \infty} \lim_{\tau \rightarrow -\infty} {}^{(1)}\langle 0_{R,-} | {}^{(2)}\langle 0_{R,-} | \sigma_{2,+}(\tau' + i\sigma) \sigma_2^+(\tau + i\sigma) | 0_R^- \rangle^{(1)} | 0_R^- \rangle^{(2)} = 1 \quad (5.9)$$

We write

$$|0_R^- \rangle \equiv \lim_{\tau \rightarrow -\infty} \sigma_2^+(\tau + i\sigma) |0_R^- \rangle^{(1)} |0_R^- \rangle^{(2)} \quad (5.10)$$

This is one of the two Ramond vacua of the CFT on the double circle. The spin of this vacuum is $-\frac{1}{2}$, arising from the spin $-\frac{1}{2}$ on each of the two initial Ramond vacua before twisting and the spin $\frac{1}{2}$ of the twist operator σ_2^+ . Similarly, we write

$$\langle 0_{R,-} | \equiv \lim_{\tau' \rightarrow \infty} {}^{(1)}\langle 0_{R,-} | {}^{(2)}\langle 0_{R,-} | \sigma_{2,+}(\tau' + i\sigma) \quad (5.11)$$

From the relation (5.9) we have

$$\langle 0_{R,-} | 0_R^- \rangle = 1 \quad (5.12)$$

The relation (5.10) implies that if we insert σ_2^+ at a general point w , then we get a state of the form

$$\sigma_2^+(w) |0_R^- \rangle^{(1)} |0_R^- \rangle^{(2)} = |0_R^- \rangle + \dots \quad (5.13)$$

where the coefficient of the vacuum on the right-hand side (RHS) is unity, and the ‘ \dots ’ represent excited states of the CFT on the doubly wound circle. We will use this relation below.

5.2 Applying the Deformation Operator to the Vacuum

Consider the amplitude depicted in Figure 5.2. Let us write down all the states and operators in this amplitude. In the initial state, we have two component strings. Since each is in the Ramond sector, we have to choose one of the Ramond ground states. We choose

$$|\Psi\rangle_i = |0_R^{--}\rangle^{(1)} |0_R^{--}\rangle^{(2)}, \quad (5.14)$$

as the initial state. To this state we apply the deformation operator at some point w_0 to arrive at the “final state:”

$$|\Psi\rangle_f = \mathcal{T}_{\dot{A}\dot{B}}(w_0) |\Psi\rangle_i = \left[\int_{w_0} \frac{dw}{2\pi i} G_A^-(w) \right] \left[\int_{\bar{w}_0} \frac{d\bar{w}}{2\pi i} \bar{G}_B^-(\bar{w}) \right] \sigma_2^{++}(w_0) |0_R^{--}\rangle^{(1)} |0_R^{--}\rangle^{(2)} \quad (5.15)$$

The final state contains one component string with winding number 2, since the deformation operator contains the twist σ_2 . From this stage on, we will write only the left moving part of the state, and join it up with the right moving part at the end. Thus we write

$$|\Psi\rangle_f = |\psi\rangle |\bar{\psi}\rangle \quad (5.16)$$

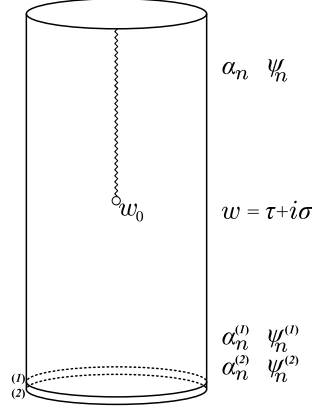


Figure 5.2: Before the twist insertion we have boson and fermion modes on two copies of the $c = 6$ CFT. These modes are labeled with superscripts (1) and (2), respectively. The twist inserted at w_0 joins these to one copy for $\tau > \tau_0$; the modes here do not carry a superscript. The branch cut above w_0 indicates that we have two sets of fields at any given σ ; these two sets go smoothly into each other as we go around the cylinder, giving a continuous field on a doubly wound circle.

and work with $|\psi\rangle$ in what follows.

5.2.1 Outline of the Computation

Let us outline our steps for computing $|\psi\rangle$.

1. The essence of the computation lies in the nature of the deformation operator. This operator is given by a supercharge acting on the twist operator σ_2^+ . This supercharge is given by a contour integral of G_A^- around the twist insertion. We first deform this contour to a pair of contours: one above and one below the insertion. These contours give zero modes of the supercurrent on the states before and after the twist insertion. We handle these zero modes at the end, and focus first on the state produced by just the twist insertion σ_2^+ ; we call this state $|\chi\rangle$.
2. Let us now look at the nature of the twist operator for bosonic fields. As we circle the twist, the two copies of the boson go into each other. The twist operator is defined by cutting a small hole around its insertion w_0 , and taking boundary condition at the edge of this hole given by filling the hole in the *covering space* with a disc; i.e. there are no operator insertions in this covering space and we have just the vacuum state [151]. To use this structure of the twist operator, we first map the cylinder to the plane via $z = e^w$, and then pass to the covering space t by the map $z = z_0 + t^2$ (here $z_0 = e^{w_0}$ is the location of the twist). The small hole cut out on the cylinder around

w_0 becomes a small hole around $t = 0$. Since the boundary condition on the edge of this hole is generated by filling this hole by a disc, we get just the vacuum state at the origin in the t plane. This observation takes into account the entire effect of the twist on the bosons.

3. On the cylinder we can specify the initial state of the system on the two circles at $\tau \rightarrow -\infty$ corresponding to the two copies of the $c = 6$ CFT. On the t plane these circles map to punctures at $t = \pm z_0^{\frac{1}{2}} \equiv \pm ia$. Since we have taken no bosonic excitations in our initial state, the bosonic part of the states at these punctures is just the vacuum, and we can close these punctures smoothly, just like the hole at $t = 0$. Thus we have no insertions anywhere in the t plane.
4. Our goal is to find the state at a circle $\tau \rightarrow \infty$ on the cylinder. But this circle maps to the circle $|t| = \infty$ on the t plane. Thus what we need is the state in the t plane at infinity. But since there are no insertions anywhere on the t plane, this state is just the t plane vacuum $|0\rangle_t$. One might think that this means there are no excitations in the final state, but this is not the case: the vacuum on the t plane is killed by positive energy modes defined with respect to the t coordinate, and these will map to a linear combination of positive and negative energy modes in the original cylinder coordinate w . Thus all we have to do is express the state $|0\rangle_t$ in terms of the modes on the cylinder, and we would have obtained the bosonic part of the state arising from the twist insertion.
5. Let us now ask if we can guess the nature of this state in terms of the modes on the cylinder. In the treatment of quantum fields on curved space we often come across a situation where we have to express the vacuum with respect to one set of field modes in terms of operators defined with respect to another set of field modes. The state with respect to the latter modes has the form of an exponential of a quadratic, i.e. of the form $e^{\gamma_{mn} a_m^\dagger a_n^\dagger} |0\rangle$. The essential reason for getting this form for the state can be traced to the fact that free fields have a quadratic action, and if there are no operator insertions anywhere then in all descriptions of the state we can only observe exponentials of a quadratic form.

For our problem, we make the ansatz that the state $|\chi\rangle$ has a similar exponential form. We find the γ_{mn} by computing the inner product of the state with a state containing a pair of operator modes. In Appendix E we prove that this exponential ansatz is indeed correct to all orders. A state of this form is frequently called a squeezed state in atomic physics.

6. Let us now ask if similar arguments can be applied to the fermionic field. The initial state on the cylinder has Ramond vacua for the two copies of the CFT. If we map to

the t plane these would give nontrivial states at $t = \pm ia$. Thus we first perform a spectral flow on the cylinder, which maps the problem to one where these Ramond vacua map to NS vacua at $\tau \rightarrow -\infty$ on the cylinder. These NS vacua will map to NS vacua at $t = \pm ia$, so there will be no operator insertions in the t plane at these points. We should also check the effect of this spectral flow on the twist $\sigma_2^+(w_0)$. From (5.6) we find that $\sigma_2^+(w_0)$ will change by just a multiplicative constant. This constant will not matter at the end since we know the normalization of our final state by (5.13).

We can now pass to the covering space t . We must now ask for the state at the edge of the hole around $t = 0$. One finds that the fermions in the t plane are antiperiodic around $t = 0$ [152]. Thus the state given by the operator σ_2^+ corresponds to having the positive spin Ramond vacuum $|0_R^+\rangle_t$. As it stands this implies that we have a nontrivial state at $t = 0$, but we perform another spectral flow, this time in the t plane. Under this second spectral flow the Ramond vacuum $|0_R^+\rangle_t$ maps to the NS vacuum of the t plane $|0\rangle_t$. We take the normalization

$${}_t\langle 0|0\rangle_t = 1 \quad (5.17)$$

for this NS vacuum. At this stage we have indeed no insertions anywhere in the t plane, and the state at $t = \infty$ is just the t plane vacuum for the fermions. Since all coordinate maps and spectral flows were linear in the operator modes, we again expect the state to be given by the exponential of a bilinear in fermion modes. We write such an ansatz, and find the coefficients in the exponential.

7. We can summarize the above discussion in the following general relation

$$\langle 0_{R,-} | \left(\mathcal{O}_1 \mathcal{O}_2 \dots \mathcal{O}_n \right) \sigma_2^+(w_0) | 0_R^- \rangle^{(1)} | 0_R^- \rangle^{(2)} = {}_t\langle 0 | \left(\mathcal{O}'_1, \mathcal{O}'_2, \dots, \mathcal{O}'_n \right) | 0 \rangle_t \quad (5.18)$$

The state $\langle 0_{R,-} |$ is defined in (5.11). \mathcal{O}_i are any operators inserted after the twist insertion (we will need to insert boson and fermion modes in finding the coefficients γ_{mn}). On the RHS, the operators \mathcal{O}'_i are obtained by mapping the operators \mathcal{O}_i through all coordinate changes and spectral flows till we reach the t plane with the NS vacuum at $t = 0$. The normalizations (5.12) and (5.17) tell us that there is no extra constant relating the left-hand side (LHS) to the right-hand side (RHS) of (5.18).

8. After obtaining the state $|\chi\rangle$ generated by the action of the twist σ_2^+ on $|0_R^- \rangle^{(1)} | 0_R^- \rangle^{(2)}$, we act with the zero mode of the supercurrent to obtain the final state $|\psi\rangle$ obtained by the action of the full deformation operator on $|0_R^- \rangle^{(1)} | 0_R^- \rangle^{(2)}$.

5.2.2 Mode Expansions on the Cylinder

Let us give the mode expansions on the cylinder, where the CFT is defined. Below the twist insertion, $\tau < \tau_0$, the fields are 2π -periodic and we define the modes as

$$\alpha_{A\dot{A},n}^{(i)} = \int_{\sigma=0}^{2\pi} \frac{dw}{2\pi} \partial_w X_{A\dot{A}}^{(i)}(w) e^{nw} \quad i = 1, 2 \quad (5.19a)$$

$$\psi_n^{(i)\alpha\dot{A}} = \int_{\sigma=0}^{2\pi} \frac{dw}{2\pi i} \psi^{(i)\alpha\dot{A}}(w) e^{nw} \quad i = 1, 2 \quad (5.19b)$$

which gives the inverse relationship,

$$\partial_w X_{A\dot{A}}^{(i)}(w) = -i \sum_n \alpha_{A\dot{A},n}^{(i)} e^{-nw} \quad i = 1, 2 \quad (5.20a)$$

$$\psi^{(i)\alpha\dot{A}}(w) = \sum_n \psi_n^{(i)\alpha\dot{A}} e^{-nw} \quad i = 1, 2. \quad (5.20b)$$

The commutation relations are

$$[\alpha_{A\dot{A},m}^{(i)}, \alpha_{B\dot{B},n}^{(j)}] = -\epsilon_{AB} \epsilon_{\dot{A}\dot{B}} \delta^{ij} m \delta_{m+n,0} \quad (5.21a)$$

$$\{\psi_m^{(i)\alpha\dot{A}}, \psi_n^{(j)\beta\dot{B}}\} = -\epsilon^{\alpha\beta} \epsilon^{\dot{A}\dot{B}} \delta^{ij} \delta_{m+n,0} \quad (5.21b)$$

Above the twist, $\tau > \tau_0$, we have a doubly twisted circle and the 4π -periodic. We have a choice of normalization in how we define modes on the doubly wound circle, and we take

$$\alpha_{A\dot{A},n} = \int_{\sigma=0}^{4\pi} \frac{dw}{2\pi} \partial_w X_{A\dot{A}}(w) e^{\frac{n}{2}w} \quad (5.22a)$$

$$\psi_n^{\alpha\dot{A}} = \int_{\sigma=0}^{4\pi} \frac{dw}{2\pi i} \psi^{\alpha\dot{A}}(w) e^{\frac{n}{2}w} \quad (5.22b)$$

Taking the normalizations as above, one finds

$$\partial_w X_{A\dot{A}}(w) = -\frac{1}{2} i \sum_n \alpha_{A\dot{A},n} e^{-\frac{n}{2}w} \quad (5.23a)$$

$$\psi^{\alpha\dot{A}}(w) = \frac{1}{2} \sum_n \psi_n^{\alpha\dot{A}} e^{-\frac{n}{2}w}. \quad (5.23b)$$

Note the factor of $\frac{1}{2}$ that appears in these equations. The commutation relations turn out to be

$$[\alpha_{A\dot{A},m}, \alpha_{B\dot{B},n}] = -\epsilon_{AB} \epsilon_{\dot{A}\dot{B}} m \delta_{m+n,0} \quad (5.24a)$$

$$\{\psi_m^{\alpha\dot{A}}, \psi_n^{\beta\dot{B}}\} = -2\epsilon^{\alpha\beta} \epsilon^{\dot{A}\dot{B}} \delta_{m+n,0}. \quad (5.24b)$$

Again note the factor of 2 in the fermion relation. The difference between the boson and the fermion cases arises from the fact that they have different scaling dimensions.

5.2.3 The $G_{A,-\frac{1}{2}}^-$ Operator

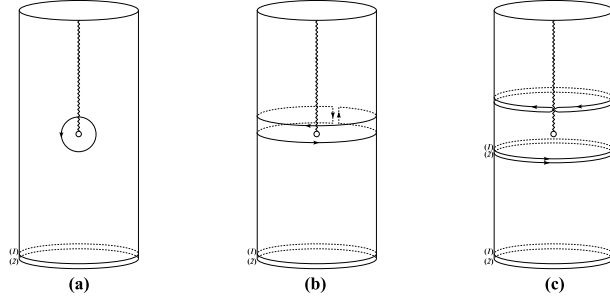


Figure 5.3: (a) The supercharge in the deformation operator is given by integrating G_A^- around the insertion at w_0 . (b) We can stretch this contour as shown, so that we get a part above the insertion and a part below, joined by vertical segments where the contributions cancel. (c) The part above the insertion gives the zero mode of the supercharge on the doubly wound circle, while the parts below give the sum of this zero mode for each of the two initial copies of the CFT.

Let us first put the $\int_{w_0} \frac{dw}{2\pi i} G_A^-(w)$ operator in (5.15) in a more convenient form. The contour in this operator runs circles the insertion w_0 (Figure 5.3(a)). We can stretch this to a contour that runs around the rectangle shown in figure 5.3(b). The vertical sides of the contour cancel out. We can thus break the contour into a part above the insertion and a part below the insertion (Figure 5.3(c)). The lower leg gives

$$\int_{w=\tau_0-\epsilon}^{\tau_0-\epsilon+2\pi i} \frac{dw}{2\pi i} G_A^-(w) = \int_{w=\tau_0-\epsilon}^{\tau_0-\epsilon+2\pi i} \frac{dw}{2\pi i} [G_A^{(1)-}(w) + G_A^{(2)-}(w)] \equiv G_{A,0}^{(1)-} + G_{A,0}^{(2)-} \quad (5.25)$$

The upper leg gives

$$- \int_{w=\tau_0+\epsilon}^{\tau_0+\epsilon+4\pi i} \frac{dw}{2\pi i} G_A^-(w) \equiv -G_{A,0}^- \quad (5.26)$$

where we note that the two copies of the CFT have linked into one copy on a doubly wound circle, and we just get the zero mode of G_A^- on this single copy.

Note that

$$G_{A,0}^{(i)-} |0_R^{--}\rangle^{(i)} = 0, \quad i = 1, 2 \quad (5.27)$$

since the α index of $|0_R^{\alpha-}\rangle^{(i)}$ forms a doublet under $SU(2)_L$, and we cannot further lower the spin of $|0_R^{\alpha-}\rangle^{(i)}$ without increasing the energy level. Thus the lower contour gives nothing, and we have

$$|\psi\rangle = -G_{A,0}^-\sigma_2^+(w_0)|0_R^-\rangle^{(1)}|0_R^-\rangle^{(2)}. \quad (5.28)$$

We find it convenient to write this as

$$|\psi\rangle = -G_{A,0}^-|\chi\rangle, \quad (5.29)$$

where

$$|\chi\rangle = \sigma_2^+(w_0)|0_R^-\rangle^{(1)}|0_R^-\rangle^{(2)}. \quad (5.30)$$

5.2.4 Ansatz for $|\chi\rangle$

Let us leave aside the action of $G_{A,0}^-$ for the moment, and consider the state $|\chi\rangle$.

The spin of $|\chi\rangle$ is $-\frac{1}{2}$, since each of the two Ramond ground states have spin $-\frac{1}{2}$ and σ_2^+ has spin $\frac{1}{2}$. Further, the fermions on the double circle produced after the twist are periodic after we go around the double circle; this follows by noting that these fermions were periodic on each of the two copies before the twist, and we have simply cut and rejoined the copies into one long loop. Thus the state $|\chi\rangle$ can be considered as built up by adding excitations (with total charge zero) to the Ramond vacuum $|0_R^-\rangle$ of the doubly twisted theory (we assume that this vacuum is normalized to unit norm)

$$|\chi\rangle = \prod\{\alpha_{C\dot{C},m_i}\}\prod\{\psi_{\dot{D},n_j}^\beta\}|0_R^-\rangle \quad (5.31)$$

As discussed in section (5.2.1), the state $|\chi\rangle$ should have the form of an exponential in the boson and fermion creation operators. Let us write down the ansatz and then explain some of its points. In Appendix E we show that for the bosonic case this ansatz is correct to all orders in the number of excitations; the fermionic case can be done in a similar way. We write

$$|\chi\rangle = \exp \left[-\frac{1}{2} \sum_{m \geq 1, n \geq 1} \gamma_{mn}^B \epsilon^{AB} \epsilon^{\dot{A}\dot{B}} \alpha_{A\dot{A},-m} \alpha_{B\dot{B},-n} + \sum_{m \geq 0, n \geq 1} \gamma_{mn}^F \epsilon_{\dot{A}\dot{B}} \psi_{-m}^{+\dot{A}} \psi_{-n}^{-\dot{B}} \right] |0_R^-\rangle \quad (5.32)$$

Below we define more precisely the modes $\alpha_{A\dot{A},n}, \psi_n^{\alpha\dot{A}}$ on the double circle. For now, let us note some points about the above expression:

1. From eq. (5.13) we see that there will not be any additional multiplicative constant on the RHS; the coefficient of first term obtained by expanding the exponential (i.e. the number unity) is set by (5.13).

2. The initial state $|0_R^-\rangle$ is a singlet of $SO(4)_I$, the symmetry group in the torus directions. The operator σ_2^+ is a singlet under this group also. Thus the state $|\chi\rangle$ will have to be a singlet under this group. Thus we have written the ansatz in a way that the A and \dot{A} indices of $\alpha_{A\dot{A}}$ and $\psi^{\alpha\dot{A}}$ are grouped to make singlets under $SO(4)_I$.

3. We have

$$\alpha_{A\dot{A},0}|0_R^-\rangle = 0 \quad (5.33)$$

since there is no momentum in the state. Thus the mode summations for the bosons start with $m, n = 1$ and not with $m, n = 0$.

4. We have

$$\psi_0^{-\dot{A}}|0_R^-\rangle = 0 \quad (5.34)$$

Thus the sum over fermion modes starts with $n = 1$ for ψ^{--}, ψ^{-+} and with $m = 0$ for ψ^{++}, ψ^{+-} . By writing modes this way we remove a normal ordering term that can arise from the anticommutation of zero modes; such a contribution would then have to be reabsorbed in an overall normalization constant in front of the exponential. We will find later that the value $m = 0$ does not occur either because the γ_{mn}^F vanish for that case; in fact we will find that γ_{mn}^B and γ_{mn}^F are nonzero only for m, n odd.

5.2.5 The First Spectral Flow

Let us continue to work with the state $|\chi\rangle$, and return to $|\psi\rangle$ at the end. First, we perform a spectral flow (2.66) with parameter $\alpha = 1$. Let the resulting state be called $|\chi\rangle_{\alpha=1}$. This spectral flow has the following effects:

1. The Ramond ground states $|0_R^-\rangle^{(i)}, i = 1, 2$ change to NS vacua

$$|0_R^-\rangle^{(1)} \rightarrow |0\rangle^{(1)} \quad |0_R^-\rangle^{(2)} \rightarrow |0\rangle^{(2)}. \quad (5.35)$$

2. The operator σ_2^+ changes by a phase which depends on its charge q ; this charge is $q = \frac{1}{2}$. So we get

$$\sigma_2^+(w_0) \rightarrow e^{-\frac{1}{2}w_0} \sigma_2^+(w_0) \quad (5.36)$$

Thus we get

$$|\chi\rangle_{\alpha=1} = e^{-\frac{1}{2}w_0} \sigma_2^+(w_0) |0\rangle^{(1)} |0\rangle^{(2)} \quad (5.37)$$

3. Modes of bosonic operators are not affected. The fermionic field changes as follows

$$\psi^{+\dot{A}}(w) \rightarrow e^{-\frac{1}{2}w} \psi^{+\dot{A}}(w), \quad \psi^{-\dot{A}}(w) \rightarrow e^{\frac{1}{2}w} \psi^{-\dot{A}}(w) \quad (5.38)$$

Thus fermionic modes change as follows

$$\psi_n^{(i)\pm\dot{A}} \rightarrow \int_{\sigma=0}^{2\pi} \frac{dw}{2\pi i} \psi^{(i)\pm\dot{A}}(w) e^{(n\mp\frac{1}{2})w}, \quad i = 1, 2 \quad (5.39a)$$

$$\psi_n^{\pm\dot{A}} \rightarrow \int_{\sigma=0}^{4\pi} \frac{dw}{2\pi i} \psi^{\pm\dot{A}}(w) e^{\frac{(n\mp 1)}{2}w}. \quad (5.39b)$$

4. For $\tau > \tau_0$, we have one copy of the CFT on a doubly long circle. Before the spectral flow, the state in this region was built by applying excitations to $|0_R^-\rangle$ in Equation(5.31). Under the spectral flow we have

$$|0_R^-\rangle \rightarrow |0_R^+\rangle. \quad (5.40)$$

5.2.6 Mode Expansions on the z Plane

We wish to go to a covering space which will allow us to see explicitly the action of the twist operator. As a preparatory step, it is convenient to map the cylinder with coordinate w to the plane with coordinate z

$$z = e^w \quad (5.41)$$

Under this map the operator modes change as follows. Before the insertion of the twist ($|z| < e^{\tau_0}$) we have

$$\alpha_{AA,n}^{(i)} \rightarrow \int_{z=0} \frac{dz}{2\pi} \partial_z X_{AA}^{(i)}(z) z^n, \quad i = 1, 2 \quad (5.42a)$$

$$\psi_n^{(i)+\dot{A}} \rightarrow \int_{z=0} \frac{dz}{2\pi i} \psi^{(i)+\dot{A}}(z) z^{n-1}, \quad i = 1, 2 \quad (5.42b)$$

$$\psi_n^{(i)-\dot{A}} \rightarrow \int_{z=0} \frac{dz}{2\pi i} \psi^{(i)-\dot{A}}(z) z^n, \quad i = 1, 2 \quad (5.42c)$$

After the twist ($|z| > e^{\tau_0}$) we have

$$\alpha_{AA,n} \rightarrow \int_{z=\infty} \frac{dz}{2\pi} \partial_z X_{AA}(z) z^{\frac{n}{2}} \quad (5.43a)$$

$$\psi_n^{+\dot{A}} \rightarrow \int_{z=\infty} \frac{dz}{2\pi i} \psi^{+\dot{A}}(z) z^{\frac{n-2}{2}} \quad (5.43b)$$

$$\psi_n^{-\dot{A}} \rightarrow \int_{z=\infty} \frac{dz}{2\pi i} \psi^{-\dot{A}}(z) z^{\frac{n}{2}} \quad (5.43c)$$

5.2.7 Mapping to the Covering Space

We pass to the cover of the z plane via the map

$$z = z_0 + t^2 \quad (5.44)$$

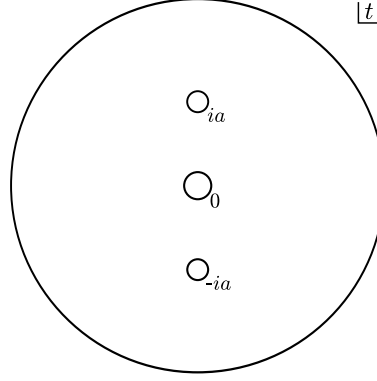


Figure 5.4: The z plane is mapped to the covering space – the t plane – by the map $z = z_0 + t^2$. The point $z = 0$ corresponds to $\tau \rightarrow -\infty$ on the cylinder, and the two copies of the CFT there correspond to the points $t = \pm ia$. The location of the twist operator maps to $t = 0$. The top the cylinder $\tau \rightarrow \infty$ maps to $t \rightarrow \infty$. After all maps and spectral flows, we have the NS vacuum at $t = 0, \pm ia$, and so we can smoothly close all these punctures. The state $|\chi\rangle$ is thus just the t plane vacuum; we must write this in terms of the original cylinder modes and apply the supercharge to get the final state $|\psi\rangle$.

where

$$z_0 = e^{w_0} \equiv a^2 \quad (5.45)$$

Thus the map from the z plane to the t plane has second order branch points at $z = z_0$ (the location of the twist σ_2^+) and at infinity (corresponding to the top of the cylinder, where we can imagine the dual twist $\sigma_{2,+}$ being placed). Under this map we have the following changes:

1. Consider the circle on the cylinder at $\tau \rightarrow -\infty$; this is the location of the initial states on the cylinder. This circle maps to $z = 0$, and then to $t = \pm ia$ on the t plane. There were two copies of the CFT at $\tau \rightarrow -\infty$ on the cylinder, and the initial state of one copy (copy (1)) will map to the point $t = ia$ and the state of the other copy (copy (2)) will map to $t = -ia$.

Note that in our present problem the states of these copies, were $|0_R^-\rangle^{(i)}$ to start with, which became NS vacua $|0\rangle^{(i)}$ after the first spectral flow. Now when we map them to the t plane we find that there is just the t plane vacuum at the points $\pm ia$, so we may smoothly close the punctures at these points with no insertions at the puncture.

2. The location of the twist insertion σ_2^+ maps to $t = 0$. At this location we have the state $|0_R^+\rangle_t$, the spin up Ramond vacuum of the t plane.

3. The operator modes before the twist become

$$\alpha_{A\dot{A},n}^{(1,2)} \rightarrow \int_{t=\pm ia} \frac{dt}{2\pi} \partial_t X_{A\dot{A}}(t) (z_0 + t^2)^n \quad (5.46a)$$

$$\psi_n^{(1,2)+\dot{A}} \rightarrow \int_{t=\pm ia} \frac{dt}{2\pi i} \psi^{+\dot{A}}(t) (z_0 + t^2)^{n-1} \sqrt{2t} \quad (5.46b)$$

$$\psi_n^{(1,2)-\dot{A}} \rightarrow \int_{t=\pm ia} \frac{dt}{2\pi i} \psi^{-\dot{A}}(t) (z_0 + t^2)^n \sqrt{2t} \quad (5.46c)$$

After the twist we have

$$\alpha_{A\dot{A},n} \rightarrow \int_{t=\infty} \frac{dt}{2\pi} \partial_t X_{A\dot{A}}(t) (z_0 + t^2)^{\frac{n}{2}} \quad (5.47a)$$

$$\psi_n^{+\dot{A}} \rightarrow \int_{t=\infty} \frac{dt}{2\pi i} \psi^{+\dot{A}}(t) (z_0 + t^2)^{\frac{n-2}{2}} \sqrt{2t} \quad (5.47b)$$

$$\psi_n^{-\dot{A}} \rightarrow \int_{t=\infty} \frac{dt}{2\pi i} \psi^{-\dot{A}}(t) (z_0 + t^2)^{\frac{n}{2}} \sqrt{2t} \quad (5.47c)$$

5.2.8 The Second Spectral Flow

We have now mapped the problem to the t plane, where we have found a state $|0_R^+\rangle_t$ at $t = 0$, and no other insertions anywhere. Let us perform a spectral flow with $\alpha = -1$ in the t plane. This has the following effects

1. The Ramond ground state at $t = 0$ maps to the NS vacuum in the t plane,

$$|0_R^+\rangle_t \rightarrow |0\rangle_t. \quad (5.48)$$

2. The operator modes change as follows. The bosons are not affected. The fermion field changes as

$$\psi^{\pm\dot{A}}(t) \rightarrow t^{\pm\frac{1}{2}} \psi^{\pm\dot{A}}(t). \quad (5.49)$$

Before the twist we get the modes

$$\alpha_{A\dot{A},n}^{(1,2)} \rightarrow \int_{t=\pm ia} \frac{dt}{2\pi} \partial_t X_{A\dot{A}}(t) (z_0 + t^2)^n \quad (5.50a)$$

$$\psi_n^{(1,2)+\dot{A}} \rightarrow \sqrt{2} \int_{t=\pm ia} \frac{dt}{2\pi i} \psi^{+\dot{A}}(t) (z_0 + t^2)^{n-1} t \quad (5.50b)$$

$$\psi_n^{(1,2)-\dot{A}} \rightarrow \sqrt{2} \int_{t=\pm ia} \frac{dt}{2\pi i} \psi^{-\dot{A}}(t) (z_0 + t^2)^n \quad (5.50c)$$

$$(5.50d)$$

After the twist we have

$$\alpha_{A\dot{A},n} \rightarrow \int_{t=\infty} \frac{dt}{2\pi} \partial_t X_{A\dot{A}}(t) (z_0 + t^2)^{\frac{n}{2}} \quad (5.51a)$$

$$\psi_n^{+\dot{A}} \rightarrow \sqrt{2} \int_{t=\infty} \frac{dt}{2\pi i} \psi^{+\dot{A}}(t) (z_0 + t^2)^{\frac{n-2}{2}} t \quad (5.51b)$$

$$\psi_n^{-\dot{A}} \rightarrow \sqrt{2} \int_{t=\infty} \frac{dt}{2\pi i} \psi^{-\dot{A}}(t) (z_0 + t^2)^{\frac{n}{2}} \quad (5.51c)$$

In the t plane, we also find it convenient to define mode operators that are natural to the t plane,

$$\tilde{\alpha}_{A\dot{A},n} \equiv \int_{t=0} \frac{dt}{2\pi} \partial_t X_{A\dot{A}}(t) t^n \quad (5.52a)$$

$$\tilde{\psi}_r^{\alpha\dot{A}} \equiv \int_{t=0} \frac{dt}{2\pi i} \psi^{\alpha\dot{A}}(t) t^{r-\frac{1}{2}}. \quad (5.52b)$$

Note that the bosonic index n is an integer while the fermionic index r is a half integer. We have

$$\tilde{\alpha}_{A\dot{A},m}|0\rangle_t = 0, \quad m \geq 0 \quad (5.53a)$$

$$\tilde{\psi}_r^{\alpha\dot{A}}|0\rangle_t = 0, \quad r > 0. \quad (5.53b)$$

The commutation relations are

$$[\tilde{\alpha}_{A\dot{A}}, \tilde{\alpha}_{B\dot{B}}] = -\epsilon_{AB}\epsilon_{\dot{A}\dot{B}} m \delta_{m+n,0} \quad (5.54a)$$

$$\{\tilde{\psi}_r^{\alpha\dot{A}}, \tilde{\psi}_s^{\beta\dot{B}}\} = -\epsilon^{\alpha\beta}\epsilon^{\dot{A}\dot{B}} \delta_{r+s,0} \quad (5.54b)$$

5.2.9 Computing γ_{mn}^B and γ_{mn}^F

In this section we compute the coefficients γ_{mn}^B and γ_{mn}^F . For this computation we use the relation (5.18) to relate correlators of operators on the cylinder to correlators on the t plane. The latter correlators can be computed very simply, and we thereby find the coefficients γ_{mn}^B and γ_{mn}^F .

The Bosonic Coefficients γ_{mn}^B

Let us compute

$$\langle 0_{R,-} | \left(\alpha_{++ ,n} \alpha_{-- ,m} \right) \sigma_2^+(w_0) | 0_R^- \rangle^{(1)} | 0_R^- \rangle^{(2)} = {}_t \langle 0 | \left(\alpha'_{++ ,n} \alpha'_{-- ,m} \right) | 0 \rangle_t \quad (5.55)$$

where the primes on the operators on the RHS signify the fact that these operators arise from the unprimed operators by the various maps leading to the spectral flowed t plane

description. Using the ansatz (5.32) we can write the LHS as

$$\begin{aligned} \langle 0_{R,-} | \left(\alpha_{++} \alpha_{--} \right) \exp \left[\sum_{m \geq 1, n \geq 1} \gamma_{mn}^B (-\alpha_{++} \alpha_{--} + \alpha_{-+} \alpha_{+-}) \right] \\ \times \exp \left[\sum_{m \geq 0, n \geq 1} \gamma_{mn}^F \epsilon_{\dot{A}\dot{B}} \psi_{-m}^{+\dot{A}} \psi_{-n}^{-\dot{B}} \right] | 0_R^- \rangle \end{aligned} \quad (5.56)$$

Expanding the exponential, and using the commutation relations (5.24a), one finds that this LHS equals

$$-mn \gamma_{mn}^B \langle 0_{R,-} | 0_R^- \rangle = -mn \gamma_{mn}^B \quad (5.57)$$

where we have used Equation (5.12).

The RHS of (5.55) can be written by expressing the inserted operators as contour integrals over circles at large t

$$_t \langle 0 | \left(\int \frac{dt_1}{2\pi i} \partial_t X_{++}(t_1) (z_0 + t_1^2)^{\frac{n}{2}} \right) \left(\int \frac{dt_2}{2\pi i} \partial_t X_{--}(t_2) (z_0 + t_2^2)^{\frac{m}{2}} \right) | 0 \rangle_t \quad (5.58)$$

with $|t_1| > |t_2|$. We have

$$(z_0 + t_1^2)^{\frac{n}{2}} = \sum_{p \geq 0} \binom{\frac{n}{2}}{p} z_0^p t_1^{n-2p} \quad (5.59a)$$

$$(z_0 + t_2^2)^{\frac{m}{2}} = \sum_{q \geq 0} \binom{\frac{m}{2}}{q} z_0^q t_2^{m-2q} \quad (5.59b)$$

Equating (5.57) and (5.58) gives

$$\gamma_{mn} = -\frac{1}{mn} \sum_{p \geq 0} \sum_{q \geq 0} \binom{\frac{n}{2}}{p} \binom{\frac{m}{2}}{q} z_0^{p+q} {}_t \langle 0 | \tilde{\alpha}_{++} \tilde{\alpha}_{--} | 0 \rangle_t \quad (5.60)$$

Using the commutation relations (5.54a) we get

$$m - 2q = -(n - 2p) \quad \Rightarrow \quad q = \frac{m+n}{2} - p \quad (5.61)$$

Since p, q are integral, either n, m are both even or both odd. Using Eq. (5.53a) we find

$$\gamma_{mn} = \frac{1}{mn} \sum_{p=0}^{\lfloor \frac{n}{2} \rfloor} \binom{\frac{n}{2}}{p} \binom{\frac{m}{2}}{\frac{m+n}{2} - p} z_0^{\frac{m+n}{2}} (n - 2p) \quad (5.62)$$

where the symbol $\lfloor \cdot \rfloor$ stands for the “floor” (i.e. “integer part of”). We can perform this sum using a symbolic manipulation program like *Mathematica*²⁹. With either n or m even

²⁹The sum can be evaluated by hand by writing it in terms of the series representation of ${}_2F_1(-\frac{m-1}{2}, 1; \frac{n-1}{2} + 2; 1)$.

we get

$$\gamma_{mn}^B = 0 \quad m \text{ or } n \text{ even.} \quad (5.63)$$

For n and m odd we write

$$m = 2m' + 1, \quad n = 2n' + 1 \quad (5.64)$$

and find

$$\gamma_{2m'+1, 2n'+1}^B = \frac{2}{(2m' + 1)(2n' + 1)(1 + m' + n')\pi} \frac{z_0^{(1+m'+n')}\Gamma(\frac{3}{2} + m')\Gamma(\frac{3}{2} + n')}{\Gamma(m' + 1)\Gamma(n' + 1)}. \quad (5.65)$$

We rewrite and summarize the result as

$$\gamma_{mn}^B = \begin{cases} \frac{4z_0^{\frac{m+n}{2}}}{mn(m+n)\pi} \frac{\Gamma(\frac{m}{2}+1)\Gamma(\frac{n}{2}+1)}{\Gamma(\frac{m+1}{2})\Gamma(\frac{n+1}{2})} & m, n \text{ odd, positive} \\ 0 & \text{otherwise} \end{cases}. \quad (5.66)$$

Note that in what follows we frequently abbreviate “odd and positive” as odd⁺.

The Fermionic Coefficients γ_{mn}^F

We follow the same steps to find γ_{mn}^F . Let us compute

$$\langle 0_{R,-} | \left(\psi_n^{++} \psi_m^{--} \right) \sigma_2^+(w_0) | 0_R^- \rangle^{(1)} | 0_R^- \rangle^{(2)} = {}_t \langle 0 | \left(\psi_n'^{++} \psi_m'^{--} \right) | 0 \rangle_t \quad (5.67)$$

We can write the LHS as

$$\begin{aligned} \langle 0_{R,-} | \psi_n^{++} \psi_m^{--} \exp \left[-\frac{1}{2} \sum_{m \geq 1, n \geq 1} \gamma_{mn}^B \epsilon^{AB} \epsilon^{\dot{A}\dot{B}} \alpha_{A\dot{A},-m} \alpha_{B\dot{B},-n} \right] \\ \times \exp \left[\sum_{m \geq 0, n \geq 1} \gamma_{mn}^F [\psi_{-m}^{++} \psi_{-n}^{--} - \psi_{-m}^{+-} \psi_{-n}^{-+}] \right] | 0_R^- \rangle \end{aligned} \quad (5.68)$$

Expanding the exponential, and using the commutation relations (5.24b), one finds that this LHS equals

$$4\gamma_{mn}^F \langle 0_{R,-} | 0_R^- \rangle = 4\gamma_{mn}^F \quad (5.69)$$

The RHS of (5.67) gives

$${}_t \langle 0 | \left[\sqrt{2} \int \frac{dt_1}{2\pi i} \psi^{++}(t_1) (z_0 + t_1^2)^{\frac{n-2}{2}} t_1 \right] \left[\sqrt{2} \int \frac{dt_2}{2\pi i} \psi^{--}(t_2) (z_0 + t_2^2)^{\frac{m}{2}} \right] | 0 \rangle_t \quad (5.70)$$

with $|t_1| > |t_2|$. We have

$$(z_0 + t_1^2)^{\frac{n-2}{2}} = \sum_{p \geq 0} \binom{\frac{n-2}{2}}{p} z_0^p t_1^{n-2-2p} \quad (5.71a)$$

$$(z_0 + t_2^2)^{\frac{m}{2}} = \sum_{q \geq 0} \binom{\frac{m}{2}}{q} z_0^q t_2^{m-2q} \quad (5.71b)$$

Equating (5.69) and (5.70) gives

$$\gamma_{mn}^F = \frac{1}{2} \sum_{p \geq 0} \sum_{q \geq 0} \binom{\frac{n-2}{2}}{p} \binom{\frac{m}{2}}{q} \langle 0 | \tilde{\psi}_{n-2p-\frac{1}{2}}^{++} \tilde{\psi}_{m-2q+\frac{1}{2}}^{--} | 0 \rangle_t. \quad (5.72)$$

Using the commutation relations (5.54b) we get

$$m - 2q + \frac{1}{2} = -(n - 2p - \frac{1}{2}) \implies q = \frac{m+n}{2} - p \quad (5.73)$$

From (5.53b) we have that

$$n - 2p - \frac{1}{2} > 0, \quad m - 2q + \frac{1}{2} < 0 \quad (5.74)$$

Thus we get

$$\gamma_{mn}^F = -\frac{1}{2} \sum_{p=0}^{\lfloor \frac{n-1}{2} \rfloor} \binom{\frac{n-2}{2}}{p} \binom{\frac{m}{2}}{\frac{m+n}{2} - p} z_0^{\frac{m+n}{2}} \quad (5.75)$$

With either n or m even we get

$$\gamma_{mn}^F = 0 \quad m \text{ or } n \text{ even.} \quad (5.76)$$

For n and m both odd we write

$$m = 2m' + 1, \quad n = 2n' + 1 \quad (5.77)$$

and find

$$\gamma_{2m'+1, 2n'+1}^F = -\frac{z_0^{(1+m'+n')}\Gamma(\frac{3}{2} + m')\Gamma(\frac{3}{2} + n')}{(2n' + 1)(1 + m' + n')\pi\Gamma(m' + 1)\Gamma(n' + 1)}. \quad (5.78)$$

We rewrite and summarize the result as

$$\gamma_{mn}^F = \begin{cases} -\frac{2z_0^{\frac{m+n}{2}}}{n(m+n)\pi} \frac{\Gamma(\frac{m}{2}+1)\Gamma(\frac{n}{2}+1)}{\Gamma(\frac{m+1}{2})\Gamma(\frac{n+1}{2})} & m, n \text{ odd}^+ \\ 0 & \text{otherwise.} \end{cases} \quad (5.79)$$

Note that if we compare this result to Equation (5.66), and take into account the normalization of α_m , the two results differ by a factor of $\sqrt{\frac{m}{n}}$. The bosons and fermions behave essentially the same, except for an asymmetry between '+' and '-', which we attribute to

the asymmetry of the twist operator and Ramond state.

5.2.10 The State $|\psi\rangle$

Finally we return to the computation of $|\psi\rangle$

$$|\psi\rangle = -G_{A,0}^- |\chi\rangle \quad (5.80)$$

We begin by applying the supercharge,

$$G_{A,0}^- = \int_{w=\tau}^{w=\tau+4\pi i} \frac{dw}{2\pi i} G_A^-(w) = -\frac{i}{2} \sum_{n=-\infty}^{\infty} \psi_n^{-\dot{A}} \alpha_{A\dot{A},-n}. \quad (5.81)$$

The positive index modes in the above expression can act on the exponential in $|\chi\rangle$, generating negative index modes. We would like to write $|\psi\rangle$ with only negative index modes acting on $|0_R^-\rangle$; these modes have trivial commutation and anticommutation relations with each other. Thus we write

$$G_{A,0}^- = -\frac{i}{2} \sum_{n>0} \psi_{-n}^{-\dot{A}} \alpha_{A\dot{A},n} - \frac{i}{2} \sum_{n>0} \psi_n^{-\dot{A}} \alpha_{A\dot{A},-n}. \quad (5.82)$$

Recall that $\gamma_{mn}^B, \gamma_{mn}^F$ are nonzero only for odd indices. Thus we write $n = 2n' + 1, m = 2m' + 1$, and find

$$-\frac{i}{2} \sum_{n>0} \psi_{-n}^{-\dot{A}} \alpha_{A\dot{A},n} |\chi\rangle = -\frac{i}{2} \sum_{n'\geq 0, m'\geq 0} (2n' + 1) \gamma_{2m'+1, 2n'+1}^B \psi_{-(2n'+1)}^{-\dot{A}} \alpha_{A\dot{A}, -(2m'+1)} |\chi\rangle \quad (5.83a)$$

$$-\frac{i}{2} \sum_{n>0} \psi_n^{-\dot{A}} \alpha_{A\dot{A},-n} |\chi\rangle = i \sum_{n'\geq 0, m'\geq 0} \gamma_{2m'+1, 2n'+1}^F \psi_{-(2n'+1)}^{-\dot{A}} \alpha_{A\dot{A}, -(2m'+1)} |\chi\rangle \quad (5.83b)$$

Thus

$$G_{A,0}^- |\chi\rangle = -i \sum_{n'\geq 0, m'\geq 0} \left((n' + \frac{1}{2}) \gamma_{2m'+1, 2n'+1}^B - \gamma_{2m'+1, 2n'+1}^F \right) \psi_{-(2n'+1)}^{-\dot{A}} \alpha_{A\dot{A}, -(2m'+1)} |\chi\rangle \quad (5.84)$$

Using the values of γ^B, γ^F from Equations (5.66) and (5.79), we find

$$\begin{aligned} & (n' + \frac{1}{2}) \gamma_{2m'+1, 2n'+1}^B - \gamma_{2m'+1, 2n'+1}^F \\ &= z_0^{m'+n'+1} \frac{\Gamma(\frac{3}{2} + m') \Gamma(\frac{3}{2} + n')}{(m' + n' + 1) \pi \Gamma(m' + 1) \Gamma(n' + 1)} \left(\frac{1}{2m' + 1} + \frac{1}{2n' + 1} \right) \\ &= z_0^{m'+n'+1} \frac{2\Gamma(\frac{3}{2} + m') \Gamma(\frac{3}{2} + n')}{\pi (2m' + 1) (2n' + 1) \Gamma(m' + 1) \Gamma(n' + 1)} \end{aligned} \quad (5.85)$$

The n' and m' sums factorize into the form

$$G_{A,0}^- |\chi\rangle = -i \left(\sum_{n' \geq 0} \frac{\sqrt{2} z_0^{n' + \frac{1}{2}} \Gamma(\frac{3}{2} + n')}{\sqrt{\pi} (2n' + 1) \Gamma(n' + 1)} \psi_{-(2n'+1)}^{-\dot{A}} \right) \times \left(\sum_{m' \geq 0} \frac{\sqrt{2} z_0^{m' + \frac{1}{2}} \Gamma(\frac{3}{2} + m')}{\sqrt{\pi} (2m' + 1) \Gamma(m' + 1)} \alpha_{A\dot{A}, -(2m'+1)} \right) |\chi\rangle, \quad (5.86)$$

which we can rewrite as

$$G_{A,0}^- |\chi\rangle = -i \frac{2}{\pi} \left[\sum_{n \text{ odd}^+} \frac{z_0^{\frac{n}{2}} \Gamma(\frac{n}{2} + 1)}{n \Gamma(\frac{n+1}{2})} \psi_{-n}^{-\dot{A}} \right] \left[\sum_{m \text{ odd}^+} \frac{z_0^{\frac{m}{2}} \Gamma(\frac{m}{2} + 1)}{m \Gamma(\frac{m+1}{2})} \alpha_{A\dot{A}, -m} \right] |\chi\rangle \quad (5.87)$$

The Final State

Finally, we write down the complete final state. Recall that we break the state into left and right sectors:

$$|\Psi\rangle_f = |\psi\rangle |\bar{\psi}\rangle. \quad (5.88)$$

The final state on the left sector is give by

$$\begin{aligned} |\psi\rangle &= -G_{A,0}^- |\chi\rangle \\ &= \frac{2i}{\pi} \left[\sum_{n \text{ odd}^+} \frac{z_0^{\frac{n}{2}} \Gamma(\frac{n}{2} + 1)}{n \Gamma(\frac{n+1}{2})} \psi_{-n}^{-\dot{A}} \right] \left[\sum_{m \text{ odd}^+} \frac{z_0^{\frac{m}{2}} \Gamma(\frac{m}{2} + 1)}{m \Gamma(\frac{m+1}{2})} \alpha_{A\dot{A}, -m} \right] \\ &\quad \times \exp \left[-\frac{1}{2} \sum_{p,q \text{ odd}^+} \gamma_{pq}^B \epsilon^{AB} \epsilon^{\dot{A}\dot{B}} \alpha_{A\dot{A}, -p} \alpha_{B\dot{B}, -q} + \sum_{p,q \text{ odd}^+} \gamma_{pq}^F \epsilon_{\dot{A}\dot{B}} \psi_{-p}^{+\dot{A}} \psi_{-q}^{-\dot{B}} \right] |0_R^-\rangle, \end{aligned} \quad (5.89)$$

with a similar expression for $|\bar{\psi}\rangle = -\bar{G}_{B,0}^- |\bar{\chi}\rangle$.

5.3 Applying the Deformation Operator to Excited States

We now wish to consider the situation where we have an excitation in the initial state on the cylinder. These excitations are generated by operators $\alpha_{A\dot{A},n}, \psi_n^{\alpha\dot{A}}$. Here we must have $n \leq -1$ for bosonic excitations, since there is no momentum and so the zero mode $\alpha_{A\dot{A},0}$ kills the vacuum. For the fermions, we have $n \leq 0$ for $\psi_n^{+\dot{A}}$ and $n < 0$ for $\psi_n^{-\dot{A}}$ since we cannot apply the zero mode $\psi_0^{-\dot{A}}$ to the vacuum $|0_R^-\rangle^{(1)} |0_R^-\rangle^{(2)}$ that we have taken as the starting point before we apply the excitation modes.

Let us note the steps we will have to perform in general:

1. In Section 5.2.3 we decomposed the action of the supercharge into an application of $-(G_{A,0}^{(1)-} + G_{A,0}^{(2)-})$ below the twist and an application of $G_{A,0}^-$ above the twist. Let us

first consider the part below the twist. We commute these supercharge modes down through any excitations $\alpha_{A\dot{A},n}, \psi_n^{\alpha\dot{A}}$ present in the initial state. After a supercharge zero mode passes all these modes it reaches the state $|0_R^-\rangle^{(1)}|0_R^-\rangle^{(2)}$ at the bottom of the cylinder, and we get zero. The commutation through the excitations can be computed by using the relations

$$[G_{A,0}^{(1)-}, \alpha_{B\dot{B},m}^{(1)}] = -i \sum_{n=-\infty}^{\infty} \psi_{-n}^{(1)-\dot{A}} [\alpha_{A\dot{A},n}^{(1)}, \alpha_{B\dot{B},m}^{(1)}] = -im\epsilon_{AB}\epsilon_{\dot{A}\dot{B}}\psi_m^{(1)-\dot{A}} \quad (5.90a)$$

$$\{G_{A,0}^{(1)-}, \psi_m^{(1)-\dot{B}}\} = 0 \quad (5.90b)$$

$$\{G_{A,0}^{(1)-}, \psi_m^{(1)+\dot{B}}\} = i\epsilon^{\dot{A}\dot{B}}\alpha_{A\dot{A},m}^{(1)}. \quad (5.90c)$$

We have exactly analogous relations for the operators in copy 2.

2. Having disposed of any supercharge present below the twist, we get the twist operator σ_2^+ acting on a set of bosonic and fermionic modes. In the sections below we will take the case where we have a single bosonic or fermionic mode below the twist σ_2^+ , and will find that this can be expressed as a linear combination of single particle modes acting *after* the twist. If we have several modes below the twist, then we can perform the same process with each mode, except that there can be in addition a “Wick contraction” between a pair of bosonic or fermionic modes. This results in a \mathbb{C} -number contribution, which we compute as well.
3. In this manner we obtain a state where we have σ_2^+ acting on the spin down Ramond vacuum, and a set of excitations acting after this twist. The action of σ_2^+ on the Ramond vacuum gives the state $|\chi\rangle$ (defined in (5.30)); this state was found in [202] and is given in (5.32). Thus we get a set of modes acting on $|\chi\rangle$. Finally we note that we have a part of the amplitude where we must act with the supercharge mode applied after all other operators. This is done using the relations

$$[G_{A,0}^-, \alpha_{B\dot{B}}] = -\frac{i}{2} \sum_{n=-\infty}^{\infty} \psi_n^{-\dot{A}} [\alpha_{A\dot{A},-n}, \alpha_{B\dot{B},m}] = -\frac{1}{2}im\epsilon_{AB}\epsilon_{\dot{A}\dot{B}}\psi_m^{-\dot{A}} \quad (5.91a)$$

$$\{G_{A,0}^-, \psi_m^{-\dot{B}}\} = 0 \quad (5.91b)$$

$$\{G_{A,0}^-, \psi_m^{+\dot{B}}\} = i\epsilon^{AB}\alpha_{A\dot{A},m} \quad (5.91c)$$

We can use these relations to commute the supercharge down through the modes now present above σ_2^+ , until it reaches the twist insertion. The supercharge applied to the twist, with the Ramond vacuum below the twist, results in the state $|\psi\rangle$ given in (5.89) [202]. Thus we end up with a set of modes on the doubly wound circle, acting on $|\chi\rangle$ and $|\psi\rangle$.

In this manner we compute the full state resulting from the action of the deformation operator on a general initial state containing excitations.

5.3.1 The Action of $\sigma_2^+(w_0)$ on a Single Bosonic Mode

We perform the following computation: we have a single excitation in the initial state, and the action of σ_2^+ on this state. The created state will have the same exponential as in the state $|\chi\rangle$ created by σ_2^+ from the vacuum, but in addition the initial excitation will split into a linear combination of single particle modes in the final state.

Let us find the state

$$|\xi\rangle = \sigma_2^+(w_0)\alpha_{A\dot{A},n}^{(1)}|0_R^{--}\rangle^{(1)}|0_R^{--}\rangle^{(2)} \quad (5.92)$$

Since the vacuum state $|0_R^{--}\rangle^{(1)}|0_R^{--}\rangle^{(2)}$ is killed by nonnegative modes of the boson, we will take

$$n \leq -1 \quad (5.93)$$

We perform the spectral flows and coordinate maps given in Section 5.2. This brings us to the t -plane with all punctures at $t = \pm ia, t = 0$, smoothly closed. Before these steps, the mode $\alpha_{A\dot{A},n}^{(1)}$ is given in (5.19a), and after all the spectral flow and coordinate maps, it is given in the t plane by (5.46a)

$$\alpha_{A\dot{A},n}^{(1)} \rightarrow \int_{t=ia} \frac{dt}{2\pi} \partial_t X_{A\dot{A}}(t) (z_0 + t^2)^n \quad (5.94)$$

We will now go through a sequence of steps to find the effect of this mode in the final state. The essence of these steps is in the following. The initial state modes (5.94) are defined by a contour around the point $t = ia$. The final state modes (5.51a) are defined at large t . They involve the function $(z_0 + t^2)^{\frac{n}{2}}$ which has branch points in the t plane for odd n , so we cannot directly stretch the contour giving the initial state modes to get the modes in the final state. Instead, we proceed from the initial modes to the final modes through a sequence of steps that expands the initial contour into a linear combination of modes at large t .

The contour in (5.94) circles the point $t = ia$. As we saw in Section 5.2, there is no singularity at $t = ia$ after all spectral flows and coordinate maps have been done. Thus if we define modes

$$\hat{\alpha}_{A\dot{A},n}^{(1)} = \int_{t=ia} \frac{dt}{2\pi} \partial_t X_{A\dot{A}}(t) (t - ia)^n, \quad (5.95)$$

then we will find

$$\hat{\alpha}_{A\dot{A},n}|0\rangle_{ia} = 0, \quad n \geq 0 \quad (5.96)$$

where $|0\rangle_{ia}$ is the NS vacuum at the point $t = ia$, and we have noted that the zero mode vanishes since there is no momentum for the boson at any stage. The modes (5.95) have the commutation relations

$$[\hat{\alpha}_{A\dot{A},m}, \hat{\alpha}_{B\dot{B},n}] = -\epsilon_{AB}\epsilon_{\dot{A}\dot{B}}m\delta_{m+n,0} \quad (5.97)$$

Thus we would like to expand the mode (5.94) in modes of type (5.95). Writing

$$z_0 + t^2 = (t - ia)(t + ia) \quad (5.98)$$

we write the mode (5.94) as

$$\alpha_{A\dot{A},n}^{(1)} \rightarrow \int_{t=ia} \frac{dt}{2\pi} \partial_t X_{A\dot{A}}(t) (t - ia)^n (t + ia)^n \quad (5.99)$$

We have

$$\begin{aligned} (t + ia)^n &= \left(2ia + (t - ia)\right)^n \\ &= (2ia)^n \left(1 + (2ia)^{-1}(t - ia)\right)^n \\ &= \sum_{k \geq 0} \binom{n}{k} (2ia)^{(n-k)} (t - ia)^k \end{aligned} \quad (5.100)$$

We thus find

$$\alpha_{A\dot{A},n}^{(1)} \rightarrow \sum_{k \geq 0} \binom{n}{k} (2ia)^{(n-k)} \int_{ia} \frac{dt}{2\pi} \partial_t X_{A\dot{A}}(t) (t - ia)^{(n+k)} = \sum_{k \geq 0} \binom{n}{k} (2ia)^{(n-k)} \hat{\alpha}_{n+k}^{(1)}. \quad (5.101)$$

Since, there are no other insertions in the t -plane, we get a nonzero contribution only from modes with

$$n + k \leq -1 \Rightarrow k \leq -n - 1. \quad (5.102)$$

(Recall from (5.93) that n is negative.) Thus we have

$$\alpha_{A\dot{A},n}^{(1)} \rightarrow \sum_{k=0}^{-n-1} \binom{n}{k} (2ia)^{(n-k)} \hat{\alpha}_{n+k}^{(1)}. \quad (5.103)$$

Note that this is a finite sum; this is important to have convergence for sums that we will encounter below.

We can now convert the original z -plane modes to $\tilde{\alpha}$ modes defined for large t . The contour in the operators $\hat{\alpha}_{A\dot{A},n}$ circles $t = ia$. But as we have seen in Section 5.2, there are no singularities at other points in the t plane, so we can stretch this contour into a contour

at large t , which we write as $\int_{t=\infty}$. We get

$$\hat{\alpha}_{A\dot{A},m}^{(1)} \rightarrow \int_{t=\infty} \frac{dt}{2\pi} \partial_t X_{A\dot{A}}(t) (t - ia)^m, \quad (5.104)$$

which we can plug into with

$$(t - ia)^m = \sum_{k' \geq 0} \binom{m}{k'} (-ia)^{k'} t^{m-k'}. \quad (5.105)$$

Let us now define modes natural for large t in the t plane,

$$\tilde{\alpha}_{A\dot{A},m} \equiv \int_{t=\infty} \frac{dt}{2\pi} \partial_t X_{A\dot{A}}(t) t^m, \quad (5.106)$$

which satisfy

$$[\tilde{\alpha}_{A\dot{A}}, \tilde{\alpha}_{B\dot{B}}] = -\epsilon_{AB} \epsilon_{\dot{A}\dot{B}} m \delta_{m+n,0}; \quad \tilde{\alpha}_{A\dot{A},m} |0\rangle_t = 0, \quad m \geq 0. \quad (5.107)$$

We can expand the modes out to

$$\hat{\alpha}_{A\dot{A},m} = \sum_{k' \geq 0} \binom{m}{k'} (-ia)^{k'} \tilde{\alpha}_{A\dot{A},m-k'}. \quad (5.108)$$

Let us now substitute this expansion for $\hat{\alpha}_{A\dot{A},m}$ into (5.103). We get

$$\alpha_{A\dot{A},n}^{(1)} \rightarrow \sum_{k=0}^{-n-1} \binom{n}{k} (2ia)^{(n-k)} \sum_{k' \geq 0} \binom{n+k}{k'} (-ia)^{k'} \tilde{\alpha}_{A\dot{A},n+k-k'}. \quad (5.109)$$

Let us look at the coefficient of $\tilde{\alpha}_{A\dot{A},q}$. Thus

$$q = n + k - k' \Rightarrow k' = n + k - q. \quad (5.110)$$

Since we have $k' \geq 0$, we find

$$n + k - q \geq 0 \Rightarrow k \geq q - n \quad (5.111)$$

Thus the k sum runs over the following range

$$\begin{aligned} q - n \leq 0 : \quad k &\in [0, -n - 1] \\ q - n \geq 0 : \quad k &\in [q - n, -n - 1] \end{aligned} \quad (5.112)$$

Recall that $n \leq -1$. The second of these equations tells us that there is no summation range at all for $q \geq 0$. Thus we only generate negative index modes $\tilde{\alpha}_{A\dot{A},q}$ from our expansion:

$$q \leq -1 \quad (5.113)$$

We now have

$$\begin{aligned}\alpha_{A\dot{A},n}^{(1)} &\rightarrow \sum_{q \leq -1} \left[\sum_{k=0}^{-n-1} \binom{n}{k} (2ia)^{(n-k)} \binom{n+k}{n+k-q} (-ia)^{n+k-q} \right] \tilde{\alpha}_{A\dot{A},q}, & q \leq n \\ \alpha_{A\dot{A},n}^{(1)} &\rightarrow \sum_{q \leq -1} \left[\sum_{k=q-n}^{-n-1} \binom{n}{k} (2ia)^{(n-k)} \binom{n+k}{n+k-q} (-ia)^{n+k-q} \right] \tilde{\alpha}_{A\dot{A},q}, & q \geq n.\end{aligned}\quad (5.114)$$

The sum has the same algebraic expression in both the ranges for q , and we find

$$\alpha_{A\dot{A},n}^{(1)} \rightarrow \sum_{q \leq -1} \frac{i^{-q} (-1)^n a^{2n-q} \Gamma(-\frac{q}{2})}{2\Gamma(-n)\Gamma(n+1-\frac{q}{2})} \tilde{\alpha}_{A\dot{A},q}. \quad (5.115)$$

Now, we wish to convert the z -plane modes before the twist into z -plane modes after the twist. These are the modes on the cylinder at $\tau \rightarrow \infty$, given in (5.51a)

$$\alpha_{A\dot{A},p} \rightarrow \int_{t=\infty} \frac{dt}{2\pi} \partial_t X_{A\dot{A}}(t) (z_0 + t^2)^{\frac{p}{2}} \quad (5.116)$$

Write

$$t' = \sqrt{t^2 + z_0} \Rightarrow t = (t'^2 - z_0)^{\frac{1}{2}} \quad (5.117)$$

with the sign of the square root chosen to give $t' \sim t$ near infinity. Then we have

$$t^q = (t'^2 - z_0)^{\frac{q}{2}} = t'^q \left(1 - z_0 t'^{-2}\right)^{\frac{q}{2}} = \sum_{k \geq 0} \binom{\frac{q}{2}}{k} (-z_0)^k t'^{q-2k} = \sum_{k \geq 0} \binom{\frac{q}{2}}{k} (-z_0)^k (z_0 + t^2)^{\frac{q-2k}{2}}. \quad (5.118)$$

Substituting this expansion in (5.106) we find that

$$\tilde{\alpha}_{A\dot{A},q} = \int \frac{dt}{2\pi} \partial_t X_{A\dot{A}}(t) \sum_{k \geq 0} \binom{\frac{q}{2}}{k} (-z_0)^k (z_0 + t^2)^{\frac{q-2k}{2}}. \quad (5.119)$$

Using (5.116) we find

$$\tilde{\alpha}_{A\dot{A},q} = \sum_{k \geq 0} \binom{\frac{q}{2}}{k} (-z_0)^k \alpha_{A\dot{A},q-2k} \quad (5.120)$$

We substitute the expansion (5.120) into (5.115), getting

$$\alpha_{A\dot{A},n}^{(1)} \rightarrow \sum_{q \leq -1} \frac{i^{-q} (-1)^n a^{2n-q} \Gamma(-\frac{q}{2})}{2\Gamma(-n)\Gamma(n+1-\frac{q}{2})} \sum_{k \geq 0} \binom{\frac{q}{2}}{k} (-z_0)^k \alpha_{A\dot{A},q-2k} \quad (5.121)$$

Let us look at the coefficient of $\alpha_{A\dot{A},p}$ in this sum. This gives

$$p = q - 2k \quad (5.122)$$

Note that since $q \leq -1$ and $k \geq 0$, we have

$$p \leq -1 \quad (5.123)$$

From (5.122) we see that if p is even only even values of q contribute to this sum, and if p is odd then only odd values of q contribute. For the even p case we write $p = 2p'$, $q = 2q'$. From (5.122) we set $k = q' - p'$. Since $k \geq 0$, the range of the q' sum becomes $p' \leq q' \leq -1$. We get the sum

$$\sum_{q'=p'}^{-1} \frac{(-1)^{q'+n} a^{2n-2q'} \Gamma(-q')}{2\Gamma(-n)\Gamma(n+1-q')} \binom{q'}{q'-p'} (-z_0)^{q'-p'} = \frac{1}{2} \delta_{n,p'} \quad (5.124)$$

For odd p we write $p = 2p' + 1$, $q = 2q' + 1$. From (5.122) we again get $k = q' - p'$. Since $k \geq 0$, the range of q' is $p' \leq q' \leq -1$. We get the sum

$$\begin{aligned} \sum_{q'=p'}^{-1} \frac{i^{-1} (-1)^{q'+n} a^{2n-2q'-1} \Gamma(-q' - \frac{1}{2})}{2\Gamma(-n)\Gamma(n + \frac{1}{2} - q')} \binom{q' + \frac{1}{2}}{q' - p'} (-z_0)^{q'-p'} \\ = \frac{ia^{2(n-p')-1}}{\pi(2n-2p'-1)} \frac{\Gamma(\frac{1}{2}-n)}{\Gamma(-n)} \frac{\Gamma(-\frac{1}{2}-p')}{\Gamma(-p')} \end{aligned} \quad (5.125)$$

Now that we have converted the initial mode $\alpha_{A\dot{A},n}^{(1)}$ to modes at large t , we note that we are left with the NS vacuum $|0\rangle_t$ of the t plane inside these modes. This vacuum just gave us the state $|\chi\rangle$ on the cylinder [202]

$$\sigma_2^+(w_0) |0_R^{--}\rangle^{(1)} |0_R^{--}\rangle^{(2)} = |\chi\rangle \quad (5.126)$$

Putting the above results together, we see that for $n < 0$

$$\begin{aligned} \sigma_2^+(w_0) \alpha_{A\dot{A},n}^{(1)} |0_R^{--}\rangle^{(1)} |0_R^{--}\rangle^{(2)} \\ = \left(\frac{1}{2} \alpha_{A\dot{A},2n} + \sum_{p' \leq -1} \left(\frac{ia^{2(n-p')-1}}{\pi(2n-2p'-1)} \frac{\Gamma(\frac{1}{2}-n)}{\Gamma(-n)} \frac{\Gamma(-\frac{1}{2}-p')}{\Gamma(-p')} \right) \alpha_{A\dot{A},2p'+1} \right) |\chi\rangle \\ \equiv \sum_p f_{n,p}^B \alpha_{A\dot{A},p} |\chi\rangle \end{aligned} \quad (5.127)$$

where we have defined the coefficients $f_{n,p}^B$ for later convenience. For $n \geq 0$ we will just have

$$\sigma_2^+(w_0) \alpha_{A\dot{A},n}^{(1)} |0_R^{--}\rangle^{(1)} |0_R^{--}\rangle^{(2)} = 0 \quad (5.128)$$

since positive modes annihilate the Ramond vacuum state.

We see that the even modes in the final state get a simple contribution; this is related to the fact that the twist operator σ_2 does not affect such modes when it cuts and joins

together the two copies of the $c = 6$ CFT. The odd modes of all levels are excited.

5.3.2 The Action of $\sigma_2^+(w_0)$ on a Single Fermionic Mode

Let us repeat the above computation for a fermionic mode in the initial state. There is a slight difference between the cases of $\psi_n^{-\dot{A}}$ and $\psi_n^{+\dot{A}}$ since the starting vacuum state $|0_R^{--}\rangle^{(1)}|0_R^{--}\rangle^{(2)}$ breaks the charge symmetry, and the spectral flows we do also break this symmetry.

Let us start with the first case, $\psi_n^{(1)-\dot{A}}$. We start with Equation (5.46a), which we write as

$$\psi_n^{(1)-\dot{A}} \rightarrow \sqrt{2} \int_{ia} \frac{dt}{2\pi i} \psi_t^{-\dot{A}}(t) (t - ia)^n (t + ia)^n \quad (5.129)$$

We perform the spectral flows and coordinate maps in Section 5.2 to reach the t plane with all punctures smoothly closed. Define natural modes around the point $t = ia$ in the t plane

$$\hat{\psi}_r^{-\dot{A}} = \int_{ia} \frac{dt}{2\pi i} \psi_t^{-\dot{A}}(t) (t - ia)^{r-\frac{1}{2}} \quad (5.130)$$

where r is a half-integer. Writing $t + ia = 2ia + (t - ia)$, we expand in powers of $(t - ia)$. Noting that operators $\hat{\psi}_r^{-\dot{A}}$ with $r > 0$ kill the NS vacuum at $t = ia$, we find

$$\psi_n^{(1)-\dot{A}} \rightarrow \sqrt{2} \sum_{k=0}^{-n-1} \binom{n}{k} (2ia)^{n-k} \hat{\psi}_{n+k+\frac{1}{2}}^{-\dot{A}} \quad (5.131)$$

The RHS in the above equation is a finite sum of operators, each given by a contour integral around $t = ia$. Since there are no singularities anywhere on the t plane, we can expand each contour to one at large t . We define operators natural for expansion around infinity in the t plane

$$\tilde{\psi}_r^{-\dot{A}} = \int_{t=\infty} \frac{dt}{2\pi i} \psi_t^{-\dot{A}}(t) t^{r-\frac{1}{2}} \quad (5.132)$$

where r is a half-integer. The commutation relations are

$$\{\tilde{\psi}_r^{\alpha\dot{A}}, \tilde{\psi}_s^{\beta\dot{B}}\} = -\epsilon^{\alpha\beta} \epsilon^{\dot{A}\dot{B}} \delta_{r+s,0} \quad (5.133)$$

We find

$$\hat{\psi}_r^{-\dot{A}} = \sum_{k' \geq 0} \binom{r-\frac{1}{2}}{k'} (-ia)^{k'} \tilde{\psi}_{r-k'}^{-\dot{A}} \quad (5.134)$$

Finally we can expand the operators $\tilde{\psi}_r^{-\dot{A}}$ in terms of the final state modes (5.47a), finding

$$\tilde{\psi}_r^{-\dot{A}} = \frac{1}{\sqrt{2}} \sum_{k \geq 0} \binom{r-\frac{1}{2}}{k} (-a^2)^k \psi_{r-2k-\frac{1}{2}}^{-\dot{A}}. \quad (5.135)$$

We then find

$$\begin{aligned}
& \sigma_2^+(w_0) \psi_n^{(1)-\dot{A}} |0_R^{--}\rangle^{(1)} |0_R^{--}\rangle^{(2)} \\
&= \left(\frac{1}{2} \psi_{2n}^{-\dot{A}} + \sum_{p' \leq -1} \frac{ia^{2(n-p')-1}}{\pi(2n-2p'-1)} \frac{\Gamma(\frac{1}{2}-n)}{\Gamma(-n)} \frac{\Gamma(-\frac{1}{2}-p')}{\Gamma(-p')} \psi_{2p'+1}^{-\dot{A}} \right) |\chi\rangle \\
&\equiv \sum_p f_{n,p}^{F-} \psi_p^{-\dot{A}} |\chi\rangle
\end{aligned} \tag{5.136}$$

We now turn to the second case, where we have $\psi^{(1)+\dot{A}}$ before the twist. We start with Equation (5.46a), which we write as

$$\psi_n^{(1)+\dot{A}} \rightarrow \sqrt{2} \int_{ia} \frac{dt}{2\pi i} \psi_t^{+\dot{A}}(t) (t-ia)^{n-1} (t+ia)^{n-1} t \tag{5.137}$$

We perform the steps in Section 5.2 as before. The natural modes around $t = ia$ are

$$\hat{\psi}_r^{+\dot{A}} = \int_{ia} \frac{dt}{2\pi i} \psi_t^{+\dot{A}}(t) (t-ia)^{r-\frac{1}{2}} \tag{5.138}$$

This time we must expand in (5.137) the factor $t + ia = 2ia + (t - ia)$ as well as the factor $t = ia + (t - ia)$. This generates two terms

$$\psi_n^{(1)+\dot{A}} \rightarrow \frac{1}{\sqrt{2}} \sum_{k=0}^{-n} \binom{n-1}{k} (2ia)^{n-k} \hat{\psi}_{n+k-\frac{1}{2}}^{+\dot{A}} + \sqrt{2} \sum_{k=0}^{-n-1} \binom{n-1}{k} (2ia)^{n-k-1} \hat{\psi}_{n+k+\frac{1}{2}}^{+\dot{A}}. \tag{5.139}$$

Define natural modes at large t

$$\tilde{\psi}_r^{+\dot{A}} = \int_{t=\infty} \frac{dt}{2\pi i} \psi_t^{+\dot{A}}(t) t^{r-\frac{1}{2}} \tag{5.140}$$

We find

$$\hat{\psi}_r^{+\dot{A}} = \sum_{k \geq 0} \binom{r-\frac{1}{2}}{k} (-ia)^k \tilde{\psi}_{r-k}^{+\dot{A}} \tag{5.141}$$

Finally we can expand the modes $\tilde{\psi}^{+\dot{A}}$ in terms of the final state modes in Equation (5.47a), finding

$$\tilde{\psi}_r^{+\dot{A}} = \frac{1}{\sqrt{2}} \sum_{k \geq 0} \binom{r-\frac{3}{2}}{k} (-a^2)^k \psi_{r-2k+\frac{1}{2}}^{+\dot{A}}. \tag{5.142}$$

Putting all these expansions together, we find

$$\begin{aligned}
& \sigma_2^+(w_0) \psi_n^{(1)+\dot{A}} |0_R^{--}\rangle^{(1)} |0_R^{--}\rangle^{(2)} \\
&= \left(\frac{1}{2} \psi_{2n}^{+\dot{A}} + \sum_{p' \leq -1} \frac{ia^{2(n-p')-1}}{\pi(2n-2p'-1)} \frac{\Gamma(\frac{1}{2}-n)}{\Gamma(1-n)} \frac{\Gamma(\frac{1}{2}-p')}{\Gamma(-p')} \psi_{2p'+1}^{+\dot{A}} \right) |\chi\rangle
\end{aligned}$$

$$\equiv \sum_p f_{n,p}^{F+} \psi_p^{+\dot{A}} |\chi\rangle. \quad (5.143)$$

The computations of this section are very basic to understanding the effect of the deformation operator: taken by itself, any single particle mode below the twist insertion $\sigma_2^+(w_0)$ spreads into a linear combination of single particle modes after the twist, and we have found the coefficients of this linear combination for both bosonic and fermionic excitations. In addition the twist creates the same exponential that arises in the action of the twist of the vacuum (5.32), so the action of the twist on a single particle initial state gives rise to states with 1, 3, 5, ... excitations.

5.3.3 Two Bosonic Modes

Now let us consider the situation where we have two excitations in the initial twist. Upon the action of the twist σ_2^+ there will be two kinds of terms. One, where the modes move separately to the final state; this contribution can thus be computed by using the expressions of the last section. The other contribution results from an interaction between the two modes. Since we are dealing with a theory of free bosons and free fermions, the only possible interactions between modes is a “Wick contraction,” which produces a C-number term.

Let us consider the state

$$\sigma_2^+(w_0) \alpha_{A\dot{A},n_1}^{(1)} \alpha_{B\dot{B},n_2}^{(1)} |0_R^{--}\rangle^{(1)} |0_R^{--}\rangle^{(2)} \quad (5.144)$$

with $n_1 < 0, n_2 < 0$. We wish to move the modes $\alpha_{A\dot{A},n_i}^{(1)}$ to operator modes acting after the σ_2^+ operator. We will get the terms corresponding to each of these modes moving across separately, but there will also be a term resulting from the interaction between the two modes.

We follow the sequence of spectral flows and dualities given in Section 5.2. We reach the t plane with all punctures closed and the operator modes (cf. Equation (5.46a))

$$\alpha_{A\dot{A},n_1}^{(1)} \alpha_{B\dot{B},n_2}^{(1)} \rightarrow \left(\int_{t=ia} \frac{dt_1}{2\pi} \partial_t X_{A\dot{A}}(t_1) (z_0 + t_1^2)^{n_1} \right) \left(\int_{t=ia} \frac{dt_2}{2\pi} \partial_t X_{B\dot{B}}(t_2) (z_0 + t_2^2)^{n_2} \right) \quad (5.145)$$

with the t_1 contour outside the t_2 contour.

There is no singularity inside the t_2 contour, so we can expand the t_2 contour as in Section 5.3.1 to get (cf. Equation (5.103))

$$\alpha_{B\dot{B},n_2}^{(1)} \rightarrow \sum_{k_2=0}^{-n_2-1} \binom{n_2}{k_2} (2ia)^{(n_2-k_2)} \hat{\alpha}_{B\dot{B},n_2+k_2}^{(1)} \quad (5.146)$$

For the t_1 contour we can get a contribution from both positive and negative $\hat{\alpha}$ modes, since the t_2 contour gives an operator inside the t_1 contour. Thus we write the general expansion (5.101) for this contour

$$\alpha_{A\dot{A},n_1}^{(1)} \rightarrow \sum_{k_1=0}^{\infty} \binom{n_1}{k_1} (2ia)^{(n_1-k_1)} \hat{\alpha}_{A\dot{A},n_1+k_1}^{(1)} \quad (5.147)$$

and consider separately two cases:

1. The range of k_1 where $n_1+k_1 \leq -1$. This gives negative index modes just like (5.146). These modes commute with the modes in (5.146), so we have no interaction between the two operators, and we get (cf. (5.103))

$$\alpha_{A\dot{A},n_1}^{(1)} \rightarrow \sum_{k_1=0}^{-n_1-1} \binom{n_1}{k_1} (2ia)^{(n_1-k_1)} \hat{\alpha}_{A\dot{A},n_1+k_1}^{(1)} \quad (5.148)$$

2. The range where $n_1+k_1 \geq 0$. Now these modes can annihilate the negative modes created by the t_2 contour. This results in a \mathbb{C} -number contribution

$$C_{A\dot{A}B\dot{B}}^B[n_1, n_2] = \sum_{k_1=-n_1}^{\infty} \sum_{k_2=0}^{-n_2-1} \binom{n_1}{k_1} (2ia)^{n_1-k_1} \binom{n_2}{k_2} (2ia)^{(n_2-k_2)} [\hat{\alpha}_{A\dot{A},n_1+k_1}^{(1)}, \hat{\alpha}_{B\dot{B},n_2+k_2}^{(1)}] \quad (5.149)$$

Using the commutation relation (5.97) we get

$$\begin{aligned} C_{A\dot{A}B\dot{B}}^B[n_1, n_2] &= -\epsilon_{AB}\epsilon_{\dot{A}\dot{B}} \sum_{k_2=0}^{-n_2-1} (-(n_2+k_2)) \binom{n_1}{-n_1-n_2-k_2} \binom{n_2}{k_2} (2ia)^{2(n_1+n_2)} \\ &= \epsilon_{AB}\epsilon_{\dot{A}\dot{B}} \frac{a^{2(n_1+n_2)} \Gamma(-n_1+\frac{1}{2}) \Gamma(-n_2+\frac{1}{2})}{2\pi(n_1+n_2) \Gamma(-n_1) \Gamma(-n_2)} \end{aligned} \quad (5.150)$$

Note that this is symmetric in n_1 and n_2 , as it should be since the modes in (5.144) commute and so can be put in either order.

Apart from this \mathbb{C} -number term, we still have the contribution where the two contours in the initial state produce the modes in Equation (5.146) and (5.148). We can proceed to expand the modes $\hat{\alpha}$ in these sums into modes of type $\tilde{\alpha}$. We note from (5.113) that each set of modes generates only negative index modes $\tilde{\alpha}_q$. Thus we cannot get any additional \mathbb{C} -number contributions from commutators between the $\tilde{\alpha}$ modes arising from our two operators.

Next we convert the modes $\tilde{\alpha}$ to modes of type α . From (5.123) we see that we again generate only negative index modes α_p from each of the two sets of modes. Thus there cannot be any additional \mathbb{C} -number contribution from commutation between the modes α arising from our two operators. In short, the only \mathbb{C} -number contribution we get from

“Wick contraction” is (5.150), and the remaining part of the state is given by independently moving the two initial state modes past σ_2^+ in the manner given in (5.127).

Putting this “Wick contraction” term together with the contribution of the uncontracted terms we get

$$\begin{aligned} \sigma_2^+(w_0) \alpha_{A\dot{A},n_1}^{(1)} \alpha_{B\dot{B},n_2}^{(1)} |0_R^{--}\rangle^{(1)} |0_R^{--}\rangle^{(2)} \\ = \left[\left(\sum_{p_1} f_{n_1,p_1}^B \alpha_{A\dot{A},p_1} \right) \left(\sum_{p_2} f_{n_2,p_2}^B \alpha_{B\dot{B},p_2} \right) + C_{A\dot{A}B\dot{B}}^B[n_1, n_2] \right] |\chi\rangle. \end{aligned} \quad (5.151)$$

5.3.4 Two Fermionic Modes

Let us repeat this computation for two fermions in the initial state. Since the spectral flow treats positive and negative charges differently, we work with the pair $\psi^{++} \psi^{--}$ and later write the result for general charges.

Consider

$$\sigma_2^+(w_0) \psi_{n_1}^{(1),++} \psi_{n_2}^{(1),--} |0_R^{--}\rangle^{(1)} |0_R^{--}\rangle^{(2)} \quad (5.152)$$

with $n_1 \leq 0, n_2 < 0$. We wish to move the modes to those acting after the σ_2^+ operator. We will get the terms corresponding to each of these modes moving across separately, but there will also be a term resulting from the interaction between the two modes.

Following the sequence of spectral flows and dualities we reach the t plane with all punctures closed and the operator modes (cf. Equation (5.46a))

$$\psi_{n_1}^{(1),++} \psi_{n_2}^{(1),--} \rightarrow \left(\sqrt{2} \int_{t=ia} \frac{dt_1}{2\pi i} \psi_t^{++}(t_1) (z_0 + t_1^2)^{n_1-1} t_1 \right) \left(\sqrt{2} \int_{t=ia} \frac{dt_2}{2\pi i} \psi_t^{--}(t_2) (z_0 + t_2^2)^{n_2} \right) \quad (5.153)$$

with the t_1 contour outside the t_2 contour.

There is no singularity inside the t_2 contour so we get

$$\psi_{n_2}^{(1),--} \rightarrow \sqrt{2} \sum_{k_2=0}^{-n_2-1} \binom{n_2}{k_2} (2ia)^{n_2-k_2} \hat{d}_{n_2+k_2+\frac{1}{2}}^{--} \quad (5.154)$$

For $\psi_{n_1}^{(1),++}$ we write the full sum over modes

$$\psi_{n_1}^{(1)+\dot{A}} \rightarrow \frac{1}{\sqrt{2}} \sum_{k_1=0}^{\infty} \binom{n_1-1}{k_1} (2ia)^{n_1-k_1} \hat{\psi}_{n_1+k_1-\frac{1}{2}}^{+\dot{A}} + \sqrt{2} \sum_{k_1=0}^{\infty} \binom{n_1-1}{k_1} (2ia)^{n_1-k_1-1} \hat{\psi}_{n_1+k_1+\frac{1}{2}}^{+\dot{A}} \quad (5.155)$$

The anticommutator arising from the first term gives

$$-(2ia)^{2(n_1+n_2)} \sum_{k_2=0}^{-n_2-1} \binom{n_1-1}{-n_1-n_2-k_2} \binom{n_2}{k_2} \quad (5.156)$$

while the anticommutator from the second term gives

$$-2(2ia)^{2(n_1+n_2)} \sum_{k_2=0}^{-n_2-1} \binom{n_1-1}{-n_1-n_2-k_2-1} \binom{n_2}{k_2}. \quad (5.157)$$

The sum of these two contributions can be simplified to give (we now include the result for the pair ψ^{+-}, ψ^{-+})

$$C^{F,\alpha A\beta B}[n_1, n_2] = -\epsilon^{\alpha\beta} \epsilon^{AB} \frac{a^{2(n_1+n_2)} \Gamma(-n_1 + \frac{1}{2}) \Gamma(-n_2 + \frac{1}{2})}{2\pi n_1(n_1+n_2) \Gamma(-n_1) \Gamma(-n_2)} \quad (5.158)$$

Note that this is not symmetric in n_1, n_2 since the choice of Ramond vacuum $|0_R^{--}\rangle^{(1)} |0_R^{--}\rangle^{(2)}$ breaks the symmetry between $+$ and $-$ charge fermions.

Putting this “Wick contraction” term together with the contribution of the uncontracted terms we get

$$\begin{aligned} \sigma_2^+(w_0) \psi_{n_1}^{(1),++} \psi_{n_2}^{(1),--} |0_R^{--}\rangle^{(1)} |0_R^{--}\rangle^{(2)} \\ = \left[\left(\sum_{p_1} f_{n_1,p_1}^{F+} \psi_{p_1}^{++} \right) \left(\sum_{p_2} f_{n_2,p_2}^{F-} \psi_{p_2}^{--} \right) + C_{n_1,n_2}^{F,++--} \right] |\chi\rangle. \end{aligned} \quad (5.159)$$

Summary

We have computed the \mathbb{C} -number “Wick contraction” term that results from the interaction between two initial state modes. Note that after all the spectral flows we perform, we are dealing with a theory of free bosons and fermions. Thus even if we had several modes in the initial state, we can break up the effect of the twist σ_2^+ into pairwise “Wick contractions” (with value given by C^B and C^F computed above), and moving any uncontracted modes past the twist σ_2^+ using the expressions in Sections 5.3.1 and 5.3.2. So the computations of Sections 5.3.1 and 5.3.2, and the present section allow us to find the effect of σ_2^+ on any initial state.

5.3.5 Complete Action of the Deformation Operator on a Bosonic Mode

In the last two sections we have focused on the effect of the twist σ_2^+ . Let us now compute an example where we combine this with the action of the supercharge described in the beginning of Section 5.3.

We start with the state containing one bosonic excitation, and find the state created by the action of the deformation operator. Thus we wish to find the state

$$|\psi\rangle_f = \mathcal{T}_{\dot{A}} \alpha_{\dot{C}\dot{C},n}^{(1)} |0_R^{--}\rangle^{(1)} |0_R^{--}\rangle^{(2)} \quad (5.160)$$

with $n \leq -1$.

We follow the steps outlined in the beginning of Section 5.3. We have

$$|\psi\rangle_f = \left(-\sigma_2^+(w_0) G_{A,0}^{(1)-} \alpha_{C\dot{C},n}^{(1)} + G_{A,0}^- \sigma_2^+(w_0) \alpha_{C\dot{C},n}^{(1)} \right) |0_R^-\rangle^{(1)} |0_R^-\rangle^{(2)}. \quad (5.161)$$

We have

$$\begin{aligned} \sigma_2^+(w_0) G_{A,0}^{(1)-} \alpha_{C\dot{C},n}^{(1)} |0_R^-\rangle^{(1)} |0_R^-\rangle^{(2)} &= \sigma_2^+(w_0) [G_{A,0}^{(1)-}, \alpha_{C\dot{C},n}^{(1)}] |0_R^-\rangle^{(1)} |0_R^-\rangle^{(2)} \\ &= (-\epsilon_{AC} \epsilon_{\dot{A}\dot{C}}) i n \sigma_2^+(w_0) \psi_n^{(1)-\dot{A}} |0_R^-\rangle^{(1)} |0_R^-\rangle^{(2)} \end{aligned} \quad (5.162)$$

We can now write down $\sigma_2^+(w_0) \psi_n^{(1)-\dot{A}} |0_R^-\rangle^{(1)} |0_R^-\rangle^{(2)}$ from (5.136). For the other term, we first compute $\sigma_2^+(w_0) \alpha_{C\dot{C},m}^{(1)} |0_R^-\rangle^{(1)} |0_R^-\rangle^{(2)}$ from (5.127), and apply the operator $G_{A,0}^-$ using

$$\begin{aligned} G_{A,0}^- \alpha_{C\dot{C},p} \sigma_2^+ |0_R^-\rangle^{(1)} |0_R^-\rangle^{(2)} &= [G_{A,0}^-, \alpha_{C\dot{C},p}] \sigma_2^+ |0_R^-\rangle^{(1)} |0_R^-\rangle^{(2)} + \alpha_{C\dot{C},p} G_{A,0}^- \sigma_2^+ |0_R^-\rangle^{(1)} |0_R^-\rangle^{(2)} \\ &= (-\epsilon_{AC} \epsilon_{\dot{A}\dot{C}}) \frac{ip}{2} \psi_p^{-\dot{A}} |\chi\rangle + \alpha_{C\dot{C},p} |\psi\rangle \end{aligned} \quad (5.163)$$

where $|\psi\rangle$ is given in (5.89). Putting together these two contributions, we get

$$\mathcal{T}_{\dot{A}} \alpha_{C\dot{C},n}^{(1)} |0_R^-\rangle^{(1)} |0_R^-\rangle^{(2)} = -\epsilon_{AC} \epsilon_{\dot{A}\dot{C}} \sum_{p \text{ odd}^+} \frac{a^{2n+p} \Gamma(\frac{1}{2} - n) \Gamma(\frac{p}{2})}{2\pi \Gamma(-n) \Gamma(\frac{p+1}{2})} \psi_p^{-\dot{A}} |\chi\rangle + \frac{1}{2} \alpha_{C\dot{C},2n} |\psi\rangle \quad (5.164)$$

where the states $|\chi\rangle$ and $|\psi\rangle$ are given in Equations (5.32) and (5.89).

5.4 Intertwining Relations

We first present a formal, intuitive derivation of the intertwining relations, which relate modes of the untwisted sector to modes of the twisted sector. In Section 5.4.3, we show how the derived relations lead to multi-dimensional infinite series whose value depends on how one takes the limit of the partial sums going to infinity. We then give a more rigorous derivation of the relations, which suggests a prescription on how to evaluate the ambiguous series.

5.4.1 Basic Derivation

We are interested in finding a relationship between modes in the untwisted sector, “before the twist,” and modes in the twisted sector, “after the twist.” More precisely we would like to know in general how to write

$$\begin{aligned} \sigma_2^+(z_0) (\text{excitations before the twist}) |0_R^-\rangle^{(1)} |0_R^-\rangle^{(2)} \\ = (\text{excitations after the twist}) \sigma_2^+(z_0) |0_R^-\rangle^{(1)} |0_R^-\rangle^{(2)} \\ = (\text{excitations after the twist}) |\chi\rangle. \end{aligned} \quad (5.165)$$

In [203], an algorithm was found for doing just that; however, the question this section addresses is whether there is a more general relation between individual modes before the twist operator and after the twist operator.

Since our argument does not depend on $SU(2)_L$ or $SU(2)_1 \times SU(2)_2$, we suppress the indices on the bosons and fermions. We begin by noting that before the twist the correct field expansions are

$$i\partial X^{(1)}(z) = \sum_n \frac{\alpha_n^{(1)}}{z^{n+1}} \quad i\partial X^{(2)}(z) = \sum_n \frac{\alpha_n^{(2)}}{z^{n+1}} \quad |z| < |z_0|, \quad (5.166)$$

and

$$\psi^{(1)}(z) = \sum_{n \in \mathbb{Z} + \frac{1}{2}} \frac{\psi_n^{(1)}}{z^{n+\frac{1}{2}}} \quad \psi^{(2)}(z) = \sum_{n \in \mathbb{Z} + \frac{1}{2}} \frac{\psi_n^{(2)}}{z^{n+\frac{1}{2}}} \quad |z| < |z_0|. \quad (5.167)$$

After the twist, the correct expansions are given by

$$i\partial X^{(1)}(z) = \frac{1}{2} \sum_n \frac{\alpha_n}{z^{\frac{n}{2}+1}} \quad i\partial X^{(2)}(z) = \frac{1}{2} \sum_n \frac{(-1)^n \alpha_n}{z^{\frac{n}{2}+1}} \quad |z| > |z_0|, \quad (5.168)$$

and

$$\psi^{(1)}(z) = \frac{1}{2} \sum_n \frac{\psi_n}{z^{\frac{n}{2}+\frac{1}{2}}} \quad \psi^{(2)}(z) = \frac{1}{2} \sum_n \frac{(-1)^n \psi_n}{z^{\frac{n}{2}+\frac{1}{2}}} \quad |z| > |z_0|. \quad (5.169)$$

Note that after the twist, there is no unique way of distinguishing copies (1) and (2), but the above expansions correspond to a way of defining (1) and (2). Following [202, 203], we define the modes in the twisted sector with an extra factor of 2 so that we can work with integers.

Now, recall that the fields $\partial X(z)$ and $\psi(z)$ should be holomorphic functions except at isolated points where there are other operator insertions. In particular, there is nothing special that occurs on the circle $|z| = |z_0|$ (there is something special at the isolated point z_0). The curve is the boundary between our twisted and untwisted mode expansions about the origin $z = 0$, but if one were to do mode expansions about a different point in the complex plane then the expansions would change across a different curve (that still passes through z_0). Therefore, *at least away from the twist operator at z_0* , we expect that the fields $\partial X(z)$ and $\psi(z)$ should be continuous across $|z| = |z_0|$.

Thus, on the circle $|z| = |z_0|$ (excluding some neighborhood around $z = z_0$) we may identify

$$\sum_n \frac{\alpha_n^{(1)}}{z^{n+1}} = \frac{1}{2} \sum_n \frac{\alpha_n}{z^{\frac{n}{2}+1}} \quad \sum_n \frac{\alpha_n^{(2)}}{z^{n+1}} = \frac{1}{2} \sum_n \frac{(-1)^n \alpha_n}{z^{\frac{n}{2}+1}}, \quad |z| = |z_0| \quad (5.170)$$

and

$$\sum_{n \in \mathbb{Z} + \frac{1}{2}} \frac{\psi_n^{(1)}}{z^{n+\frac{1}{2}}} = \frac{1}{2} \sum_n \frac{\psi_n}{z^{\frac{n}{2}+\frac{1}{2}}} \quad \sum_{n \in \mathbb{Z} + \frac{1}{2}} \frac{\psi_n^{(2)}}{z^{n+\frac{1}{2}}} = \frac{1}{2} \sum_n \frac{(-1)^n \psi_n}{z^{\frac{n}{2}+\frac{1}{2}}}, \quad |z| = |z_0|. \quad (5.171)$$

Multiplying (5.170) by z^m and integrating along the circle $|z| = |z_0|$, we get

$$\begin{aligned} \alpha_m^{(1)} &= \frac{1}{2} \sum_n \alpha_n \int \frac{dz}{2\pi i} z^{m-\frac{n}{2}-1} \\ &= \frac{1}{2} \sum_n \alpha_n \int_0^{2\pi} \frac{d\theta}{2\pi} (z_0 e^{i\theta})^{m-\frac{n}{2}} \\ &= \frac{1}{2} \alpha_{2m} + \frac{i}{2\pi} \sum_{n \text{ odd}} \frac{z_0^{m-\frac{n}{2}}}{m-\frac{n}{2}} \alpha_n, \end{aligned} \quad (5.172)$$

and similarly

$$\alpha_m^{(2)} = \frac{1}{2} \alpha_{2m} - \frac{i}{2\pi} \sum_{n \text{ odd}} \frac{z_0^{m-\frac{n}{2}}}{m-\frac{n}{2}} \alpha_n, \quad (5.173)$$

where the sum over the odds is both positive and negative. These are the desired relations between modes before the twist and modes after the twist. The relations are analogous to the more general Bogolyubov transformations discussed in condensed matter in [206]. Note that the contour in (5.172) is open, since we must exclude some infinitesimal neighborhood around z_0 . It is straightforward to find the analogous relation for fermions in the R sector:

$$\psi_n^{(1,2)} = \frac{1}{2} \psi_{2n} \pm \frac{i}{2\pi} \sum_{k \text{ odd}} \frac{z_0^{n-\frac{k}{2}}}{n-\frac{k}{2}} \psi_k. \quad (5.174)$$

Given the delicate nature of the above argument, in particular with regard to what is happening around z_0 , one may not be surprised that there are some hidden subtleties with these relations. Note also that the derivation would seem to work for any holomorphic field $\mathcal{O}(z)$, which *cannot be correct* since some modes have a nontrivial commutator with the twist operator, e.g. J_0^- . We should be careful in what we mean when we write “=” in the above expressions. For example in Equation (5.172), we implicitly mean the operator relation

$$\sigma_2^+(z_0) \alpha_m^{(1)} = \left[\frac{1}{2} \alpha_{2m} + \frac{i}{2\pi} \sum_{n \text{ odd}} \frac{z_0^{m-\frac{n}{2}}}{m-\frac{n}{2}} \alpha_n \right] \sigma_2^+(z_0) \quad (5.175)$$

with the above radial ordering. The usage should be clear from the context.

Before showing what goes wrong, let us first explore what goes right. First of all this is the kind of relation we were hoping for: it relates positive and negative modes before the twist to positive and negative modes after the twist directly. The method given in [203] can only relate states to states; it cannot relate an individual mode before the twist to modes

after the twist without knowing what other excitations one has before the twist.

An important requirement for Bogolyubov coefficients is that they respect the commutation relations. We can check that the above relations are consistent with the commutation relations by computing, for instance,

$$\begin{aligned} [\alpha_m^{(1)}, \alpha_n^{(1)}] &= \left[\frac{1}{2} \alpha_{2m} + \frac{i}{2\pi} \sum_{k \text{ odd}} \frac{z_0^{m-\frac{k}{2}}}{m-\frac{k}{2}} \alpha_k, \frac{1}{2} \alpha_{2n} + \frac{i}{2\pi} \sum_{l \text{ odd}} \frac{z_0^{n-\frac{l}{2}}}{n-\frac{l}{2}} \alpha_l \right] \\ &= \frac{m}{2} \delta_{m+n,0} - \frac{z_0^{m+n}}{4\pi^2} \sum_{k \text{ odd}} \frac{k}{(m-\frac{k}{2})(n+\frac{k}{2})}. \end{aligned} \quad (5.176)$$

The sum is divergent; however, if we make the relatively modest assumption that we should cutoff the sum symmetrically for positive and negative k , then we find³⁰

$$\lim_{L \rightarrow \infty} \sum_{\substack{|k| < L \\ k \text{ odd}}} \frac{k}{(m-\frac{k}{2})(n+\frac{k}{2})} = -2m\pi^2 \delta_{m+n,0}, \quad (5.177)$$

which gives the correct answer. Similar calculations go through for the other (anti-)commutations.

Second, it gets the right answer for moving a single mode through the twist operator. For instance,

$$\begin{aligned} \sigma_2^+(z_0) \alpha_{AA,n}^{(1)} |0_R^-\rangle^{(1)} |0_R^-\rangle^{(2)} &= \left(\frac{1}{2} \alpha_{AA,2n} + \frac{i}{2\pi} \sum_{k \text{ odd}} \frac{z_0^{n-\frac{k}{2}}}{n-\frac{k}{2}} \alpha_{AA,k} \right) \sigma_2^+(z_0) |0_R^-\rangle^{(1)} |0_R^-\rangle^{(2)} \\ &= \left(\frac{1}{2} \alpha_{AA,2n} + \frac{i}{2\pi} \sum_{k \text{ odd}} \frac{z_0^{n-\frac{k}{2}}}{n-\frac{k}{2}} \alpha_{AA,k} \right) |\chi\rangle \\ &= \left[\frac{1}{2} \alpha_{AA,2n} + \frac{i}{2\pi} \left(\sum_{k \text{ odd}^+} \frac{z_0^{n+\frac{k}{2}}}{n+\frac{k}{2}} \alpha_{AA,-k} + \sum_{k,l \text{ odd}^+} \frac{z_0^{n-\frac{k}{2}}}{n-\frac{k}{2}} \gamma_{kl}^B k \alpha_{AA,-l} \right) \right] |\chi\rangle. \end{aligned} \quad (5.178)$$

Making use of the identity in (F.1) one sees that

$$\sum_{k \text{ odd}^+} \frac{z_0^{n-\frac{k}{2}} k \gamma_{kl}^B}{n-\frac{k}{2}} = \frac{z_0^{n+\frac{l}{2}}}{n+\frac{l}{2}} \left(\frac{\Gamma(\frac{l}{2}) \Gamma(-n+\frac{1}{2})}{\Gamma(\frac{l+1}{2}) \Gamma(-n)} - 1 \right), \quad (5.179)$$

³⁰This mild UV ambiguity might be seen as a hint of the other UV issues with the intertwining relations; however, this issue does not arise for the fermions, and it is of a different character. The UV issues that we discuss at length arise with multidimensional series; whereas the above is arguably the only reasonable regularization of the series in (5.176). For example, if one cuts off the positive modes at L and the negative modes at $-2L$ then one *does* get a different answer, but it is not a consistent truncation of the Hilbert space to have a creation operator without its corresponding annihilation operator.

and thus

$$\sigma_2^+(z_0)\alpha_{A\dot{A},n}^{(1)}|0_R^-\rangle^{(1)}|0_R^-\rangle^{(2)} = \left[\frac{1}{2}\alpha_{A\dot{A},2n} + \frac{i}{2\pi} \sum_{l \text{ odd}^+} \frac{z_0^{n+\frac{l}{2}}}{n+\frac{l}{2}} \frac{\Gamma(\frac{l}{2})\Gamma(-n+\frac{1}{2})}{\Gamma(\frac{l+1}{2})\Gamma(-n)} \alpha_{A\dot{A},-l} \right] |\chi\rangle. \quad (5.180)$$

For n positive the above vanishes as it should, since the positive even mode in the first term annihilates $|\chi\rangle$ and $\Gamma(-n)$ kills the second term. For n negative this reproduces the result found in [203] for a single mode in the initial state.

Similarly, if one performs the analogous calculation for fermions with (5.174), then one can use

$$\psi_{+k}^{\alpha\dot{A}}|\chi\rangle = 2 \sum_{p \text{ odd}^+} \left(\gamma_{pk}^F \delta_+^{\alpha\dot{A}} \psi_{-p}^{+\dot{A}} - \gamma_{kp}^F \delta_-^{\alpha\dot{A}} \psi_{-p}^{-\dot{A}} \right) |\chi\rangle \quad k \text{ odd, positive}, \quad (5.181)$$

to find

$$\sigma_2^+(z_0)\psi_n^{(1)+\dot{A}}|0_R^-\rangle^{(1)}|0_R^-\rangle^{(2)} = \left[\frac{1}{2}\psi_{2n}^{+\dot{A}} + \frac{i}{2\pi} \sum_{p \text{ odd}^+} \frac{z_0^{n+\frac{p}{2}}}{n+\frac{p}{2}} \frac{\Gamma(\frac{p}{2}+1)\Gamma(-n+\frac{1}{2})}{\Gamma(\frac{p+1}{2})\Gamma(-n+1)} \psi_{-p}^{+\dot{A}} \right] |\chi\rangle \quad (5.182a)$$

$$\sigma_2^+(z_0)\psi_n^{(1)-\dot{A}}|0_R^-\rangle^{(1)}|0_R^-\rangle^{(2)} = \left[\frac{1}{2}\psi_{2n}^{-\dot{A}} + \frac{i}{2\pi} \sum_{p \text{ odd}^+} \frac{z_0^{n+\frac{p}{2}}}{n+\frac{p}{2}} \frac{\Gamma(\frac{p}{2})\Gamma(-n+\frac{1}{2})}{\Gamma(\frac{p+1}{2})\Gamma(-n)} \psi_{-p}^{-\dot{A}} \right] |\chi\rangle. \quad (5.182b)$$

This agrees with [203].

5.4.2 Problems

There are two problems with the above derivation. One is that this formal derivation only makes use of the holomorphicity of the fields, which means that one could make the same argument for any other holomorphic field. For instance, consider $J^a(z)$, one would get

$$J_n^{a(1,2)} \stackrel{?}{=} \frac{1}{2}J_{2n}^a \pm \frac{i}{2\pi} \sum_{k \text{ odd}} \frac{z_0^{n-\frac{k}{2}}}{n-\frac{k}{2}} J_k^a, \quad (5.183)$$

which leads to

$$[J_0^-, \sigma_2^+(z_0)] = J_0^- \sigma_2^+(z_0) - \sigma_2^+(z_0)(J_0^{(1)} + J_0^{(2)}) \stackrel{?}{=} 0. \quad (5.184)$$

One should find $\sigma_2^-(z_0)$, not zero. One finds similar contradictions if one tries to use the same argument for $T(z)$, too.

The second problem, alluded to above, concerns using the intertwining relations with more than one mode. The simplest instance may be to consider

$$\sigma_2^+(z_0)\alpha_{++ , m}^{(1)}\alpha_{-- , -n}^{(1)}|0_R^-\rangle^{(1)}|0_R^-\rangle^{(2)} = -m\delta_{m,n}|\chi\rangle \quad m, n > 0. \quad (5.185)$$

If we use Equation (5.172), then we get

$$\begin{aligned} -m\delta_{m,n}|\chi\rangle &\stackrel{?}{=} \left(\frac{1}{2}\alpha_{++ , 2m} + \frac{i}{2\pi} \sum_{k \text{ odd}} \frac{z_0^{m-\frac{k}{2}}}{m-\frac{k}{2}} \alpha_{++ , k} \right) \left(\frac{1}{2}\alpha_{-- , -2n} + \frac{i}{2\pi} \sum_{l \text{ odd}} \frac{z_0^{-n-\frac{l}{2}}}{-n-\frac{l}{2}} \alpha_{-- , l} \right) |\chi\rangle \\ &= -\frac{m}{2}\delta_{m,n}|\chi\rangle - \frac{1}{4\pi^2} \left(\sum_{k \text{ odd}} \frac{z_0^{m-\frac{k}{2}}}{m-\frac{k}{2}} \alpha_{++ , k} \right) \left(\sum_{l \text{ odd}} \frac{z_0^{-n-\frac{l}{2}}}{-n-\frac{l}{2}} \alpha_{-- , l} \right) |\chi\rangle \\ &= -\frac{m}{2}\delta_{m,n}|\chi\rangle \\ &\quad - \frac{1}{4\pi^2} \left(\sum_{k \text{ odd}} \frac{z_0^{m-\frac{k}{2}}}{m-\frac{k}{2}} \alpha_{++ , k} \right) \left[\sum_{j \text{ odd}^+} \alpha_{-- , -j} \left(\frac{z_0^{-n+\frac{j}{2}}}{-n+\frac{j}{2}} + \sum_{l \text{ odd}^+} \frac{z_0^{-n-\frac{l}{2}} l \gamma_{lj}}{-n-\frac{l}{2}} \right) \right] |\chi\rangle \end{aligned} \quad (5.186)$$

Note that the even-odd cross-terms vanish since they commute and either the $\alpha_{++ , 2m}$ or the $\alpha_{++ , k}$ -sum kills $|\chi\rangle$ (from (5.180)). Similarly, we need only look at the commutator of the $\alpha_{++ , k}$ -sum and the square-bracketed expression, which gives

$$\begin{aligned} &- \left(\sum_{k \text{ odd}^+} \frac{k z_0^{m-\frac{k}{2}}}{m-\frac{k}{2}} \right) \left(\frac{z_0^{-n+\frac{k}{2}}}{-n+\frac{k}{2}} + \sum_{l \text{ odd}^+} \frac{z_0^{-n-\frac{l}{2}} l \gamma_{lk}}{-n-\frac{l}{2}} \right) \\ &= z_0^{m-n} \sum_{k \text{ odd}^+} \left(\frac{k}{(m-\frac{k}{2})(n-\frac{k}{2})} + \sum_{l \text{ odd}^+} \frac{z_0^{-\frac{k}{2}-\frac{l}{2}} k l \gamma_{kl}}{(m-\frac{k}{2})(n+\frac{l}{2})} \right). \end{aligned} \quad (5.187)$$

We would like the above expression to evaluate to $2\pi^2 m \delta_{m,n}$ in order to get the correct answer; however, the above summations depend sensitively on the order in which one adds the infinite number of terms. For instance, if we attempt to perform the k -sum *first*, then the first term is divergent and the second term, using (5.179), gives

$$- \sum_{l \text{ odd}^+} \frac{l}{(m+\frac{l}{2})(n+\frac{l}{2})}, \quad (5.188)$$

which is also divergent.

On the other hand, if we perform the l sum first, using (5.179) we find

$$z_0^{m-n} \sum_{k \text{ odd}^+} \left(\frac{k}{(m-\frac{k}{2})(n-\frac{k}{2})} + \sum_{l \text{ odd}^+} \frac{z_0^{-\frac{k}{2}-\frac{l}{2}} k l \gamma_{kl}}{(m-\frac{k}{2})(n+\frac{l}{2})} \right)$$

$$\begin{aligned}
&= z_0^{m-n} \sum_{k \text{ odd}^+} \left(\frac{k}{(m - \frac{k}{2})(n - \frac{k}{2})} + \frac{k}{(m - \frac{k}{2})(n - \frac{k}{2})} \left[\frac{\Gamma(\frac{k}{2})\Gamma(n + \frac{1}{2})}{\Gamma(\frac{k+1}{2})\Gamma(n)} - 1 \right] \right) \\
&= z_0^{m-n} \frac{\Gamma(n + \frac{1}{2})}{\Gamma(n)} \sum_{k \text{ odd}^+} \left(\frac{k}{(m - \frac{k}{2})(n - \frac{k}{2})} \frac{\Gamma(\frac{k}{2})}{\Gamma(\frac{k+1}{2})} \right), \tag{5.189}
\end{aligned}$$

which using another identity,

$$\sum_{k \text{ odd}^+} \frac{k}{(m - \frac{k}{2})(n - \frac{k}{2})} \frac{\Gamma(\frac{k}{2})}{\Gamma(\frac{k+1}{2})} = 2\pi^2 m \frac{\Gamma(n)}{\Gamma(n + \frac{1}{2})} \delta_{m,n} \quad m, n > 0, \tag{5.190}$$

gives the correct answer.

How should we think of the ambiguity in Equation (5.187)? Any infinite series is implicitly evaluated by determining the limit of a sequence of *partial sums*. In our case, higher values of k and l correspond to higher modes, so it is natural to think of imposing UV cut-offs on the sums, $k < L_1$ and $l < L_2$. We then wish to take the limit as $L_1, L_2 \rightarrow \infty$, but there are many different ways to do that. If we define $b = L_1/L_2$ to parameterize the different ways of evaluating (5.187), then evaluating the k -sum first corresponds to $b = \infty$, while evaluating the l -sum first corresponds to $b = 0$. These are just two of an infinite number of ways to evaluate the double-sum.

Given that these ambiguous multi-dimensional series are rampant in this formalism and that frequently the correct method of evaluating them may be much less obvious,³¹ we need a well-motivated principle that determines the correct way to handle the UV physics.

5.4.3 A More Rigorous Derivation

We now present a more rigorous derivation of the intertwining relations in Equations (5.172), (5.173), and (5.174). By continuously deforming the contour integral for an initial state mode outward only where the integrand is holomorphic, we can treat the point z_0 more carefully. This resolves the two problems outlined above.

Bosons

Working with the bosons first, let us note that

$$\alpha_n^{(1)} = \oint_{C_1} \frac{dz}{2\pi i} i\partial X^{(1)}(z) z^n, \tag{5.191}$$

where C_1 is a circular contour with radius less than $|z_0|$ shown in Figure 5.5(a), and $i\partial X^{(1)}(z)$ is a holomorphic function except at $z = z_0$ (and excluding any other operator

³¹For instance, there are cases involving triple-sums, where more than one order of evaluating the sums give distinct, finite results.

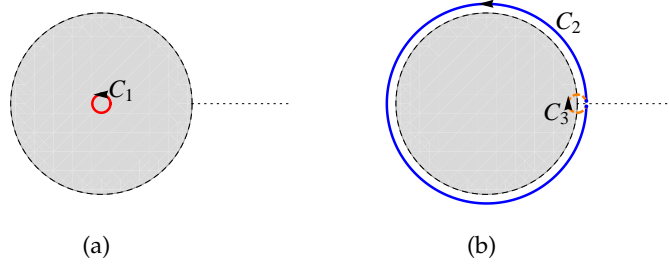


Figure 5.5: In the z -plane, showing how the contour C_1 (solid, red) in (a) may be deformed out and around the branch cut into contours C_2 (solid, blue) and C_3 (dashed, orange) in (b). The gray circular region is the “before the twist” region, $|z| < |z_0|$. The branch cut is indicated by the dashed black line extending out from the circle.

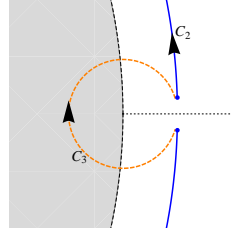


Figure 5.6: A close-up depiction of contours C_2 and C_3 meeting. Note that we have added an artificial gap around the branch cut for illustrative purposes only—in fact, both C_2 and C_3 are full circles.

insertions). Thus, we may deform the contour into an open circle C_2 of radius larger than $|z_0|$ and a contour, C_3 , sneaking around the branch cut starting at $z = z_0$, as shown in Figures 5.5 and 5.6. We take C_3 to be a circle of radius ε , which we eventually take to zero. The orientations of the contours are shown in the figures.

We write the above contour integral as

$$\alpha_n^{(1)} = \int_{C_2} \frac{dz}{2\pi i} i\partial X^{(1)}(z) z^n + \int_{C_3} \frac{dz}{2\pi i} i\partial X^{(1)}(z) z^n. \quad (5.192)$$

The C_2 term, is what we have been calculating and is given by (with ε corrections)

$$\begin{aligned} \int_{C_2} \frac{dz}{2\pi i} i\partial X(z) z^n &= \frac{i}{2} \sum_k \alpha_k \int_{C_2} \frac{dz}{2\pi i} z^{n-\frac{k}{2}-1} \\ &= \frac{1}{4\pi} \sum_k \alpha_k (z_0 + \varepsilon)^{n-\frac{k}{2}} \int_0^{2\pi} d\theta e^{i(n-\frac{k}{2})\theta} \end{aligned}$$

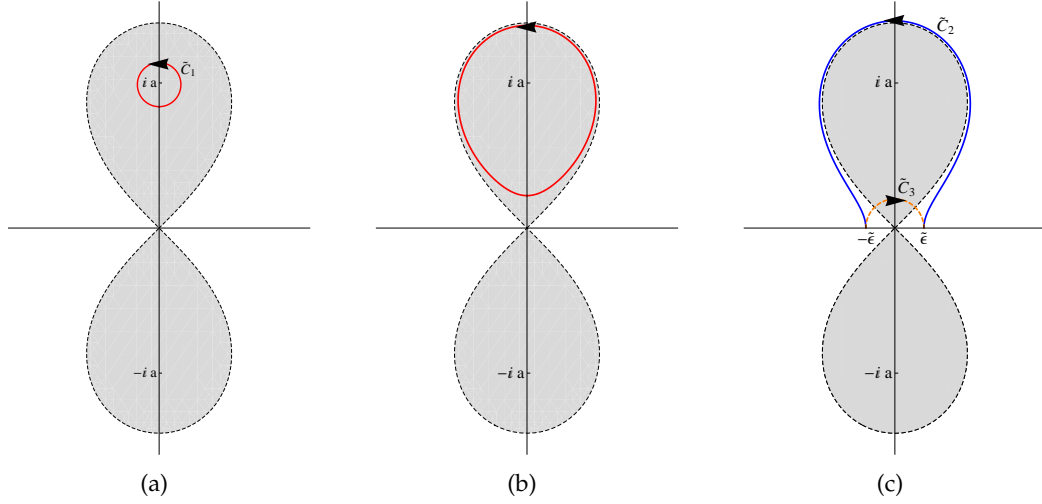


Figure 5.7: We show the t -plane where there is no branch cut and the fields are single-valued. We start in (a) with the \tilde{C}_1 contour (solid, red), which we finally deform out into \tilde{C}_2 (solid, blue) and \tilde{C}_3 (dashed, orange) in (c).

$$= \frac{1}{2} \alpha_{2n} + \frac{i}{2\pi} \sum_{k \text{ odd}} \frac{(z_0 + \varepsilon)^{n - \frac{k}{2}}}{n - \frac{k}{2}} \alpha_k. \quad (5.193)$$

At this point, it becomes necessary to introduce the covering space where the fields are well-defined. We map to the covering space coordinate t via

$$z = z_0 + t^2 \quad a^2 = z_0. \quad (5.194)$$

The points ia and $-ia$ are the two images of the origin $z = 0$, one corresponding to each copy of the fields. Mapping the z -plane contours in Figure 5.5 to the t -plane results in Figure 5.7.

We compute the C_3 term by going to the t -plane

$$\int_{C_3} \frac{dz}{2\pi i} \partial X(z) z^n = \int_{\tilde{C}_3} \frac{dt}{2\pi i} \partial X(t) (z_0 + t^2)^n \xrightarrow{\tilde{\varepsilon} \rightarrow 0} 0, \quad (5.195)$$

where the radius of the semicircular contour in the t -plane, \tilde{C}_3 , is given by $\tilde{\varepsilon}$. The contour gives zero contribution since there is no bosonic insertion at $t = 0$ and the integrand is therefore analytic. As the length of the contour goes to zero, therefore, so does the integral. Thus, we see that the story for the bosons is exactly as stated, and in the limit as $\varepsilon \rightarrow 0$ we

reproduce our previous result,

$$\alpha_n^{(1,2)} = \frac{1}{2}\alpha_{2n} \pm \frac{i}{2\pi} \sum_{k \text{ odd}} \frac{z_0^{n-\frac{k}{2}}}{n-\frac{k}{2}} \alpha_k. \quad (5.196)$$

Fermions

For the fermions we have

$$\psi_n^{(1)} = \oint_{C_1} \frac{dz}{2\pi i} \psi(z) z^{n-\frac{1}{2}}, \quad (5.197)$$

which becomes

$$\psi_n^{(1)} = \int_{C_2} \frac{dz}{2\pi i} \psi(z) z^{n-\frac{1}{2}} + \int_{C_3} \frac{dz}{2\pi i} \psi(z) z^{n-\frac{1}{2}} \quad (5.198)$$

The C_2 term is what we have computed for the fermions previously, and is given by

$$\begin{aligned} \int_{C_2} \frac{dz}{2\pi i} \psi(z) z^{n-\frac{1}{2}} &= \frac{1}{2} \sum_k \psi_k \int_{C_2} \frac{dz}{2\pi i} z^{n-\frac{k}{2}-1} \\ &= \frac{1}{2} \psi_{2n} \pm \frac{i}{2\pi} \sum_{k \text{ odd}} \frac{z_0^{n-\frac{k}{2}}}{n-\frac{k}{2}} \psi_k. \end{aligned} \quad (5.199)$$

The C_3 contribution also goes to zero for the fermions. When one goes to the t -plane, one finds

$$\int_{\tilde{C}_3} \frac{dt}{2\pi i} \psi(t) \sqrt{2t} (z_0 + t^2)^{n-\frac{1}{2}}, \quad (5.200)$$

which acts on the spin field $S(t=0)$. The most singular term in the OPE between $\psi(t)$ and $S(0)$ is proportional to $1/\sqrt{t}$, and so one again finds that the semi-circular contour vanishes.

At this point, we see the resolution of the first problem we found with our formal derivation. If the field has an OPE with the spin-field in the covering space which is singular enough, then the C_3 -contribution is nonvanishing in the limit as $\tilde{\varepsilon} \rightarrow 0$. This extra contribution gives exactly the correct answer for J_0^- , for instance, as we demonstrate in Section 5.5.1.

Multiple Contours

Having resolved the first problem with the formal derivation, we should now discuss the UV issues that arise with multiple contours.³²

³²Recall that the definition of the twist operator σ_2 involves a hole in the z -plane, whose radius is carefully taken to zero [15]. One might suspect that this limit has important consequences for these UV issues and that the size of the hole plays the role of a UV cutoff. In fact, the hole is taken to zero size *before* any of the issues discussed in this section, and does not play any role here. The actual issue is the interaction between neighboring contours, as discussed.

Let us write ε_i for the radius of the i th mode's C_3 semi-circle. For instance, consider an initial state

$$\alpha_{n_1}^{(1)} \alpha_{n_2}^{(1)} |0_R^-\rangle^{(1)} |0_R^-\rangle^{(2)}. \quad (5.201)$$

Then the C_3 part coming from $\alpha_{n_1}^{(1)}$ has radius ε_1 in the z -plane and therefore the semi-circle in the t -plane has radius $\sqrt{\varepsilon_1}$. Similarly, for $\alpha_{n_2}^{(1)}$. If we require that the C_2 parts of α_{n_1} and α_{n_2} preserve the same ordering, then the semi-circles in the t -plane satisfy

$$\varepsilon_2 < \varepsilon_1. \quad (5.202)$$

We now argue that, in fact, we should have $\varepsilon_2 \ll \varepsilon_1$ in order to use the intertwining relations as we want to. Consider the two semi-circular C_3 contours at leading order in ε_1 and ε_2 :

$$\begin{aligned} & \int_{\tilde{C}_3(\varepsilon_1)} \frac{dt}{2\pi i} \partial X(t) (z_0 + t^2)^{n_1} \int_{\tilde{C}_3(\varepsilon_2)} \frac{dt'}{2\pi i} \partial X(t') (z_0 + t'^2)^{n_2} \\ & \sim \int_{\tilde{C}_3(\varepsilon_1)} \frac{dt}{2\pi i} (z_0 + t^2)^{n_1} \int_{\tilde{C}_3(\varepsilon_2)} \frac{dt'}{2\pi i} \frac{(z_0 + t'^2)^{n_2}}{(t - t')^2} \\ & \sim \int_{\tilde{C}_3(\varepsilon_1)} \frac{dt}{2\pi i} z_0^{n_1} \int_{\tilde{C}_3(\varepsilon_2)} \frac{dt'}{2\pi i} \frac{z_0^{n_2}}{(t - t')^2} \\ & \sim z_0^{n_1+n_2} \log \frac{1 - \sqrt{\frac{\varepsilon_2}{\varepsilon_1}}}{1 + \sqrt{\frac{\varepsilon_2}{\varepsilon_1}}} \\ & \sim z_0^{n_1+n_2} \sqrt{\frac{\varepsilon_2}{\varepsilon_1}} + \dots \end{aligned} \quad (5.203)$$

This vanishes only if $\varepsilon_2 \ll \varepsilon_1$. Note that this argument is unaffected if the modes are on different copies (the integrals work out in essentially the same way).

Taking $\varepsilon_2 \ll \varepsilon_1$ suggests a particular way to take the limit for double-sums: if L_i is the cutoff on the $\alpha_{n_i}^{(1)}$ -sum, then we should take

$$L_2 \gg L_1, \quad (5.204)$$

that is, evaluate the L_2 -sum first and then the L_1 -sum. This is exactly the way that we got the correct answer, when the issue was demonstrated in (5.186).

The Prescription

We now develop the precise prescription that resolves the UV ambiguities. Before we state the prescription, we should mention that there are two kinds of sums over modes. There are the after-the-twist intertwining sums, which have ordering ambiguities among themselves, and there can also be before-the-twist sums on modes before the twist operator. For

example, consider a composite operator like

$$J_n^{a(1)} = -\frac{1}{4}(\sigma^{aT})^\alpha{}_\beta \sum_{j=-\infty}^{\infty} \psi_{\alpha A, n-j}^{(1)\dagger} \psi_j^{(1)\beta A}. \quad (5.205)$$

In fact, these sums also have UV-limit issues when combined with the intertwining relations as is demonstrated in Section 5.5.2. If we look at the intertwining relation in (5.172), for example, with the implicit cutoff on the sum,

$$\alpha_m^{(2)} = \frac{1}{2}\alpha_{2m} - \frac{i}{2\pi} \sum_{n \text{ odd}}^{|n| < L} \frac{z_0^{m-\frac{n}{2}}}{m-\frac{n}{2}} \alpha_n, \quad (5.206)$$

we see that we are approximating a mode m as a linear combination of modes with UV cutoff L . In order for this approximation to become an exact expansion we must take $L \rightarrow \infty$ with m fixed. That is we need to have much higher frequency modes in our sum than the mode that we are expanding. Therefore, we need to cutoff the before-the-twist sum in (5.205) and ensure that its cutoff is much less than the after-the-twist cutoff in (5.206).

Before proceeding, let us consider more generally what sort of multi-dimensional series we can get in this formalism. If we have a bunch of modes in the initial state that we pull across using the intertwining relations, then there are several different types of terms that can arise. There is a term in which all of the positive modes act on $|\chi\rangle$ separately, and we are left with a product of one-dimensional sums that result in either (5.180) or (5.182). Then, there are terms where the positive modes from one sum contract with negative modes of another. This gives a double sum, like the one in (5.187). If there is a sum on the before-the-twist modes, then we can get a triple sum if those two modes contract. This is the most complicated sum possible.

Finally, we are ready to state the prescription that ensures that the multi-dimensional series converge to the correct answer. The prescription is

1. The after-the-twist intertwining sums should be performed from innermost contour (right-most mode) to outermost contour (left-most mode). This ensures that the C_3 -terms can be dropped.
2. Any sums on before-the-twist modes should be performed *last*. There is no UV-ambiguity among the before-the-twist sums.

Note that with this prescription we have a weakened version of our goal. Because of the UV sensitive series, one cannot directly map operators to operators since one requires knowledge of what other modes are around in order to correctly evaluate the series. While the modes that we start with before the twist operator may commute, we need to think about them pulling across the twist operator in a particular order. It is in this sense, that we have intertwining relations and not Bogolyubov coefficients.

5.5 An Example: Intertwining Relations for J_n^a

There are two equivalent ways of calculating the effect of the twist operator on composite operators such as J_n^a . One way is to use the contour deformation method described in this section, being careful not to throw away the small contour C_3 . The other way is to write J^a as the product of fermion modes and use the intertwining relations for the fermions, being careful to use the prescriptions described in Section 5.4.3.

5.5.1 The Contour Method

We first describe the contour method mentioned above. If we go through the argument described in Section 5.4.3 then

$$J_n^{a(1)} = \frac{1}{2} J_{2n}^a + \frac{i}{2\pi} \sum_{k \text{ odd}} \frac{z_0^{n-\frac{k}{2}}}{n-\frac{k}{2}} J_k^a + \lim_{\varepsilon \rightarrow 0} \int_{C_3} \frac{dz}{2\pi i} J^{a(1)}(z) z^n, \quad (5.207)$$

but this time we find a nonvanishing contribution coming from the C_3 contour. As we pull the $J_n^{a(1)}$ contour out, it acts on the twist operator (or equivalently, the spin field in the covering space) and can switch a σ_2^+ to σ_2^- . Therefore, let us consider σ_2^α .

We can evaluate the C_3 contour by going to the t -plane, where $\sigma_2^\alpha(z_0)$ leaves only a spin field $S^\alpha(t=0)$. The image of C_3 in the t -plane, \tilde{C}_3 , is a semi-circle around the origin as shown in Figure 5.7. Thus, the \tilde{C}_3 contour implicitly acts on the spin field:

$$\begin{aligned} \int_{C_3} \frac{dz}{2\pi i} J^{(1)a}(z) z^n &= \left[\int_{\tilde{C}_3} \frac{dt}{2\pi i} J^a(t) (z_0 + t^2)^n \right] S^\alpha(0) \\ &= \frac{1}{2} (\sigma^{aT})^\alpha{}_\beta S^\beta(0) \int_{\tilde{C}_3} \frac{dt}{2\pi i} \frac{(z_0 + t^2)^n}{t} \\ &= \frac{1}{2} (\sigma^{aT})^\alpha{}_\beta S^\beta(0) \frac{1}{2\pi i} \left(z_0^n \log t \Big|_{-\varepsilon}^\varepsilon + O(\varepsilon) \right) \\ &= -\frac{z_0^n}{4} (\sigma^{aT})^\alpha{}_\beta S^\beta(0), \end{aligned} \quad (5.208)$$

where we have given the result after taking $\varepsilon \rightarrow 0$. When we go back to the z -plane we should write the above result as

$$\sigma_2^\alpha(z_0) J_n^{a(1)} = \left[\frac{1}{2} J_{2n}^a + \frac{i}{2\pi} \sum_{k \text{ odd}} \frac{z_0^{n-\frac{k}{2}}}{n-\frac{k}{2}} J_k^a \right] \sigma_2^\alpha(z_0) - \frac{z_0^n}{4} (\sigma^{aT})^\alpha{}_\beta \sigma_2^\beta(z_0). \quad (5.209)$$

If we had considered $J_n^{a(2)}$, then we obtain a similar result. We can summarize the two relations and write them in a suggestive form as

$$\sigma_2^\alpha(z_0) J_n^{a(1,2)} = \left[\frac{1}{2} J_{2n}^a \pm \frac{i}{2\pi} \sum_{k \text{ odd}} \frac{z_0^{n-\frac{k}{2}}}{n-\frac{k}{2}} J_k^a \right] \sigma_2^\alpha(z_0) - \frac{z_0^n}{2} [J_0^a, \sigma_2^\alpha(z_0)]. \quad (5.210)$$

We see that if we use these intertwining relations, then we get the correct answer in (5.184).

While the above intertwining relation is correct, it may not be the most useful form. Because we have switched the charge on the twist operator, we now must think about a new state $|\chi\rangle$ created by the negatively-charged operator acting on the vacuum.

An Example

For concreteness, let us consider

$$\sigma_2^+(z_0) J_n^{-(1)} |0^-\rangle^{(1)} |0^-\rangle^{(2)}, \quad n < 0, \quad (5.211)$$

then we have

$$\left[\frac{1}{2} J_{2n}^- + \frac{i}{2\pi} \sum_{k \text{ odd}} \frac{z_0^{n-\frac{k}{2}}}{n-\frac{k}{2}} J_k^- - \frac{z_0^n}{2} J_0^- \right] |\chi\rangle. \quad (5.212)$$

Thus, our first task is to compute the three terms,

$$J_{2n}^- |\chi\rangle \quad J_k^- |\chi\rangle \text{ } k \text{ odd} \quad J_0^- |\chi\rangle. \quad (5.213)$$

There are no real complications in working the terms out. For instance, for the first term, one starts with³³

$$J_{2n}^- = -\frac{1}{4} \sum_j \psi_{+\dot{A}, 2n-j}^\dagger \psi_j^{-\dot{A}}, \quad (5.214)$$

then breaks the sum into terms with both modes negative and terms with odd positive modes that act on $|\chi\rangle$. One can write the result in the form

$$J_{2n}^- |\chi\rangle = -\frac{1}{4} \sum_{2n+1 \leq j \leq -1} \psi_{+\dot{A}, 2n-j}^\dagger \psi_j^{-\dot{A}} |\chi\rangle + \sum_{j, p \text{ odd}^+} \gamma_{jp}^F \psi_{+\dot{A}, -p}^\dagger \psi_{2n-j}^{-\dot{A}} |\chi\rangle. \quad (5.215)$$

Similarly, J_0^- becomes

$$J_0^- |\chi\rangle = \sum_{j, p \text{ odd}^+} \gamma_{jp}^F \psi_{+\dot{A}, -j}^\dagger \psi_{-p}^{-\dot{A}} |\chi\rangle. \quad (5.216)$$

The J_k^- term is not much work, but there are two distinct cases, corresponding to whether or not there are terms where both ψ s are raising operators: $k \leq -3$ and $k \geq -1$.

³³Note that the J after the twist has an extra factor of 1/2 from before the twist, which arises from the fermion–fermion anticommutator having an extra factor of 2 after the twist.

One finds

$$J_k^- |\chi\rangle = -\frac{1}{4} \sum_{k+1 \leq j \leq -1} \psi_{+\dot{A},k-j}^\dagger \psi_j^{-\dot{A}} |\chi\rangle + \sum_{j,p \text{ odd}^+} \gamma_{jp}^F \psi_{+\dot{A},k-j}^\dagger \psi_{-p}^{-\dot{A}} |\chi\rangle \quad k \leq -3, \text{ odd} \quad (5.217)$$

and

$$J_k^- |\chi\rangle = \sum_{j,p \text{ odd}^+} \gamma_{k+j+1,p}^F \psi_{+\dot{A},-j-1}^\dagger \psi_{-p}^{-\dot{A}} |\chi\rangle \quad k \geq -1, \text{ odd}. \quad (5.218)$$

The slightly more difficult task is the sum over k , which can be written as

$$\begin{aligned} \sum_{k \text{ odd}} \frac{z_0^{n-\frac{k}{2}}}{n-\frac{k}{2}} J_k^- |\chi\rangle &= \sum_{k \text{ odd}}^{k \leq -3} \frac{z_0^{n-\frac{k}{2}}}{n-\frac{k}{2}} J_k^- |\chi\rangle + \sum_{k \text{ odd}}^{k \geq -1} \frac{z_0^{n-\frac{k}{2}}}{n-\frac{k}{2}} J_k^- |\chi\rangle \\ &= -\frac{1}{2} \sum_{j,p \text{ odd}^+} \frac{z_0^{n+\frac{j+p+1}{2}}}{n+\frac{j+p+1}{2}} \psi_{+\dot{A},-j-1}^\dagger \psi_{-p}^{-\dot{A}} \\ &\quad + \sum_{j \text{ odd}}^{j \geq 3} \sum_{p \text{ odd}^+} \left(\sum_{k \text{ odd}}^{-j \leq k \leq -3} \frac{z_0^{n-\frac{k}{2}}}{n-\frac{k}{2}} \gamma_{k+j+1,p}^F \right) \psi_{+\dot{A},-j-1}^\dagger \psi_{-p}^{-\dot{A}} \\ &\quad + \sum_{j,p \text{ odd}^+} \left(\sum_{k \text{ odd}}^{k \geq -1} \frac{z_0^{n-\frac{k}{2}}}{n-\frac{k}{2}} \gamma_{k+j+1,p}^F \right) \psi_{+\dot{A},-j-1}^\dagger \psi_{-p}^{-\dot{A}}, \end{aligned} \quad (5.219)$$

after a few manipulations. Note that all of the terms on the right implicitly act on $|\chi\rangle$. Finally, using (F.3b) one arrives at

$$\sum_{k \text{ odd}} \frac{z_0^{n-\frac{k}{2}}}{n-\frac{k}{2}} J_k^- |\chi\rangle = - \sum_{j,p \text{ odd}^+} \frac{z_0^{n+\frac{j+p+1}{2}}}{2(n+\frac{j+p+1}{2})} \frac{\Gamma(\frac{p}{2})\Gamma(-n-\frac{j}{2})}{\Gamma(\frac{p+1}{2})\Gamma(-n-\frac{j+1}{2})} \psi_{+\dot{A},-j-1}^\dagger \psi_{-p}^{-\dot{A}} |\chi\rangle \quad (5.220)$$

Putting it all together, we have

$$\begin{aligned} \sigma_2^+(z_0) J_n^{-(1)} |0^-\rangle^{(1)} |0^-\rangle^{(2)} &= -\frac{1}{8} \sum_{j=n+1}^{-1} \psi_{+\dot{A},2n-2j}^\dagger \psi_{2j}^{-\dot{A}} |\chi\rangle \\ &\quad - \frac{i}{4\pi} \sum_{j=1}^{\infty} \sum_{p \text{ odd}^+} \frac{z_0^{n+j+\frac{p}{2}}}{n+j+\frac{p}{2}} \frac{\Gamma(\frac{p}{2})\Gamma(-n-j+\frac{1}{2})}{\Gamma(\frac{p+1}{2})\Gamma(-n-j)} \psi_{+\dot{A},-2j}^\dagger \psi_{-p}^{-\dot{A}} |\chi\rangle \\ &\quad + \frac{1}{2} \sum_{j,p \text{ odd}^+} \left[-\frac{1}{4} \delta_{j+p+2n,0} + \frac{\gamma_{2n+p,j}^F + \gamma_{2n+j,p}^F}{2} - z_0^n \frac{\gamma_{jp}^F + \gamma_{pj}^F}{2} \right] \psi_{+\dot{A},-j}^\dagger \psi_{-p}^{-\dot{A}} |\chi\rangle, \end{aligned} \quad (5.221)$$

where for ease of comparison we have broken the result into even-even, even-odd, and odd-odd terms. In the above expression, we define γ^F with negative indices to be zero.

Furthermore, we have explicitly symmetrized over j and p in the last term since

$$\psi_{+\dot{A},-j}^\dagger \psi_{-p}^{-\dot{A}} = \psi_{+\dot{A},-p}^\dagger \psi_{-j}^{-\dot{A}}. \quad (5.222)$$

Below, we compare this result with what one finds when one breaks the $J_n^{-(1)}$ into fermions and uses the fermion intertwining relations.

5.5.2 The Composite Method

We now show how to reproduce the above result by using the fermion intertwining relations and our prescription.

We start by writing

$$J_n^{a(1)} = -\frac{1}{4}(\sigma^{aT})^\alpha{}_\beta \sum_{j=-\infty}^{\infty} \psi_{\alpha\dot{A},n-j}^{(1)\dagger} \psi_j^{(1)\beta\dot{A}}, \quad (5.223)$$

and note that the sum on j is a sum over “before-the-twist” modes and therefore should be evaluated last according to the prescription. We then can use our intertwining relations to write this directly as

$$J_n^{a(1)} = -\frac{1}{4}(\sigma^{aT})^\alpha{}_\beta \sum_{j=-\infty}^{\infty} \left[\frac{1}{2} \psi_{\alpha\dot{A},2n-2j}^\dagger + \frac{i}{2\pi} \sum_{k \text{ odd}} \frac{z_0^{n-j-\frac{k}{2}}}{n-j-\frac{k}{2}} \psi_{\alpha\dot{A},k}^\dagger \right] \left[\frac{1}{2} \psi_{2j}^{\beta\dot{A}} + \frac{i}{2\pi} \sum_{l \text{ odd}} \frac{z_0^{j-\frac{l}{2}}}{j-\frac{l}{2}} \psi_l^{\beta\dot{A}} \right]. \quad (5.224)$$

At this point, we can say nothing further until we know what $J_n^{a(1)}$ acts on. Of course, when faced with an expression like the above it is rather tempting to evaluate the j -sum using

$$\sum_{j=-\infty}^{\infty} \frac{1}{(n-j-\frac{k}{2})(j-\frac{l}{2})} = -\pi^2 \delta_{\frac{l}{2}, n-\frac{k}{2}} \quad k, l \text{ odd}, \quad (5.225)$$

which immediately leads to the false relation

$$J_n^{a(1)} = \frac{1}{2} J_{2n}^a + \frac{i}{2\pi} \sum_{k \text{ odd}} \frac{z_0^{n-\frac{k}{2}}}{n-\frac{k}{2}} J_k^a \quad (\text{false relation}). \quad (5.226)$$

This demonstrates the need for the restriction on before-the-twist sums.

In order to proceed and compare to (5.210), let us again consider the state

$$\sigma_2^+(z_0) J_n^{-(1)} |0_R^-\rangle^{(1)} |0_R^-\rangle^{(2)}. \quad (5.227)$$

Now, one could make the j -sum in (5.224) finite by considering the above; however, our prescription ensures that one gets the correct answer even if one leaves it as an infinite series.

If we act on the vacuum as in (5.227), then we get (5.224) acting on $|\chi\rangle$. The $\psi^{\beta\dot{A}}$ is the rightmost mode and so the l -sum should be evaluated first, followed by the k -sum, and then finally the j -sum. We can use (5.182) to quickly read off the result of the l -sum. There are now two distinct terms to consider for the k -sum. There is the possibility of the $\psi_{\alpha\dot{A}}^\dagger$ contracting with the result of the l -sum, and the ψ^\dagger can pass through and act on $|\chi\rangle$ (and we can again use (5.182)). The contraction gives zero. For other composite operators, however, the contraction term can be nonzero.

Following the above procedure, we get

$$-\frac{1}{2} \sum_{j=-\infty}^{\infty} \left[\frac{1}{2} \psi_{+\dot{A}, 2(n-j)}^\dagger + \frac{i}{2\pi} \sum_{p \text{ odd}^+} \frac{z_0^{n-j+\frac{p}{2}}}{n-j+\frac{p}{2}} \frac{\Gamma(\frac{p}{2})\Gamma(-n+j+\frac{1}{2})}{\Gamma(\frac{p+1}{2})\Gamma(-n+j)} \psi_{+\dot{A}, -p}^\dagger \right] \quad (5.228)$$

$$\left[\frac{1}{2} \psi_{2j}^{-\dot{A}} + \frac{i}{2\pi} \sum_{q \text{ odd}^+} \frac{z_0^{j+\frac{q}{2}}}{j+\frac{q}{2}} \frac{\Gamma(\frac{q}{2})\Gamma(-j+\frac{1}{2})}{\Gamma(\frac{q+1}{2})\Gamma(-j)} \psi_{-q}^{-\dot{A}} \right].$$

There are four terms from the above multiplication.

The even-even term is

$$(\text{even-even}) = -\frac{1}{8} \sum_{j=n+1}^{-1} \psi_{+\dot{A}, 2n-2j}^\dagger \psi_{2j}^{-\dot{A}}. \quad (5.229)$$

One can show that the two even-odd cross-terms are identical, and sum to

$$(\text{even-odd}) = -\frac{i}{4\pi} \sum_{j=-\infty}^{-1} \sum_{p \text{ odd}^+} \frac{z_0^{n-j+\frac{p}{2}}}{n-j+\frac{p}{2}} \frac{\Gamma(\frac{p}{2})\Gamma(-n+j+\frac{1}{2})}{\Gamma(\frac{p+1}{2})\Gamma(-n+j)} \psi_{+\dot{A}, -p}^\dagger \psi_{2j}^{-\dot{A}} \quad (5.230)$$

One may write the odd-odd term as

$$(\text{odd-odd}) = \frac{1}{8\pi^2} \sum_{p, q \text{ odd}^+} \psi_{+\dot{A}, -p}^\dagger \psi_{-q}^{-\dot{A}} z_0^{n+\frac{p+q}{2}} \frac{\Gamma(\frac{p}{2})\Gamma(\frac{q}{2})}{\Gamma(\frac{p+1}{2})\Gamma(\frac{q+1}{2})} S(n, p, q), \quad (5.231)$$

where

$$S(n, p, q) = \sum_{j=n+1}^{-1} \frac{1}{(n-j+\frac{p}{2})(j+\frac{q}{2})} \frac{\Gamma(-n+j+\frac{1}{2})\Gamma(-j+\frac{1}{2})}{\Gamma(-n+j)\Gamma(-j)}. \quad (5.232)$$

Comparing the above to the three terms in Equation (5.221), one finds agreement provided

$$\frac{z_0^{n+\frac{j+p}{2}}}{8\pi^2} \frac{\Gamma(\frac{j}{2})\Gamma(\frac{p}{2})}{\Gamma(\frac{j+1}{2})\Gamma(\frac{p+1}{2})} S(n, j, p) = \frac{1}{2} \left[-\frac{1}{4} \delta_{j+p+2n, 0} + \frac{\gamma_{2n+p, j}^F + \gamma_{2n+j, p}^F}{2} - z_0^n \frac{\gamma_{jp}^F + \gamma_{pj}^F}{2} \right]. \quad (5.233)$$

This equation follows from the identity

$$\sum_{k=0}^{\mu} \frac{1}{(\mu - k - \frac{\alpha}{2})(k - \frac{\beta}{2})} \frac{\Gamma(\mu - k + \frac{3}{2})\Gamma(k + \frac{3}{2})}{\Gamma(\mu - k + 1)\Gamma(k + 1)} \\ = \pi - \frac{\pi}{\frac{\alpha+\beta}{2} - \mu} \left(\frac{\Gamma(\frac{\alpha+3}{2})\Gamma(\frac{\alpha}{2} - \mu)}{\Gamma(\frac{\alpha}{2} + 1)\Gamma(\frac{\alpha-1}{2} - \mu)} + \frac{\Gamma(\frac{\beta+3}{2})\Gamma(\frac{\beta}{2} - \mu)}{\Gamma(\frac{\beta}{2} + 1)\Gamma(\frac{\beta-1}{2} - \mu)} \right), \quad (5.234)$$

where the left-hand side is $S(n, p, q)$ with $\mu = -n - 2$, $\alpha = p - 2$, and $\beta = q - 2$. If we call the above sum $F(\mu, \alpha, \beta)$, then one can prove the identity by showing that both sides of Equation (5.234) obey the four-term recursion relation

$$f_0(\mu, \alpha, \beta)F(\mu, \alpha, \beta) + f_1(\mu, \alpha, \beta)F(\mu + 1, \alpha, \beta) \\ + f_2(\mu, \alpha, \beta)F(\mu + 2, \alpha, \beta) + f_3(\mu, \alpha, \beta)F(\mu + 3, \alpha, \beta) = 0, \quad (5.235)$$

with

$$f_0(\mu, \alpha, \beta) = (-3 + \alpha - 2\mu)(\alpha + \beta - 2\mu)(3 - \beta + 2\mu)(\alpha + \beta - 6(3 + \mu)) \quad (5.236a)$$

$$f_1(\mu, \alpha, \beta) = 3(\alpha + \beta - 2(1 + \mu))(-2\beta^2(2 + \mu) + \alpha^2(\beta - 2(2 + \mu)) + \beta(79 + 8\mu(9 + 2\mu)) \\ + \alpha(79 + \beta^2 + 8\mu(9 + 2\mu) - 2\beta(12 + 5\mu)) - 2(128 + \mu(175 + 4\mu(20 + 3\mu)))) \quad (5.236b)$$

$$f_2(\mu, \alpha, \beta) = 3(\alpha + \beta - 2(2 + \mu))(\beta^2(5 + 2\mu) + \alpha^2(5 - \beta + 2\mu) + 4(2 + \mu)(43 + 32\mu + 6\mu^2) \\ - 2\beta(47 + \mu(39 + 8\mu)) - \alpha(94 + \beta^2 - 2\beta(12 + 5\mu) + 2\mu(39 + 8\mu))) \quad (5.236c)$$

$$f_3(\mu, \alpha, \beta) = (\alpha + \beta - 6(2 + \mu))(\alpha - 2(3 + \mu))(\beta - 2(3 + \mu))(\alpha + \beta - 2(3 + \mu)). \quad (5.236d)$$

Thus the identity holds by induction once one confirms that it holds for $\mu = 0, 1, 2$. It may be helpful to use an algebraic manipulation program such as *Mathematica* to show the above.

5.6 Discussion

We developed technology for computing the effect of the blow-up mode deformation operator on untwisted states of the D1D5 CFT. We would be remiss, if we did not note that the methods presented here should generalize to higher order twist operators.

In Section 5.2, we showed that one could manipulate the supercharge contour so that it acts before and after the twist. We then showed that the twist operator acts on the vacuum to create a squeezed state in terms of the twisted sector modes. The coefficients of the bosonic and fermionic excitations appear in Equations (5.66) and (5.79) and the full state appears in Equation (5.89). We can analyze the large m and n limit of the coefficients, by noting the asymptotic behavior

$$\frac{\Gamma(x + 1)}{\Gamma(x + \frac{1}{2})} \sim \sqrt{x} e^{-\frac{1}{8x} + O(\frac{1}{x^2})}, \quad (5.237)$$

which can be derived from Stirling's approximation. The large m and n behavior is

$$\gamma_{mn}^B \sim \frac{2z_0^{\frac{m+n}{2}}}{(m+n)\pi} \frac{1}{\sqrt{mn}} \quad (5.238a)$$

$$\gamma_{mn}^F \sim -\frac{z_0^{\frac{m+n}{2}}}{(m+n)\pi} \sqrt{\frac{m}{n}}. \quad (5.238b)$$

Let us note that the behavior of γ_{mn}^B is more properly multiplied by \sqrt{mn} if we want unit-normalized raising operators $a_m^\dagger = \alpha_{-m}/\sqrt{m}$. Thus, when $m \sim n$ the fermions and bosons behave essentially the same. The asymmetry between m and n results from the asymmetry between $+$ and $-J_0^3$ -charge in our setup.

Let us note that the state appearing in Equation (5.89) is before the integral over the z and \bar{z} coordinates that give rise to an energy-conserving delta-function. No terms can contribute in Equation (5.89), and thus the Ramond vacuum is invariant under the deformation to first order in perturbation theory. This is expected from supersymmetry. It is convenient to have an off-shell expression for later calculations, however.

In Section 5.3, we computed the effect of the deformation operator on some simple excited states. First, a single bosonic and fermionic excitation, as given in Equations (5.127) and (5.143). In both, expressions there is a “diagonal” component in which an initial $\alpha_m^{(1)}$ mode becomes α_{2m} in the final state. Recalling our convention for the twisted sector, these both have the same energy and moding. Then, there is the off-diagonal contribution which consists of only odd modes. Because the exponential gives pairs of odd modes, the only part that conserves L_0 is the diagonal contribution. Again, it is still useful to have the off-shell expression. We then computed the effect of the twist operator on two bosonic and two fermionic modes in Sections 5.3.3 and 5.3.4. The calculation culminates in Equations (5.151) and (5.159), before the application of the supercharge. In Section 5.3.5, we included the effect of the supercharge in Equation (5.164). The supercharge changes some bosonic excitations to fermionic excitations, but it does not change our conclusion about going on-shell for a single bosonic excitation.

While the (untwisted) Ramond vacuum and single bosonic or fermionic excitations do not have very exciting physics when we go on-shell, let us consider two bosonic excitations. Looking at the expression in (5.151), we see that there is no even-odd problem like for a single mode and so there is an off-diagonal contribution on-shell. Applying the supercharge does not alter the weights of the modes, and does not effect our argument. For concreteness consider the case in which we have two initial bosonic modes with combined weight 10 and for which there is no \mathbb{C} -number contribution. We first have the two f^B terms. We could take them both to be α_{-1} -modes, for instance. This contributes weight 1 out of the original 10. The remaining 9, can be made up out of the exponential in $|\chi\rangle$ in many different ways. For instance, one could have 9 pairs of additional α_{-1} modes.

Therefore, even on-shell there is a nonzero probability for the two original excitations to fragment into as many as 20 bosonic lower weight modes. This is all only first-order in perturbation theory!

In Section 5.4, we developed a different method to compute the effect of the twist operator on excited states. The technique makes the Bogolyubov-nature of the deformation operator more transparent. There were some UV ambiguous sums that were tamed with the prescription in Section 5.4.3. With the prescription the results are self-consistent and agree with those of the previous sections.

Using the technology and understanding developed here, we hope to address some important outstanding questions concerning the D1D5 CFT and black hole physics. In particular, we hope to elucidate the nature of the proposed “non-renormalization” theorem [96]; how states of the CFT fragment, thereby “scrambling” information [207, 208]; black hole formation; and the in-falling observer. All of these are important and deep issues that will probably require lots of work to resolve; however, the work shown here should serve as a step toward these goals.

All of the calculations here and in [202–204] have been off-shell. A more modest next step would be to analyze the physics that arise on-shell. Another task is to systematically analyze the combinatorial factors that arise at different orders in perturbation theory. We defer these steps for future calculations.

Chapter 6

CONCLUSIONS AND OUTLOOK

The D1D5 system has been and remains indispensable in the theoretical study of black holes in string theory. In Chapter 2, we gave an overview of the D1D5 system and its CFT description. Describing the same process using both supergravity and CFT descriptions is one of the best ways to gain understanding of black holes. We have focused on the CFT description here, emphasizing its utility in understanding some of the mysteries of the gravitational description.

In Chapter 3, we outlined how to perturbatively relax the decoupling limit allowing the supergravity fields in flat space to interact with the AdS/CFT. The results of this chapter apply equally well to other incarnations of the AdS–CFT correspondence so we do not restrict ourselves to $\text{AdS}_3\text{--CFT}_2$. The general interaction term is given in Equation (3.52). This can be used to compute absorption, emission, or even more general scattering processes. While some similar calculations were performed in [157], we have made a much more general and systematic treatment. In particular we have taken the effect of the neck into account.

In Chapter 4, we applied the technique of Chapter 3 to reproduce the ergoregion emission from JMaRT geometries from a CFT amplitude. Since ergoregion emission from the JMaRT geometries and Hawking radiation from a black hole use the same vertex operator, we argued that the ergoregion emission is the Hawking radiation from the particular microstate. This point of view was first advanced in [180–182], but there were several important missing links. First, the coupling between the asymptotic flat space and the CFT was fixed by demanding agreement with Hawking radiation, which may be a bit unsatisfying. Second, only partial spectrums had been reproduced from a subset of the JMaRT solitons. In Chapter 3, we fix the coupling by demanding agreement between gravity and CFT for a two-point function *within* AdS; this step does not require us to relax the decoupling limit. This addresses the first issue. In Chapter 4, we reproduce the *full* spectrum from *all* of the JMaRT geometries.

In our computation of the full spectrum, there are several points of interest. One is

that we demonstrate how spectral flow and Hermitian conjugation can be used to relate a single CFT calculation to many different gravitational processes. In particular, for $\kappa = 1$, we first computed the emission of a single quantum out of the geometry. We then related this amplitude to the JMaRT ergoregion emission. A second point is that in our calculation of emission for $\kappa > 1$, we had to make a conjecture of the form of supergravity excitations in κ -orbifolded geometries. This conjecture seems natural from the perspective that all of the modes for $\kappa = 1$ get “divided by” κ . It would be interesting to understand this last issue better.

Finally, in Chapter 5 we describe technology that allows one to compute the effect of deforming the CFT off its orbifold point. More specifically we studied a single application of the marginal 2-twist deformation operator. A surprisingly rich structure emerges from the twisting. The effect of the twist operator is to very similar to a Bogolyubov transformation. Much of this material should go through with only minor alteration to higher-twist operators. So this is relevant to anyone interested in describing the physics of $S_{N_1 N_5}$ -twist operators using a Hamiltonian description. A lot of the results reported in this chapter require more calculation and analysis to elucidate the black hole physics of interest, which we put off for future papers. Note, however, that the basic physics of interest we can already see, as discussed in Section 5.6. At first order in perturbation theory, we find that a few high-energy excitations can fragment into many low-energy excitations.

There are many puzzles left for black holes in string theory. We expect that the D1D5 CFT will be useful in resolving them. Many outstanding questions about the fuzzball proposal and black holes revolve around dynamical questions: How do black holes thermalize and what is the role of quasi-normal modes? How does one get into a fuzzball state? What does an infalling observer experience? What happens to a infalling spherical shell of matter? The marginal deformation that we add to the CFT can be treated in time-dependent perturbation theory. It is hoped, then, that the D1D5 CFT and the results in Chapter 5 will address some of those questions.

Appendix A

NOTATION AND CONVENTIONS FOR THE ORBIFOLD CFT

Here, we carefully define the notation and conventions used throughout this paper, and to be used in future work. The system we describe lives in $M_{4,1} \times T^4 \times S^1$. We restrict our attention to the case where the compact space is a torus, although one may also consider K3.

The base space of the CFT is the S^1 and time (\mathbb{R}) , with fields living in the orbifolded target space: $(T^4)^{N_1 N_5} / S_{N_1 N_5}$. The expressions in this appendix are exclusively given for the complex plane.

A.1 Symmetries and Indices

The symmetries of our theory are $SU(2)_L \times SU(2)_R$ and the $SO(4)_I \simeq SU(2)_1 \times SU(2)_2$ rotations of the torus. Indices correspond to the following representations

$$\begin{array}{llll}
 \alpha, \beta & \text{doublet of } SU(2)_L & \dot{\alpha}, \dot{\beta} & \text{doublet of } SU(2)_R \\
 A, B & \text{doublet of } SU(2)_1 & \dot{A}, \dot{B} & \text{doublet of } SU(2)_2 \\
 i, j & \text{vector of } SO(4). & &
 \end{array}$$

One can project vectors of $SO(4)$ into the doublets of $SU(2)_1 \times SU(2)_2$, using the usual Pauli spin matrices and the identity matrix

$$(\sigma^i)^{\dot{A}A}, \quad \sigma^4 = i\mathbb{1}_2.$$

The indices are such that, for instance, $(\sigma^2)^{\dot{2}1} = i$.

We use indices $a, b, c = 1, 2, 3$ for the triplet of any $SU(2)$. Their occurrence is rare enough that which $SU(2)$ is being referred to should be unambiguous. Note that the $SU(2)$ generators $(\sigma^a)_\alpha^\beta$ naturally come with one index raised and one index lowered. On the other hand the Clebsch-Gordan coefficients to project a vector of $SO(4)$ into two $SU(2)$'s

naturally come with both indices raised (or lowered), as above.

We raise and lower all $SU(2)$ doublet indices in the same way so that

$$\epsilon_{\alpha\beta}v^\beta = v_\alpha \quad v^\alpha = \epsilon^{\alpha\beta}v_\beta, \quad (\text{A.1})$$

where

$$\epsilon_{12} = -\epsilon_{21} = \epsilon^{21} = -\epsilon^{12} = 1, \quad (\text{A.2})$$

and therefore

$$\epsilon_{\alpha\beta}\epsilon^{\beta\gamma} = \delta_\alpha^\gamma. \quad (\text{A.3})$$

A.2 Field Content

The bosonic field content of each copy of the CFT consists of a vector of $SO(4)_I$, $X^i(z, \bar{z})$, giving the position of that effective string in the torus. The fermions on the left sector have indices in $SU(2)_L \times SU(2)_2$, while the fermions in the right sector have indices in $SU(2)_R \times SU(2)_2$:

$$\psi^{\alpha\dot{A}}(z) \quad \bar{\psi}^{\dot{A}}(\bar{z}). \quad (\text{A.4})$$

These fermions are complex, so there are two complex fermions and their Hermitian conjugates in the left sector and two complex fermions and their Hermitian conjugates in the right sector.

Note that we use the abbreviated notation

$$[X]^{\dot{A}\dot{A}} = \frac{1}{\sqrt{2}}X^i(\sigma^i)^{\dot{A}\dot{A}}. \quad (\text{A.5})$$

A.3 Currents

The holomorphic currents of our theory that form a closed OPE algebra are an $SU(2)_L$ current, $J^a(z)$; the supersymmetry currents, $G^{\alpha\dot{A}}(z)$; and the stress-energy $T(z)$. The right sector has the corresponding anti-holomorphic currents. Obviously, in this case, the index a on J transforms in $SU(2)_L$.

For each copy of the CFT, the currents are realized in terms of the fields as

$$J^a(z) = \frac{1}{4}\epsilon_{\dot{A}\dot{B}}\psi^{\alpha\dot{A}}\epsilon_{\alpha\beta}(\sigma^{*a})^\beta_\gamma\psi^{\gamma\dot{B}} \quad (\text{A.6a})$$

$$G^{\alpha\dot{A}}(z) = \psi^{\alpha\dot{A}}[\partial X]^{\dot{B}\dot{A}}\epsilon_{\dot{A}\dot{B}} \quad (\text{A.6b})$$

$$T(z) = \frac{1}{2}\epsilon_{\dot{A}\dot{B}}\epsilon_{AB}[\partial X]^{\dot{A}\dot{A}}[\partial X]^{\dot{B}\dot{B}} + \frac{1}{2}\epsilon_{\alpha\beta}\epsilon_{\dot{A}\dot{B}}\psi^{\alpha\dot{A}}\partial\psi^{\beta\dot{B}}. \quad (\text{A.6c})$$

Note that the $SO(4)_I$ of the torus is an outer automorphism and so while we can make a generator that acts appropriately on the fermions we cannot make one that also acts

appropriately on the bosons.

A.4 Hermitian Conjugation

Because we work in a Euclidean time formalism, one must address Hermitian conjugation carefully so that it is consistent with the physical, real-time formalism.

A quasi-primary field of weight $(\Delta, \bar{\Delta})$ is Hermitian conjugated as [150]

$$[\mathcal{O}(z, \bar{z})]^\dagger = \bar{z}^{-2\Delta} z^{-2\bar{\Delta}} \mathcal{O}^\dagger\left(\frac{1}{\bar{z}}, \frac{1}{z}\right), \quad (\text{A.7})$$

where $\mathcal{O}^\dagger(z, \bar{z})$ has the opposite charges under $SU(2)_L \times SU(2)_R \times SO(4)_I$.

The fermions Hermitian conjugate as

$$(\psi^{\alpha\dot{A}})^\dagger(z) = -\epsilon_{\alpha\beta}\epsilon_{\dot{A}\dot{B}}\psi^{\beta\dot{B}}(z) = -\psi_{\alpha\dot{A}}(z). \quad (\text{A.8})$$

This reality condition ensures that there are only four real degrees of freedom in both the left and right sectors. The specific sign can be determined from the basic fermion correlator and demanding a positive-definite norm.

The bosons conjugate as

$$(X^i)^\dagger(z, \bar{z}) = X^i(z, \bar{z}) \quad ([X]^{\dot{A}\dot{A}})^\dagger(z, \bar{z}) = -\epsilon_{\dot{A}\dot{B}}\epsilon_{AB}[X]^{\dot{B}B}(z, \bar{z}). \quad (\text{A.9})$$

The stress energy tensor and the $SU(2)_L$ current are both Hermitian and so conjugate trivially; whereas, the supercurrents conjugate as

$$(G^{\alpha A})^\dagger(z) = -\epsilon_{\alpha\beta}\epsilon_{AB}G^{\beta B}(z). \quad (\text{A.10})$$

Again, the specific sign is determined by requiring the norm to be positive-definite.

The Ramond vacua conjugate as

$$(|\emptyset\rangle_R^\alpha)^\dagger = {}^R\langle\emptyset|_\alpha \quad {}^R\langle\emptyset|_\alpha |\emptyset\rangle_R^\beta = \delta_\alpha^\beta. \quad (\text{A.11})$$

A.5 OPE

We normalize the fields so that the basic correlators are

$$\langle X^i(z)X^j(w) \rangle = -2\delta^{ij} \log |z - w| \quad (\text{A.12a})$$

$$\langle \psi^{\alpha\dot{A}}(z)\psi^{\beta\dot{B}}(w) \rangle = -\frac{\epsilon^{\alpha\beta}\epsilon^{\dot{A}\dot{B}}}{z - w}, \quad (\text{A.12b})$$

where it is also useful to note that Equation (A.12a) implies

$$\langle [X]^{\dot{A}\dot{A}}(z)[X]^{\dot{B}B}(w) \rangle = 2\epsilon^{\dot{A}\dot{B}}\epsilon^{AB} \log |z - w|. \quad (\text{A.13})$$

From which, the commonly used

$$[\partial X(z)]^{\dot{A}A}[\partial X(w)]^{\dot{B}B} \sim \frac{\epsilon^{\dot{A}\dot{B}}\epsilon^{AB}}{(z-w)^2}, \quad (\text{A.14})$$

immediately follows.

The OPE current algebra for a single copy of the $\mathcal{N} = 4$ CFT is

$$J^a(z)J^b(w) \sim \frac{c}{12} \frac{\delta^{ab}}{(z-w)^2} + i\epsilon^{ab} \frac{J^c(w)}{z-w} \quad (\text{A.15a})$$

$$J^a(z)G^{\alpha A}(w) \sim \frac{1}{2}(\sigma^{*a})^\alpha{}_\beta \frac{G^{\beta A}(w)}{z-w} \quad (\text{A.15b})$$

$$G^{\alpha A}(z)G^{\beta B}(w) \sim -\frac{c}{3} \frac{\epsilon^{AB}\epsilon^{\alpha\beta}}{(z-w)^3} + \epsilon^{AB}\epsilon^{\beta\gamma}(\sigma^{*a})^\alpha{}_\gamma \left[\frac{2J^a(w)}{(z-w)^2} + \frac{\partial J^a(w)}{z-w} \right] - \epsilon^{AB}\epsilon^{\alpha\beta} \frac{T(w)}{z-w} \quad (\text{A.15c})$$

$$T(z)J^a(w) \sim \frac{J^a(w)}{(z-w)^2} + \frac{\partial J^a(w)}{z-w} \quad (\text{A.15d})$$

$$T(z)G^{\alpha A}(w) \sim \frac{\frac{3}{2}G^{\alpha A}(w)}{(z-w)^2} + \frac{\partial G^{\alpha A}(w)}{z-w} \quad (\text{A.15e})$$

$$T(z)T(w) \sim \frac{c}{2} \frac{1}{(z-w)^4} + 2 \frac{T(w)}{(z-w)^2} + \frac{\partial T(w)}{z-w}, \quad (\text{A.15f})$$

which agrees with the above correlators for $c = 6$.

For convenient reference, we include the OPEs of the currents with the basic primary fields, ∂X and ψ :

$$J^a(z)\psi^{\alpha\dot{A}}(w) \sim \frac{1}{2}(\sigma^{*a})^\alpha{}_\beta \frac{\psi^{\beta\dot{A}}(w)}{z-w} \quad (\text{A.16a})$$

$$G^{\alpha A}(z)[\partial X(w)]^{\dot{B}B} \sim \epsilon^{AB} \left(\frac{\psi^{\alpha\dot{B}}(w)}{(z-w)^2} + \frac{\partial \psi^{\alpha\dot{B}}(w)}{z-w} \right) \quad (\text{A.16b})$$

$$G^{\alpha A}(z)\psi^{\beta\dot{A}}(w) \sim \epsilon^{\alpha\beta} \frac{[\partial X(w)]^{\dot{A}A}}{z-w} \quad (\text{A.16c})$$

$$T(z)[\partial X(w)]^{\dot{A}A} \sim \frac{[\partial X(w)]^{\dot{A}A}}{(z-w)^2} + \frac{[\partial^2 X(w)]^{\dot{A}A}}{z-w} \quad (\text{A.16d})$$

$$T(z)\psi^{\alpha\dot{A}}(w) \sim \frac{\frac{1}{2}\psi^{\alpha\dot{A}}(w)}{(z-w)^2} + \frac{\partial \psi^{\alpha\dot{A}}(w)}{z-w}. \quad (\text{A.16e})$$

A.6 Mode Algebra

We define the modes corresponding to the above currents according to their weight, Δ , by

$$\begin{aligned}\mathcal{O}_m &= \oint \frac{dz}{2\pi i} \mathcal{O}(z) z^{\Delta+m-1} \\ \mathcal{O}(z) &= \sum_m \mathcal{O}_m z^{-(\Delta+m)}.\end{aligned}\tag{A.17}$$

The weight may be read off from the OPE of the current with the stress–energy tensor. Fermionic currents have half-integer weight. In the NS sector, fermions are periodic in the plane and therefore we need integer powers of z . This means the fermionic currents have modes labeled by half-integer m .

Using the OPE current algebra above, one finds that the modes form an algebra:

$$[J_m^a, J_n^b] = \frac{c}{12} m \delta^{ab} \delta_{m+n,0} + i \epsilon^{ab}{}_c J_{m+n}^c \tag{A.18a}$$

$$[J_m^a, G_n^{\alpha A}] = \frac{1}{2} (\sigma^{*a})^\alpha{}_\beta G_{m+n}^{\beta A} \tag{A.18b}$$

$$\{G_m^{\alpha A}, G_n^{\beta B}\} = -\frac{c}{6} (m^2 - \frac{1}{4}) \epsilon^{AB} \epsilon^{\alpha\beta} \delta_{m+n,0} + (m-n) \epsilon^{AB} \epsilon^{\beta\gamma} (\sigma^{*a})^\alpha{}_\gamma J_{m+n}^a - \epsilon^{AB} \epsilon^{\alpha\beta} L_{m+n} \tag{A.18c}$$

$$[L_m, J_n^a] = -n J_{m+n}^a \tag{A.18d}$$

$$[L_m, G_n^{\alpha A}] = (\frac{m}{2} - n) G_{m+n}^{\alpha A} \tag{A.18e}$$

$$[L_m, L_n] = c \frac{m^3 - m}{12} \delta_{m+n,0} + (m-n) L_{m+n}. \tag{A.18f}$$

The infinite-dimensional algebra has a finite, anomaly-free subalgebra which is of primary importance for the AdS–CFT correspondence. The anomaly-free subalgebra has a basis of $\{J_0^a, G_{\pm\frac{1}{2}}^{\alpha A}, L_0, L_{\pm 1}\}$. The smaller subalgebra spanned by $\{J_0^3, L_0\}$ is the Cartan subalgebra, which means we may label states and operators by their charge m and their weight h .

For reference, we provide the mode algebra of the two canonical primary fields. The ∂X 's modes are α_n .

$$[\alpha_m^{\dot{A}A}, \alpha_n^{\dot{B}B}] = m\epsilon^{\dot{A}\dot{B}}\epsilon^{AB}\delta_{n+m,0} \quad (\text{A.19a})$$

$$\{\psi_m^{\alpha\dot{A}}, \psi_n^{\beta\dot{B}}\} = -\epsilon^{\alpha\beta}\epsilon^{\dot{A}\dot{B}}\delta_{m+n,0} \quad (\text{A.19b})$$

$$[J_m^a, \psi_n^{\alpha\dot{A}}] = \frac{1}{2}(\sigma^{*a})^\alpha{}_\beta\psi_{m+n}^{\beta\dot{A}} \quad (\text{A.19c})$$

$$[G_m^{\alpha A}, \alpha_n^{\dot{B}B}] = -n\epsilon^{AB}\psi_{m+n}^{\alpha\dot{B}} \quad (\text{A.19d})$$

$$\{G_m^{\alpha A}, \psi_n^{\beta\dot{A}}\} = \epsilon^{\alpha\beta}\alpha_{m+n}^{\dot{A}A} \quad (\text{A.19e})$$

$$[L_m, \alpha_n^{\dot{A}A}] = -n\alpha_{m+n}^{\dot{A}A} \quad (\text{A.19f})$$

$$[L_m, \psi_n^{\alpha\dot{A}}] = -(\frac{m}{2} + n)\psi_{m+n}^{\alpha\dot{A}}. \quad (\text{A.19g})$$

A.7 Useful Identities

These identities are useful for relating vectors of $SO(4)_I$ to tensors in $SU(2)_1 \times SU(2)_2$:

$$\epsilon_{\dot{A}\dot{B}}\epsilon_{AB}(\sigma^i)^{\dot{A}A}(\sigma^j)^{\dot{B}B} = -2\delta^{ij} \quad (\text{A.20a})$$

$$(\sigma^i)^{\dot{A}A}(\sigma^i)^{\dot{B}B} = -2\epsilon^{\dot{A}\dot{B}}\epsilon^{AB}. \quad (\text{A.20b})$$

It is useful to know how to relate the $(+, -, 3)$ basis for the triplet of $SU(2)$ to the $(1, 2, 3)$ basis:

$$\delta^{++} = \delta^{--} = \delta_{++} = \delta_{--} = 0 \quad (\text{A.21a})$$

$$\delta^{+-} = \delta^{-+} = 2 \quad \delta_{+-} = \delta_{-+} = \frac{1}{2} \quad (\text{A.21b})$$

$$\epsilon^{+-3} = -2i \quad (\text{A.21c})$$

$$\sigma^+ = \begin{pmatrix} 0 & 2 \\ 0 & 0 \end{pmatrix} \quad \sigma^- = \begin{pmatrix} 0 & 0 \\ 2 & 0 \end{pmatrix}. \quad (\text{A.21d})$$

One can raise and lower the '3' index with impunity.

A.8 n -twisted Sector Mode Algebra

In the n -twisted sector, by which we mean modes whose contour orbits a twist operator, we can only define the modes by summing over all n -copies of the field. This allows us to define fractional modes. The modes are defined by [152]

$$\mathcal{O}_{\frac{m}{n}} = \oint_0 \frac{dz}{2\pi i} \sum_{k=1}^n \mathcal{O}^{(k)}(z) e^{2\pi i \frac{m}{n}(k-1)} z^{\Delta + \frac{m}{n} - 1}. \quad (\text{A.22})$$

One can confirm that the integrand is 2π -periodic and therefore well-defined. If one lifts to a covering space using a map that locally behaves as

$$z = bt^n, \quad (\text{A.23})$$

then the mode in the base z -space can be related to a mode in the t -space:

$$\mathcal{O}_{\frac{m}{n}}^{(z)} = b^{\frac{m}{n}} n^{1-\Delta} \mathcal{O}_m^{(t)}, \quad (\text{A.24})$$

where Δ is the weight of the field.

To compute a correlator in the twisted sector, one may either work in the base space with the summed-over-copies modes or one may work in the covering space with the opened-up mode. If one works in the base space, then one should use the algebra with the *total* central charge

$$c_{\text{tot.}} = nc; \quad (\text{A.25})$$

the algebra is otherwise unchanged. If one works in the covering space then one uses the central charge of a single copy of the CFT, but must remember to write all of the factors that come in lifting to the cover. These two methods give identical answers.

A.9 Spectral Flow

The $\mathcal{N} = 4$ algebra is a vector space at every point z in the complex plane, spanned by the local operators $\{J^a(z), G^{\alpha A}(z), T(z)\}$. This vector space closes under the OPE. It is possible to make a z -dependent change of basis and preserve the algebra.

Making an $SU(2)_L$ transformation in the ‘3’ direction to the local operators by an angle, $\eta(z) = i\alpha \log z$, at every point z is called “spectral flow” by α units. While this may look like a nontrivial transformation, the new algebra is isomorphic to the old algebra [149].

It is important to remember that $\log z$ has a branch cut, which we put on the real axis for the following discussion. Let us suppose we start in the NS sector, where the local operators are periodic in the complex plane. Let us spectral flow the local operators by α units. Suppose we start on the (positive imaginary side of the) positive real axis, where $\eta = 0$ and the new operators are the same as the old operators. As we make a counter-clockwise circle in the complex plane, the angle between the old operators and the new operators increases. Across the branch cut on the real axis, where before the operators were continuous, now there is a large, finite $SU(2)_L$ transformation.

More illustratively, consider how the fermions behave under spectral flow, as described above:

$$\psi^{\pm\dot{A}}(z) \mapsto \psi^{\pm\dot{A}'}(z) = e^{\pm\frac{i}{2}\eta(z)} \psi^{\pm\dot{A}}(z) = z^{\mp\frac{\alpha}{2}} \psi^{\pm\dot{A}}(z). \quad (\text{A.26})$$

We see that except for even α , there is a branch cut. Moreover, if we spectral flow by an odd number of units, then the new operators $\psi'(z)$ have the opposite periodicity from $\psi(z)$. In general, one expects that an operator with charge m under $SU(2)_L$ transforms as

$$\mathcal{O}(z) \mapsto z^{-\alpha m} \mathcal{O}(z); \quad (\text{A.27})$$

however, the superconformal algebra and its $SU(2)_L$ subalgebra, in particular, is anomalous which leads to nontrivial transformations of some operators.

Since the spectral flowed algebra and the original algebra are isomorphic, there is a bijective mapping from states living in the representations of one algebra to states living in the representation of its spectral flow. Since the NS sector and the R sector are related by spectral flow, we can map problems in one sector into problems in the other.

The operator which maps states into their spectral flow images, we call \mathcal{U}_α ,

$$|\psi'\rangle = \mathcal{U}_\alpha |\psi\rangle. \quad (\text{A.28})$$

Formally, then, we may write the action of spectral flow on operators as

$$\mathcal{O}'(z) = \mathcal{U}_\alpha \mathcal{O}(z) \mathcal{U}_\alpha^{-1}, \quad (\text{A.29})$$

so that amplitudes are invariant under spectral flow. The spectral flow operator, \mathcal{U}_α may be roughly defined as an “improper gauge transformation” [149, 153, 199].

The spectral flow operator is most naturally defined in the context of bosonized fermions. We can bosonize the fermions as (conventions chosen to be consistent with [152])

$$\psi^{+1} = e^{-i\phi_6} \quad \psi^{+2} = e^{i\phi_5} \quad \psi^{-1} = e^{-i\phi_5} \quad \psi^{-2} = -e^{i\phi_6}, \quad (\text{A.30})$$

which gives the $SU(2)_L$ current in the form³⁴

$$J^3(z) = \frac{i}{2} (\partial\phi_5(z) - \partial\phi_6(z)) \quad J^+(z) = e^{-i\phi_6} e^{i\phi_5}(z) \quad J^-(z) = e^{-i\phi_5} e^{i\phi_6}(z). \quad (\text{A.31})$$

The fields ϕ_5 and ϕ_6 are the (holomorphic half of) real bosons normalized such that

$$\langle \phi_i(z) \phi_j(w) \rangle = -\delta_{ij} \log(z - w). \quad (\text{A.32})$$

They may be expanded as

$$\phi_i = q_i - \frac{i}{2} p_i \log z + (\text{modes}), \quad (\text{A.33})$$

³⁴There are implicit cocycles on the exponentials, which make unrelated fermions anticommute. Thus, the order of exponentials in expressions matters.

where q_i and p_i are the zero-mode position and momentum which satisfy

$$[q_i, p_j] = i\delta_{ij}. \quad (\text{A.34})$$

With this bosonization, the spectral flow operator can be written as [153]

$$\mathcal{U}_\alpha = e^{i\alpha(q_5 - q_6)}. \quad (\text{A.35})$$

We see that spectral flow corresponds to increasing and decreasing the zero mode momentum of the fields ϕ_5 and ϕ_6 used to bosonize the fermions. The Baker–Campbell–Hausdorff formula implies

$$e^{i\alpha q_i} e^{i\beta p_j} = e^{-i\alpha\beta\delta_{ij}} e^{i\beta p_j} e^{i\alpha q_i}, \quad (\text{A.36})$$

which one can use to confirm that this operator has the correct action on fermions.

From this perspective, one can see that any operator that is “pure exponential” in ϕ_5 and ϕ_6 transforms as in Equation (A.27). If one considers any of the chiral primaries of the $\mathcal{N} = 4$ orbifold theory, one finds that all of the chiral primaries are “pure exponential” and therefore transform using Equation (A.27).

We define the periodicity of the fermions in the complex plane via the parameter β_\pm :

$$\psi^{\pm\dot{A}}(ze^{2\pi i}) = e^{i\pi\beta_\pm} \psi^{\pm\dot{A}}(z) \quad \bar{\psi}^{\pm\dot{A}}(\bar{z}e^{2\pi i}) = e^{i\pi\bar{\beta}_\pm} \bar{\psi}^{\pm\dot{A}}(\bar{z}). \quad (\text{A.37})$$

Obviously β_\pm is only defined modulo 2 under addition. We use spectral flow to alter the fermion content of the CFT states and to go from the NS sector, $\beta_\pm = 0$, to the R sector $\beta_\pm = 1$. The effect of spectral flow by α units on the left and $\bar{\alpha}$ units on the right is

$$\beta_\pm \mapsto \beta'_\pm = \beta_\pm \pm \alpha \quad \bar{\beta}_\pm \mapsto \bar{\beta}'_\pm = \bar{\beta}_\pm \pm \bar{\alpha}. \quad (\text{A.38})$$

One finds that the the currents transform under spectral flow as follows

$$\begin{aligned} J^3(z) &\mapsto J^3(z) - \frac{c\alpha}{12z} \\ J^\pm(z) &\mapsto z^{\mp\alpha} J^\pm(z) \\ G^{\pm A}(z) &\mapsto z^{\mp\frac{\alpha}{2}} G^{\pm A}(z) \\ T(z) &\mapsto T(z) - \frac{\alpha}{z} J^3(z) + \frac{c\alpha^2}{24z^2}, \end{aligned} \quad (\text{A.39})$$

which gives rise to the transformation of the modes,

$$\begin{aligned}
J_m^3 &\mapsto J_m^3 - \frac{c\alpha}{12}\delta_{m,0} \\
J_m^\pm &\mapsto J_{m\mp\alpha}^\pm \\
G_m^{\pm A} &\mapsto G_{m\mp\frac{\alpha}{2}}^{\pm A} \\
L_m &\mapsto L_m - \alpha J_m^3 + \frac{c\alpha^2}{24}\delta_{m,0}.
\end{aligned} \tag{A.40}$$

Spectral flow also acts on states, changing the weight and charge by

$$h \mapsto h' = h + \alpha m + \frac{c\alpha^2}{24} \tag{A.41a}$$

$$m \mapsto m' = m + \frac{c\alpha}{12}, \tag{A.41b}$$

which can be read off from L_0 and J_0^3 . Frequently, one can deduce the spectral-flowed state from the weight and charge.

Note that spectral flow by α_1 units followed by spectral flow by α_2 units is equivalent to spectral flow by $\alpha_1 + \alpha_2$ units. Therefore, spectral flow forms an abelian group, and

$$\mathcal{U}_\alpha^{-1} = \mathcal{U}_{-\alpha}. \tag{A.42}$$

A.10 Ramond Sector

The CFT in the complex plane naturally has periodic fermions, which corresponds to the NS sector. One can, however, spectral flow by an odd number of units to the Ramond sector. If one starts with the NS vacuum and then spectral flows with $\alpha = -1$, then the state in the R sector has

$$h = \frac{1}{4} \quad m = \frac{1}{2}. \tag{A.43}$$

From the weight we see that this must be the R ground state. Let us call this state

$$|\emptyset\rangle_R^+. \tag{A.44}$$

Since, we are now in the Ramond ground state we have fermion zero modes, and therefore may act with J_0^- , which gives us the state

$$|\emptyset\rangle_R^- = J_0^- |\emptyset\rangle_R^+ = -\frac{1}{2}\epsilon_{AB}\psi_0^{-\dot{A}}\psi_0^{-\dot{B}} |\emptyset\rangle_R^+ = \psi_0^{-\dot{2}}\psi_0^{-\dot{1}} |\emptyset\rangle_R^+. \tag{A.45}$$

The normalization is fixed by the commutation relations of J_0^a . Since J_0^- has zero weight, one can be sure that this state is also a member of the R vacuum. Acting twice with J_0^- annihilates the state, from which one concludes that these states form a doublet of $SU(2)_L$,

$$|\emptyset\rangle_R^\alpha, \quad (\text{A.46})$$

and one also can determine that

$$|\emptyset\rangle_R^+ = J_0^+ |\emptyset\rangle_R^- = \frac{1}{2} \epsilon_{\dot{A}\dot{B}} \psi_0^{+\dot{A}} \psi_0^{+\dot{B}} |\emptyset\rangle_R^- = \psi_0^{+1} \psi_0^{+2} |\emptyset\rangle_R^-. \quad (\text{A.47})$$

What happens if we act on these states not with a pair of fermion zero modes in the current J , but with a single fermion zero mode directly? Since one cannot raise the charge of the state $|\emptyset\rangle_R^+$ or lower the charge of the state $|\emptyset\rangle_R^-$, one must have

$$\psi_0^{+\dot{A}} |\emptyset\rangle_R^+ = 0 \quad \psi_0^{-\dot{A}} |\emptyset\rangle_R^- = 0. \quad (\text{A.48})$$

This can also be seen from Equations (A.45) and (A.47). However, one ought to be able to contract the fermion zero mode index with the R vacuum doublet index to form

$$|\emptyset\rangle_R^{\dot{A}} = \frac{1}{\sqrt{2}} \epsilon_{\alpha\beta} \psi_0^{\alpha\dot{A}} |\emptyset\rangle_R^\beta, \quad (\text{A.49})$$

where the normalization is determined from the fermion mode anticommutation relations. Since there are four fermion zero modes (in the left sector), we expect four Ramond vacuum. We see that those vacua form a doublet of $SU(2)_L$ and a doublet of $SU(2)_2$.

Of course, the same story holds on the right sector of the theory as well, which gives a total of 16 Ramond vacua:

$$|\emptyset\rangle_R^{\alpha\dot{\alpha}} \quad |\emptyset\rangle_R^{\dot{A}\dot{\alpha}} \quad |\emptyset\rangle_R^{\alpha\dot{A}} \quad |\emptyset\rangle_R^{\dot{A}\dot{B}}. \quad (\text{A.50})$$

Note that we must be very careful to always write the index corresponding to the left zero modes first and the index corresponding to the right zero modes second.

What are the images of the Ramond vacua in the NS sector? From the action of spectral flow on the charge and weight of a state, one can conclude that the Ramond vacua are one unit of spectral flow from chiral primary ($h = m$) states in the NS sector; or equivalently, negative one units of spectral flow from anti-chiral primary ($h = -m$) states. Therefore, there is a one-to-one correspondence between the R vacua and the NS chiral primary states. There are four left chiral primary states in the NS sector,

$$|\emptyset\rangle_{NS} \quad \psi_{-\frac{1}{2}}^{+\dot{A}} |\emptyset\rangle_{NS} \quad \epsilon_{\dot{A}\dot{B}} \psi_{-\frac{1}{2}}^{+\dot{A}} \psi_{-\frac{1}{2}}^{+\dot{B}} |\emptyset\rangle_{NS}, \quad (\text{A.51})$$

and there are also four states in the right sector. Thus a total of 16 chiral primary states in the NS sector that get mapped onto the 16 Ramond vacua via spectral flow. These are all of the chiral primary states for a single strand of the CFT. In the twisted sector, there are more chiral primary states which correspond to Ramond “vacua” in the twisted sector.

Appendix B

CARTESIAN TO SPHERICAL CLEBSCH–GORDAN COEFFICIENTS

In this section, we outline our conventions for relating irreducible spherical tensors to ordinary Cartesian tensors in flat space. This fixes the factors in going from Equation (3.52) to Equation (3.63) for the D1D5 case, and explains how we define the correctly normalized differential operator, so that Equation (3.39) is satisfied.

Our goal is to show how to construct the coefficients, $Y_{l,m_\psi,m_\phi}^{j_1\dots j_l}$, that define the differential operator in Equation (3.38) such that it satisfies Equation (3.39),

$$Y_{l,m_\psi,m_\phi}^{k_1 k_2 \dots k_l} \partial_{k_1} \partial_{k_2} \dots \partial_{k_l} [r^l Y_{l',m'_\psi,m'_\phi}(\Omega_3)] = \delta_{ll'} \delta_{m_\psi m'_\psi} \delta_{m_\phi m'_\phi}.$$

We take the spherical harmonics as a starting point. The Cartesian coordinates for the noncompact space are related to the angular coordinates via

$$\begin{aligned} x^1 &= r \cos \theta \cos \psi \\ x^2 &= r \cos \theta \sin \psi \\ x^3 &= r \sin \theta \cos \phi \\ x^4 &= r \sin \theta \sin \phi, \end{aligned} \tag{B.1}$$

where the (θ, ψ, ϕ) are restricted to

$$\theta \in [0, \frac{\pi}{2}) \quad \psi, \phi \in [0, 2\pi). \tag{B.2}$$

Spherical harmonics can be written as a homogeneous polynomial of the Cartesian unit vector components of the form

$$Y_{l,m_\psi,m_\phi}(\Omega_3) = \frac{1}{r^l} \mathcal{Y}_{j_1\dots j_l}^{l,m_\psi,m_\phi} x^{j_1} \dots x^{j_l} = \mathcal{Y}_{j_1\dots j_l}^{l,m_\psi,m_\phi} n^{j_1} \dots n^{j_l}. \tag{B.3}$$

The \mathcal{Y} must be pairwise symmetric and traceless. One can compute these tensors by the usual methods of breaking up a tensor into irreducible components, or by inspection of

the explicit form of the spherical harmonics in angular components.

Given the spherical harmonic normalization

$$\int Y_{l,m_\psi,m_\phi}^* Y_{l',m'_\psi,m'_\phi} d\Omega = \delta_{ll'} \delta_{m_\psi m'_\psi} \delta_{m_\phi m'_\phi}, \quad (\text{B.4})$$

one can determine an orthogonality relation for the \mathcal{Y} 's:

$$(\mathcal{Y}_{j_1 \dots j_l}^{l,m_\psi,m_\phi})^* \mathcal{Y}_{k_1 \dots k_{l'}}^{l',m'_\psi,m'_\phi} \int (n^{j_1} \dots n^{j_l})(n^{k_1} \dots n^{k_{l'}}) d\Omega = \delta_{ll'} \delta_{m_\psi m'_\psi} \delta_{m_\phi m'_\phi}. \quad (\text{B.5})$$

The integral over $l + l'$ unit vectors defines a natural inner product on the Clebsch–Gordan coefficients \mathcal{Y} .

We label the integral

$$I^{j_1 \dots j_l k_1 \dots k_{l'}}, \quad (\text{B.6})$$

and note that I must be symmetric in all of its indices. Furthermore, from the symmetry of the integral one must conclude that I vanishes unless every index appears an even number of times. For instance,

$$I^j = \int n^j d\Omega = 0. \quad (\text{B.7})$$

As a corollary, I vanishes unless it has an even number of indices. Having picked off the easiest properties, let's without further comment give the general form. Let a_i be the total number of times the index i appears in the collection of indices on I , then

$$\begin{aligned} I^{[a_1, a_2, a_3, a_4]} &= \int (n^1)^{a_1} (n^2)^{a_2} (n^3)^{a_3} (n^4)^{a_4} d\Omega_3 \\ &= \left[\int_0^{\frac{\pi}{2}} \cos^{a_1+a_2+1} \theta \sin^{a_3+a_4+1} \theta d\theta \right] \left[\int_0^{2\pi} \cos^{a_1} \psi \sin^{a_2} \psi d\psi \right] \left[\int_0^{2\pi} \cos^{a_3} \phi \sin^{a_4} \phi d\phi \right]. \end{aligned} \quad (\text{B.8})$$

We recognize the above definite integrals as different representations of the beta function:

$$\int_0^{\frac{\pi}{2}} \cos^\alpha \theta \sin^\beta \theta d\theta = \frac{1}{2} B\left(\frac{\alpha+1}{2}, \frac{\beta+1}{2}\right) \quad (\text{B.9a})$$

$$\int_0^{2\pi} \cos^\alpha \theta \sin^\beta \theta d\theta = \frac{1}{2} [1 + (-1)^\alpha + (-1)^{\alpha+\beta} + (-1)^\beta] B\left(\frac{\alpha+1}{2}, \frac{\beta+1}{2}\right), \quad (\text{B.9b})$$

where the second equation follows from the first. Therefore, one sees that *provided all the a_i are even*

$$\begin{aligned} I^{[a_1, a_2, a_3, a_4]} &= 2B\left(\frac{a_1+a_2+2}{2}, \frac{a_3+a_4+2}{2}\right) B\left(\frac{a_1+1}{2}, \frac{a_2+1}{2}\right) B\left(\frac{a_3+1}{2}, \frac{a_4+1}{2}\right) \\ &= 2\pi^2 \left(\frac{1}{\pi^2} \frac{\Gamma\left(\frac{a_1+1}{2}\right) \Gamma\left(\frac{a_2+1}{2}\right) \Gamma\left(\frac{a_3+1}{2}\right) \Gamma\left(\frac{a_4+1}{2}\right)}{\Gamma\left(\frac{a_1+a_2+a_3+a_4+4}{2}\right)} \right) \end{aligned}$$

$$= \frac{2\pi^2(a_1-1)!(a_2-1)!(a_3-1)!(a_4-1)!}{2^{a_1+a_2+a_3+a_4-4}\left(\frac{a_1}{2}-1\right)!\left(\frac{a_2}{2}-1\right)!\left(\frac{a_3}{2}-1\right)!\left(\frac{a_4}{2}-1\right)!\left(\frac{a_1+a_2+a_3+a_4}{2}+1\right)!} \quad (\text{B.10})$$

Note that in the last line one must use the limit

$$\lim_{x \rightarrow 0} \frac{(x-1)!}{\left(\frac{x}{2}-1\right)!} = \frac{1}{2}, \quad (\text{B.11})$$

in the event that some of the a_i are zero.

The orthogonality condition from Equation (B.5) is

$$I^{j_1 \dots j_l k_1 \dots k_l} (\mathcal{Y}_{j_1 \dots j_l}^{l, m_\psi, m_\phi})^* \mathcal{Y}_{k_1 \dots k_l}^{l', m'_\psi, m'_\phi} = \delta_{ll'} \delta_{m_\psi m'_\psi} \delta_{m_\phi m'_\phi}, \quad (\text{B.12})$$

which motivates the choice of

$$Y_{l, m_\psi, m_\phi}^{j_1 \dots j_l} \propto I^{j_1 \dots j_l k_1 \dots k_l} (\mathcal{Y}_{k_1 \dots k_l}^{l, m_\psi, m_\phi})^*. \quad (\text{B.13})$$

We can think of the $2l$ -index I as defining an inner product on the space of symmetric traceless l -index tensors, spanned by the $\mathcal{Y}_{j_1 \dots j_l}^{l, m_\psi, m_\phi}$. Then, we can think of Y_{l, m_ψ, m_ϕ} as (proportional to) the dual of $\mathcal{Y}_{j_1 \dots j_l}^{l, m_\psi, m_\phi}$.

Since the l derivatives are symmetrized and the spherical harmonic's Cartesian form is also symmetrized, we get a factor of $l!$. One finds that

$$I^{j_1 \dots j_l k_1 \dots k_l} (\mathcal{Y}_{k_1 \dots k_l}^{l, m_\psi, m_\phi})^* \partial_{j_1} \dots \partial_{j_l} r^l Y_{l, m_\psi, m_\phi}(\theta, \psi, \phi) \Big|_{r \rightarrow 0} = l! \quad (\text{B.14})$$

and therefore we define

$$Y_{l, m_\psi, m_\phi}^{j_1 \dots j_l} = \frac{1}{l!} I^{j_1 \dots j_l k_1 \dots k_l} (\mathcal{Y}_{k_1 \dots k_l}^{l, m_\psi, m_\phi})^*. \quad (\text{B.15})$$

The first few normalized spherical harmonics are given by

$$\sqrt{2\pi}Y_{0,0,0} = 1 \quad (\text{B.16a})$$

$$\sqrt{2\pi}Y_{1,1,0} = \sqrt{2}\frac{x^1 + ix^2}{r} = \sqrt{2}\cos\theta e^{i\psi} \quad (\text{B.16b})$$

$$\sqrt{2\pi}Y_{1,0,1} = \sqrt{2}\frac{x^3 + ix^4}{r} = \sqrt{2}\sin\theta e^{i\phi} \quad (\text{B.16c})$$

$$\sqrt{2\pi}Y_{2,2,0} = \sqrt{3}\left(\frac{x^1 + ix^2}{r}\right)^2 = \sqrt{3}\cos^2\theta e^{i\psi} \quad (\text{B.16d})$$

$$\sqrt{2\pi}Y_{2,0,2} = \sqrt{3}\left(\frac{x^3 + ix^4}{r}\right)^2 = \sqrt{3}\sin^2\theta e^{2i\phi} \quad (\text{B.16e})$$

$$\sqrt{2\pi}Y_{2,1,1} = \sqrt{6}\frac{(x^1 + ix^2)(x^3 + ix^4)}{r^2} = \sqrt{6}\sin\theta\cos\theta e^{i\psi+i\phi} \quad (\text{B.16f})$$

$$\sqrt{2\pi}Y_{2,1,-1} = \sqrt{6}\frac{(x^1 + ix^2)(x^3 - ix^4)}{r^2} = \sqrt{6}\sin\theta\cos\theta e^{i\psi-i\phi} \quad (\text{B.16g})$$

$$\sqrt{2\pi}Y_{2,0,0} = \sqrt{3}\frac{(x^1 + ix^2)(x^1 - ix^2) - (x^3 + ix^4)(x^3 - ix^4)}{r^2} = \sqrt{3}(\cos^2\theta - \sin^2\theta) \quad (\text{B.16h})$$

Since

$$Y_{l,m_\psi,m_\phi}^* = Y_{l,-m_\psi,-m_\phi}, \quad (\text{B.17})$$

one can find the rest of the $l = 0, 1, 2$ spherical harmonics by complex conjugation. The first few Clebsch–Gordan coefficients are given by

$$\sqrt{2\pi}\mathcal{Y}^{0,0,0} = 1 \quad (\text{B.18a})$$

$$\sqrt{2\pi}\mathcal{Y}_j^{1,1,0} = \sqrt{2}(\delta_j^1 + i\delta_j^2) \quad (\text{B.18b})$$

$$\sqrt{2\pi}\mathcal{Y}_j^{1,0,1} = \sqrt{2}(\delta_j^3 + i\delta_j^4) \quad (\text{B.18c})$$

$$\sqrt{2\pi}\mathcal{Y}_{ij}^{2,2,0} = \sqrt{3}[\delta_i^1\delta_j^1 - \delta_i^2\delta_j^2 + 2i\delta_i^1\delta_j^2] \quad (\text{B.18d})$$

$$\sqrt{2\pi}\mathcal{Y}_{ij}^{2,0,2} = \sqrt{3}[\delta_i^3\delta_j^3 - \delta_i^4\delta_j^4 + 2i\delta_i^3\delta_j^4] \quad (\text{B.18e})$$

$$\sqrt{2\pi}\mathcal{Y}_{ij}^{2,1,1} = \sqrt{6}[\delta_i^1\delta_j^3 - \delta_i^2\delta_j^4 + i\delta_i^1\delta_j^4 + i\delta_i^2\delta_j^3] \quad (\text{B.18f})$$

$$\sqrt{2\pi}\mathcal{Y}_{ij}^{2,1,-1} = \sqrt{6}[\delta_i^1\delta_j^3 + \delta_i^2\delta_j^4 - i\delta_i^1\delta_j^4 + i\delta_i^2\delta_j^3] \quad (\text{B.18g})$$

$$\sqrt{2\pi}\mathcal{Y}_{ij}^{2,0,0} = \sqrt{3}[\delta_i^1\delta_j^1 + \delta_i^2\delta_j^2 - \delta_i^3\delta_j^3 - \delta_i^4\delta_j^4]. \quad (\text{B.18h})$$

For compactness, we have neglected to symmetrize the indices above. Finally, we should list the first few I 's. The zero-index I is

$$I_{(0)} = 2\pi^2; \quad (\text{B.19a})$$

the 2-index I can be written as a matrix,

$$I_{(2)}^{ij} = \frac{\pi^2}{2} \begin{pmatrix} 1 & & & \\ & 1 & & \\ & & 1 & \\ & & & 1 \end{pmatrix}^{ij}. \quad (\text{B.19b})$$

The following two components of the 4-index I suffice to deduce the rest of the components from symmetry:

$$I_{(4)}^{1111} = \frac{\pi^2}{4} \quad I_{(4)}^{1122} = \frac{\pi^2}{12}. \quad (\text{B.19c})$$

Finally, we write down the $l = 0$ and $l = 1$ coefficients for the derivative operators:

$$Y_{0,0,0} = \sqrt{2}\pi \quad (\text{B.20a})$$

$$Y_{1,1,0}^j = \frac{\pi}{2}(\delta_j^1 + i\delta_j^2) \quad (\text{B.20b})$$

$$Y_{1,0,1}^j = \frac{\pi}{2}(\delta_j^3 + i\delta_j^4), \quad (\text{B.20c})$$

and the $l = 2$ coefficients

$$Y_{2,2,0}^{ij} = \frac{1}{2!} \frac{\sqrt{3}}{\sqrt{2}\pi} (I^{ij11} - I^{ij22} - 2iI^{ij12})$$

$$= \frac{1}{\sqrt{6}} \frac{\pi}{4} \begin{pmatrix} 1 & -i \\ -i & -1 \end{pmatrix}^{ij} \quad (\text{B.20d})$$

$$Y_{2,0,2}^{ij} = \frac{1}{\sqrt{6}} \frac{\pi}{4} \begin{pmatrix} & & \\ & 1 & -i \\ -i & -1 & \end{pmatrix}^{ij} \quad (\text{B.20e})$$

$$Y_{2,1,1}^{ij} = \frac{\pi}{8\sqrt{3}} \begin{pmatrix} & & 1 & -i \\ & & -i & -1 \\ 1 & -i & & \\ -i & -1 & & \end{pmatrix}^{ij} \quad (\text{B.20f})$$

$$Y_{2,1,-1}^{ij} = \frac{\pi}{8\sqrt{3}} \begin{pmatrix} & & 1 & -i \\ & & i & 1 \\ 1 & i & & \\ -i & 1 & & \end{pmatrix}^{ij} \quad (\text{B.20g})$$

$$Y_{2,0,0}^{ij} = \frac{\pi}{8} \sqrt{\frac{3}{2}} \begin{pmatrix} 1 & & & \\ & 1 & & \\ & & -1 & \\ & & & -1 \end{pmatrix}^{ij} \quad (\text{B.20h})$$

Again, the remaining coefficients can be found by complex conjugation. Clearly, it is not too difficult to find higher l coefficients as needed.

Appendix C

NORMALIZING THE CFT STATE AND THE VERTEX OPERATOR

Here we present the normalization calculation for the $\kappa = 1$ initial state of Chapter 4, along with that of the vertex operator for emission of ϕ_{ij} .

C.1 Normalizing the Initial State

To find the normalization constant \mathcal{C}_L , we take the Hermitian conjugate to find

$${}^L_{A\dot{A}}\langle\phi_{N+1}^{\frac{l}{2},\frac{l}{2}-k}| = -\mathcal{C}_L^* {}_{NS}\langle\emptyset|\tilde{\sigma}_{l+1}\epsilon_{\dot{A}\dot{B}}\psi_{\frac{1}{2}}^{-\dot{B}}\epsilon_{AB}G_{\frac{1}{2}}^{+B}(J_0^+)^k L_1^N, \quad (\text{C.1})$$

and then compute the norm,

$$\begin{aligned} & {}^L_{A\dot{A}}\langle\phi_{N+1}^{\frac{l}{2},\frac{l}{2}-k}|\phi_{N+1}^{\frac{l}{2},\frac{l}{2}-k}\rangle_L^{B\dot{B}} \\ &= -|\mathcal{C}_L|^2 \epsilon_{\dot{A}\dot{C}}\epsilon_{AC} {}_{NS}\langle\emptyset|\tilde{\sigma}_{l+1}^0\psi_{\frac{1}{2}}^{-\dot{C}}G_{\frac{1}{2}}^{+C}(J_0^+)^k L_1^N L_{-1}^N (J_0^-)^k G_{-\frac{1}{2}}^{-B}\psi_{-\frac{1}{2}}^{+\dot{B}}\sigma_{l+1}^0|\emptyset\rangle_{NS} \\ &= -|\mathcal{C}_L|^2 \epsilon_{\dot{A}\dot{C}}\epsilon_{AC} {}_{NS}\langle\emptyset|\tilde{\sigma}_{l+1}^0\psi_{\frac{1}{2}}^{-\dot{C}}G_{\frac{1}{2}}^{+C}(J_0^+)^k \left(\prod_{j=1}^N j(2L_0 + j - 1)\right) (J_0^-)^k G_{-\frac{1}{2}}^{-B}\psi_{-\frac{1}{2}}^{+\dot{B}}\sigma_{l+1}^0|\emptyset\rangle_{NS} \\ &= -\frac{N!(N+l+1)!}{(l+1)!} |\mathcal{C}_L|^2 \epsilon_{\dot{A}\dot{C}}\epsilon_{AC} {}_{NS}\langle\emptyset|\tilde{\sigma}_{l+1}^0\psi_{\frac{1}{2}}^{-\dot{C}}G_{\frac{1}{2}}^{+C}(J_0^+)^k (J_0^-)^k G_{-\frac{1}{2}}^{-B}\psi_{-\frac{1}{2}}^{+\dot{B}}\sigma_{l+1}^0|\emptyset\rangle_{NS} \\ &= -\frac{k!l!}{(l-k)!} \frac{N!(N+l+1)!}{(l+1)!} |\mathcal{C}_L|^2 \epsilon_{\dot{A}\dot{C}}\epsilon_{AC} {}_{NS}\langle\emptyset|\tilde{\sigma}_{l+1}^0\psi_{\frac{1}{2}}^{-\dot{C}}G_{\frac{1}{2}}^{+C}G_{-\frac{1}{2}}^{-B}\psi_{-\frac{1}{2}}^{+\dot{B}}\sigma_{l+1}^0|\emptyset\rangle_{NS} \\ &= -\delta_A^B \frac{k!l!}{(l-k)!} \frac{N!(N+l+1)!}{(l+1)!} |\mathcal{C}_L|^2 \epsilon_{\dot{A}\dot{C}} {}_{NS}\langle\emptyset|\tilde{\sigma}_{l+1}^0\psi_{\frac{1}{2}}^{-\dot{C}}(L_0 + J_0^3)\psi_{-\frac{1}{2}}^{+\dot{B}}\sigma_{l+1}^0|\emptyset\rangle_{NS}. \quad (\text{C.2}) \end{aligned}$$

Proceeding with the calculation, one finds

$$\begin{aligned} & {}^L_{A\dot{A}}\langle\phi_{N+1}^{\frac{l}{2},\frac{l}{2}-k}|\phi_{N+1}^{\frac{l}{2},\frac{l}{2}-k}\rangle_L^{B\dot{B}} = -(l+1)\delta_A^B \epsilon_{\dot{A}\dot{C}} \frac{k!l!}{(l-k)!} \frac{N!(N+l+1)!}{(l+1)!} |\mathcal{C}_L|^2 {}_{NS}\langle\emptyset|\tilde{\sigma}_{l+1}^0\psi_{\frac{1}{2}}^{-\dot{C}}\psi_{-\frac{1}{2}}^{+\dot{B}}\sigma_{l+1}^0|\emptyset\rangle_{NS} \\ &= -\delta_A^B \frac{N!(N+l+1)!k!}{(l-k)!} |\mathcal{C}_L|^2 \epsilon_{\dot{A}\dot{C}} {}_{NS}\langle\emptyset|\tilde{\sigma}_{l+1}^0\psi_{\frac{1}{2}}^{-\dot{C}}\psi_{-\frac{1}{2}}^{+\dot{B}}\sigma_{l+1}^0|\emptyset\rangle_{NS} \end{aligned}$$

$$= \delta_A^B \delta_{\dot{A}}^{\dot{B}} \frac{N!(N+l+1)!k!}{(l-k)!} (l+1) |\mathcal{C}_L|^2, \quad (\text{C.3})$$

where we have used the fact that the chiral primary twist operators are correctly normalized. The factor of $l+1$ comes from the fermion anticommutator, since in the twisted sector there are $l+1$ copies of the fermion field that go into what we call ψ . One can understand this factor most easily by using Equation (A.24). By demanding that

$${}_{A\dot{A}}^L \langle \phi_{N+1}^{\frac{l}{2}, \frac{l}{2}-k} | \phi_{N+1}^{\frac{l}{2}, \frac{l}{2}-k} \rangle_L^{B\dot{B}} = \delta_A^B \delta_{\dot{A}}^{\dot{B}}, \quad (\text{C.4})$$

we conclude that the normalized state (with the left *and* right parts) is

$$|\phi\rangle^{A\dot{A}B\dot{B}} = \sqrt{\frac{(l-k)!(l-\bar{k})!}{N!\bar{N}!(N+l+1)!(\bar{N}+l+1)!k!\bar{k}!(l+1)^2}} \\ \times L_{-1}^N (J_0^-)^k G_{-\frac{1}{2}}^{-A} \psi_{-\frac{1}{2}}^{+\dot{A}} \bar{L}_{-1}^{\bar{N}} (\bar{J}_0^-)^{\bar{k}} \bar{G}_{-\frac{1}{2}}^{-\dot{B}} \bar{\psi}_{-\frac{1}{2}}^{+\dot{B}} \sigma_{l+1}^0 |\emptyset\rangle_{NS}. \quad (\text{C.5})$$

In this computation we use the identity

$$\prod_{j=1}^k (jl - j(j-1)) = \frac{k! l!}{(l-k)!}. \quad (\text{C.6})$$

C.2 Normalizing the Vertex Operator

The left part of the vertex operator is given by

$$\mathcal{V}_{L;l,k}^{A\dot{A}}(z) = N_L \left((J_0^+)^k G_{-\frac{1}{2}}^{+A} \psi_{-\frac{1}{2}}^{-\dot{A}} \tilde{\sigma}_{l+1}^0(z) \right)_z. \quad (\text{C.7})$$

We need to normalize the vertex operator. To that end, we begin by writing its Hermitian conjugate:

$$\mathcal{V}_{L;l,k}^{A\dot{A}}{}^\dagger(z) = -(-1)^{k+1} \epsilon_{AB} \epsilon_{\dot{A}\dot{B}} N_L^* \left((J_0^-)^k G_{-\frac{1}{2}}^{-B} \psi_{-\frac{1}{2}}^{+\dot{B}} \sigma_{l+1}^0(z) \right)_z = \epsilon_{AB} \epsilon_{\dot{A}\dot{B}} \mathcal{V}_{l,2l-k}^{B\dot{B}}(z), \quad (\text{C.8})$$

where the second equality is the condition needed to ensure the total interaction action is Hermitian.

The factor of $(-1)^{k+1}$ comes from the G and the J_0 's. We illustrate below with J_0^+ :

$$\begin{aligned} [(J_0^+)_z]^\dagger &= \left[\oint_z \frac{dz'}{2\pi i} J^+(z') \right]^\dagger \\ &= - \oint_{\bar{z}} \frac{d\bar{z}'}{2\pi i} J^-\left(\frac{1}{\bar{z}'}\right) \frac{1}{\bar{z}'^2} \\ &= - \oint_{\frac{1}{\bar{z}}} \frac{d\xi}{2\pi i} J^-(\xi) \end{aligned}$$

$$= -(J_0^-)_{\frac{1}{\bar{z}}}, \quad (\text{C.9})$$

where when making the change of variables $\xi = 1/\bar{z}'$ there are two minus signs. One comes from the Jacobian $d\bar{z}' = -1/\xi^2 d\xi$, and the other comes from making the contour counter-clockwise. The $G_{-\frac{1}{2}}$ behaves in the same way; however, the $\psi_{-\frac{1}{2}}$ is different:

$$\begin{aligned} \left[(\psi_{-\frac{1}{2}}^{-\dot{A}})_z \right]^\dagger &= \left[\oint_z \frac{dz'}{2\pi i} \frac{\psi^{-\dot{A}}(z')}{z' - z} \right]^\dagger \\ &= -(-\epsilon_{-+} \epsilon_{\dot{A}\dot{B}}) \oint_{\bar{z}} \frac{d\bar{z}'}{2\pi i} \psi^{+\dot{B}}(\frac{1}{\bar{z}'}) \frac{1}{\bar{z}'(\bar{z}' - \bar{z})} \\ &= -\epsilon_{\dot{A}\dot{B}} \oint_{\frac{1}{\bar{z}}} \frac{d\xi}{2\pi i} \psi^{+\dot{B}}(\xi) \frac{1}{\xi \left(\frac{1}{\xi} - \bar{z} \right)} \\ &= \frac{\epsilon_{\dot{A}\dot{B}}}{\bar{z}} \oint_{\frac{1}{\bar{z}}} \frac{d\xi}{2\pi i} \frac{\psi^{+\dot{B}}(\xi)}{\xi - \frac{1}{\bar{z}}} \\ &= \frac{\epsilon_{\dot{A}\dot{B}}}{\bar{z}} (\psi_{-\frac{1}{2}}^{+\dot{B}})_{\frac{1}{\bar{z}}}; \end{aligned} \quad (\text{C.10})$$

it receives an extra minus sign from the integrand.

We use the notation

$$\langle \cdot \rangle = {}_{NS} \langle \emptyset | \cdot | \emptyset \rangle_{NS} \quad (\text{C.11})$$

for the NS-vacuum expectation value. Proceeding with the normalization, the 2-point function is given by

$$\begin{aligned} \left\langle \mathcal{V}_{L;l,k}^{A\dot{A}}{}^\dagger(z) \mathcal{V}_{L;l,k}^{B\dot{B}}(0) \right\rangle &= (-1)^{k+2} |N_L|^2 \epsilon_{AC} \epsilon_{\dot{A}\dot{C}} \left\langle \left((J_0^-)^k G_{-\frac{1}{2}}^{-C} \psi_{-\frac{1}{2}}^{+\dot{C}} \sigma_{l+1}^0(z) \right)_z \left((J_0^+)^k G_{-\frac{1}{2}}^{+B} \psi_{-\frac{1}{2}}^{-\dot{B}} \tilde{\sigma}_{l+1}^0(0) \right)_0 \right\rangle \\ &= -|N_L|^2 \epsilon_{AC} \epsilon_{\dot{A}\dot{C}} \left\langle \left(\psi_{-\frac{1}{2}}^{+\dot{C}} \sigma_{l+1}^0(z) \right)_z \left(G_{-\frac{1}{2}}^{-C} (J_0^-)^k (J_0^+)^k G_{-\frac{1}{2}}^{+B} \psi_{-\frac{1}{2}}^{-\dot{B}} \tilde{\sigma}_{l+1}^0(0) \right)_0 \right\rangle \\ &= -|N_L|^2 \epsilon_{AC} \epsilon_{\dot{A}\dot{C}} \frac{k! l!}{(l-k)!} \left\langle \left(\psi_{-\frac{1}{2}}^{+\dot{C}} \sigma_{l+1}^0(z) \right)_z \left(G_{-\frac{1}{2}}^{-C} G_{-\frac{1}{2}}^{+B} \psi_{-\frac{1}{2}}^{-\dot{B}} \tilde{\sigma}_{l+1}^0(0) \right)_0 \right\rangle \\ &= |N_L|^2 \delta_A^B \epsilon_{\dot{A}\dot{C}} \frac{k! l!}{(l-k)!} \left\langle \left(\psi_{-\frac{1}{2}}^{+\dot{C}} \sigma_{l+1}^0(z) \right)_z \left(L_{-1} \psi_{-\frac{1}{2}}^{-\dot{B}} \tilde{\sigma}_{l+1}^0(0) \right)_0 \right\rangle \\ &= |N_L|^2 \delta_A^B \epsilon_{\dot{A}\dot{C}} \frac{k! l!}{(l-k)!} \lim_{v \rightarrow 0} \partial_v \left\langle \left(\psi_{-\frac{1}{2}}^{+\dot{C}} \sigma_{l+1}^0(z) \right)_z \left(\psi_{-\frac{1}{2}}^{-\dot{B}} \tilde{\sigma}_{l+1}^0(v) \right)_v \right\rangle \\ &= |N_L|^2 \delta_A^B \epsilon_{\dot{A}\dot{C}} \epsilon^{\dot{C}\dot{B}} \frac{k! l!}{(l-k)!} \lim_{v \rightarrow 0} \partial_v \frac{l+1}{(z-v)^{l+1}} \\ &= |N_L|^2 \delta_A^B \delta_{\dot{A}}^{\dot{B}} \frac{k! (l+1)!}{(l-k)!} (l+1) \frac{1}{z^{l+2}}. \end{aligned} \quad (\text{C.12})$$

The factor of $l+1$ has the same origin as in the normalization of the initial state. Using the above, one finds

$$N_L = \sqrt{\frac{(l-k)!}{k! (l+1)! (l+1)}}, \quad (\text{C.13})$$

and thus the left part of the vertex operator is

$$\mathcal{V}_{L;l,k}^{AA}(z) = \sqrt{\frac{(l-k)!}{k!(l+1)!(l+1)}} \left((J_0^+)^k G_{-\frac{1}{2}}^{+A} \psi_{-\frac{1}{2}}^{-\dot{A}} \tilde{\sigma}_{l+1}^0(z) \right)_z. \quad (\text{C.14})$$

The normalization is chosen such that the vertex operator in the complex plane satisfies

$$\begin{aligned} \langle \mathcal{V}_{l,-m_\psi,-m_\phi}^{A\dot{A}B\dot{B}}(z) \mathcal{V}_{l,m_\psi,m_\phi}^{C\dot{C}D\dot{D}}(0) \rangle &= \frac{\epsilon^{AC} \epsilon^{\dot{A}\dot{C}} \epsilon^{BD} \epsilon^{\dot{B}\dot{D}}}{|z|^{l+2}} \\ \langle \mathcal{V}_{l,-m_\psi,-m_\phi}^{ij}(z) \mathcal{V}_{l,m_\psi,m_\phi}^{kl}(0) \rangle &= \frac{\delta^{ik} \delta^{jl}}{|z|^{l+2}}. \end{aligned} \quad (\text{C.15})$$

Appendix D

COMPUTING CORRELATION FUNCTIONS OF $S_{N_1 N_5}$ -TWIST OPERATORS

We use the methods developed in [151, 152] to compute correlation functions of $S_{N_1 N_5}$ -twist operators. We call the physical space where the problem is posed the “base space” which has the coordinates complex z and \bar{z} . In the base space, the basic fields are multi-valued. The basic method for computing the correlators of twist operators consists of using a meromorphic mapping to a covering space where there is one set of single-valued fields. Having single-valued fields comes at the expense of introducing curvature in the covering space. Fortunately, we can conformally map the curved covering space to a manifold with metric in a fiducial (flat) form. Because of the conformal curvature anomaly, the path integral is not invariant under conformal mappings; however, the path integral changes in a calculable way. Note that we do not compute the combinatorial factors that result from properly symmetrizing over the copies of the orbifold theory.

D.1 Basic Method

Suppose we compute the path integral of our conformal field theory on the manifold with fiducial metric \hat{ds}^2 , which we call \hat{Z} . The path integral of the same conformal field theory on a manifold with metric $ds^2 = e^\phi \hat{ds}^2$ which we call Z , is related to \hat{Z} by [209]

$$Z = e^{S_L} \hat{Z}, \tag{D.1}$$

where the Liouville action, S_L , is given by

$$S_L = \frac{c}{96\pi} \int d^2t \sqrt{-\hat{g}} \left[\hat{g}^{\mu\nu} \partial_\mu \phi \partial_\nu \phi + 2\hat{R}\phi \right]. \tag{D.2}$$

\hat{g} is the fiducial metric, \hat{R} is the Ricci scalar of the *fiducial* metric, and c is the central charge of a *single* copy of the fields ($c = 6$ in our case).

We now outline the precise steps needed to compute correlators of twist operators, as given in [151]. The problem is posed in terms of some twist operators inserted at various points z_i in the base space. To make the fields well-defined, we cut a small hole of radius ε_i around each z_i and demand that the fields have the correct twisted boundary conditions around that hole. Furthermore, we regulate the path integral by putting the correlator on a disc of radius $1/\delta$, which encloses all of the z_i except twist operators that are inserted at infinity. To define the boundary conditions on the edge of the disc, we glue a second flat disc onto the edge of the first, giving the base space the topology of a sphere. We insert any twist operators located at infinity at the center of this second disc. We work on the base space with metric

$$ds^2 = \begin{cases} dz d\bar{z}, & |z| < \frac{1}{\delta} \\ d\tilde{z} d\bar{\tilde{z}}, & |\tilde{z}| < \frac{1}{\delta} \end{cases}, \quad \tilde{z} = \frac{1}{\delta^2} \frac{1}{z}. \quad (\text{D.3})$$

The path integral with the various regularizations on the above metric we write as

$$Z_{\varepsilon, \delta}^{(s)}[\sigma_{n_1}(z_1) \cdots \sigma_{n_N}(z_N)]. \quad (\text{D.4})$$

We can map to a covering space with metric ds'^2 with coordinates t and \bar{t} via a meromorphic function $z = z(t)$. Then, the path integral is given by

$$Z_{\varepsilon, \delta}^{(s)}[\sigma_{n_1}(z_1) \cdots \sigma_{n_N}(z_N)] = Z_{\varepsilon, \delta}^{(s')}, \quad (\text{D.5})$$

where

$$ds^2 = dz d\bar{z} \implies ds'^2 = \frac{dz}{dt} \frac{d\bar{z}}{d\bar{t}} dt d\bar{t}. \quad (\text{D.6})$$

When we write $Z^{(s')}$ with no square brackets we mean that there are no insertions in the path integral. Throughout this discussion, we assume that we are computing the correlator of bare twists which leave no insertions in the covering space. If this is not the case as in Chapter 4, then the right hand side of Equation (D.5) is multiplied by the separately computed correlator of those insertions in the covering space [151, 152].

The sizes of the various holes in the t coordinates are determined by the mapping. The boundary conditions at the edges of the holes are defined by pasting in flat pieces of manifold in the covering space.³⁵

³⁵If the twist operators are not bare twists, then there would also be some operator insertions in the covering space; however, here we just discuss bare twists.

The induced metric on the covering space, ds'^2 , is conformally related to the fiducial metric we choose to work with

$$\widehat{ds}^2 = \begin{cases} dt d\tilde{t}, & |t| < \frac{1}{\delta'} \\ d\tilde{t} d\tilde{\tilde{t}}, & |\tilde{t}| < \frac{1}{\delta'} \end{cases}, \quad \tilde{t} = \frac{1}{\delta'^2} \frac{1}{t}. \quad (\text{D.7})$$

Thus, we can write

$$Z_{\varepsilon, \delta}^{(s)}[\sigma_{n_1}(z_1) \cdots \sigma_{n_N}(z_N)] = e^{S_L} Z_{\varepsilon, \delta, \delta'}^{(\hat{s})}. \quad (\text{D.8})$$

The correlator of the regularized twist operators is defined by

$$\langle \sigma_{n_1}(z_1) \cdots \sigma_{n_N}(z_N) \rangle_{\varepsilon, \delta} = \frac{Z_{\varepsilon, \delta}^{(s)}[\sigma_{n_1}(z_1) \cdots \sigma_{n_N}(z_N)]}{(Z_\delta)^s} = e^{S_L} \frac{Z_{\varepsilon, \delta, \delta'}^{(\hat{s})}}{(Z_\delta)^s}, \quad (\text{D.9})$$

where the s in the denominator is the number of Riemann sheets or the number of copies involved in the correlator (not to be confused with the metric). The path integral in the numerator, then, is also only over the twisted copies of the CFT, while the path integral with no insertions in the denominator, Z_δ , is the path integral of a single copy of the CFT with the metric in Equation (D.3).

The path integrals on the right-hand side of Equation (D.9) have no insertions and are on a metric of identical form. For the case where the covering space manifold has spherical topology, the path integrals cancel out up to the δ and δ' dependence. Ultimately, we want to normalize the twist operators (and correlator) and take the limit of $\varepsilon, \delta, \delta' \rightarrow 0$. We normalize the ε -dependence by demanding that the two-point function of two twist operators is fixed. The δ' -dependence cancels out as it should, and any δ -dependence that remains corresponds to twist operators at infinity. This δ -dependence can be cancelled out by appropriate normalization of the two-point function with one twist at infinity.

We should mention that there is an important final step to compute the correlation function. The twist operators σ_n are implicitly labeled by a certain n -cycle element of $S_{N_1 N_5}$; however, we are modding out by $S_{N_1 N_5}$, so we should really label the twists with *conjugacy classes* [151]. This fact is taken into account combinatorial in the body of the text. One can understand the structure and relation of these combinatorial factors to the genus of the covering space via diagrammatic methods developed in [201].

D.2 Spherical Correlation Functions of Twist Operators

Our goal in this appendix is to simplify and algorithmize correlation functions of bare twist operators using the Liouville action method. We restrict our consideration to correlation functions that have spherical genus, because they have a couple of simplifications and give the leading contribution in a large- $N_1 N_5$ expansion [151].

Consider a correlator of the form

$$Z = \langle \sigma_{p_1}(z_1) \sigma_{p_2}(z_2) \cdots \sigma_{p_M}(z_M) \sigma_{q_0}(\infty) \sigma_{q_1}(\infty) \sigma_{q_2}(\infty) \cdots \sigma_{q_{N-1}}(\infty) \rangle, \quad (\text{D.10})$$

where these are the normalized twist operators that have unit correlator with themselves at unit separation in the z -plane. We come to the normalization later. The p_i and q_j are the lengths of the S_N -cycles for the corresponding twist operators. We have M twists in the finite z -plane and N twists at $z = \infty$. This is the most general correlator of bare twists one could consider. Note that one could alternatively consider only twists in the finite z -plane and then take the limit as some of the z_i go to infinity.

The genus of the covering space is determined by the Riemann–Hurwitz formula

$$g = \frac{1}{2} \sum_{i=1}^M (p_i - 1) + \frac{1}{2} \sum_{j=0}^{N-1} (q_j - 1) - s + 1, \quad (\text{D.11})$$

where s is the total number of sheets, or copies, involved in the correlator. We restrict our attention to the sphere, $g = 0$. In which case, we do not have to compute the path integral, as we see when we normalize the twist operators.

D.3 Properties of the Map

One needs to find the map to the covering space. This is the difficult part of the problem. One can use a differential equation approach, as demonstrated in [151] or other methods. We do not treat this aspect of the problem here.

The map must have certain properties. It should be meromorphic with three types of points where the map's local properties become important: images of the twists, infinite images of infinity, and finite images of infinity. We parameterize the behavior as follows

$$\begin{aligned} z - z_i &\approx a_i (t - t_i)^{p_i} & z &\approx z_i, t \approx t_i \\ z &\approx b_0 t^{q_0} & z &\rightarrow \infty, t \rightarrow \infty \\ z &\approx \frac{b_j}{(t - t_\infty^j)^{q_j}} & z &\rightarrow \infty, t \approx t_\infty^j, \end{aligned} \quad (\text{D.12})$$

where we only care about the leading term displayed above. In the end, the correlator depends only on the a_i , b_j , p_i , and q_j .

We should specify exactly how many different images of infinity the map has. We claim that we can arrange the map so that q_0 through q_{N-1} are as above and all additional finite images of infinity are of order 1, and furthermore

$$q_0 + \sum_{j=1}^M q_j = \sum_{j=0}^{N-1} q_j + \sum_{j=N}^F q_j = s, \quad (\text{D.13})$$

where q_N through q_F are all unity. This means that the number of distinct images of infinity is

$$F = s + N - \sum_{j=0}^{N-1} q_j. \quad (\text{D.14})$$

D.4 Computing the Liouville Action

The correct way to define the correlator in Equation (D.10) is to cut holes in the z plane around the z_i with radius ε and then a large cut at $|z| = 1/\delta$ [151]. The small holes around the z_i have the appropriate boundary conditions for the twist operators. Upon the cut at $|z| = 1/\delta$, we glue a second flat disc with complex coordinate \tilde{z} . The center of this second disc has a hole of size $\tilde{\varepsilon}$, which has the boundary conditions appropriate for the N twists at infinity. The metric on this manifold is

$$ds^2 = \begin{cases} dzd\bar{z} & |z| < \frac{1}{\delta} \\ d\tilde{z}d\bar{\tilde{z}} & |\tilde{z}| < \frac{1}{\delta} \end{cases} \quad (\text{D.15})$$

$$z = \frac{1}{\delta^2 \tilde{z}}.$$

Note that there is a ring of curvature at $|z| = 1/\delta$. The base space with holes for the correlator in Chapter 4 is pictured in Figure D.1.

We map to a covering space with coordinates t and \bar{t} using the map given in Equation (D.12). The manifold still has holes from the images of the twist operators. We close all of the holes in the manifold by pasting in flat patches. Then, the covering space manifold, which we call Σ , becomes compact with the topology of a sphere. The Riemann–Hurwitz formula (D.11) determines the genus of the covering space. We restrict our attention to $g = 0$, but in other cases one can get higher genus covering spaces, as discussed in [151]. The N twist operators which corresponded to a single hole in the base space at $\tilde{z} = 0$ map to different holes in the covering space, all but one in the finite- t plane and one at infinity. These holes we also close with flat patches. The covering space for the case needed in Section 4.3.5 is pictured in Figure D.1.

The metric induced on the manifold Σ from the base metric (D.15) is conformally related to the fiducial metric for the t -sphere,

$$\hat{ds}^2 = \begin{cases} dt d\bar{t} & |t| < \frac{1}{\delta'} \\ d\tilde{t} d\bar{\tilde{t}} & |\tilde{t}| < \frac{1}{\delta'} \end{cases} \quad (\text{D.16})$$

$$t = \frac{1}{\delta'^2 \tilde{t}}.$$

We choose δ' such that the outermost image of $|z| = \frac{1}{\delta}$ is contained in the first half of the t -sphere.

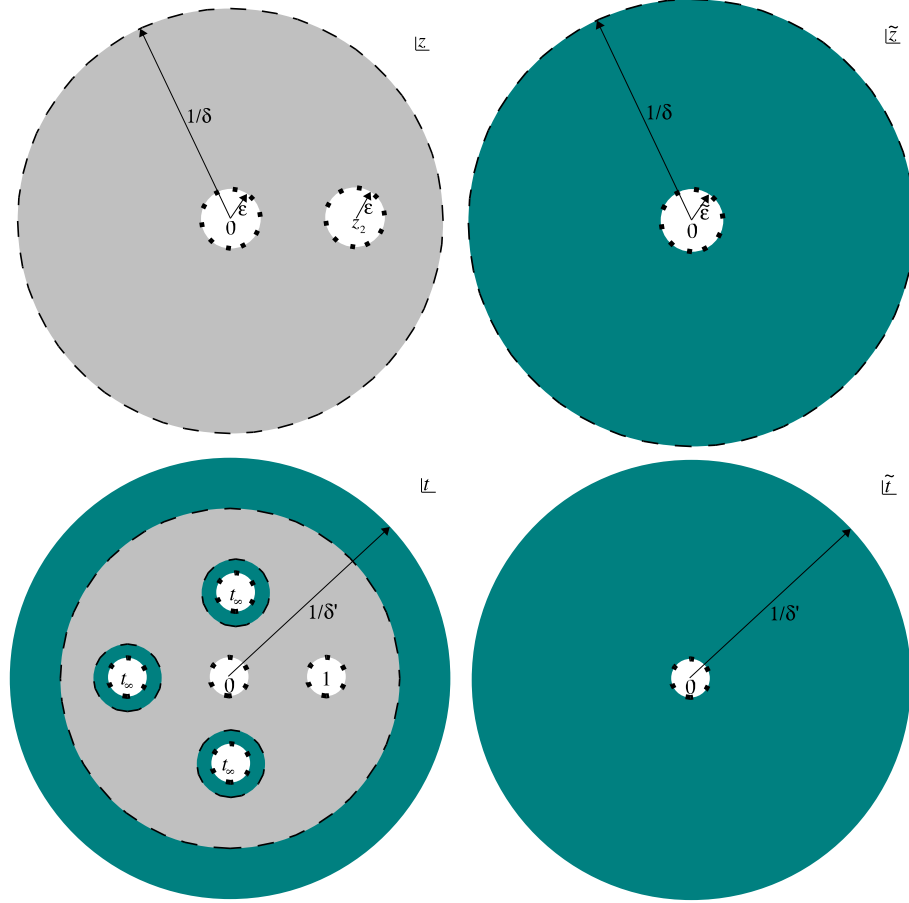


Figure D.1: The figure depicts the effect of the map, and the various regions which contribute to the Liouville action for a correlator with two twist operators in the finite z -plane and some twist operators at infinity. This can be thought of as a special case of the correlator needed to compute the twist Jacobian factor T in Chapter 4. The relative sizes are not accurate. The top two circles show the z -sphere, while the bottom two show the covering space, or t -sphere.

The Liouville field ϕ is defined by

$$ds^2 = e^\phi \hat{ds}^2. \quad (\text{D.17})$$

We break the manifold Σ into a “regular region,” which is the image of the “first half” of

the z -sphere with the holes cut out; the “annuli,” which consist of the images of the second half of the z -sphere with the hole around $\tilde{z} = 0$ cut out; the “second half” of the t -sphere with the hole cut out; and finally, the flat patches which we pasted in to make the manifold compact. Using this categorization, we can write ϕ as

$$\phi = \begin{cases} \log \left| \frac{dz}{dt} \right|^2; & \text{regular region} \\ \log \left| \frac{d\tilde{z}}{dt} \right|^2; & \text{annuli} \\ \log \left| \frac{d\tilde{z}}{dt} \right|^2; & \text{second half of the } t\text{-sphere} \\ (\text{constant}); & \text{flat patches} \end{cases}. \quad (\text{D.18})$$

Note that ϕ is a continuous function over Σ , but its first derivative is discontinuous across the boundaries between the above regions.

The goal of this section is to compute the Liouville action,

$$S_L = \frac{c}{96\pi} \int_{\hat{\Sigma}} d^2t \sqrt{\hat{g}} \left[\partial_\mu \phi \partial_\nu \phi \hat{g}^{\mu\nu} + 2\hat{R}\phi \right], \quad (\text{D.19})$$

in the limit of small ε , $\tilde{\varepsilon}$, δ , and δ' . Any regularization dependence drops out once we normalize the twist operators to have unit 2-point function with themselves at unit separation. It is important to note that the curvature and metric in the above equation are on the fiducial manifold $\hat{\Sigma}$, and not the more complicated curved manifold Σ . This means, for instance, the only curvature contribution comes from the ring of concentrated curvature at $|t| = 1/\delta'$ where the two discs of the fiducial metric are glued together.

There are the following nonzero contributions to the Liouville action:

1. a contribution $S_L^{(1)}$ from the regular region R (light gray in the figure).
2. a contribution $S_L^{(2)}$ from the annulus A , between the outer image of $|z| = \frac{1}{\delta}$ and $|t| = 1/\delta'$.
3. a contribution $S_L^{(3)}$ from the ring of curvature concentrated at $|t| = 1/\delta'$.
4. a contribution $S_L^{(4)}$ from the second half of the t -sphere, but outside of the patched hole around $\tilde{t} = 0$,
5. a contribution $S_L^{(5)}$ from the annuli around the finite images of infinity between the image of $|\tilde{z}| = \tilde{\varepsilon}$ and the image of $|z| = |\tilde{z}| = 1/\delta$.

The flat patches (and the various boundaries between the regions) do not contribute. In the flat regions, there is no curvature of the fiducial metric and ϕ is constant; therefore, there can be no contribution. On their boundaries, $\partial\phi$ is nonzero, but bounded and is integrated over a set of measure zero. Therefore, the edges of the filled holes do not contribute either.

There can be no curvature contribution beyond $S_L^{(3)}$, but one may worry about possible kinetic term contributions from various boundaries; however, these cannot contribute as long as $\partial\phi$ is bounded, which means that as long as ϕ is continuous, there is no contribution from the kinetic term on boundaries. Note that the fourth and fifth contributions are zero for the calculations performed in [151].

D.4.1 Kinetic Contributions to the Liouville Action

We break the t -sphere into the following regions where we need to compute the contributions to the Liouville action kinetic term:

1. the regular region, R . R is defined as the image of the first half of the z -sphere under the map.
2. the outer annulus, A_0 . A_0 is bounded by $|z| > 1/\delta$ and $|t| < 1/\delta'$.
3. the second half of the t -sphere, S . S is bounded by $|\tilde{z}| > \tilde{\varepsilon}$ and $|\tilde{t}| < 1/\delta'$.
4. the annuli surround the finite images of infinity, A_j . These annuli are bounded by the images of $|\tilde{z}| < 1/\delta$ and $|\tilde{z}| > \tilde{\varepsilon}$.

We can integrate by parts, by noting

$$\partial_\mu \phi \partial^\mu \phi = \partial_\mu (\phi \partial^\mu \phi) - \phi \partial_\mu \partial^\mu \phi. \quad (\text{D.20})$$

The second term vanishes for any holomorphic transformation. Therefore, we are left with

$$S_L = \frac{c}{96\pi} \int_\Sigma \partial_\mu (\phi \partial^\mu \phi) dA = \frac{c}{96\pi} \int_{\partial\Sigma} g^{\mu\nu} n_\mu \phi \partial_\nu \phi d\ell. \quad (\text{D.21})$$

In our case, the metric is given by

$$ds^2 = dz d\bar{z} \quad \implies \quad g_{z\bar{z}} = \frac{1}{2} \quad g^{z\bar{z}} = 2. \quad (\text{D.22})$$

Thus, we may write

$$S_L = 2 \frac{c}{96\pi} \int_{\partial\Sigma} n_{\bar{z}} \phi \partial_z \phi d\ell + 2 \frac{c}{96\pi} \int_{\partial\Sigma} n_z \phi \partial_{\bar{z}} \phi d\ell = I + \bar{I}, \quad (\text{D.23})$$

where we recognize that the second term is just the complex conjugate of the first. Let us suppose that $\partial\Sigma$ has two types of contours: internal and external. We need to treat these separately,

$$I = \sum I_{\text{int}} + I_{\text{ext}}. \quad (\text{D.24})$$

Note that there will only be one external contour. It is convenient at this point to introduce real coordinates:

$$\begin{aligned} z &= x + iy & \bar{z} &= x - iy \\ ds^2 &= dx^2 + dy^2 \\ n_{\bar{z}} &= \frac{n_x + in_y}{2} & n_z &= \frac{n_x - in_y}{2}. \end{aligned} \quad (\text{D.25})$$

Consider one of the internal boundaries of Σ . Let's parameterize the contour (counterclockwise, of course) as

$$\begin{aligned} z &= F(s) & \bar{z} &= \bar{F}(s) & s &\in [0, 1) \\ F(s) &= f(s) + ig(s) & F(0) &= F(1) \\ d\ell &= |F'(s)| ds, \end{aligned} \quad (\text{D.26})$$

where F is a holomorphic function and f and g are real-valued functions.

The normal should point *out of* Σ and therefore *into the hole*. We claim, that this means that (since the contour is counterclockwise)

$$n_x = -\frac{g'(s)}{\sqrt{f'(s)^2 + g'(s)^2}} = -\frac{g'(s)}{|F'(s)|} \quad n_y = \frac{f'(s)}{\sqrt{f'(s)^2 + g'(s)^2}} = \frac{f'(s)}{|F'(s)|}, \quad (\text{D.27})$$

which leads one to conclude

$$n_{\bar{z}} = \frac{1}{2|F'(s)|} (-g'(s) + if'(s)) = \frac{i}{2} \frac{F'(s)}{|F'(s)|}. \quad (\text{D.28})$$

Plugging in,

$$\begin{aligned} I_{\text{int}} &= 2 \frac{c}{96\pi} \int_{\text{hole}} \left(\frac{iF'(s)}{2|F'(s)|} \right) \phi \partial \phi |F'(s)| ds \\ &= i \frac{c}{96\pi} \int_{\text{hole}} \phi \partial \phi F'(s) ds \\ &= i \frac{c}{96\pi} \int_{\text{hole}} \phi \partial \phi dz, \end{aligned} \quad (\text{D.29})$$

where again the contour is counter clockwise.

What changes for the external boundary? For the external boundary, the normal points *outward and away from the enclosed area*, which means that n_x and n_y flip signs. Therefore, we pick up an extra minus sign. We can absorb this extra minus sign by remembering to use a convention: internal boundaries counter clockwise, external boundaries clockwise. Then, we always can use the formula

$$S_L^{\text{kinetic}} = \frac{c}{96\pi} \left[i \int_{\partial \Sigma} \phi \partial \phi dz + \text{c.c.} \right], \quad (\text{D.30})$$

where c.c. indicates the complex conjugate.

The Regular Region

Here we compute the contributions to the regular region. We integrate by parts in which case we need only compute the contributions from the various curves making up the boundary of R .

We begin with the boundaries from the twists, defined by

$$|z - z_j| = \varepsilon \implies |t - t_j| = \left(\frac{\varepsilon_j}{|a_i|} \right)^{\frac{1}{p_i}}. \quad (\text{D.31})$$

The Liouville scalar ϕ in the regular region is given by

$$\phi = \log \frac{dz}{dt} + \log \frac{d\bar{z}}{d\bar{t}} = 2 \log \left| \frac{dz}{dt} \right|. \quad (\text{D.32})$$

Near the twists, then, we have

$$\phi = 2 \log (p_i |a_i| |t - t_i|^{p_i-1}) \quad \partial \phi = \frac{p_i - 1}{t - t_i}. \quad (\text{D.33})$$

The contribution from the twist boundaries, then, is given by

$$\begin{aligned} S_L^i &= -\frac{c}{12} (p_i - 1) \left[\log |a_i| + \log p_i + (p_i - 1) \log \left(\frac{\varepsilon_i}{|a_i|} \right)^{\frac{1}{p_i}} \right] \\ &= -\frac{c}{12} (p_i - 1) \left[\frac{1}{p_i} \log |a_i| + \log p_i + \frac{p_i - 1}{p_i} \log \varepsilon_i \right]. \end{aligned} \quad (\text{D.34})$$

Next, we have the outer boundary, defined by

$$|z| = \frac{1}{\delta} \implies |t| = \frac{1}{(|b_0| \delta)^{\frac{1}{q_0}}}. \quad (\text{D.35})$$

The field ϕ is given by

$$\phi = 2 \log (q_0 |b_0| |t|^{q_0-1}) \quad \partial \phi = \frac{q_0 - 1}{t} \quad (\text{D.36})$$

The contribution (remembering the extra minus sign for an outer boundary) is

$$S_L^{\infty,0} = \frac{c}{12} (q_0 - 1) \left[\frac{1}{q_0} \log |b_0| + \log q_0 - \frac{q_0 - 1}{q_0} \log \delta \right]. \quad (\text{D.37})$$

Finally, we have the boundaries from the finite images of infinity, defined by

$$|z| = \frac{1}{\delta} \implies |t - t_\infty^j| = (|b_j| \delta)^{\frac{1}{q_j}} \quad (\text{D.38})$$

where

$$\phi = 2 \log \left[\frac{|b_j| q_j}{|t - t_\infty^j|^{q_j+1}} \right] \quad \partial \phi = -\frac{q_j + 1}{t - t_\infty^j}. \quad (\text{D.39})$$

Thus, the contribution from these boundaries is given by

$$S_L^{\infty, j} = -\frac{c}{12} (q_j + 1) \left[\frac{1}{q_j} \log |b_j| - \log q_j + \frac{q_j + 1}{q_j} \log \delta \right]. \quad (\text{D.40})$$

The “Outer” Annulus A_0

For A_0 , the field is defined by

$$\phi = \log \frac{d\tilde{z}}{dt} + \log \frac{d\bar{\tilde{z}}}{d\bar{t}} = 2 \log \left| \frac{d\tilde{z}}{dt} \right|. \quad (\text{D.41})$$

In this region ϕ , always has the same form:

$$\phi = 2 \log \left(\frac{q_0}{|b_0| \delta^2} |t|^{-(q_0+1)} \right) \quad \partial \phi = -\frac{q_0 + 1}{t}. \quad (\text{D.42})$$

The contribution to the Liouville action from the outer annulus, then, is given by

$$S_L = \frac{c}{12} (q_0 + 1)^2 \log |t| \Big|_{\text{inner}}^{\text{outer}}, \quad (\text{D.43})$$

where the outer boundary is given by

$$|t| = \frac{1}{\delta'}, \quad (\text{D.44})$$

and the inner boundary is given by

$$|z| = \frac{1}{\delta} \implies |t| = (\delta |b_0|)^{-\frac{1}{q_0}}. \quad (\text{D.45})$$

Therefore, the contribution is given by

$$S_L = \frac{c}{12} (q_0 + 1)^2 \left[\frac{1}{q_0} \log |b_0| + \frac{1}{q_0} \log \delta - \log \delta' \right]. \quad (\text{D.46})$$

The “Inner” Annuli, A_j

For the inner annuli, the field is given by

$$\phi = \log \frac{d\tilde{z}}{dt} + \log \frac{d\bar{\tilde{z}}}{d\bar{t}} = 2 \log \left| \frac{d\tilde{z}}{dt} \right|. \quad (\text{D.47})$$

From the local behavior of the map, one finds that

$$\phi = 2 \log \frac{q_j}{|b_j| \delta^2} |t - t_\infty^j|^{q_j-1} \quad \partial \phi = \frac{q_j - 1}{t}. \quad (\text{D.48})$$

As above, the form of the field does not change over the annuli, hence

$$S_L^j = \frac{c}{12} (q_j - 1)^2 \log |t - t_\infty^j| \Big|_{\text{inner}}^{\text{outer}}, \quad (\text{D.49})$$

where the outer boundary is

$$|\tilde{z}| = \frac{1}{\delta} \implies |t - t_\infty^j| = (|b_j| \delta)^{\frac{1}{q_j}} \quad (\text{D.50})$$

and the inner boundary is given by

$$|\tilde{z}| = \tilde{\varepsilon} \implies |t - t_\infty^j| = (|b_j| \tilde{\varepsilon} \delta^2)^{\frac{1}{q_j}}. \quad (\text{D.51})$$

Thus,

$$S_L^j = -\frac{c}{12} \frac{(q_j - 1)^2}{q_j} \log(\tilde{\varepsilon} \delta). \quad (\text{D.52})$$

Second Half of the t -sphere, S

For the second half of the t -sphere, the field ϕ is defined via

$$\phi = \log \frac{d\tilde{z}}{d\tilde{t}} + \log \frac{d\bar{\tilde{z}}}{d\bar{\tilde{t}}} = 2 \log \left| \frac{d\tilde{z}}{d\tilde{t}} \right|. \quad (\text{D.53})$$

Again, the field has the same form over this region:

$$\phi = 2 \log \frac{\delta'^{2q_0} q_0}{\delta^2 |b_0|} |\tilde{t}|^{q_0-1} \quad \partial \phi = \frac{q_0 - 1}{\tilde{t}}. \quad (\text{D.54})$$

The contribution to the Liouville action from S , is given by

$$S_L = \frac{c}{12} (q_0 - 1)^2 \log |\tilde{t}| \Big|_{\text{inner}}^{\text{outer}}. \quad (\text{D.55})$$

The outer boundary is given by

$$|\tilde{t}|_{\text{outer}} = 1/\delta', \quad (\text{D.56})$$

while the inner boundary is given by

$$|\tilde{z}| = \tilde{\varepsilon} \implies |\tilde{t}|_{\text{inner}} = \frac{1}{\delta'^2} (\delta^2 \tilde{\varepsilon} |b_0|)^{\frac{1}{q_0}}. \quad (\text{D.57})$$

Thus, the contribution to the Liouville action from the second half of the t -sphere is given by

$$S_L^S = -\frac{c}{12} \frac{(q_0 - 1)^2}{q_0} [\log |b_0| + \log \tilde{\varepsilon} + 2 \log \delta - q_0 \log \delta'] \quad (\text{D.58})$$

The Total Kinetic Contribution

Adding up the sundry contributions to the kinetic part of the Liouville action, one finds that the total contribution to the Liouville action from the kinetic term is

$$\begin{aligned} S_L^{\text{kinetic}} = & -\frac{c}{12} \left\{ \sum_i \frac{p_i - 1}{p_i} \log |a_i| + \sum_j \frac{q_j + 1}{q_j} \log |b_j| - \frac{5q_0 - 1}{q_0} \log |b_0| \right. \\ & + \sum_i (p_i - 1) \log p_i - \sum_j (q_j + 1) \log q_j - (q_0 - 1) \log q_0 \\ & + \sum_i \frac{(p_i - 1)^2}{p_i} \log \varepsilon_i + \left[\sum_j \frac{(q_j - 1)^2}{q_j} + \frac{(q_0 - 1)^2}{q_0} \right] \log \tilde{\varepsilon} \\ & + 2 \left[\sum_j \frac{q_j^2 + 1}{q_j} + \frac{q_0^2 - 4q_0 + 1}{q_0} \right] \log \delta \\ & \left. + 4q_0 \log \delta' \right\} \quad (\text{D.59}) \end{aligned}$$

D.4.2 The Curvature Contribution

All of the curvature in the fiducial metric is concentrated on a ring at $|t| = 1/\delta'$. Since we have restricted our consideration to correlation functions that are on a sphere, we may write

$$S_L^{\text{curvature}} = \frac{c}{48\pi} \int d^2t \hat{R} \phi = \frac{c}{6} \phi \Big|_{|t|=1/\delta'}. \quad (\text{D.60})$$

The value the field takes is

$$\phi = 2 \log \left(\frac{q_0 \delta'^{q_0+1}}{|b_0| \delta^2} \right), \quad (\text{D.61})$$

and thus

$$\begin{aligned} S_L^{\text{curvature}} &= \frac{c}{3} \log \left(\frac{q_0 \delta'^{q_0+1}}{|b_0| \delta^2} \right) \\ &= -\frac{c}{12} \left[4 \log |b_0| - 4 \log q_0 + 8 \log \delta - 4(q_0 + 1) \log \delta' \right] \quad (\text{D.62}) \end{aligned}$$

Adding this to the kinetic contribution, one finds

$$\begin{aligned}
S_L^{\text{total}} = & -\frac{c}{12} \left\{ \sum_i \frac{p_i - 1}{p_i} \log |a_i| + \sum_j \frac{q_j + 1}{q_j} \log |b_j| - \frac{q_0 - 1}{q_0} \log |b_0| \right. \\
& + \sum_i (p_i - 1) \log p_i - \sum_j (q_j + 1) \log q_j - (q_0 + 3) \log q_0 \\
& + \sum_i \frac{(p_i - 1)^2}{p_i} \log \varepsilon_i + \left[\sum_j \frac{(q_j - 1)^2}{q_j} + \frac{(q_0 - 1)^2}{q_0} \right] \log \tilde{\varepsilon} \\
& + 2 \left[\sum_j \frac{q_j^2 + 1}{q_j} + \frac{q_0^2 + 1}{q_0} \right] \log \delta \\
& \left. - 4 \log \delta' \right\}
\end{aligned} \tag{D.63}$$

D.5 The Unnormalized Correlator

The correlator of twists is defined by

$$Z = \langle \cdot \rangle = \frac{\langle \cdot \rangle_{\delta, \varepsilon}}{\langle \emptyset | \emptyset \rangle_{\delta, \varepsilon}} = e^{S_L} \frac{Z'_{\delta'}}{(Z_\delta)^s}, \tag{D.64}$$

where s is the number of sheets involved in the correlator and \cdot is the twist operators in the correlator. Z_δ is the partition function on the z -sphere, and $Z'_{\delta'}$ is the partition function on the t -sphere with the fiducial metric. One can extract the dependence on the cutoff from the partition function and write

$$Z_\delta = Q \delta^{-\frac{c}{3}} \quad Z'_{\delta'} = Q' \delta'^{-\frac{c}{3}}. \tag{D.65}$$

The cutoff-independent factors Q and Q' depend on the precise shape that the z -sphere and the covering space have, respectively. We have chosen the metric on the base space and the covering space in such a way that $Q = Q'$; however, it will be instructive to leave Q' 's in for now.

Thus, the unnormalized correlator is given by

$$Z = e^{S_L} \frac{Q' \delta'^{-\frac{c}{3}}}{Q^s \delta^{-s \frac{c}{3}}}. \tag{D.66}$$

One can immediately see that the δ' -dependence cancels out, as it should.

D.6 Normalizing the Twist Operators

We normalize the twist operators by demanding that they have unit correlator with themselves at unit separation in the z -plane. For the two-point function

$$\langle \sigma_n(0) \sigma_n(z_2) \rangle, \quad (\text{D.67})$$

the map is of the form

$$z = z_2 \frac{t^n}{t^n - (t-1)^n} \quad (\text{D.68})$$

which behaves as

$$\begin{aligned} z &\approx (-1)^{n+1} z_2 t^n & z &\approx 0, t \approx 0 \\ z - z_2 &\approx z_2 (t-1)^n & z &\approx z_2, t \approx 1 \\ z &\approx \frac{z_2}{n} t & z &\rightarrow \infty, t \rightarrow \infty \\ z &\approx -\frac{z_2}{n} \frac{\alpha_j}{(1-\alpha_j)^2} \frac{1}{t - t_\infty^j} & z &\rightarrow \infty, t \rightarrow t_\infty^j. \end{aligned} \quad (\text{D.69})$$

The finite images of infinite satisfy

$$t_\infty^j = \frac{1}{1 - \alpha_j} \quad (\alpha_j)^n = 1, \quad (\text{D.70})$$

where the α_j are the n roots of unity, and $\alpha_0 = 1$. Therefore, j runs from 0 to $n-1$.

For the two-point function, we identify the important parameters

$$\begin{aligned} a_1 &= (-1)^{n+1} z_2 & p_1 &= n \\ a_2 &= z_2 & p_2 &= n \\ b_0 &= \frac{z_2}{n} & q_0 &= 1 \\ b_j &= \frac{z_2}{n} \frac{\alpha_j}{(1-\alpha_j)^2} & q_j &= 1. \end{aligned} \quad (\text{D.71})$$

The Liouville action is given by

$$S_L^{\text{total}} = -\frac{c}{12} \left\{ 2 \frac{n-1}{n} \log |z_2| + 2 \sum_{j=1}^{n-1} \log |b_j| + 2(n-1) \log n + \frac{(n-1)^2}{n} \log \varepsilon_1 \varepsilon_2 + 4n \log \delta - 4 \log \delta' \right\}. \quad (\text{D.72})$$

We compute

$$\begin{aligned} \sum_{j=1}^{n-1} \log |b_j| &= (n-1) \log \frac{z_2}{n} + \log \left| \prod_{j=1}^{n-1} \frac{\alpha_j}{(1-\alpha_j)^2} \right| \\ &= (n-1) \log \frac{z_2}{n} - \log n^2 \end{aligned}$$

$$= (n-1) \log z_2 - (n+1) \log n, \quad (\text{D.73})$$

and therefore

$$S_L^{\text{total}} = -\frac{c}{12} \left\{ 2(n-1) \frac{n+1}{n} \log |z_2| - 4 \log n + \frac{(n-1)^2}{n} \log \varepsilon_1 \varepsilon_2 + 4n \log \delta - 4 \log \delta' \right\}. \quad (\text{D.74})$$

The unnormalized two point correlator, then, is given by

$$\langle \sigma_n^{\varepsilon_1}(0) \sigma_n^{\varepsilon_2} \rangle_\delta = \frac{Q'}{Q^n} |z_2|^{-\frac{c}{6}(n-\frac{1}{n})} n^{\frac{c}{3}} (\varepsilon_1 \varepsilon_2)^{-\frac{c}{12} \frac{(n-1)^2}{n}}. \quad (\text{D.75})$$

Note that since $s = n$ for the correlator, the δ -dependence cancelled out as it should. Therefore, the normalized twist operator is defined by

$$\sigma_n = \sqrt{\frac{Q^n}{Q'}} n^{-\frac{c}{6}} \varepsilon^{\frac{c}{12} \frac{(n-1)^2}{n}} \sigma_n^\varepsilon \quad (\text{D.76})$$

D.7 The General Correlator

We are now ready to put all of the pieces together to compute the normalized correlator of twists in Equation (D.10) for spherical genus.

The correlator of the normalized twists is given by

$$\begin{aligned} Z^{\text{norm.}} &= \frac{Q^{\frac{1}{2} \sum_{i=1}^M p_i + \frac{1}{2} \sum_{j=0}^{N-1} q_j}}{Q'^{\frac{M+N}{2}}} \left(\prod_{i=1}^M p_i \prod_{j=0}^{N-1} q_j \right)^{-\frac{c}{6}} \prod_{i=1}^M \varepsilon_i^{\frac{c}{12} \frac{(p_i-1)^2}{p_i}} \tilde{\varepsilon}^{\frac{c}{12} \sum_{j=0}^{N-1} \frac{(q_j-1)^2}{q_j}} Z \\ &= \frac{Q^{\frac{1}{2} \sum_{i=1}^M p_i + \frac{1}{2} \sum_{j=0}^{N-1} q_j - s}}{Q'^{\frac{M+N}{2} - 1}} \left(\prod_{i=1}^M p_i \prod_{j=0}^{N-1} q_j \right)^{-\frac{c}{6}} \prod_{i=1}^M \varepsilon_i^{\frac{c}{12} \frac{(p_i-1)^2}{p_i}} \tilde{\varepsilon}^{\frac{c}{12} \sum_{j=0}^{N-1} \frac{(q_j-1)^2}{q_j}} \left(\frac{\delta^s}{\delta'} \right)^{\frac{c}{3}} e^{S_L} \\ &= \frac{Q^{\frac{M+N}{2} - 1 + g}}{Q'^{\frac{M+N}{2} - 1}} \left(\prod_{i=1}^M p_i \prod_{j=0}^{N-1} q_j \right)^{-\frac{c}{6}} \prod_{i=1}^M \varepsilon_i^{\frac{c}{12} \frac{(p_i-1)^2}{p_i}} \tilde{\varepsilon}^{\frac{c}{12} \sum_{j=0}^{N-1} \frac{(q_j-1)^2}{q_j}} \left(\frac{\delta^s}{\delta'} \right)^{\frac{c}{3}} e^{S_L} \\ &= Q^g \left(\frac{Q}{Q'} \right)^{\frac{M+N}{2} - 1} \left(\prod_{i=1}^M p_i \prod_{j=0}^{N-1} q_j \right)^{-\frac{c}{6}} \prod_{i=1}^M \varepsilon_i^{\frac{c}{12} \frac{(p_i-1)^2}{p_i}} \tilde{\varepsilon}^{\frac{c}{12} \sum_{j=0}^{N-1} \frac{(q_j-1)^2}{q_j}} \left(\frac{\delta^s}{\delta'} \right)^{\frac{c}{3}} e^{S_L} \quad (\text{D.77}) \end{aligned}$$

We see that as long as we restrict our attention to correlators whose covering space is a sphere, and we carefully ensure that $Q = Q'$, then we never have to compute the path integral. This is exactly what we are doing, and thus

$$Z^{\text{norm.}} = \left(\prod_{i=1}^M p_i \prod_{j=0}^{N-1} q_j \right)^{-\frac{c}{6}} \prod_{i=1}^M \varepsilon_i^{\frac{c}{12} \frac{(p_i-1)^2}{p_i}} \tilde{\varepsilon}^{\frac{c}{12} \sum_{j=0}^{N-1} \frac{(q_j-1)^2}{q_j}} \left(\frac{\delta^s}{\delta'} \right)^{\frac{c}{3}} e^{S_L}. \quad (\text{D.78})$$

The δ' , ε_j , and $\tilde{\varepsilon}$ dependence all cancels out. The power of δ is

$$\begin{aligned}
\delta : \quad & \frac{c}{3}s - \frac{c}{6} \sum_{j=0}^F \frac{q_j^2 + 1}{q_j} \\
&= \frac{c}{3}s - \frac{c}{6}s - \frac{c}{6} \sum_{j=0}^F \frac{1}{q_j} \\
&= \frac{c}{6} \left(s - \sum_{j=1}^F \frac{1}{q_j} \right) \\
&= \frac{c}{6} \sum_{j=0}^F \left(q_j - \frac{1}{q_j} \right) \\
&= 4 \sum_{j=0}^{N-1} \Delta_{q_j}
\end{aligned} \tag{D.79}$$

If there are no twists at infinity then the power vanishes, appropriately. Typically, one divides this dependence out when one inserts twists at infinity, but we leave them explicitly here, for now. Let us call the total weight of all the operators at infinity

$$\Delta_\infty = \sum_{j=0}^{N-1} \Delta_{q_j} \tag{D.80}$$

We can rewrite the correlator in the slightly nicer form:

$$\begin{aligned}
Z^{\text{norm.}} &= \delta^{4\Delta_\infty} \left(\prod_{i=1}^M p_i \prod_{j=0}^{N-1} q_j \right)^{-\frac{c}{6}} \left(\prod_{i=1}^M |a_i|^{\frac{1}{p_i}} p_i \right)^{-\frac{c}{12}(p_i-1)} \prod_{j=1}^F \left(\frac{|b_j|^{\frac{1}{q_j}}}{q_j} \right)^{-\frac{c}{12}(q_j+1)} |b_0|^{\frac{c}{12} \frac{q_0-1}{q_0}} q_0^{\frac{c}{12}(q_0+3)} \\
&= \delta^{4\Delta_\infty} \left(\prod_{i=1}^M p_i^{-\frac{c}{12}(p_i+1)} \right) \left(\prod_{j=1}^{N-1} q_j^{\frac{c}{12}(q_j-1)} \right) q_0^{\frac{c}{12}(q_0+1)} \left(\prod_{i=1}^M |a_i|^{-\frac{c}{12} \frac{p_i-1}{p_i}} \right) \left(\prod_{j=1}^F |b_j|^{-\frac{c}{12} \frac{q_j+1}{q_j}} \right) |b_0|^{\frac{c}{12} \frac{q_0-1}{q_0}} \\
&= \delta^{4\Delta_\infty} \left(\prod_{i=1}^M p_i^{-\frac{c}{12}(p_i+1)} \right) \left(\prod_{j=0}^{N-1} q_j^{\frac{c}{12}(q_j-1)} \right) \left(\prod_{i=1}^M |a_i|^{-\frac{c}{12} \frac{p_i-1}{p_i}} \right) \left(\prod_{j=0}^F |b_j|^{-\frac{c}{12} \frac{q_j+1}{q_j}} \right) |b_0|^{\frac{c}{6}} q_0^{\frac{c}{6}}
\end{aligned} \tag{D.81}$$

It would be nice if we could say something about the a_i and b_j . For instance, we should think about what happens if we multiply the whole map by a constant scale factor. If one wants to consider a case when there are no twists at infinity, then one should set the $q_j = 1$ and $F = s$ to obtain the simpler formula

$$Z^{\text{norm.}} = \left(\prod_{i=1}^M p_i^{-\frac{c}{12}(p_i+1)} \right) \left(\prod_{i=1}^M |a_i|^{-\frac{c}{12} \frac{p_i-1}{p_i}} \right) \left(\prod_{j=0}^s |b_j|^{-\frac{c}{6}} \right) |b_0|^{\frac{c}{6}}. \tag{D.82}$$

Note that the b_0 dependence cancels out.

D.7.1 Checking the Correlator

What happens if we multiply the map by a complex prefactor α ? This corresponds to scaling and rotating the positions of all of the twist operators, but preserving the origin. If the map is of the form

$$z = f(t), \quad (\text{D.83})$$

for some holomorphic function f , then we consider the transformation

$$z = f(t) \quad \mapsto \quad z' = \alpha f(t). \quad (\text{D.84})$$

The only effect is rescaling all of the a_i and b_j by α . Thus, we observe that

$$Z^{\text{norm.}} \mapsto Z' = |\alpha|^D Z^{\text{norm.}}, \quad (\text{D.85})$$

where

$$\begin{aligned} D &= -\frac{c}{12} \sum_{i=1}^M \frac{p_i - 1}{p_i} - \frac{c}{12} \sum_{j=0}^F \frac{q_j + 1}{q_j} + \frac{c}{6} \\ &= \frac{c}{12} \sum_{i=1}^M \frac{1}{p_i} - \frac{c}{12} \sum_{j=0}^F \frac{1}{q_j} - \frac{c}{12} (M + F - 2) \\ &= 2\Delta_\infty - 2 \sum_{i=1}^M \Delta_{p_i} - \frac{c}{12} (s + F - 2) + \frac{c}{12} \sum_{i=1}^M (p_i - 1) \\ &= 2\Delta_\infty - 2 \sum_{i=1}^M \Delta_{p_i}. \end{aligned} \quad (\text{D.86})$$

Therefore, we see that the effect of scaling by α is

$$Z' = \frac{1}{|\alpha|^{2 \sum \Delta_{p_i} - 2\Delta_\infty}} Z, \quad (\text{D.87})$$

as it should be. This is a good check that the formula is correct.

Appendix E

THE EXPONENTIAL ANSATZ

In this appendix we check that the exponential ansatz in Equation (5.32) for the bosonic excitations is indeed correct; the fermionic case works in a similar way.

The bosonic fields completely decouple from the fermionic fields. Further, the set $\{\alpha_{++}, \alpha_{--}, n\}$ decouples from the set $\{\alpha_{+-}, \alpha_{-+}, n\}$. Thus in what follows we write only the modes $\{\alpha_{++}, \alpha_{--}, n\}$.

We have from the basic relation (5.18)

$$\langle 0_{R,-} | \left(\alpha_{++}, n_1 \alpha_{--}, n_2 \dots \right) \sigma_2^+(w_0) | 0_R^- \rangle^{(1)} | 0_R^- \rangle^{(2)} = {}_t \langle 0 | \left(\alpha'_{++}, n_1 \alpha'_{--}, n_2 \dots \right) | 0 \rangle_t \quad (\text{E.1})$$

where the operators α' arise from following the various coordinate changes and spectral flows that bring us from the original operators α on the cylinder to operators on the t plane (with the state $|0\rangle_t$ at $t = 0$). If we can understand all amplitudes of this type, then we will have a complete understanding of the state $\sigma_2^+(w_0) | 0_R^- \rangle^{(1)} | 0_R^- \rangle^{(2)}$. Our ansatz for this state is

$$\sigma_2^+(w_0) | 0_R^- \rangle^{(1)} | 0_R^- \rangle^{(2)} = e^{-\sum_{m>0, n>0} \gamma_{mn}^B \alpha_{++}, m \alpha_{--}, n} | 0_R^- \rangle \quad (\text{E.2})$$

The initial operators α are given by eq.(5.22a), and their map to the final form in the t plane is given by eq.(5.51a). We can expand the latter form in terms of natural modes on the t plane (5.52a)

$$\begin{aligned} \alpha_{A\dot{A}, n} &\rightarrow \int_{t=-\infty}^{\infty} \frac{dt}{2\pi i} \partial_t X_{A\dot{A}}(t) (z_0 + t^2)^{\frac{n}{2}} \\ &= \int_{t=-\infty}^{\infty} \frac{dt}{2\pi i} \partial_t X_{A\dot{A}}(t) \sum_{k \geq 0} \binom{\frac{n}{2}}{k} z_0^k t^{n-2k} \\ &= \sum_{k \geq 0} \binom{\frac{n}{2}}{k} z_0^k \tilde{\alpha}_{A\dot{A}, n-2k} \end{aligned} \quad (\text{E.3})$$

All we need to know is that this is a linear relation

$$\alpha_{A\dot{A},n} = \sum_{p=-\infty}^{\infty} B_{n,p} \tilde{\alpha}_{A\dot{A},p} \quad (\text{E.4})$$

with some constant coefficients B_{np} . Since the relation (E.4) is linear in the field operators, we will have as many operators inserted between the parenthesis $()$ on the RHS of (E.1) as on the LHS. But on the RHS we just have these mode operators sandwiched between the t plane vacuum state. Thus the amplitude will be evaluated by Wick contractions between these operators. From this fact we can immediately note two things: we must have an even number of insertions, and there must be an equal number of α_{++} and α_{--} modes.

Let us start with the simplest case: two operator insertions, which is computation we encountered in finding γ_{mn}^B . We have (with $n_1 > 0, n_2 > 0$)

$$\langle 0_{R,-} | \left(\alpha_{++ , n_1} \alpha_{-- , n_2} \right) \sigma_2^+(w_0) | 0_R^- \rangle^{(1)} | 0_R^- \rangle^{(2)} = {}_t \langle 0 | \left(\alpha'_{++ , n_1} \alpha'_{-- , n_2} \right) | 0 \rangle_t \quad (\text{E.5})$$

With the ansatz (E.2), the LHS gives

$$\begin{aligned} \langle 0_{R,-} | \left(\alpha_{++ , n_1} \alpha_{-- , n_2} \right) \sigma_2^+(w_0) | 0_R^- \rangle^{(1)} \otimes | 0_R^- \rangle^{(2)} \\ = \langle 0_{R,-} | \left(\alpha_{++ , n_1} \alpha_{-- , n_2} \right) e^{-\sum_{m_1 > 0, m_2 > 0} \gamma_{m_1 m_2}^B \alpha_{++ , -m_1} \alpha_{-- , -m_2}} | 0_R^- \rangle \end{aligned} \quad (\text{E.6})$$

The contribution to this amplitude comes from expanding the exponential to first order giving

$$\langle 0_{R,-} | \left(\alpha_{++ , n_1} \alpha_{-- , n_2} \right) (-1) \sum_{m_1 > 0, m_2 > 0} \gamma_{m_1 m_2}^B \alpha_{++ , -m_1} \alpha_{-- , -m_2} | 0_R^- \rangle = (-1) n_1 n_2 \gamma_{n_2 n_1}^B \quad (\text{E.7})$$

The RHS of (E.5) gives

$${}_t \langle 0 | \sum_{p_1, p_2} B_{n_1, p_1} B_{n_2, p_2} \tilde{\alpha}_{++ , p_1} \tilde{\alpha}_{-- , p_2} | 0 \rangle_t = \sum_{p_1 > 0} p_1 B_{n_1, p_1} B_{n_2, -p_1} \quad (\text{E.8})$$

Thus we get the relation

$$(-1) n_1 n_2 \gamma_{n_2 n_1}^B = \sum_{p_1 > 0} p_1 B_{n_1, p_1} B_{n_2, -p_1} \quad (\text{E.9})$$

which gives the γ_{mn}^B in (5.66) when we use (E.3).

Let us now consider the next simplest case: four operator insertions. The LHS of (E.1) gives ($n_1, n_2, n_3, n_4 > 0$)

$$\langle 0_{R,-} | \left(\alpha_{++ , n_1} \alpha_{-- , n_2} \alpha_{++ , n_3} \alpha_{-- , n_4} \right) \sigma_2^+(w_0) | 0_R^- \rangle^{(1)} | 0_R^- \rangle^{(2)} \quad (\text{E.10})$$

We must now expand the exponential in the ansatz (E.2) to second order, getting for the LHS of (E.1)

$$\begin{aligned} & {}^{(2)}\langle 0_{R,-} | \left(\alpha_{++ , n_1} \alpha_{-- , n_2} \alpha_{++ , n_3} \alpha_{-- , n_4} \right) \frac{1}{2!} (-1)^2 \\ & \times \left(\sum_{m_1 > 0, m_2 > 0} \gamma_{m_1 m_2}^B \alpha_{++ , -m_1} \alpha_{-- , -m_2} \right) \left(\sum_{m_3 > 0, m_4 > 0} \gamma_{m_3 m_4}^B \alpha_{++ , -m_3} \alpha_{-- , -m_4} \right) | 0_R^- \rangle \end{aligned} \quad (\text{E.11})$$

This gives

$$\frac{1}{2!} (-1)^2 (2!) n_1 n_2 n_3 n_4 \left(\gamma_{n_2 n_1}^B \gamma_{n_4 n_3}^B + \gamma_{n_4 n_1}^B \gamma_{n_2 n_3}^B \right) \quad (\text{E.12})$$

where the factor (2!) comes from the fact that the set $\alpha_{++ , n_1} \alpha_{-- , n_2}$ can contract with the operators from either of the two γ^B factors.

The RHS of (E.1) gives

$$\begin{aligned} & {}_t \langle 0 | \sum_{p_1, p_2, p_3, p_4} B_{n_1, p_1} B_{n_2, p_2} B_{n_3, p_3} B_{n_4, p_4} \tilde{\alpha}_{++ , p_1} \tilde{\alpha}_{-- , p_2} \tilde{\alpha}_{++ , p_3} \tilde{\alpha}_{-- , p_4} | 0 \rangle_t \\ & = \left(\sum_{p_1 > 0} p_1 B_{n_1, p_1} B_{n_2, -p_1} \right) \left(\sum_{p_3 > 0} p_3 B_{n_3, p_3} B_{n_4, -p_3} \right) \\ & \quad + \left(\sum_{p_1 > 0} p_1 B_{n_1, p_1} B_{n_4, -p_1} \right) \left(\sum_{p_3 > 0} p_3 B_{n_3, p_3} B_{n_2, -p_3} \right) \end{aligned} \quad (\text{E.13})$$

On using (E.9) this gives

$$n_1 n_2 n_3 n_4 \left(\gamma_{n_2 n_1}^B \gamma_{n_4 n_3}^B + \gamma_{n_4 n_1}^B \gamma_{n_2 n_3}^B \right) \quad (\text{E.14})$$

which agrees with (E.12).

Thus we have verified the ansatz to order four in the bosonic field operators. Proceeding in this way we can verify the complete exponential ansatz.

The fermionic case is similar. Modes on the cylinder map linearly to the modes for the case where we are on the t plane and we have the NS vacuum at $t = 0$. On this t plane the modes must appear in pairs to allow the amplitude to be nonvanishing, thus we must have an even number of modes in each term in the ansatz. Our ansatz allows all modes that are nonvanishing on the chosen vacuum state; thus the situation is similar to the bosonic case where we allowed all negative index bosonic operators in the ansatz. Thus the fermionic part of the ansatz can be verified in the same way as the bosonic part.

Appendix F

SOME USEFUL SERIES

In this appendix, we collect some series we find useful in the main text. Some of the identities can be proved using hypergeometric series, while others we know of no conclusive proof; however, we are confident they are correct after numerical study. These series arise when considering a single boson and fermion.

$$\sum_{k \text{ odd}^+} \frac{1}{(n - \frac{k}{2})(k + l)} \frac{\Gamma(\frac{k}{2} + 1)}{\Gamma(\frac{k+1}{2})} = \frac{\pi l \Gamma(\frac{l+1}{2})}{4\Gamma(\frac{l}{2} + 1)} \frac{1}{n + \frac{l}{2}} \left(\frac{\Gamma(\frac{l}{2})\Gamma(-n + \frac{1}{2})}{\Gamma(\frac{l+1}{2})\Gamma(-n)} - 1 \right) \quad (\text{F.1})$$

$$\sum_{k \text{ odd}^+} \frac{1}{k(p + k)(n - \frac{k}{2})} \frac{\Gamma(\frac{k}{2} + 1)}{\Gamma(\frac{k+1}{2})} = -\frac{\pi \Gamma(\frac{p+1}{2})}{4\Gamma(\frac{p}{2} + 1)} \frac{1}{n + \frac{p}{2}} \left(\frac{\Gamma(\frac{p}{2} + 1)\Gamma(-n + \frac{1}{2})}{\Gamma(\frac{p+1}{2})\Gamma(1 - n)} - 1 \right) \quad (\text{F.2})$$

These series arise when considering a single fermion:

$$\sum_{k \text{ odd}^+} \frac{z_0^{n-\frac{k}{2}} \gamma_{pk}^F}{n - \frac{k}{2}} = \frac{z_0^{n+\frac{p}{2}}}{2(n + \frac{p}{2})} \left(\frac{\Gamma(\frac{p}{2} + 1)\Gamma(-n + \frac{1}{2})}{\Gamma(\frac{p+1}{2})\Gamma(-n + 1)} - 1 \right) \quad (\text{F.3a})$$

$$\sum_{k \text{ odd}^+} \frac{z_0^{n-\frac{k}{2}} \gamma_{kp}^F}{n - \frac{k}{2}} = -\frac{z_0^{n+\frac{p}{2}}}{2(n + \frac{p}{2})} \left(\frac{\Gamma(\frac{p}{2})\Gamma(-n + \frac{1}{2})}{\Gamma(\frac{p+1}{2})\Gamma(-n)} - 1 \right). \quad (\text{F.3b})$$

Some other useful series are

$$\sum_{k \text{ odd}^+} \frac{\Gamma(\frac{k}{2})}{\Gamma(\frac{k+1}{2})(m + \frac{k}{2})} = \pi \frac{\Gamma(m + \frac{1}{2})}{\Gamma(m + 1)} \quad (\text{F.4a})$$

$$\sum_{l \text{ odd}^+} \frac{l}{(m - \frac{l}{2})(n - \frac{l}{2})} \frac{\Gamma(\frac{l}{2})}{\Gamma(\frac{l+1}{2})} = 2\pi^2 m \frac{\Gamma(n)}{\Gamma(n + \frac{1}{2})} \delta_{m,n} \quad m, n > 0 \quad (\text{F.4b})$$

BIBLIOGRAPHY

- [1] **The Virgo Collaboration**, T. L. S. Collaboration *et al.*, “Searches for gravitational waves from known pulsars with S5 LIGO data,” *Astrophys. J.* **713** (2010) 671–685, [arXiv:0909.3583 \[astro-ph.HE\]](#).
- [2] R. Feynman, F. Morinigo, W. Wagner, D. Pines, and e. Hatfield, B., *Feynman lectures on gravitation*. Westview Press, Boulder, 2003.
- [3] S. W. Hawking and R. Penrose, “The Singularities of gravitational collapse and cosmology,” *Proc. Roy. Soc. Lond.* **A314** (1970) 529–548.
- [4] S. W. Hawking and G. Ellis, *The Large Scale Structure of Spacetime*. Cambridge University Press, Cambridge, 1973.
- [5] J. R. Oppenheimer and H. Snyder, “On Continued gravitational contraction,” *Phys. Rev.* **56** (1939) 455–459.
- [6] A. Celotti, J. C. Miller, and D. W. Sciama, “Astrophysical evidence for the existence of black holes,” *Class. Quant. Grav.* **16** (1999) A3, [arXiv:astro-ph/9912186](#).
- [7] R. M. Wald, *General Relativity*. The University of Chicago Press, Chicago, 1984.
- [8] G. T. Horowitz and R. C. Myers, “The value of singularities,” *Gen. Rel. Grav.* **27** (1995) 915–919, [arXiv:gr-qc/9503062](#).
- [9] S. Weinberg, “The cosmological constant problems,” [arXiv:astro-ph/0005265](#).
- [10] S. W. Hawking, “Black hole explosions,” *Nature* **248** (1974) 30–31.
- [11] J. B. Hartle and S. W. Hawking, “Path Integral Derivation of Black Hole Radiance,” *Phys. Rev.* **D13** (1976) 2188–2203.
- [12] D. N. Page, “Particle Emission Rates from a Black Hole: Massless Particles from an Uncharged, Nonrotating Hole,” *Phys. Rev.* **D13** (1976) 198–206.
- [13] S. W. Hawking, “Particle Creation by Black Holes,” *Commun. Math. Phys.* **43** (1975) 199–220.
- [14] S. Fulling, *Aspects of Quantum Field Theory in Curved Space-time*. Cambridge University Press, Cambridge, 1989.

- [15] M. Visser, “Essential and inessential features of Hawking radiation,” *Int. J. Mod. Phys. D* **12** (2003) 649–661, [arXiv:hep-th/0106111](#).
- [16] F. Belgiorno *et al.*, “Hawking radiation from ultrashort laser pulse filaments,” [arXiv:1009.4634 \[gr-qc\]](#).
- [17] J. D. Bekenstein, “Black holes and entropy,” *Phys. Rev. D* **7** (1973) 2333–2346.
- [18] J. A. Harvey and A. Strominger, “Quantum aspects of black holes,” [arXiv:hep-th/9209055](#).
- [19] J. Preskill, “Do black holes destroy information?,” [arXiv:hep-th/9209058](#).
- [20] D. N. Page, “Black hole information,” [arXiv:hep-th/9305040](#).
- [21] S. B. Giddings, “Quantum mechanics of black holes,” [arXiv:hep-th/9412138](#).
- [22] S. D. Mathur, “The Information Paradox: A Pedagogical Introduction,” *Class. Quant. Grav.* **26** (2009) 224001, [arXiv:0909.1038 \[hep-th\]](#).
- [23] S. D. Mathur, “Fuzzballs and the information paradox: a summary and conjectures,” [arXiv:0810.4525 \[hep-th\]](#).
- [24] J. Stachel, “Einstein and michelson - the context of discovery and the context of justification,” *Astronomische Nachrichten* **303** (1982) 47–53.
- [25] M. Froissart, “Asymptotic behavior and subtractions in the Mandelstam representation,” *Phys. Rev.* **123** (1961) 1053–1057.
- [26] M. H. Goroff and A. Sagnotti, “The Ultraviolet Behavior of Einstein Gravity,” *Nucl. Phys. B* **266** (1986) 709.
- [27] M. H. Goroff and A. Sagnotti, “QUANTUM GRAVITY AT TWO LOOPS,” *Phys. Lett. B* **160** (1985) 81.
- [28] A. E. M. van de Ven, “Two loop quantum gravity,” *Nucl. Phys. B* **378** (1992) 309–366.
- [29] P. Horava, “Quantum Gravity at a Lifshitz Point,” *Phys. Rev. D* **79** (2009) 084008, [arXiv:0901.3775 \[hep-th\]](#).
- [30] T. P. Sotiriou, “Horava-Lifshitz gravity: a status report,” [arXiv:1010.3218 \[hep-th\]](#).
- [31] H. Nicolai, K. Peeters, and M. Zamaklar, “Loop quantum gravity: An outside view,” *Class. Quant. Grav.* **22** (2005) R193, [arXiv:hep-th/0501114](#).
- [32] S. Weinberg, “Ultraviolet divergences in quantum theories of gravitation,” in *General Relativity: An Einstein centenary survey*, S. W. Hawking & W. Israel, ed., pp. 790–831. 1979.
- [33] J. Gomis and S. Weinberg, “Are Nonrenormalizable Gauge Theories Renormalizable?,” *Nucl. Phys. B* **469** (1996) 473–487, [arXiv:hep-th/9510087](#).

- [34] M. Reuter and F. Saueressig, “Functional Renormalization Group Equations, Asymptotic Safety, and Quantum Einstein Gravity,” [arXiv:0708.1317 \[hep-th\]](#).
- [35] M. Niedermaier, “The asymptotic safety scenario in quantum gravity: An introduction,” *Class. Quant. Grav.* **24** (2007) R171, [arXiv:gr-qc/0610018](#).
- [36] B. S. DeWitt, “Quantum theory of gravity. II. The manifestly covariant theory,” *Phys. Rev.* **162** (1967) 1195–1239.
- [37] E. Witten, “String theory and the universe.” IOP Isaac Newton Lecture, July, 2010. Available online at <http://www.iop.org>.
- [38] O. Aharony and T. Banks, “Note on the quantum mechanics of M theory,” *JHEP* **03** (1999) 016, [arXiv:hep-th/9812237](#).
- [39] T. Banks, “TASI Lectures on Holographic Space-Time, SUSY and Gravitational Effective Field Theory,” [arXiv:1007.4001 \[hep-th\]](#).
- [40] A. Shomer, “A pedagogical explanation for the non-renormalizability of gravity,” [arXiv:0709.3555 \[hep-th\]](#).
- [41] M. B. Green, J. H. Schwarz, and E. Witten, *Superstring Theory: Introduction*, vol. 1. Cambridge University Press, Cambridge, 1987.
- [42] M. B. Green, J. H. Schwarz, and E. Witten, *Superstring Theory: Loop Amplitudes, Anomalies and Phenomenology*, vol. 1. Cambridge University Press, Cambridge, 1987.
- [43] J. Polchinski, *String Theory: An Introduction to the Bosonic String*, vol. 1. Cambridge University Press, Cambridge, 1998.
- [44] J. Polchinski, *String Theory: Superstring Theory and Beyond*, vol. 2. Cambridge University Press, Cambridge, 1998.
- [45] J. M. Maldacena, “The large N limit of superconformal field theories and supergravity,” *Adv. Theor. Math. Phys.* **2** (1998) 231–252, [arXiv:hep-th/9711200](#).
- [46] S. S. Gubser, I. R. Klebanov, and A. M. Polyakov, “Gauge theory correlators from non-critical string theory,” *Phys. Lett. B* **428** (1998) 105–114, [arXiv:hep-th/9802109](#).
- [47] E. Witten, “Anti-de Sitter space and holography,” *Adv. Theor. Math. Phys.* **2** (1998) 253–291, [arXiv:hep-th/9802150](#).
- [48] D. Mateos, “String Theory and Quantum Chromodynamics,” *Class. Quant. Grav.* **24** (2007) S713–S740, [arXiv:0709.1523 \[hep-th\]](#).
- [49] S. A. Hartnoll, “Lectures on holographic methods for condensed matter physics,” *Class. Quant. Grav.* **26** (2009) 224002, [arXiv:0903.3246 \[hep-th\]](#).
- [50] J. McGreevy, “Holographic duality with a view toward many-body physics,” *Adv. High Energy Phys.* **2010** (2010) 723105, [arXiv:0909.0518 \[hep-th\]](#).

- [51] C. V. Johnson, *D-Branes*. Cambridge University Press, Cambridge, 2003.
- [52] K. Becker, M. Becker, and J. H. Schwarz, *String Theory and M-Theory*. Cambridge University Press, Cambridge, 2007.
- [53] E. Kiritsis, *String Theory in a Nutshell*. Princeton University Press, Princeton, 2007.
- [54] L. Brink, P. Di Vecchia, and P. S. Howe, "A Locally Supersymmetric and Reparametrization Invariant Action for the Spinning String," *Phys. Lett.* **B65** (1976) 471–474.
- [55] S. Deser and B. Zumino, "A Complete Action for the Spinning String," *Phys. Lett.* **B65** (1976) 369–373.
- [56] A. M. Polyakov, "Quantum geometry of bosonic strings," *Phys. Lett.* **B103** (1981) 207–210.
- [57] S. Deser, "Self-interaction and gauge invariance," *Gen. Rel. Grav.* **1** (1970) 9–18, [arXiv:gr-qc/0411023](#).
- [58] D. G. Boulware and S. Deser, "Classical General Relativity Derived from Quantum Gravity," *Ann. Phys.* **89** (1975) 193.
- [59] S. Deser, "GRAVITY FROM SELFINTERACTION IN A CURVED BACKGROUND," *Class. Quant. Grav.* **4** (1987) L99.
- [60] R. H. Kraichnan, "Special-Relativistic Derivation of Generally Covariant Gravitation Theory," *Phys. Rev.* **98** (1955) 1118–1122.
- [61] S. N. Gupta, "Gravitation and Electromagnetism," *Phys. Rev.* **96** (1954) 1683–1685.
- [62] L. M. Butcher, M. Hobson, and A. Lasenby, "Bootstrapping gravity: a consistent approach to energy- momentum self-coupling," *Phys. Rev.* **D80** (2009) 084014, [arXiv:0906.0926 \[gr-qc\]](#).
- [63] E. B. Bogomolny, "Stability of Classical Solutions," *Sov. J. Nucl. Phys.* **24** (1976) 449.
- [64] M. K. Prasad and C. M. Sommerfield, "An Exact Classical Solution for the 't Hooft Monopole and the Julia-Zee Dyon," *Phys. Rev. Lett.* **35** (1975) 760–762.
- [65] E. D'Hoker and D. Z. Freedman, "Supersymmetric gauge theories and the AdS/CFT correspondence," [arXiv:hep-th/0201253](#). TASI 2001 Lecture Notes.
- [66] O. Aharony, S. S. Gubser, J. M. Maldacena, H. Ooguri, and Y. Oz, "Large N field theories, string theory and gravity," *Phys. Rept.* **323** (2000) 183–386, [arXiv:hep-th/9905111](#).
- [67] L. Susskind, "The World as a hologram," *J. Math. Phys.* **36** (1995) 6377–6396, [arXiv:hep-th/9409089](#).
- [68] G. 't Hooft, "Dimensional reduction in quantum gravity," [arXiv:gr-qc/9310026](#).

- [69] S. Coleman, *Aspects of Symmetry*. Cambridge University Press, Cambridge, 1985. Selected Erice lectures of Sidney Coleman.
- [70] G. 't Hooft, "A PLANAR DIAGRAM THEORY FOR STRONG INTERACTIONS," *Nucl. Phys.* **B72** (1974) 461.
- [71] I. Heemskerk, J. Penedones, J. Polchinski, and J. Sully, "Holography from Conformal Field Theory," *JHEP* **10** (2009) 079, [arXiv:0907.0151 \[hep-th\]](#).
- [72] M. Natsuume, "The singularity problem in string theory," [arXiv:gr-qc/0108059](#).
- [73] C. V. Johnson, A. W. Peet, and J. Polchinski, "Gauge theory and the excision of repulson singularities," *Phys. Rev.* **D61** (2000) 086001, [arXiv:hep-th/9911161](#).
- [74] S. S. Gubser, "Curvature singularities: The good, the bad, and the naked," *Adv. Theor. Math. Phys.* **4** (2000) 679–745, [arXiv:hep-th/0002160](#).
- [75] S. D. Mathur, "The fuzzball proposal for black holes: An elementary review," *Fortsch. Phys.* **53** (2005) 793–827, [arXiv:hep-th/0502050](#).
- [76] S. D. Mathur, "The quantum structure of black holes," *Class. Quant. Grav.* **23** (2006) R115, [arXiv:hep-th/0510180](#).
- [77] I. Bena and N. P. Warner, "Black holes, black rings and their microstates," *Lect. Notes Phys.* **755** (2008) 1–92, [arXiv:hep-th/0701216](#).
- [78] K. Skenderis and M. Taylor, "The fuzzball proposal for black holes," *Phys. Rept.* **467** (2008) 117–171, [arXiv:0804.0552 \[hep-th\]](#).
- [79] V. Balasubramanian, J. de Boer, S. El-Showk, and I. Messamah, "Black Holes as Effective Geometries," *Class. Quant. Grav.* **25** (2008) 214004, [arXiv:0811.0263 \[hep-th\]](#).
- [80] B. D. Chowdhury and A. Virmani, "Modave Lectures on Fuzzballs and Emission from the D1-D5 System," [arXiv:1001.1444 \[hep-th\]](#).
- [81] I. Mandal and A. Sen, "Black Hole Microstate Counting and its Macroscopic Counterpart," [arXiv:1008.3801 \[hep-th\]](#).
- [82] A. Sen, "Black hole solutions in heterotic string theory on a torus," *Nucl. Phys.* **B440** (1995) 421–440, [arXiv:hep-th/9411187 \[hep-th\]](#).
- [83] A. Sen, "Extremal black holes and elementary string states," *Mod. Phys. Lett.* **A10** (1995) 2081–2094, [arXiv:hep-th/9504147 \[hep-th\]](#).
- [84] A. Strominger and C. Vafa, "Microscopic Origin of the Bekenstein-Hawking Entropy," *Phys. Lett.* **B379** (1996) 99–104, [arXiv:hep-th/9601029](#).
- [85] P. T. Chrusciel, "'No hair' theorems: Folklore, conjectures, results," *Contemp. Math.* **170** (1994) 23–49, [arXiv:gr-qc/9402032](#).

- [86] J. D. Bekenstein, “Black hole hair: Twenty-five years after,” [arXiv:gr-qc/9605059](#).
- [87] O. Lunin and S. D. Mathur, “AdS/CFT duality and the black hole information paradox,” *Nucl. Phys.* **B623** (2002) 342–394, [arXiv:hep-th/0109154](#).
- [88] O. Lunin and S. D. Mathur, “Statistical interpretation of Bekenstein entropy for systems with a stretched horizon,” *Phys. Rev. Lett.* **88** (2002) 211303, [arXiv:hep-th/0202072](#).
- [89] O. Lunin and S. D. Mathur, “Metric of the multiply wound rotating string,” *Nucl. Phys.* **B610** (2001) 49–76, [arXiv:hep-th/0105136](#).
- [90] M. Taylor, “General 2 charge geometries,” *JHEP* **03** (2006) 009, [arXiv:hep-th/0507223](#).
- [91] I. Bena and N. P. Warner, “One ring to rule them all ... and in the darkness bind them?,” *Adv. Theor. Math. Phys.* **9** (2005) 667–701, [arXiv:hep-th/0408106](#).
- [92] I. Bena and N. P. Warner, “Bubbling supertubes and foaming black holes,” *Phys. Rev.* **D74** (2006) 066001, [arXiv:hep-th/0505166](#).
- [93] I. Bena, N. Bobev, S. Giusto, C. Ruef, and N. P. Warner, “An Infinite-Dimensional Family of Black-Hole Microstate Geometries,” [arXiv:1006.3497 \[hep-th\]](#).
- [94] J. de Boer, S. El-Showk, I. Messamah, and D. Van den Bleeken, “A bound on the entropy of supergravity?,” *JHEP* **02** (2010) 062, [arXiv:0906.0011 \[hep-th\]](#).
- [95] S. D. Mathur, “Tunneling into fuzzball states,” *Gen. Rel. Grav.* **42** (2010) 113–118, [arXiv:0805.3716 \[hep-th\]](#).
- [96] J. R. David, G. Mandal, and S. R. Wadia, “Microscopic formulation of black holes in string theory,” *Phys. Rept.* **369** (2002) 549–686, [arXiv:hep-th/0203048](#).
- [97] M. R. Douglas, “Branes within branes,” [arXiv:hep-th/9512077](#).
- [98] C. Vafa, “Instantons on D-branes,” *Nucl. Phys.* **B463** (1996) 435–442, [arXiv:hep-th/9512078](#).
- [99] R. Dijkgraaf, “Instanton strings and hyperKaehler geometry,” *Nucl. Phys.* **B543** (1999) 545–571, [arXiv:hep-th/9810210](#).
- [100] A. Giveon, D. Kutasov, and N. Seiberg, “Comments on string theory on AdS(3),” *Adv. Theor. Math. Phys.* **2** (1998) 733–780, [arXiv:hep-th/9806194](#).
- [101] D. Kutasov and N. Seiberg, “More comments on string theory on AdS(3),” *JHEP* **04** (1999) 008, [arXiv:hep-th/9903219](#).
- [102] N. Seiberg and E. Witten, “The D1/D5 system and singular CFT,” *JHEP* **04** (1999) 017, [arXiv:hep-th/9903224](#).
- [103] F. Larsen and E. J. Martinec, “U(1) charges and moduli in the D1-D5 system,” *JHEP* **06** (1999) 019, [arXiv:hep-th/9905064](#).

- [104] A. Jevicki, M. Mihailescu, and S. Ramgoolam, “Gravity from CFT on $S^{*}N(X)$: Symmetries and interactions,” *Nucl. Phys.* **B577** (2000) 47–72, [arXiv:hep-th/9907144](#).
- [105] R. Dijkgraaf, E. P. Verlinde, and H. L. Verlinde, “BPS spectrum of the five-brane and black hole entropy,” *Nucl. Phys.* **B486** (1997) 77–88, [arXiv:hep-th/9603126](#).
- [106] R. Dijkgraaf, E. P. Verlinde, and H. L. Verlinde, “BPS quantization of the five-brane,” *Nucl. Phys.* **B486** (1997) 89–113, [arXiv:hep-th/9604055](#).
- [107] J. de Boer, “Six-dimensional supergravity on $S^{*}3 \times \text{AdS}(3)$ and 2d conformal field theory,” *Nucl. Phys.* **B548** (1999) 139–166, [arXiv:hep-th/9806104](#).
- [108] C. M. Hull and P. K. Townsend, “Unity of superstring dualities,” *Nucl. Phys.* **B438** (1995) 109–137, [arXiv:hep-th/9410167](#).
- [109] A. A. Tseytlin, “Harmonic superpositions of M-branes,” *Nucl. Phys.* **B475** (1996) 149–163, [arXiv:hep-th/9604035](#).
- [110] S. F. Hassan, “T-duality, space-time spinors and R-R fields in curved backgrounds,” *Nucl. Phys.* **B568** (2000) 145–161, [arXiv:hep-th/9907152](#).
- [111] V. Balasubramanian, J. de Boer, E. Keski-Vakkuri, and S. F. Ross, “Supersymmetric conical defects: Towards a string theoretic description of black hole formation,” *Phys. Rev.* **D64** (2001) 064011, [arXiv:hep-th/0011217](#).
- [112] J. M. Maldacena and L. Maoz, “De-singularization by rotation,” *JHEP* **12** (2002) 055, [arXiv:hep-th/0012025](#).
- [113] V. S. Rychkov, “D1-D5 black hole microstate counting from supergravity,” *JHEP* **01** (2006) 063, [arXiv:hep-th/0512053](#).
- [114] B. C. Palmer and D. Marolf, “Counting supertubes,” *JHEP* **06** (2004) 028, [arXiv:hep-th/0403025](#).
- [115] D. Bak, Y. Hyakutake, S. Kim, and N. Ohta, “A geometric look on the microstates of supertubes,” *Nucl. Phys.* **B712** (2005) 115–138, [arXiv:hep-th/0407253](#).
- [116] A. Sen, “Two Charge System Revisited: Small Black Holes or Horizonless Solutions?,” *JHEP* **05** (2010) 097, [arXiv:0908.3402 \[hep-th\]](#).
- [117] A. Dabholkar, “Exact counting of black hole microstates,” *Phys.Rev.Lett.* **94** (2005) 241301, [arXiv:hep-th/0409148 \[hep-th\]](#).
- [118] A. Dabholkar, R. Kallosh, and A. Maloney, “A Stringy cloak for a classical singularity,” *JHEP* **0412** (2004) 059, [arXiv:hep-th/0410076 \[hep-th\]](#).
- [119] M. Banados, C. Teitelboim, and J. Zanelli, “The Black hole in three-dimensional space-time,” *Phys. Rev. Lett.* **69** (1992) 1849–1851, [arXiv:hep-th/9204099](#).
- [120] M. Banados, M. Henneaux, C. Teitelboim, and J. Zanelli, “Geometry of the (2+1) black hole,” *Phys. Rev.* **D48** (1993) 1506–1525, [arXiv:gr-qc/9302012](#).

- [121] S. Giusto, S. D. Mathur, and A. Saxena, “Dual geometries for a set of 3-charge microstates,” *Nucl. Phys.* **B701** (2004) 357–379, [arXiv:hep-th/0405017](#).
- [122] S. Giusto, S. D. Mathur, and A. Saxena, “3-charge geometries and their CFT duals,” *Nucl. Phys.* **B710** (2005) 425–463, [arXiv:hep-th/0406103](#).
- [123] I. Bena, C.-W. Wang, and N. P. Warner, “The foaming three-charge black hole,” *Phys. Rev.* **D75** (2007) 124026, [arXiv:hep-th/0604110](#).
- [124] E. Witten, “On the conformal field theory of the Higgs branch,” *JHEP* **07** (1997) 003, [arXiv:hep-th/9707093](#).
- [125] J. M. Maldacena and J. G. Russo, “Large N limit of non-commutative gauge theories,” *JHEP* **09** (1999) 025, [arXiv:hep-th/9908134](#).
- [126] A. Dhar, G. Mandal, S. R. Wadia, and K. P. Yogendran, “D1/D5 system with B-field, noncommutative geometry and the CFT of the Higgs branch,” *Nucl. Phys.* **B575** (2000) 177–194, [arXiv:hep-th/9910194](#).
- [127] S. Ferrara, R. Kallosh, and A. Strominger, “N=2 extremal black holes,” *Phys. Rev.* **D52** (1995) 5412–5416, [arXiv:hep-th/9508072](#).
- [128] S. Ferrara, G. W. Gibbons, and R. Kallosh, “Black holes and critical points in moduli space,” *Nucl. Phys.* **B500** (1997) 75–93, [arXiv:hep-th/9702103](#).
- [129] S. Ferrara and R. Kallosh, “Universality of Supersymmetric Attractors,” *Phys. Rev.* **D54** (1996) 1525–1534, [arXiv:hep-th/9603090](#).
- [130] S. Ferrara and R. Kallosh, “Supersymmetry and Attractors,” *Phys. Rev.* **D54** (1996) 1514–1524, [arXiv:hep-th/9602136](#).
- [131] A. Sen, “Black Hole Entropy Function and the Attractor Mechanism in Higher Derivative Gravity,” *JHEP* **09** (2005) 038, [arXiv:hep-th/0506177](#).
- [132] K. Goldstein, N. Iizuka, R. P. Jena, and S. P. Trivedi, “Non-supersymmetric attractors,” *Phys. Rev.* **D72** (2005) 124021, [arXiv:hep-th/0507096](#).
- [133] A. Dabholkar, A. Sen, and S. P. Trivedi, “Black hole microstates and attractor without supersymmetry,” *JHEP* **01** (2007) 096, [arXiv:hep-th/0611143](#).
- [134] J. de Boer, J. Manschot, K. Papadodimas, and E. Verlinde, “The chiral ring of AdS3/CFT2 and the attractor mechanism,” *JHEP* **03** (2009) 030, [arXiv:0809.0507 \[hep-th\]](#).
- [135] S. F. Hassan and S. R. Wadia, “Gauge theory description of D-brane black holes: Emergence of the effective SCFT and Hawking radiation,” *Nucl. Phys.* **B526** (1998) 311–333, [arXiv:hep-th/9712213](#).
- [136] J. M. Maldacena, “Black holes in string theory,” [arXiv:hep-th/9607235](#).
- [137] M. F. Sohnius, “Introducing Supersymmetry,” *Phys. Rept.* **128** (1985) 39–204.

- [138] P. C. Argyres, “Non-perturbative dynamics of four-dimensional supersymmetric field theories,” in *Conformal Field Theory: New Non-Perturbative Methods in String and Field Theory*, Y. Nutku *et al.*, eds. Perseus, 2000.
- [139] S. R. Coleman, “There are no Goldstone bosons in two-dimensions,” *Commun. Math. Phys.* **31** (1973) 259–264.
- [140] E. Witten, “Some comments on string dynamics,” [arXiv:hep-th/9507121](#).
- [141] J. D. Brown and M. Henneaux, “Central Charges in the Canonical Realization of Asymptotic Symmetries: An Example from Three-Dimensional Gravity,” *Commun. Math. Phys.* **104** (1986) 207–226.
- [142] D.-E. Diaconescu and N. Seiberg, “The Coulomb branch of (4,4) supersymmetric field theories in two dimensions,” *JHEP* **07** (1997) 001, [arXiv:hep-th/9707158](#).
- [143] N. Seiberg, “Observations on the Moduli Space of Superconformal Field Theories,” *Nucl. Phys.* **B303** (1988) 286.
- [144] S. Cecotti, “N=2 Landau-Ginzburg versus Calabi-Yau sigma models: Nonperturbative aspects,” *Int. J. Mod. Phys.* **A6** (1991) 1749–1814.
- [145] M. F. Atiyah, N. J. Hitchin, V. G. Drinfeld, and Y. I. Manin, “Construction of instantons,” *Phys. Lett.* **A65** (1978) 185–187.
- [146] R. Rajaraman, *Solitons and Instantons: An Introduction to Solitons and Instantons in Quantum Field Theory*. Elsevier Science B.V., 1982.
- [147] E. J. Weinberg and P. Yi, “Magnetic monopole dynamics, supersymmetry, and duality,” *Phys. Rept.* **438** (2007) 65–236, [arXiv:hep-th/0609055](#).
- [148] J. Michelson, “Notes on the Supersymmetric $(T^4)^N/S_N$ CFT.” *Unpublished*, 2008.
- [149] A. Schwimmer and N. Seiberg, “Comments on the N=2, N=3, N=4 Superconformal Algebras in Two-Dimensions,” *Phys. Lett.* **B184** (1987) 191.
- [150] P. D. Francesco, P. Mathieu, and D. Sénéchal, *Conformal Field Theory*. Springer Science+Business Media, LLC, New York, 1997.
- [151] O. Lunin and S. D. Mathur, “Correlation functions for M(N)/S(N) orbifolds,” *Commun. Math. Phys.* **219** (2001) 399–442, [arXiv:hep-th/0006196](#).
- [152] O. Lunin and S. D. Mathur, “Three-point functions for M(N)/S(N) orbifolds with N = 4 supersymmetry,” *Commun. Math. Phys.* **227** (2002) 385–419, [arXiv:hep-th/0103169](#).
- [153] W. Lerche, C. Vafa, and N. P. Warner, “Chiral Rings in N=2 Superconformal Theories,” *Nucl. Phys.* **B324** (1989) 427.
- [154] M. Gunaydin, G. Sierra, and P. Townsend, “THE UNITARY SUPERMULTIPLETS OF d = 3 ANTI-DE SITTER AND d = 2 CONFORMAL SUPERALGEBRAS,” *Nucl. Phys.* **B274** (1986) 429.

- [155] E. Gava and K. S. Narain, “Proving the pp-wave / CFT(2) duality,” *JHEP* **12** (2002) 023, [arXiv:hep-th/0208081](#).
- [156] J. M. Maldacena and A. Strominger, “AdS(3) black holes and a stringy exclusion principle,” *JHEP* **12** (1998) 005, [arXiv:hep-th/9804085](#).
- [157] J. R. David, G. Mandal, and S. R. Wadia, “D1/D5 moduli in SCFT and gauge theory, and Hawking radiation,” *Nucl. Phys.* **B564** (2000) 103–127, [arXiv:hep-th/9907075](#).
- [158] S. G. Avery, B. D. Chowdhury, and S. D. Mathur, “Emission from the D1D5 CFT,” *JHEP* **10** (2009) 065, [arXiv:0906.2015 \[hep-th\]](#).
- [159] O. Lunin, J. M. Maldacena, and L. Maoz, “Gravity solutions for the D1-D5 system with angular momentum,” [arXiv:hep-th/0212210](#).
- [160] S. D. Mathur, A. Saxena, and Y. K. Srivastava, “Constructing ‘hair’ for the three charge hole,” *Nucl. Phys.* **B680** (2004) 415–449, [arXiv:hep-th/0311092](#).
- [161] I. Kanitscheider, K. Skenderis, and M. Taylor, “Fuzzballs with internal excitations,” *JHEP* **06** (2007) 056, [arXiv:0704.0690 \[hep-th\]](#).
- [162] K. Skenderis and M. Taylor, “Fuzzball solutions and D1-D5 microstates,” *Phys. Rev. Lett.* **98** (2007) 071601, [arXiv:hep-th/0609154](#).
- [163] I. Kanitscheider, K. Skenderis, and M. Taylor, “Holographic anatomy of fuzzballs,” *JHEP* **04** (2007) 023, [arXiv:hep-th/0611171](#).
- [164] I. Bena, C.-W. Wang, and N. P. Warner, “Plumbing the Abyss: Black Ring Microstates,” *JHEP* **07** (2008) 019, [arXiv:0706.3786 \[hep-th\]](#).
- [165] I. Bena, N. Bobev, and N. P. Warner, “Spectral Flow, and the Spectrum of Multi-Center Solutions,” *Phys. Rev.* **D77** (2008) 125025, [arXiv:0803.1203 \[hep-th\]](#).
- [166] I. Bena, N. Bobev, C. Ruef, and N. P. Warner, “Entropy Enhancement and Black Hole Microstates,” [arXiv:0804.4487 \[hep-th\]](#).
- [167] I. Bena, N. Bobev, C. Ruef, and N. P. Warner, “Supertubes in Bubbling Backgrounds: Born-Infeld Meets Supergravity,” [arXiv:0812.2942 \[hep-th\]](#).
- [168] V. Jejjala, O. Madden, S. F. Ross, and G. Titchener, “Non-supersymmetric smooth geometries and D1-D5-P bound states,” *Phys. Rev.* **D71** (2005) 124030, [arXiv:hep-th/0504181](#).
- [169] P. Berglund, E. G. Gimon, and T. S. Levi, “Supergravity microstates for BPS black holes and black rings,” *JHEP* **06** (2006) 007, [arXiv:hep-th/0505167](#).
- [170] V. Balasubramanian, E. G. Gimon, and T. S. Levi, “Four Dimensional Black Hole Microstates: From D-branes to Spacetime Foam,” *JHEP* **01** (2008) 056, [arXiv:hep-th/0606118](#).

- [171] E. G. Gimon and T. S. Levi, “Black Ring Deconstruction,” *JHEP* **04** (2008) 098, [arXiv:0706.3394 \[hep-th\]](#).
- [172] E. G. Gimon, T. S. Levi, and S. F. Ross, “Geometry of non-supersymmetric three-charge bound states,” *JHEP* **08** (2007) 055, [arXiv:0705.1238 \[hep-th\]](#).
- [173] J. de Boer, F. Denef, S. El-Showk, I. Messamah, and D. Van den Bleeken, “Black hole bound states in $AdS_3 \times S^2$,” *JHEP* **11** (2008) 050, [arXiv:0802.2257 \[hep-th\]](#).
- [174] J. de Boer, S. El-Showk, I. Messamah, and D. V. d. Bleeken, “Quantizing $N=2$ Multicenter Solutions,” [arXiv:0807.4556 \[hep-th\]](#).
- [175] D. Z. Freedman, S. D. Mathur, A. Matusis, and L. Rastelli, “Correlation functions in the $CFT(d)/AdS(d+1)$ correspondence,” *Nucl. Phys.* **B546** (1999) 96–118, [arXiv:hep-th/9804058](#).
- [176] O. Lunin and S. D. Mathur, “The slowly rotating near extremal D1-D5 system as a ‘hot tube’,” *Nucl. Phys.* **B615** (2001) 285–312, [arXiv:hep-th/0107113](#).
- [177] J. Callan, Curtis G., S. S. Gubser, I. R. Klebanov, and A. A. Tseytlin, “Absorption of fixed scalars and the D-brane approach to black holes,” *Nucl. Phys.* **B489** (1997) 65–94, [arXiv:hep-th/9610172](#).
- [178] V. Cardoso, O. J. C. Dias, J. L. Hovdebo, and R. C. Myers, “Instability of non-supersymmetric smooth geometries,” *Phys. Rev.* **D73** (2006) 064031, [arXiv:hep-th/0512277](#).
- [179] V. Cardoso, O. J. C. Dias, and R. C. Myers, “On the gravitational stability of D1-D5-P black holes,” *Phys. Rev.* **D76** (2007) 105015, [arXiv:0707.3406 \[hep-th\]](#).
- [180] B. D. Chowdhury and S. D. Mathur, “Radiation from the non-extremal fuzzball,” *Class. Quant. Grav.* **25** (2008) 135005, [arXiv:0711.4817 \[hep-th\]](#).
- [181] B. D. Chowdhury and S. D. Mathur, “Pair creation in non-extremal fuzzball geometries,” *Class. Quant. Grav.* **25** (2008) 225021, [arXiv:0806.2309 \[hep-th\]](#).
- [182] B. D. Chowdhury and S. D. Mathur, “Non-extremal fuzzballs and ergoregion emission,” *Class. Quant. Grav.* **26** (2009) 035006, [arXiv:0810.2951 \[hep-th\]](#).
- [183] S. G. Avery and B. D. Chowdhury, “Emission from the D1D5 CFT: Higher Twists,” [arXiv:0907.1663 \[hep-th\]](#).
- [184] G. E. Arutyunov and S. A. Frolov, “Virasoro amplitude from the $S(N) R^{*24}$ orbifold sigma model,” *Theor. Math. Phys.* **114** (1998) 43–66, [arXiv:hep-th/9708129](#).
- [185] G. E. Arutyunov and S. A. Frolov, “Four graviton scattering amplitude from $S(N) R^{*8}$ supersymmetric orbifold sigma model,” *Nucl. Phys.* **B524** (1998) 159–206, [arXiv:hep-th/9712061](#).
- [186] J. R. David, G. Mandal, S. Vaidya, and S. R. Wadia, “Point mass geometries, spectral flow and $AdS(3)$ - $CFT(2)$ correspondence,” *Nucl. Phys.* **B564** (2000) 128–141, [arXiv:hep-th/9906112](#).

- [187] M. Cvetič and D. Youm, “General Rotating Five Dimensional Black Holes of Toroidally Compactified Heterotic String,” *Nucl. Phys.* **B476** (1996) 118–132, [arXiv:hep-th/9603100](#).
- [188] M. Cvetič and F. Larsen, “General rotating black holes in string theory: Greybody factors and event horizons,” *Phys. Rev.* **D56** (1997) 4994–5007, [arXiv:hep-th/9705192](#).
- [189] O. Lunin, “Adding momentum to D1-D5 system,” *JHEP* **04** (2004) 054, [arXiv:hep-th/0404006](#).
- [190] W. H. Press and S. A. Teukolsky, “Floating Orbits, Superradiant Scattering and the Black-hole Bomb,” *Nature* **238** (1972) 211–212.
- [191] J. L. Friedman, “Ergosphere instability,” *Commun. Math. Phys.* **63** (1978) 243.
- [192] N. Comins and B. F. Schutz, “On the ergoregion instability,” *Proc. R. Soc. Lond.* **A364** (1978) 211.
- [193] A. Ashtekar and A. Magnon, “Sublimation d’ergospheres,” *Comptes Rendus Academie des Sciences (Paris)* **281** (1975) 875–878.
- [194] C. G. Callan and J. M. Maldacena, “D-brane Approach to Black Hole Quantum Mechanics,” *Nucl. Phys.* **B472** (1996) 591–610, [arXiv:hep-th/9602043](#).
- [195] A. Dhar, G. Mandal, and S. R. Wadia, “Absorption vs decay of black holes in string theory and T-symmetry,” *Phys. Lett.* **B388** (1996) 51–59, [arXiv:hep-th/9605234](#).
- [196] S. R. Das and S. D. Mathur, “Comparing decay rates for black holes and D-branes,” *Nucl. Phys.* **B478** (1996) 561–576, [arXiv:hep-th/9606185](#).
- [197] S. R. Das and S. D. Mathur, “Interactions involving D-branes,” *Nucl. Phys.* **B482** (1996) 153–172, [arXiv:hep-th/9607149](#).
- [198] J. M. Maldacena and A. Strominger, “Black hole greybody factors and D-brane spectroscopy,” *Phys. Rev.* **D55** (1997) 861–870, [arXiv:hep-th/9609026](#).
- [199] M. Yu, “THE UNITARY REPRESENTATIONS OF THE N=4 SU(2) EXTENDED SUPERCONFORMAL ALGEBRAS,” *Nucl. Phys.* **B294** (1987) 890.
- [200] A. Pakman, L. Rastelli, and S. S. Razamat, “Extremal Correlators and Hurwitz Numbers in Symmetric Product Orbifolds,” [arXiv:0905.3451 \[hep-th\]](#).
- [201] A. Pakman, L. Rastelli, and S. S. Razamat, “Diagrams for Symmetric Product Orbifolds,” [arXiv:0905.3448 \[hep-th\]](#).
- [202] S. G. Avery, B. D. Chowdhury, and S. D. Mathur, “Deforming the D1D5 CFT away from the orbifold point,” [arXiv:1002.3132 \[hep-th\]](#).
- [203] S. G. Avery, B. D. Chowdhury, and S. D. Mathur, “Excitations in the deformed D1D5 CFT,” [arXiv:1003.2746 \[hep-th\]](#).

- [204] S. G. Avery and B. D. Chowdhury, “Intertwining Relations for the Deformed D1D5 CFT,” [arXiv:1007.2202 \[hep-th\]](#).
- [205] J. Gomis, L. Motl, and A. Strominger, “pp-wave / CFT(2) duality,” *JHEP* **11** (2002) 016, [arXiv:hep-th/0206166](#).
- [206] P. G. de Gennes, *Superconductivity in Metals and Alloys*. Benjamin, New York, 1966.
- [207] Y. Sekino and L. Susskind, “Fast Scramblers,” *JHEP* **10** (2008) 065, [arXiv:0808.2096 \[hep-th\]](#).
- [208] P. Hayden and J. Preskill, “Black holes as mirrors: quantum information in random subsystems,” *JHEP* **09** (2007) 120, [arXiv:0708.4025 \[hep-th\]](#).
- [209] D. Friedan, “INTRODUCTION TO POLYAKOV’S STRING THEORY,”. To appear in Proc. of Summer School of Theoretical Physics: Recent Advances in Field Theory and Statistical Mechanics, Les Houches, France, Aug 2-Sep 10, 1982.